Engineering and Physical Sciences Research Council

Modified Folates for Selective Delivery into Cancer Cells

A thesis submitted to Cardiff university for the degree of Doctor of Philosophy by:

Gareth E. S. Smith MChem(Hons)

Submission 29-September-2022

Successful Defence 27-February-2023

Corrected Submission 25-April-2023

Supervisors:

Prof. Dr. Rudolf K. Allemann

Dr. Louis Y. P. Luk

02-July-2018 – 31-March-2022

Table of Contents

List of Figures

List of Schemes

List of Tables

Acknowledgements

All glory to Jesus Christ the son of God.

Habakkuk 3:19

“The sovereign Lord is my strength; He makes my feet like the feet of a deer; He enables me to tread on the heights.”

Job 8:7

“Your beginnings will seem humble, so prosperous will your future be.”

1 Corinthians 15:33

“Do not be misled: Bad company corrupts good character.”

Luke 1:37

“For nothing will be impossible with God.”

John 13:7

“Jesus replied, ‘You do not realize now what I am doing, but later you will understand.’”

Hebrews 10:36

"For you have need of endurance, so that when you have done the will of God you may receive what is promised."

Mathew 24:13

“But the one who endures to the end will be saved.”

1 Peter 5:7

“Casting all your anxieties on him, because he cares for you.”

To Henrietta Lacks, I am grateful for your enormous contributions towards science and medicine. Without your contributions, we wouldn't have the current progression and advances that we have today. Praise the good Lord God. Thank you.

To my nearest and dearest friends, I love you and will forever appreciate your support. My closest friend Dr. Tyler Thomas and I would spend countless hours studying together in Starbucks coffee shops when we were undergraduates and later party the night away. I have so many fantastic memories with you here at Cardiff university. I truly believe that if it were not for your help, I would not be in the position that I am in today. Thank you from the bottom of my heart brother.

Thank you to my crew, coach Jamie Price, my sisters Emilohi Adedeji and talented graduate chemist Dina Dawit, my family dog Piper, fellow peptide chemists Dr. Alexander Lander and Dr. Davide Cardella, pastor Dave Gobbett, Dr. Irene Castellan, and High Fields Church.

Thank you to my lovely wife Nokhuthula Nyoni-Smith RD for your amazing support before and during my Ph.D. studies. You have been by my side every step of the way. I look forward to what God has in store for us next. Life is great.

Thank you to my parents Carmelita and Graham Arthur-Leroy Smith BSc(Hons) CChem MSci FRSC and my A-Level chemistry teacher Dr. Mike Beer, who just like my father inspired me to pursue chemistry.

To the incredibly talented post-doctoral researchers Dr. Aduragbemi Adesina, Dr. Alan Scott and Dr. Luke Johnson who helped guide me during my research studies. Thank you all for your expertise and kindness. Thank you to Dr. Sahar Kandill, Dr. David Miller and Prof. Dr. John A. Pickett for their contributions towards correcting my thesis. Thank you to Dr. Robert Mart for his deep knowledge of science which he was happy to lend me as well as his upkeep of all the labs that I worked in during his time at Cardiff university.

To my secondary Ph.D. project supervisor, masters project supervisor and IBCarb funded summer placement supervisor Dr. Louis Luk. You were instrumental in my development as a chemist. Thank you for all the support you gave me and the hours spent together working out at PureGym. Louis taught me a valuable lesson that “less is more.” It took me a while to grasp this. I’m still working on it. But I think it shows in my presentations that I’ve been delivering during the last four years.

I am extremely grateful to my primary Ph.D. project supervisor Prof. Dr. Rudolf Allemann for selecting me as his student in March 2018. In addition to this, I would like to express extra gratitude to Ruedi for allowing me take on my Ph.D. project. I will always be thankful that you selected me to be a part of your research group and giving me the opportunity to work on a project that I adored. Furthermore, I am also grateful for the tremendous support that both Ruedi and Louis Luk provided during tough stretches in my Ph.D. studies. I cannot thank you both enough for kindly lending me your time from your busy schedules, and on one occasion Ruedi rearranging his meetings to lend me a helping hand during a very tough hour. Thank you so much.

To the first post-doc that I had worked with on this project, Dr. Antonio Angelastro, thank you for introducing me to essential skills such as solid phase peptide synthesis. This helped me progress in my studies.

Thank you all.

My Ph.D. work and thesis was written in dedication to my father Graham Arthur-Leroy Smith BSc(Hons) MSci CChem FRSC.

Abstract

Small molecule drugs suffer from prompt resistance and off-site activity. To address these problems, small molecules were substituted with peptides that mediate more sophisticated pathways such as apoptosis through more specific and intricate cellular interactions that require more time to develop resistance. In this research, a dual conjugate system was developed using a luminescent protein such as super folder green fluorescent protein (*e.g* sfGFP) for highlighting and a pro-apoptotic peptide (*e.g.* Bid-BH3) for killing. Both were labelled with folate which provided both protein and peptide increased cell target specificity. Folic acid is a high affinity ligand for its dedicated membrane receptor folate receptor alpha (FR-α) which is overexpressed in one third of all cancer. Therefore, folic acid was employed as a protein and peptide delivery motif because the expression pattern of FR-α in healthy cells is largely non-existent. The folic acid labelled sfGFP had preference to interact with FR-α positive cells (*e.g.* KB cells), and no interaction with FR-α negative HEK293 cells when tested at concentrations below 10 μM. Folate labelled sfGFP was found to interact with KB cells at 10 nM according to FACS. Once this was discovered, sfGFP was swapped for Bid-BH3 for conjugation with folic acid and this was compared alongside its unmodified sequence. It was found that the folate labelled sequence retained its cytotoxicity when compared to the native sequence on KB cells in the absence of free folic acid (*e.g.* ± 0.5, 5.3 μM vs. ± 1.0, 6.2 μM respectively). In the presence of free folic acid cytotoxicity of the folate labelled peptide diminished, whereas the native sequence cytotoxicity was unaffected. This result was also observed when both sequences were tested on FR-α-negative HEK293 cells.

In other works, the synthesis cell penetrating peptides (CPP) based on TAT and aurein-1.2 connected to folic acid was attempted. These sequences were planned for conjugation to sfGFP to generate a protein-based conjugate with a combination of cell targeting and endosome escape. The plan was to swap sfGFP for a cytotoxic protein once ideal concentrations allowing for cell targeting and endosome escape were found. Many issues were found when synthesising the TAT sequences such as glutarimide formation, truncation and failed folic acid labelling. The aurein-1.2 sequences were significantly easier to synthesise, however, folate labelling was problematic, and the peptide sequence was found to rapidly self-cleave from sfGFP in phosphate buffered saline. Because of these results, alternative synthetic techniques for producing folate-CPP conjugated to sfGFP will need to be considered.

Glossary of Abbreviations

ABC transporter – Adenosin triphosphate binding cassette transporter

AIF – Apoptosis inducing factor

Alloc – Allyloxycarbonyl ester protecting group

Allyl – Allyl ester protecting group

APAF-1 – Apoptotic protease activating factor 1

ARP2/3 – Actin related protein 2/3

ATP – Adenosine-5'-triphosphate

BCl-2 – B-cell lymphoma 2

BME – β-Mercaptoethanol

C_{18} – HPLC column containing octadecylsilane comprised of 18 carbons bound to the silica

CDC42 – Cell division control 42

CEM – Chemical engineering machines

CLIC – Clathrin independent carrier

CPP – Cell penetrating peptide

DAVBLH - Desacetyl vinblastine monohydrazide

DCB – 2,6-*Di*chlorobenzoyl chloride

DCC – N,N'-Dicyclohexylcarbodiimide

DCM – Dichloromethane

dH_2O – Deionised water

DIC – *N,N'*-Diisopropylcarbodiimide

DIPEA – Diisopropylethyl amine

DMEM – Delbeco's modified eagle medium

DMF – Dimethylformamide

DMSO – Dimethyl sulfoxide

DNA – 2’-Deoxyribonucleic acid

DOD – 3,6-Dioxa-1,8-octanedithiol

ε – Molar extinction coefficient

E. coli – *Escherichia coli*

EC145 – Vintafolide

EC20 – Etarfolatide

EDTA – Ethylenediaminetetraacetic acid

eGFP – Enhanced green fluorescent protein

FACS – Fluorescence activated cell sorting

FBS – Fetal bovine serum

Fmoc – Fluorenylmethyloxy carbonyl protecting group

FPLC – Fast protein liquid chromatography

FR-α – Folate receptor alpha

GDP – Guanosine-5’-diphosphate

GEEC – Glycosylphosphatidylinositol-anchor enriched early endosomal compartment

GFP – Green fluorescent protein

GTP – Guanosine-5’-triphosphate

HATU – Hexafluorophosphate azabenzotriazole tetramethyl uronium

HBTU – Hexafluorophosphate benzotriazole tetramethyl uronium

HEK293 cells – Human embryonic kidney-293 cells

HER2 – Human epidermal growth factor receptor 2

HIV1 – Human immunodeficiency virus 1

His_6-Tag – Histidine tag

$HOBt.H_2O$ – Hydroxybenzotriazole monohydrate

HPLC – High performance liquid chromatography

IC_{50} – Inhibition concentration where binding, or response is reduced by 50%

IPTG – Isopropyl-β-D-1-thiogalactopyranoside

KB cells – Subline of keratin-producing HeLa cells comprised of human papilloma virus18

kDa – Kilo Dalton

LB Medium – Lysogeny broth

LC/MS – Liquid chromatography mass spectrometry

$^{M}/_{Z}$ – Mass to charge ratio

mbar – Millibar

MDR – Multidrug resistant protein

MPa – Megapascal

Mtt – *4*-Methyl trityl protecting group

Ni^{2+}-NTA – Nickel nitrilotriacetic acid

NMM – *N*-Methyl morpholine

OaAEP1 – *Oldenlandia affinis* asparaginyl endopeptidase

OD_{600} – Optical density at 600 nm

Pbf – 2,2,4,6,7-pentamethyldihydrobenzofuran-5-sulfonyl protecting group

PBS – Phosphate buffered saline

PEG_9 – 8-Amino-3,6-dioxaoctanoic acid

PMSF – Phenylmethylsulfonyl fluoride

ppm – Parts per million

psi – Pounds per square inch

PyBOP – Benzotriazole-1-yloxytripyrrolidinophosphonium hexafluorophoshate

RME – Receptor mediated endocytosis

RNA – Ribonucleic acid

rpm – Rotations per minutes

RPMI – Roswell Park memorial institute medium

RT – Room temperature

SDS – Sodium dodecyl sulphate

SDS-PAGE – Sodium dodecyl sulphate–polyacrylamide gel electrophoresis

sfGFP – Super folder green fluorescent protein

siRNA – Small interference ribonucleic acid

S_N2 – Bimolecular nucleophilic substitution

SPPS – Solid phase peptide synthesis

TAT – Trans-activator of transcription

^{t}Boc – Tertiary-butyloxycarbonyl protecting group

^{t}Bu – Tertiary butyl protecting group

TCEP – Tris(2-carboxyethyl)phosphine

TEMED – Tetramethylethylenediamine

TFA – Trifluoroacetic acid

TIS – Triisopropyl-silyl

TNB – 5-Thio-2-nitrobenzoic acid

Trt – Trityl protecting group

UV-Vis – Ultra violet-visible light

WASp – Wiscott-Aldrich syndrome protein

WHO – World Health Organisation

Yop effector – *Yersinia* outer protein effector

Proteinogenic L-Amino Acid Abbreviations

A – Alanine (Ala)

R – Arginine (Arg)

N – Asparagine (Asn)

D – Aspartic acid (Asp)

C – Cysteine (Cys)

Q – Glutamine (Gln)

E – Glutamic acid (Glu)

G – Glycine (Gly)

H – Histidine (His)

I – Isoleucine (Ile)

L – Leucine (Leu)

K – Lysine (Lys)

M – Methionine (Met)

F – Phenylalanine (Phe)

P – Proline (Pro)

S – Serine (Ser)

T – Threonine (Thr)

W – Tryptophan (Trp)

Y – Tyrosine (Tyr)

V – Valine (Val)

Chapter 1: Introduction

1.1 Project aim

The aim of this research was to produce site selectively labelled polypeptides containing a folic acid motif. This was to enhance selectivity and delivery of polypeptides towards cancer cells by exploiting the high affinity interaction of folate and FR-α with the purpose of creating a selective cancer cell killing system, and thus provide leads for future therapeutics aimed at tackling cancers of the female reproductive system (*e.g.* ovarian cancer).

1.2 Cancer and its Impact

During the early 20th century cancer was thought to be an age-related condition and commonly deemed the "disease of the old."[1] However, cancer occurrence amongst children,[2] adolescent and young adults[3] is becoming more frequent and coincides with a rise in global population.[1,4–6] Data provided by Cancer Research UK show that more than 164,000 people per annum died as a result of cancer in 2021 and this corresponds to 28% of total deaths.[6]

Cancer is a collection of diseases, all of which have in common uncontrolled cell proliferation. This is the result of mutations in cell regulatory machinery, and different types of cancer have different systems mutated making it impossible to treat with a single therapy. Genetic alterations that contribute towards the development of malignancies are derived from three gene types.[7] For instance, DNA repair genes are responsible for maintaining the structural integrity of genetic information. Tumour-suppressor genes and proto-oncogenes are responsible for maintaining cell growth and division. Alterations to these genes can cause healthy cells to progress into malign cells.[7] For example, DNA repair genes can result in mutations such as additional or missing gene sequences. This can impact genes responsible for cell growth and division, such as tumour-suppressor genes and proto-oncogenes, the latter developing into oncogenes due to unwanted mutations, and thus generating cells that evade maintenance mechanisms of cell death required to preserve balance in the body.[8] There are two categories of cell death; necrosis which is an unprogrammed process derived from catastrophic cellular injuries resulting in cell demise, and apoptosis, a programmed mechanism responsible for eliminating cells infected with viruses, and cells containing harmful changes to DNA.[9] Some cells carrying harmful mutations in genetic information can evade apoptosis and this can lead to the introduction of malignancies within a hosts body. Consequently, these cells can develop changes in cellular characteristics such as the number of

membrane receptors needed for nutrient uptake.[10] Alterations like this can help increase the propensity for malign cells to replicate exponentially by providing them with a system to outcompete normal functioning cells for metabolites. Therefore, resulting in the unwanted distribution of cancerous cells throughout the hosts body if left undeterred, ultimately leading to death.

A recent demographic study by the World Health Organisation (WHO) shows cancer is a leading cause of globally mortality (**Figure 1**).[11] Data compiled from 183 countries indicate cancerous diseases were the most prevalent or second major cause of premature demise in 112 countries. Furthermore, cancer was among the top ten causes of death in the remaining 71 documented countries.[11] For this reason, the development and application of methods for tackling cancer is imperative.

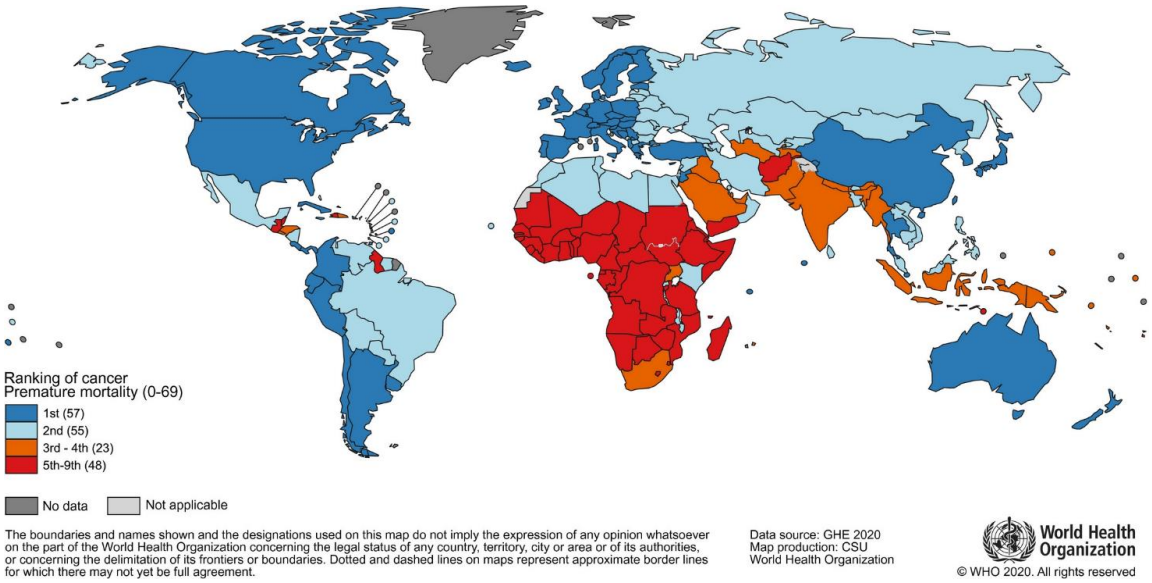

Figure 1 - Demographic chart depicting global cancer mortality from WHO.[11]

1.3 Methods for Eradicating Cancer

1.3.1 Radiotherapy

Radiotherapy is a method commonly used for treating cancer. This technique relies on directing high energy radiation at malign cells.[12] The result of exposure to high energy radiation is destruction of DNA needed for cellular replication. However, most malignancies are surrounded by non-cancerous cells and, hence radiation must travel through healthy tissues to reach tumours. A consequence of this procedure is death of surrounding healthy cells as well as cancer cells.[13]

1.3.2 Chemotherapy

An alternative procedure which is also used alongside radiotherapy is chemotherapy. This is defined as the administration of a cytotoxic agent with cell killing properties aimed at destroying tumours.[14]. Their anti-cancer activity can be defined by enzyme inhibitory characteristics or alkylating genetic information such as DNA. For example, β-chloroethyl amine[15,16] used for treating Hodgkin lymphoma[17] operates by alkylating DNA bases generating cross linked strands thereby, preventing cell replication. On the other hand, inhibitory molecules such as methotrexate bind to essential enzymes such as dihydrofolate reductase.[18] This diminishes the cell's ability to replicate because of a decline in one carbon metabolism caused by the cells inability to convert folate into tetrahydrofolate which is an essential co-factor. These are responsible for producing DNA nucleotide precursors such as purines and thymidylates (**Figure 2**).[19]

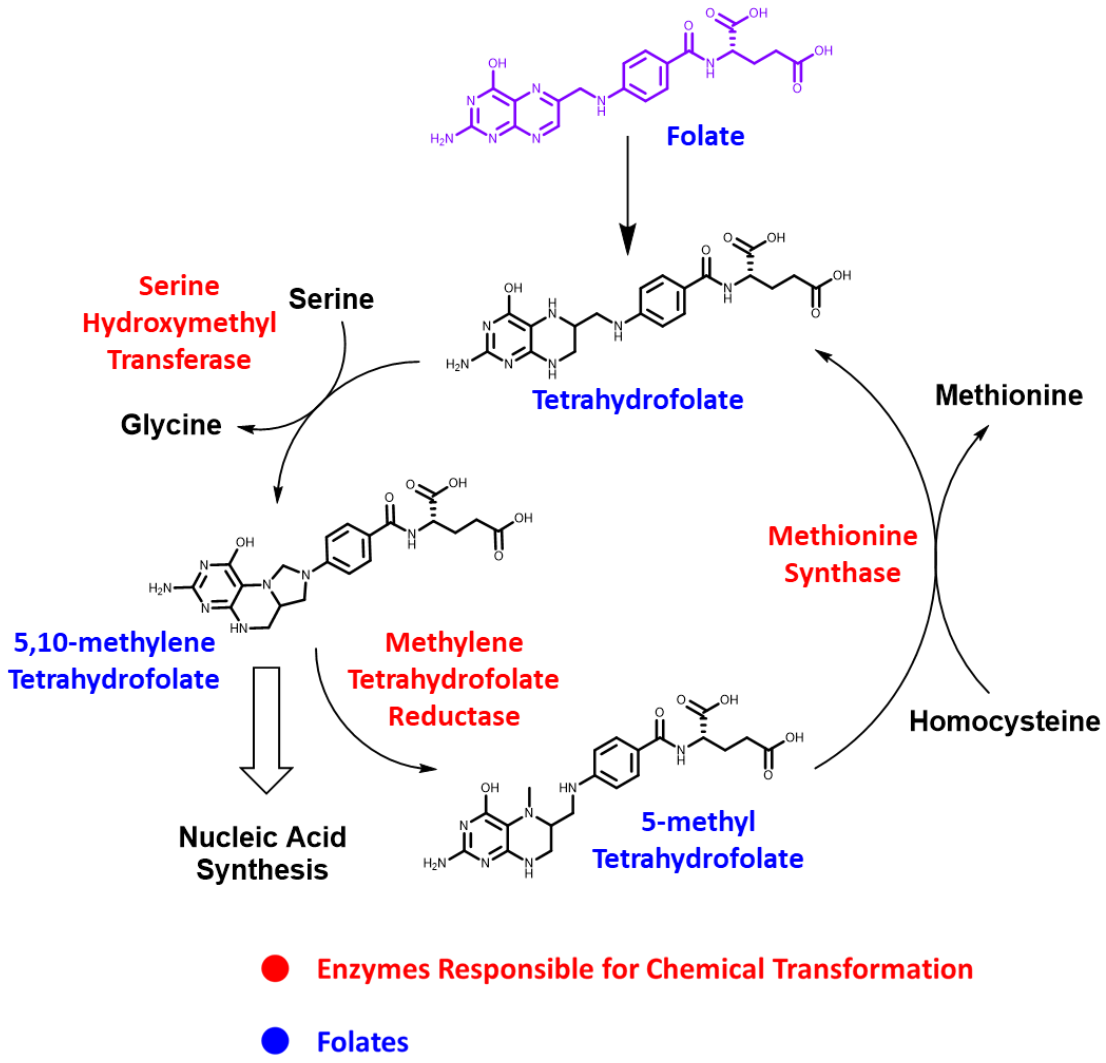

Figure 2 - Simplified one carbon metabolic cycle.

Cytotoxic agents possess the capacity to destroy tumour cells. However, they exhibit a distinct lack of cell target specificity,[20–22] resulting in the induction of apoptosis in both normal and cancer cells and subsequent decline in patient's health.[20] For instance, patients treated with methotrexate exhibited many adverse symptoms such as end-stage liver disease,[23,24] and tumour lysis syndrome.[25] This highlights the importance of new chemotherapeutic agents that selectively target cancer cells, in other words, performing 'molecular surgery' and reducing side effects, therefore eliminating cancer cells and minimising adverse effects on surrounding healthy cells.

Advances

Tumour Homing Small Molecules

Chemotherapeutic agents have been synthesised to incorporate a chemical motif that possess the propensity to discriminate between normal cells and cancer cells, and thus, increase cell target specificity and minimise side effects.[26] Vintafolide (EC145, **3 – Figure 3**) was an example of this advancement and was developed by a biotech company Endocyte Inc. It was examined in phase III global clinical trials for platinum resistant ovarian cancer but failed due to a lack of desirable activity.[27] This molecule was made of desacetyl vinblastine monohydrazide (DAVLBH **1 – Figure 3**) which is a modified vinca-alkaloid that induces apoptosis in cancer cells. This is achieved by inhibiting mitotic spindles at the metaphase/anaphase boundary of mitosis in fast replicating cancer cells.[28] DAVLBH is connected to a releasable linker system (green segment of **3 – Figure 3**) held together by a disulphide bridge *via C*-terminal cysteine incorporated into a short water-soluble peptide sequence capped with folic acid on the N-terminus. The folate motif is the tumour homing ligand used to guide the drug molecule DAVLBH towards cells that overexpress folate receptor alpha.[26]

Although EC145 demonstrated some success at killing cancer cells, a method of diagnosis was needed prior to drug deployment to identify malignant cells that highly express folate receptor alpha. Radioactive tracers are used with PET imaging to visualise abnormal activity in malign cells. Etarfolatide (EC20, **4** – **Figure 3**) is a companion imaging agent that was comprised of a folate connected to a chelated meta-stable technetium-99 radio label.[29] This radio diagnostic tool was employed to highlight FR-α overproducing cancers *via* PET images by exploiting an active uptake mechanism.

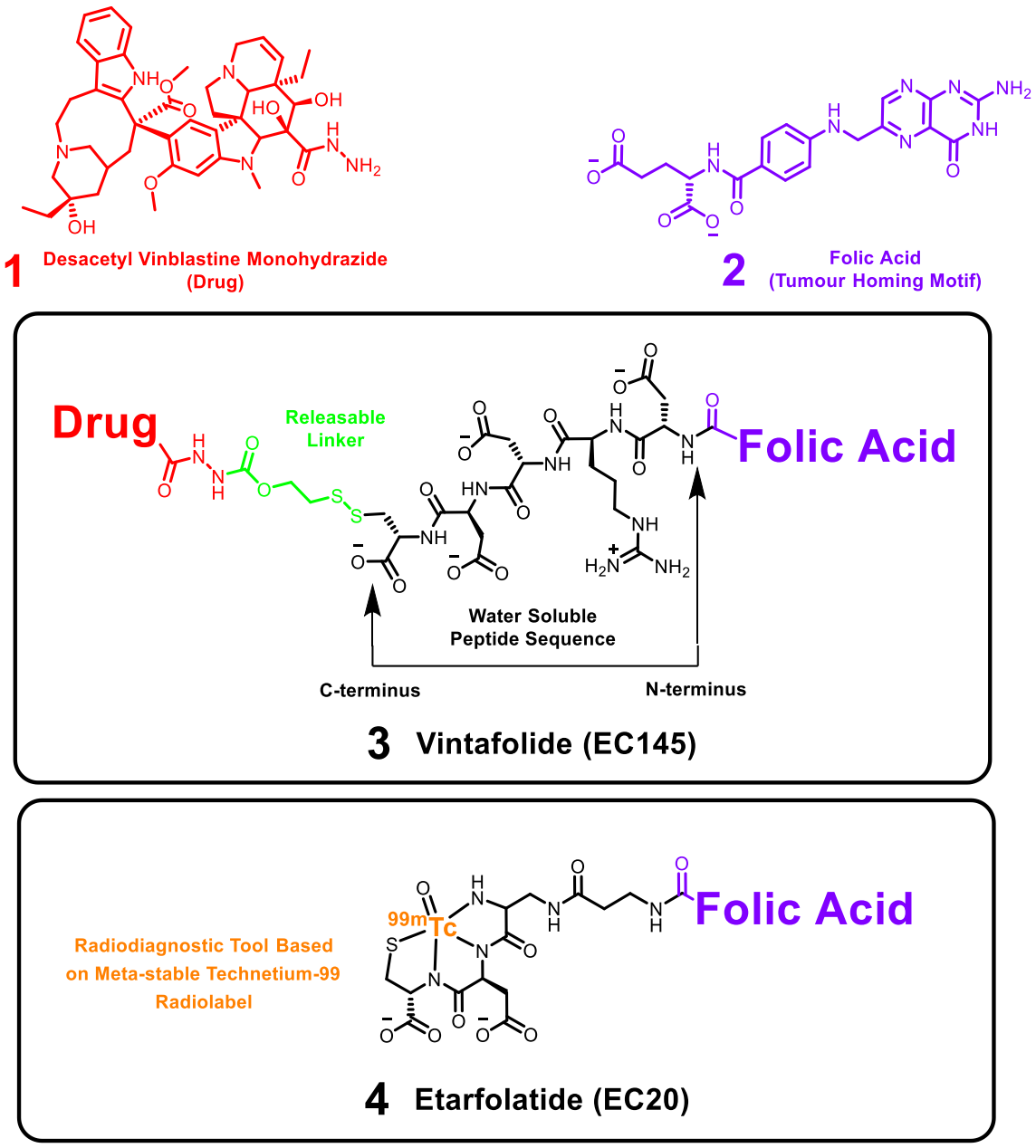

Figure 3 - Structure of DAVLBH (1), folic acid (2), vintafolide (3) and etarfolatide (4).

Exploiting Natural Uptake Mechanisms

Active Cellular Uptake

Essential metabolites such as folates and derivatives require a mode of transportation to assist their movement across the cell membrane. The lipid bilayer forms a barrier that provides the cell protection from foreign bodies such as parasites and helps to establish a concentration gradient facilitating essential nutrient upkeep.[30] Molecules can move through the cell membrane using energy dependent or independent pathways. For example, small non-polar and non-charged molecules such as O_2 and H_2O can move through the cell membrane un-impeded. However, polar and large charged molecules such as ions, amino acids, glucose and folates are unable to move across the plasma membrane without a carrier molecule assisting transportation.[30,31] A common feature shared between both uptake processes is that they are both energy independent and thus designated as translocation mechanisms.[30] On the other hand, for molecules that are needed by the cell but cannot pass through the lipid bilayer, endocytosis becomes essential. In general, endocytic processes can be categorised as follows:

- **Pinocytosis** is a ubiquitous and non-specific form of endocytosis and can be described as ‘cell drinking’ whereby solutes are actively trafficked into a cell.[32]

- **Phagocytosis** is a process utilised by the immune system employing phagocytes designed to recognise and destroy pathogens such as bacteria and viruses.[33] Pathogen-associated molecular pattern is a biomarker produced on the surface of pathogens and are recognised by complementary toll-like receptor generated by phagocytes. Through recognition and adherence, the foreign body is engulfed into phagosomes which mature into phagolysosomes containing anti-pathogenic molecules used for dismantling foreign bodies.[34]

- **Receptor mediated endocytosis (RME)** is the most specific form of endocytosis and can be sub-categorised according to the endocytic machinery used to aid vesicle formation:

A) **Clathrin-dependent RME (Figure 4 - 1)** utilises clathrin coated pits for the formation of a vesicle from the cell surface.[35] As a ligand binds to the extracellular portion of a receptor (step 1), a protein conformational change induces a tyrosine sorting signal located on a cytosplasmic extension to bind onto an adaptor protein (step 2).[36–38] As a result, clathrin molecules are recruited and bind onto the adaptor protein *via* clathrin box motif (step 3) and produce a cage like structure (step 4) forming indentations in the plasma membrane.[39–41] Large GTPases such as dynamin facilitate the completion of endosome formation by providing membrane scission. This severs the vesicle from the surface membrane and clathrin disassembly proteins remove clathrin molecules (step 5). This is then followed by the movement of ligands across the vesicle membrane and subsequent return of the receptor to the surface membrane (step 6).[42,43]

B) **Clathrin-independent RME (Figure 4 - 2)** can operate in the absence of clathrin molecules and rely on the action of small GTPases such as CDC42 for initiating endocytic uptake.[44] As a ligand binds onto a receptor (step 1), a conformational change will occur inducing effector molecules such as a guanine-nucleotide exchange factor to exchange GTP for GDP, therefore activating CDC42.[45–47] In its initiated state CDC42 can form complexes with Wiscott-Aldrich syndrome protein (WASp) used for aiding actin polymerisation.[48] CDC42-WASp complex can bind onto actin mimics such as ARP2/3 and attach to pre-formed actin fibres enabling spontaneous actin polymerisation.[49] Consequently, this polymerisation event drives membrane invaginations over regions of the surface membrane comprised of a high concentration of ligand-receptor complex (step 2, A – E).[50] Endosome formation is completed once membrane folds have ingulfed their target region and fused (step 3).[51,52] Ligands are released from their receptor (step 4) and the receptor returns to the surface membrane for further endocytosis (step 5).

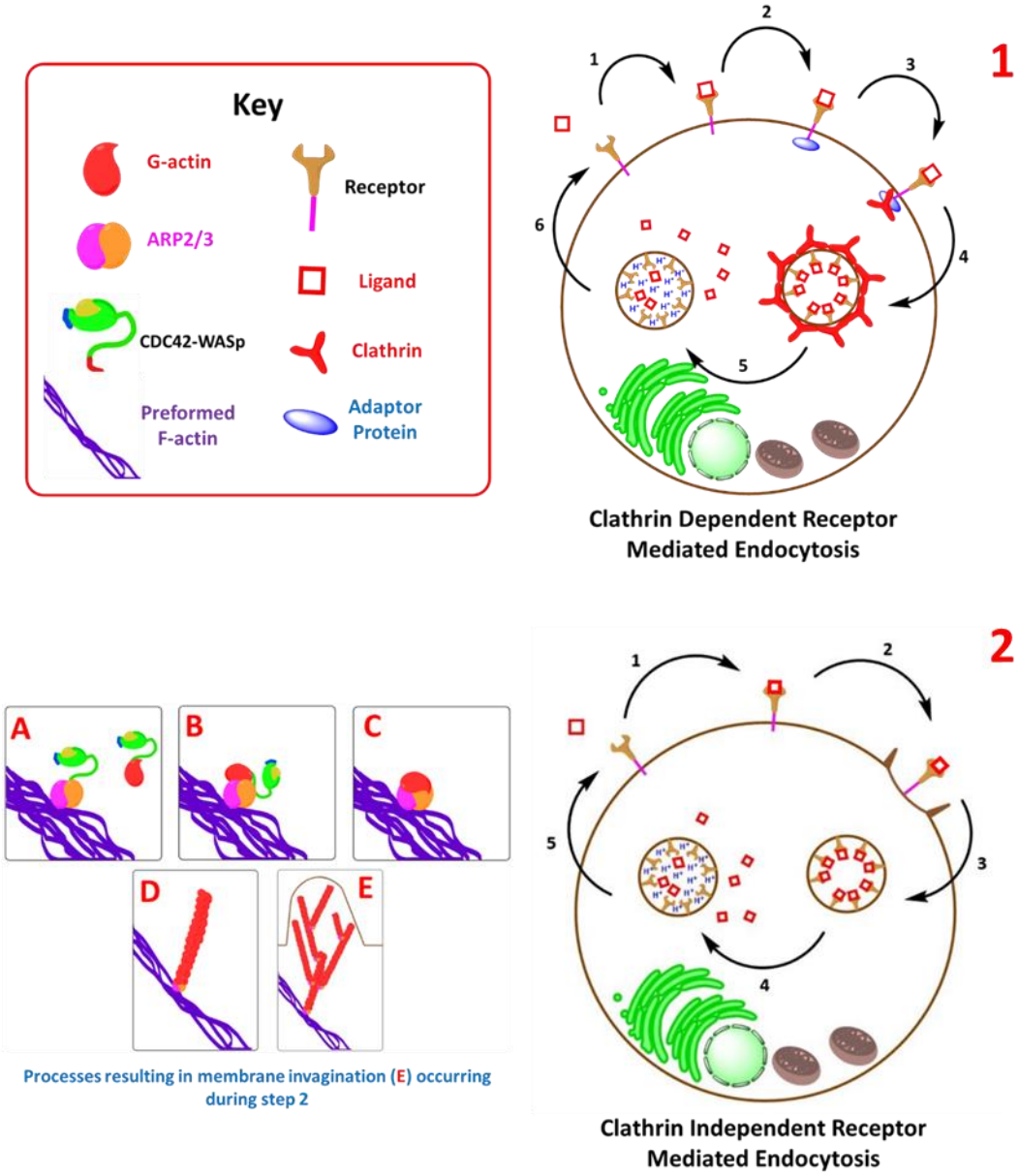

Figure 4 - Clathrin Mediated Endocytosis (1) and Clathrin Independent Receptor Meidated Endocytosis (2)

FR-α transports folic acid and its derivatives into the cytosol *via* clathrin independent receptor mediated endocytosis mechanism (**Figure 4**).[53–55] This natural mechanism has been exploited for the transit of unnatural cytotoxic molecules into cancer cells, for example EC145. Membrane invaginations fuse together forming the early endosome, otherwise known as a clathrin-independent carrier (CLIC) in FR-α mediated mechanism (**Figure 5**).[56] The interior environment of the endosome becomes increasingly acidic the further the vesicle moves into the cell and this is

caused by ATPase acting as proton pumps, and thus resulting in vesicle maturation.[53] This matured vesicle in FR-α mediated endocytosis is known as a "glycosylphosphatidylinositol-anchor enriched early endosomal compartment," (GEEC); following endosome acidification, folic acid and related derivatives dissociate from FR-α due to conformational change of the receptor protein. Subsequently, folates can exit the endocytic vehicle by a proton-coupled folate transporter into the cytosol (**Figure 5**).[57]

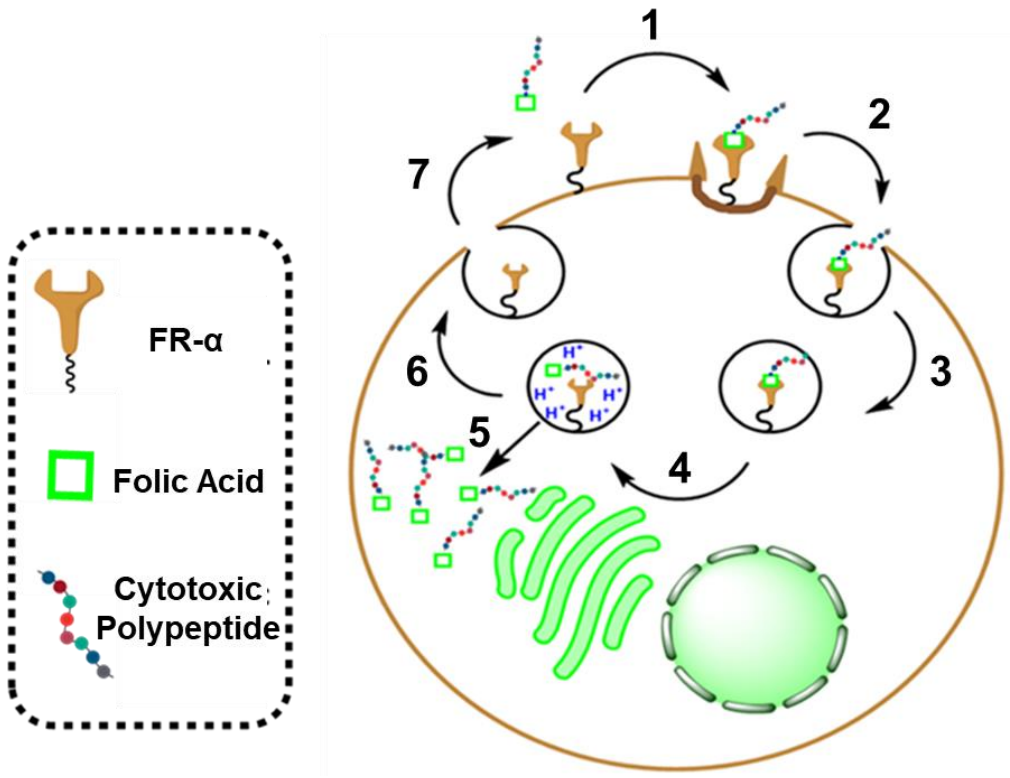

Figure 5 - FR-α endocytosis. (1) folate binding to FR-α, (2) membrane folds make CLIC, (3) CLIC carries folate/FR-α into cell, (4) Llumen acidifies forming GEEC, (5) folate exits endosome, (6) FR-α moving back to cell surface, (7) FR-α ready for further uptake

Folic acid installed into EC145 and EC20 (**Figure 3**) helps to concentrate its cargo (*i.e.* DAVLBH or ^{99m}Tc respectively) on the cell membrane. This is because folate is important in cell proliferation and the dedicated high-affinity (K_D = 0.1 – 1 nM) membrane transporter known as folate receptor alpha (FR-α) is frequently overproduced in fast-replicating malignancies.[58] Indeed, the corresponding FR-α gene (*folr1*) is overexpressed in one third of all cancer.[59] The expression pattern of

folr1, and subsequent production of the corresponding FR-α grants significant discrimination between healthy cells and cancer cells. Most normal functioning human cells produce negligible or non-existent quantities of FR-α.[60] Nonetheless, there are some examples of healthy human tissues that mass-produce FR-α, namely the choroid plexus, lungs and kidneys.[10,61] Folate labelled drugs such as EC145 were unable to directly access FR-α in the choroid plexus and lungs due to the presence of the blood brain barrier, and lack of direct contact with the blood stream respectively. However, FR-α located in the proximal tubule component of the nephron in kidneys are exposed to blood borne folates. Despite this, folate labelled drugs such as EC145 did not enforce renal cytotoxic effects,[10] and this is because FR-α within the kidneys utilise a mechanism known as transcytosis.[62,63] For higher eukaryotic organisms, this is an evolutionary trait employed to retain and recycle folates due to the absence of *de novo* folate biosynthesis.[64] Folates are filtered in the kidneys and shuttled back into blood circulation for further one carbon metabolism.[63] On the other hand, epithelial malignancies such as ovarian and endometrial carcinoma, can foster millions of copies per cell.[61] For this reason, FR-α has been utilised as a biomarker for drug delivery. In addition to FR-α, there are other examples of targeted biomarkers, for example human epidermal growth factor receptor 2 (HER2) is overexpressed in 30% of all breast cancer.[65] The monoclonal antibody herceptin discovered by Genetech Inc targets HER2 and spotlights malign cells for elimination by the immune system.[66] This is done *via* antibody dependent cell cytotoxicity whereby herceptin binds to its target receptor leaving its FC region exposed. Cytotoxic cells such as natural killer cells recognise the FC region and bind to it. This interaction results in the release of interferons which are responsible for killing the target cell. Despite the successes of targeting HER2, its corresponding gene overexpression in cancers such as ovarian and endometrial carcinoma is less frequent in comparison to FR-α.[67–69] For this reason, targeted therapies aimed at exploiting FR-α and its active uptake mechanism need to be further explored for selective delivery.

Small Molecule Problems

Endocytic uptake of EC145 (**3 – Figure 3**) using FR-α was efficient, and the subsequent release and dispatch of the drug payload DAVLBH (**1 – Figure 3**) carried in EC145 was effective. Consequently, DAVLBH can passively diffuse across the endosomal membrane and access the cell cytosol due to its small size, and hence allowing the vinca alkaloid to elicit its cytotoxic activity.[70] However, small molecules fall prey to resistance mechanisms such as upregulated assembly of multi-drug resistant (MDR) proteins and ABC-transporter pumps, diminishing the drug's efficacy.[71,72] This occurs through MDR proteins forming conjugates with cytotoxic targets such as vinca alkaloids which are recognised by ABC-transporters for cellular efflux.[73]

Despite the introduction of a folic acid moiety for selective guidance, patients treated with EC145 during phase I clinical trials were discovered to suffer from constipation, gastrointestinal toxicity, and neuropathy. This stems from offsite activity likely caused by vinca alkaloid accumulation in the bile, liver metabolism and axonal degeneration.[74-76] Efforts were made to reduce side effects, however, symptoms such as neuropathy continued to persist due to the inhibitory nature of vinca alkaloids and their propensity to prevent retrograde and anterograde axonal transportation.[74,75]

Small Molecule Alternatives

Antibodies

Alternative methods used for eliminating malignancies are based on larger molecular weight species such as antibodies, for example herceptin[76–80] These proteins contain an antigen-binding site known as a paratope. This structural feature can recognise and bind to complementary antigens generally located on the extracellular face of the cell surface. Antibody-antigen binding involves greater surface area coverage when compared to a small molecule that bind and interact with significantly smaller regions of a target. Consequently, this results in less off-site activity when compared to small cytostatic molecules.[81] Despite their ability to discriminate cancer cells, these macromolecules initiate undesirable immunogenic responses such as high blood pressure,[82–84] bleeding,[85] and blood clots.[86] Once attached to their target, antibodies recruit phagocytes, initiate the complement system, or neutralise pathogens *via* binding interactions that alter structure and function.[87]

Enzymes

Aside from antibodies, enzymes can be used to target markers and disrupt metabolic processes within cancer cells by damaging cellular machinery, thereby, directly killing a cell.[88–90] The complexity of biocatalytic processes mediated by enzymes require malignancies more time to develop resistance when compared to small molecules. Much like antibodies, enzymes also cover a large surface area when interacting with intracellular targets such as ribosomes.[91,92] Momordin is a type 1 ribosome inactivating protein (RIP) that was studied for chemical labelling with folic acid to create a protein-folate conjugate. This was destined for testing on cancer cells overproducing FR-α and these studies highlighted a significant issue with cyotosolic delivery of large molecular weight species such as enzymes. Momordin-folate conjugates were successful at targeting cancer cells due to the folic acid motif; however, cytotoxic activity was compromised. This was due to problems related to vesicular entrapment derived from the large size and charge of the protein cargo preventing it from moving through the endosomal membrane.[91,92]

Peptides

Cell Membrane Barrier

In modern medicinal research, the cell membrane presents a significant obstacle in the successful cytosolic delivery of cytotoxic molecules based on proteins. Most macromolecules are unable to access the cell cytosol from the extracellular milieu due to large molecular weight and charge. This results in endosome entrapment of macromolecules which are eventually degraded due to lysosomal conditions of late endosomes. This is an issue which has plagued intracellular delivery of large molecular weight species due to limited membrane permeability.[91,93–96] Many druggable targets are intracellular, for instance ribosomes[97,98] and RNA polymerases,[99] and thus therapeutics must be able to cross the cell membrane in order to reach their targets. To this end, significant research efforts have been made to find ways of circumventing the cell membrane. For example, recent studies show blue light activated dimerising magnetic proteins can induce fusion of lysosomal and mitochondrial membranes.[100] This system could be used for guiding toxic proteins that target organelles such as mitochondrial ribosomes. However, studies were performed *in vitro* whereby cells were subjected to transient transformation using plasmid DNA required to produce magnetic proteins.[100] Moreover, liposomes have been successfully used for enhancing stability and delivery of therapeutic molecules.[101] They are comprised of concentric amphipathic phospholipids arranged

via interactions of hydrophilic head groups, and association of hydrophobic tails. This provides a spherical structure comprised of an aqueous core that mimics the cell membrane in physiological medium. These lipid vesicles have been used to carry drug molecules such as doxorubicin and verteporfin,[102,103] and are capable of fusing with the cell membrane and unloading their cargo into the cell, therefore by-passing the cell membrane. Despite this, production of lipid vesicles can be a costly and complex multi-step process,[104,105] and thus, more convenient strategies of initiating cell permeation are being explored.

Electro-Permeabilisation

Current methods aimed at bypassing the cell membrane include electroporation which uses electricity directed at the plasma membrane for inducing pore formation.[106] This facilitates the intracellular passage of molecules such as proteins into the cytosolic space.[107] However, electro-permeabilisation and related physical techniques suffer from issues such as poor cell survival; apertures generated may be too large, and therefore the cell is unable to close membrane openings. Additionally, electroporation can't be clinically applied to patients.[106] Furthermore, such techniques suffer from non-specific transport of materials moving into and out of a cell during the application of electricity, resulting in problems such as ion imbalance and, therefore leading to cell death.[106]

Cell Penetrating Peptides (CPP)

Hydrophobic and cationic polymers were found to favour cell uptake, among these are chemical entities known as cell penetrating peptides (CPPs – **Table 1**) which are short sequences comprised of a maximum of 30 amino acids in length.[108] CPPs are a structural component discovered in pathogens such as viruses and were found to enhance their cellular uptake through the cell membrane.[109–112] A well-known example is the trans-activator of transcription (**Table 1** – TAT) discovered in 1988. It is used by the HIV1 virus for promoting trans-activation of its corresponding viral promoter.[113] In addition to this sequence, CPPs derived from Yop effector molecules originating from bacteria *Yersinia enterocolitica*[114] are used for facilitating proinflammatory cytokine downregulation.[112] These CPPs and others (**Table 1**) have been used for intracellular delivery of quantum dots,[115] siRNA,[116] plasmid DNA[117,118] and fluorescent proteins.[96,119] Despite these successes, CPPs suffer from a range of problems such as lack of cell target specificity[120] caused by interactions with ubiquitously produced

membrane components utilised for permeation. For instance, TAT and oligoarginines are known to pass through the cell membrane by interacting with heparan sulphate proteoglycans.[121]

Bearing in mind their lack of cell targeting ability, CPPs had been used in conjugation with a protein cargo to circumvent membrane barriers and promote cytosolic entry.[96] This type of system will allow a macromolecular toxin to mediate cytotoxic activity if employed, but a method for targeting cells will need to be installed due to CPPs lack of cell discriminating ability.[121,122] Therefore, folic acid can be added onto CPP sequences to improve cell targeting properties. A combination of cytotoxic macromolecule connected to CPP, both retaining functionality, and capped with folic acid will need to be found and studied.

Peptide Name	Sequence
TAT[113]	YGRKKRRQRRR
R_9[123]	RRRRRRRRR
Pep-1[124]	GALFLGFLGAAGSTMGA
TP10[125]	AGYLLGKINLKALAALAKKIL
Aurein-1.2[96]	GLFDIIKKIAESF
Xentry[125]	LCLRPVG

Table 1 - Cell penetrating peptide sequences.

CPP Chemical Properties and Membrane Interaction

Cell penetrating peptides (CPPs) are polymers that possess hydrophobic and hydrophilic amino acid side chains that can influence properties such as membrane permeation. These polymers can be used for non-invasive delivery of cytotoxic proteins. Based on the chemical characteristics of CPPs, they can be classified into cationic, amphipathic, and hydrophobic sequences.

- **Cationic CPPs** normally contain more than five positively charged residues for interacting with anionic membrane components. Arginine is preferred, because it possesses a guanidinium group that can generate bidentate hydrogen bonds with cell surface membrane components such as sulphates, carboxylates and phosphates (**Figure 6**).[123] Consequently, through interaction with negatively charged membrane constituents, cationic CPPs can initiate cellular uptake under physiological conditions.[127]

- **Amphipathic CPPs** incorporate hydrophilic residues into hydrophobic peptidyl segments. This consequently alters the chemical characteristics and thus membrane interaction. By hosting a mix of charged and non-charged amino acids, the distribution of charge within amphipathic CPPs gives rise to primary and secondary amphipathicity. Primary amphipathicity refers to sequences comprised of well-defined hydrophilic and hydrophobic portions. Peptides such as pep-1 and TP10 are examples that exhibit a preference for interacting with disordered sections of the lipid bilayer incorporating loosely packed phospholipids and curved regions. In addition, secondary amphipathic CPPs contain alternating sequence of charged and non-charged residues.[128] Aurein-1.2 is an example of secondary amphipathic CPP which has been used for the delivery of supercharged proteins,[96] and is known for possessing anticancer properties. Such peptides behave differently by performing conformational changes to structures such as α-helices specific to aurein-1.2 and β-sheets for other peptides.[128]

- **Hydrophobic CPPs** prefer to interact with more lipophilic segments of the plasma membrane for potentiating spontaneous entry into the cell cytosol. By utilising hydrophobic residues such as tryptophan, hydrophobic CPPs can use these side chains for insertion into the cell membrane. Subsequently, direct translocation from the extracellular environment into the intracellular space follows.[128]

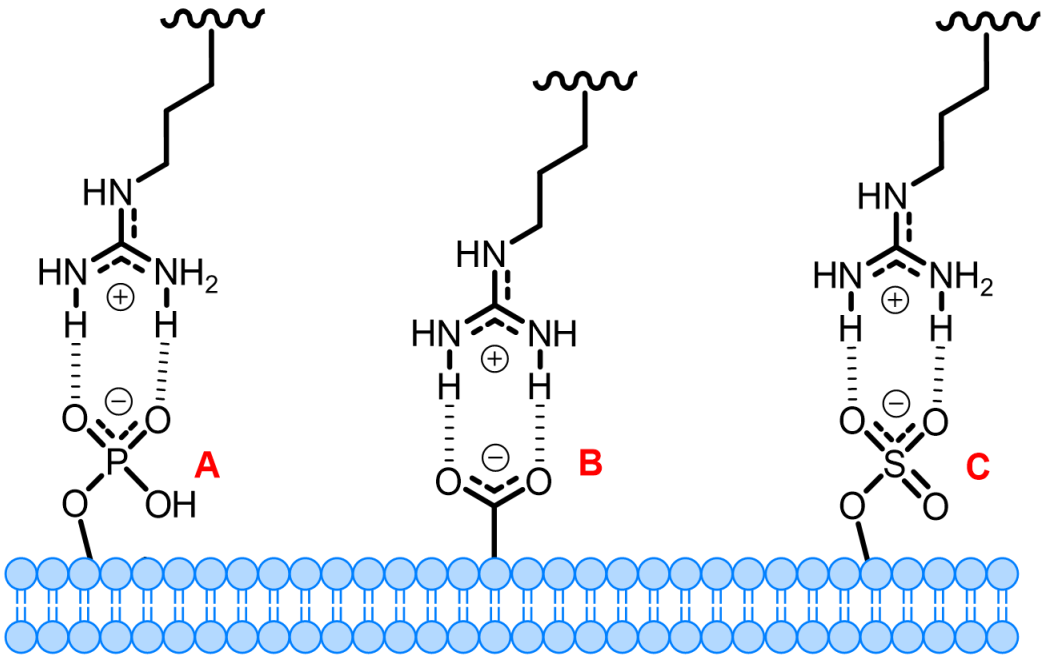

Figure 6 - Bidentate hydrogen bonding interaction between arginine guanidinium group and cell surface phosphates (A), carboxylates (B) and sulphates (C).

Natural Cytotoxic Peptides

In addition to membrane translocamotive properties, some cell permeable peptide sequences possess anticancer activity. For example, Bid-BH3 (EDIIRNIARHLAQVGDSMDR) and aurein-1.2 have demonstrated membrane penetration[96,129] and the ability to interact with a specific biological target to initiate cell death.[130,131] Such attributes make peptides such as these an interesting candidate for developing anticancer therapeutics. All cells in a multicellular organism participate in processes of growth and death and both are critical for the survival of a living system. Cell death can be initiated by harsh environmental stimuli or *via* a controlled process. In nature there are two types of cell death, and they are necrosis and apoptosis.

Necrosis

Necrosis is a passive pathological process which is detrimental to the body and involves the damage of cells resulting in an inflammatory response.[132] This is derived from the exposure of a cell to extreme conditions which differ from their normal living conditions (*e.g.* changes in pH, temperature, UV exposure or oxygen levels).[132] The cells inability to maintain normal function under harsh conditions are caused by impairment of cellular machinery, and eventually this will culminate in cell death.

Apoptosis

Apoptosis, or otherwise known as programmed cell suicide is a predetermined active physiological process necessary for the body whereby the cell participates in its own death.[132,133] This process is essential for cell proliferation and turnover, and therefore cells perish by following a route of biochemical reactions to maintain a balance in cell population. Cells within the human body have established lifespans. For instance, red blood cells live for approximately 120 days before they are programmed to die.[134] This is critical due to the potential for developing malignancies which emanate from unwanted cells evading programmed cell suicide.[135] Apoptosis pathways can be categorised according to the involvement of caspases:

- **Apoptosis Inducing Factor:** This mechanism of programmed cell death is a caspase independent process[136] and involves the use of a molecule known as an apoptosis inducing factor (AIF).[137] AIF is a flavoprotein involved in initiating apoptosis *via* release from mitochondria into the cytosol, and subsequent entry into the nucleus of a cell where condensation of chromatin and DNA fragmentation is stimulated and resulting in cell death.[137]

- **Extrinsic Pathway:** This process of cell suicide is initiated by external stimuli such as T-lymphocytes. These cells possess a protein located on the membrane surface known as Fas ligand and this is used to bind onto Fas receptors[138] resulting in the recruitment of a Fas associated death domain.[139] This complexation facilitates the activation of caspase-8,[140] and therefore giving rise to a caspase cascade resulting in the destruction of the cells interior, and thus leading to programmed cell death.

- **Intrinsic pathway:** This pathway is initiated from signals derived from within the mitochondria of a cell and culminates in a caspase-9 cascade resulting in programmed cell death.[141] Bid-BH3 is a peptide known to aid the direct activation of a pro-apoptosis inducing protein.[142,141]

Bid-BH3

Intrinsic mitochondrial apoptosis can be activated directly and indirectly (**Figure 7**). Both routes activate the pro-apoptotic protein BAX which resides in the cytosol as an inactive monomer and on the outer mitochondrial membrane inhibited by BCl-2. This apoptosis promoter is responsible for creating pores in the outer mitochondrial membrane by forming oligomers.[141] The result of outer membrane pore formation is leakage of cytochrome C into the cytoplasm of a cell. Once in the cytoplasm, cytochrome C will attach to APAF-1 creating a complex known as an apoptosome which is responsible for activating caspase-9 leading to the destruction of a cell's interior (*e.g.* organelles), and resulting in cell death.[142] Indirect BAX activation involves the BCl-2 family protein BAD which is an inhibitor of the anti-apoptotic protein BCl-2.[141] This resides on the outer mitochondrial membrane and helps to preserve its structural integrity. Once BCl-2 is inhibited by BAD, this releases BAX to create pores in the outer membrane and eventually leading to cell death *via* indirect activation (**Figure 7**).[141] On the other hand, a short peptide sequence belonging to the BCl-2 family known as Bid-BH3, originating from BH3-only proteins is capable of facilitating intrinsic apoptosis[142] by directly activating BAX (**Figure 7**). For this process to occur Bid-BH3 must be in its active alpha helical conformation to interact with and activate BAX.[141] This causes BAX to translocate to the outer mitochondrial membrane leading to oligomerisation which results in pore formation and subsequent cytochrome C leakage. This gives rise to the same caspase-9 cascade that gives rise to programmed cell death.[141]

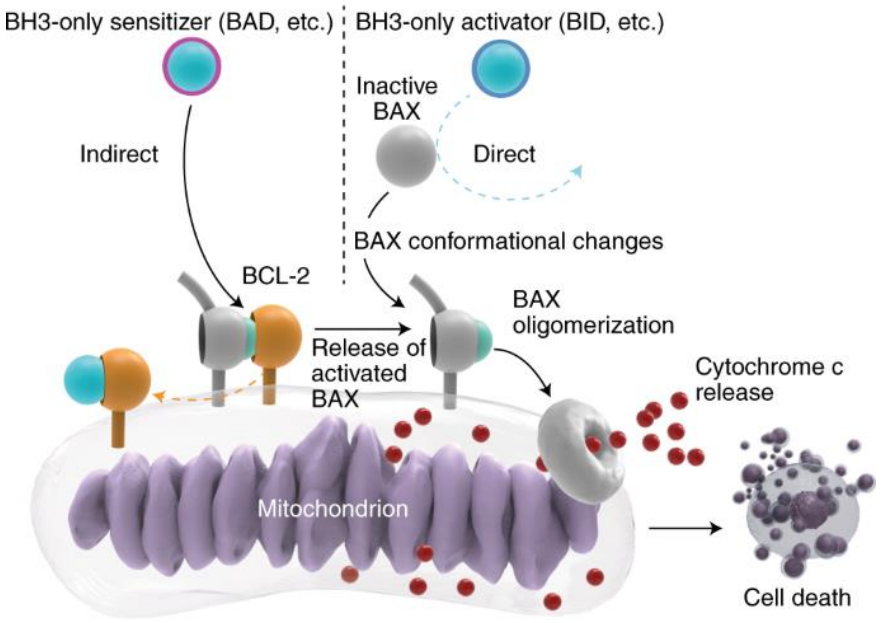

Figure 7 - Intrinsic mitochondrial apoptosis mediated by BAX activation via pro-apoptotic peptide Bid-BH3 (direct activation) and protein BAD (indirect activation).[141]

Aurein-1.2

Aurein-1.2 is a peptide derived from the defensive skin secretions of *Litoria* genus of Australian bell frogs.[131,143–145] This peptide was used for providing an endosomal escape pathway[96] for supercharged fluorescent proteins that were prone to entrapment inside of vesicles.[93,96] Despite enhancing cytosolic entry of protein, aurein-1.2 did not have preference for targeting cancerous or non-cancerous cells.[145] Aurein-1.2 operates by adopting an alpha helical conformation upon interaction with charged regions of cancer cell membranes resulting in a carpet like coverage. This causes structural perturbations resulting in membrane lysis and eventually cell death.[145]

1.4 Labelling Polypeptides

Polypeptides such as aurein-1.2 and BCl-2 family sequences such as Bid-BH3 represent an intriguing alternative to cytostatic molecules for selective delivery. They hold potential for inducing sophisticated metabolic pathways by interacting with a specific biological target,[142] whereas small molecules are largely restricted to inhibitory processes[28] that warrant prompt resistance.[73] Despite this they require guidance to reach cancer cells just like small molecules[26] and need a modification that includes a tumour homing motif such as folate. The advent of a simple labelling technique connecting a polypeptide to folic acid in a site selective manner will help expand our arsenal of anticancer therapeutics. This technology can be developed by focusing on reactive amino acid residues such as cysteine due to the known methods of chemical labelling.

1.4.1 Disulphide Bridge Conjugation

Assembly of small molecule drug conjugates such as EC145 was performed using disulphide bridge conjugation linking folate to DAVLBH (**Figure 3**)**.** This was accomplished using a bifunctional cross linker (2-[benzotriazole-1-yl-(oxycarbonyloxy)-ethyldisulfanyl]pyridine)[146] comprised of an anhydride for connecting DAVLBH, and a mixed disulphide for an exchange reaction adding the modified folate. In this case, two different chemical reactions on either side of a linker were required to create EC145.[146] On the other hand, there are reagents that allow for the direct addition of a tumour homing motif onto a cysteine residue. For example, disulphide bridge containing compound Ellman's reagent (5,5'-dithio-*bis*(2-nitrobenzoic acid)) has been used to quantify the number of sulfhydryl groups present

in solution. The disulphide motif of Ellman's reagent can readily undergo exchange with a free thiol present on a cysteine residue of a polypeptide (**Figure 8**).[147,148] The result of this reaction is an activated mixed disulphide comprised of a polypeptide linked to 5-thio-2-nitrobenzoic acid (TNB) *via* cysteine conjugation.[149] This exchange process breaks Ellman's reagent in half giving rise to the release of TNB which is a poor nucleophile due to its resonance stability.[150] The activated disulphide can undergo further disulphide exchange with another cysteine containing polypeptide to generate a conjugate.

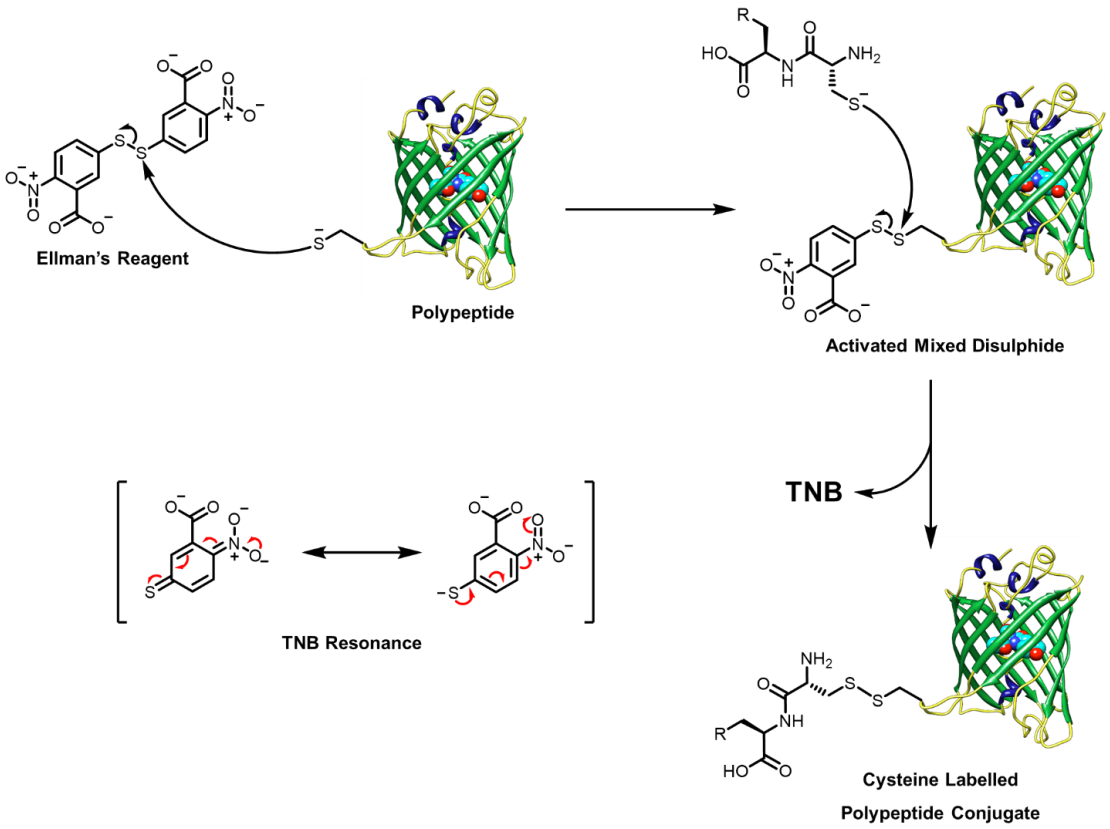

Figure 8 - Disulphide bridge conjugation facilitated by Ellman's reagent.

1.4.2 Michael Addition Conjugation

Another method of chemical labelling is the Michael reaction which involves the addition of a nucleophile, for example a thiol to a compound comprised of an α,β-unsaturated carbonyl such as a maleimide (**Figure 9**).[151] This route of thiol labelling is commonly used due to the convenient nature required to perform this chemical transformation.[152] A buffer solution with a pH residing in an approximately neutral region between 6.5 – 7.5 is employed to maintain specificity of a thiol towards the maleimide.[150] This pH range sustains structural integrity of the maleimide motif by negating potential for alkaline mediated hydrolysis at higher pH and allows for fast labelling.[153] Furthermore, buffer pH kept below 7.5 prevents amines from competing with thiols for connection to maleimides.[150]

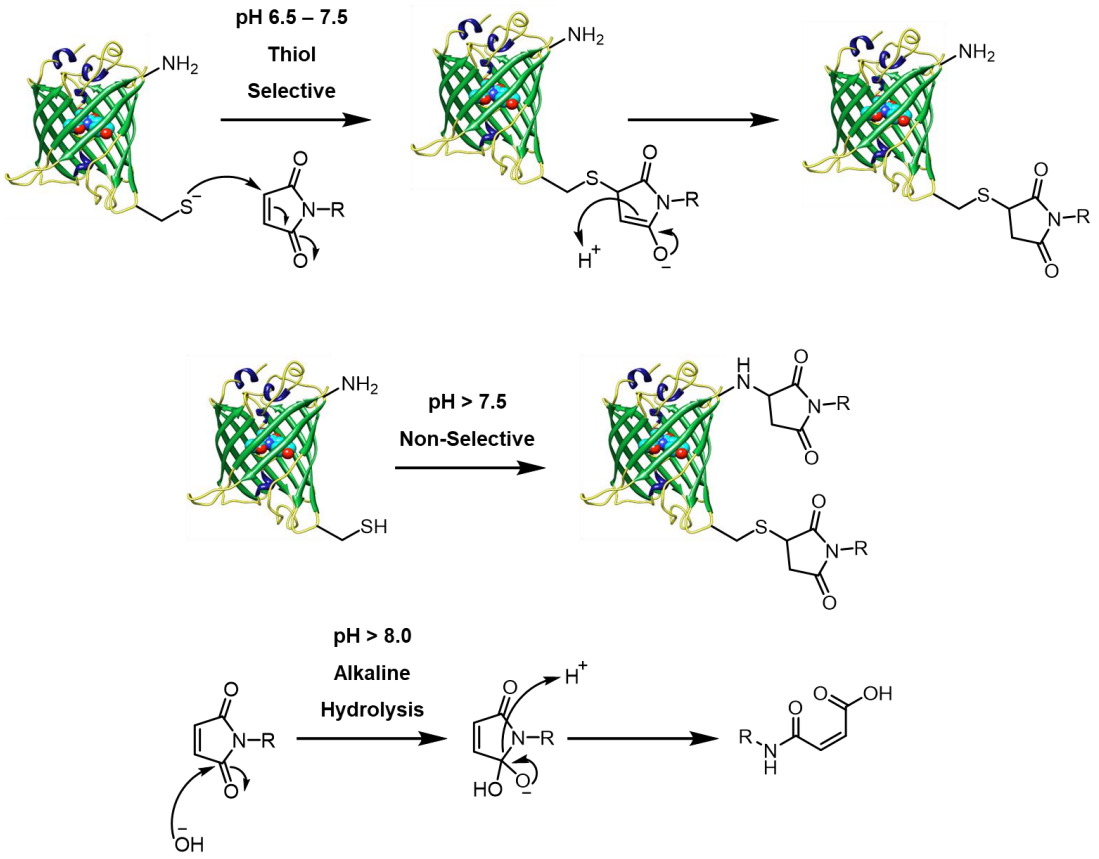

Figure 9 - The influence of pH change on maleimide selectivity towards thiols and structural stability.

1.4.3 Folate Labelling

Site selective chemical labelling of folates can be performed by exploiting thiol Michael addition or disulphide bridge conjugation techniques. Both methods of conjugation were previously employed to create small molecule drug conjugates based on vinca alkaloids.[26] However, investigations into FR-α targeted polypeptide delivery systems are limited[92,154–156] when compared to low molecular species.[26,157] Folate labelling of polypeptides was performed in previous work using a ribosome inactivating protein (RIP) momordin.[91] The resulting RIP was found to be labelled with multiple folates in mixture using a non-selective labelling method.[91] The cytotoxicity of momordin was retained despite structural changes from random labelling, however, non-discriminatory conjugation of other molecules may pose problems when identifying inactivated structural combinations. Therefore, further developments in folate labelling will need to be site-selective to identify non-active conjugates. For example, the vinca alkaloid vincristine was found to be inactivated when labelled with folic acid. On the other hand, vinblastine was discovered to retain cytotoxicity when connected to the same folate label.[158] Recent studies were carried out building on site-specific labelling of folates to polypeptides. Folic acid labelling of peptidic thymidylate synthase inhibitors were successful at selectively inhibiting cancer cell growth in multiple cervical cancer cell lines.[154] In addition to this work a prodrug delivery system involving an anticancer tripeptide was developed and demonstrated selective uptake in HeLa cells, however this system exhibited poor activity.[155]

Interestingly, a system comprised of folate conjugated to a naturally occurring polypeptide capable of selectively killing cancer cells with high potency is yet to be produced. Recent findings show folate labelling of KLAKLAK was successful at discriminating cervical cancer cells, but high micromolar concentrations were required.[159] If this type of system can be made more cytotoxic with a convenient method of assembly, for example, thiol Michael addition under mild aqueous conditions this will establish an easy folate labelling technique that can be applied to a variety of polypeptides. This technique could facilitate further research into cancer delivery systems and contribute towards the current chemotherapeutic repertoire.

1.5 Research Purpose

The goal of this research was to produce folate labelled polypeptides for selectively inducing cell death in malignancies. Folic acid was used to enhance selective delivery of polypeptides towards cancer cells by exploiting the high affinity interaction between the ligand folate and biomarker FR-α. This could provide leads to future therapeutics that could expedite the development of treatments for diseases such as ovarian cancer. Development of two systems was pursued, both based on polypeptides. The first system planned included a CPP labelled with folic acid and a conjugatable linker destined for connection to a protein in chapter 3. Proteins lacking a translocation domain were found to suffer from issues derived from vesicular entrapment and subsequent degradation in acidified environments of late endosomes.[91,92] The premise of this study was to introduce a combination of selectivity using the folate, and membrane permeability introduced by the CPP to provide an endosome escape pathway for large polypeptides. In addition to the CPP work, a cytotoxic peptide system involving naturally occurring sequences aurein-1.2 and Bid-BH3 was assembled in chapter 4. Small cytotoxic peptides were conjugated to folic acid using a convenient thiol mediated Michael reaction. Both naturally occurring cytotoxic peptides and derivatives were tested on mammalian cells *in vitro*. To accompany the folic acid tagged peptides, a diagnostic tool like EC20 (4 – **Figure 3**) was needed to study the ability of folate to guide a polypeptide towards cancer cells overproducing FR-α. Super folder green fluorescent protein (sfGFP) was tagged with folate and employed to illuminate cancer cells that produce FR-α and this was studied using fluorescence activated cell sorting in chapter 2.

Chapter 2: Large Fluorescent Polypeptide Conjugates

2.1.1 Introduction

This chapter describes the preparation of modified fluorescent proteins bearing folates to examine the efficiency of cargo delivery into FR-α producing cancer cells. A pair of peptides based on a PEG_9-DRDCG sequence containing *N*-terminal folate and pteroate respectively (**Scheme 1**) were generated using Fmoc solid phase peptide synthesis (SPPS). The key structural difference between pteroate and folate is the glutamate tail and this was studied for its effect on FR-α binding. On the *C*-terminus a cysteine was included for the purpose of generating a disulphide bridge with the solvent exposed cysteine of sfGFP. Both peptides contain a 9-atom polyethylene glycol (PEG_9) which serves as a molecular spacer between folate moiety and sfGFP. Inclusion of PEG_9, therefore, prevents sfGFP from obstructing the folate motif when attempting to bind to FR-α. Finally, peptides were capped using folate and pteroate (**Scheme 1**) for comparative studies to investigate FR-α binding and endocytic uptake of large polypeptides. It was found that the glutamate tail plays a minor role in FR-α affinity and provides significantly improved enhancement for uptake. Folate was found to be better for binding to FR-α when compared to pteroate. However, experiments demonstrate that the pteroate portion of folate is the critical component for binding to FR-α because interaction between construct 2 and FR-α was detected at concentrations as low as 100 nM.

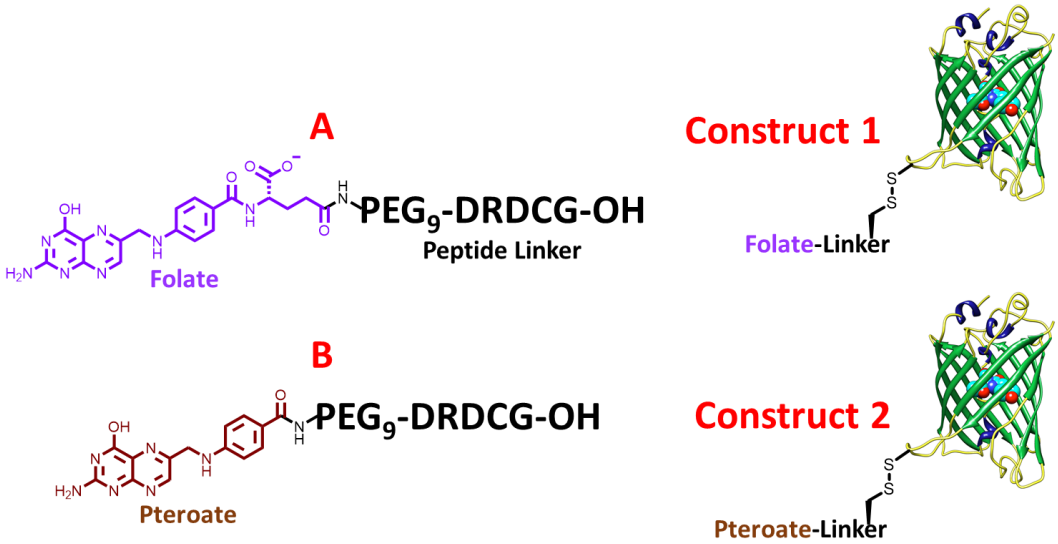

Scheme 1 - Structure of folic acid labelled peptide (A) and pteroic acid labelled peptide (B) used to produce construct 1 and construct 2.

2.1.2 Peptide Production Methods

Peptides are a promising drug delivery vehicle for facilitating the cell uptake of protein-based therapeutics due to their ability to increase membrane permeability, and hence provide access and interact with intracellular targets. Additionally, natural cytotoxic peptides with anti-cancer properties are an attractive warhead due to their ability to navigate across the cell membrane, in contrast to proteins which require CPP modification, and hence are less likely to suffer from endosome entrapment. Furthermore, they possess structural complexity, like proteins and because of this they are highly selective towards their intended biological target and can initiate complex metabolic processes like proteins. Accordingly, there is significant interest in producing synthetic peptides (*e.g.* CPPs and natural cytotoxic peptides) for therapeutic research. However, peptides are susceptible to degradation *via* protease mediated hydrolysis, and therefore reducing their half-life. Despite shortcomings such as this, there are methods that can be implemented to improve a peptides enzyme resistance. The substitution for D-amino acids, peptide cyclisation and PEGylation, among others were found improve peptide stability towards proteases.

Molecular Cloning

CPPs can be generated together with a protein *in situ* by exploiting techniques such as molecular cloning. For instance, pre-existing genes encoding the protein of interest can be added with a CPP at any desired position. This route of producing CPPs can be easy to enforce due to the use of well characterised gene expression systems (*e.g. E. coli*) allowing for easy protein biosynthesis. However, producing CPP fusion proteins can be low yielding due to issues related to bacterial cytotoxicity.[160] Furthermore, the addition of a CPP to a protein structure can adversely affect its function through structural alterations.

Solid Phase Peptide Synthesis

In synthetic organic chemistry, there is a well-established protocol used for generating amide bonds between amino acids *via* condensation reactions known as solid phase peptide synthesis (SPPS).[161] Despite using increased molar excesses of reagents and generating large quantities of waste material, SPPS is a convenient method that can be easily utilised for the generation of linear sequences. In addition to this, large and complex peptides can be rapidly synthesised using this technique. Chemical synthesis of peptides takes place from the *C*-terminus to the *N*-terminal amino acid.

Initially, a similar technique was employed for creating short polymers in solution phase, known as liquid-phase peptide synthesis.[162] Despite the ability to produce short polymers, liquid phase peptide synthesis is restricted to the construction of small and linear peptides. This required multiple demanding work-ups and purification steps, consequently resulting in less than desirable yield.[163] Therefore, this method is not suitable for building long and complex sequences[164] (**Table 2**).[165]

Table 1. Effects of accumulated errors on final product yields

No. of reactions		Yield of each reaction (%)			
		100	**99**	**95**	**90**
10	Overall yields	100	90	60	35
20		100	81	36	12
30		100	74	21	4
40		100	67	13	1
50		100	61	8	< 1

Table 2 - Illustration of how achieving less than 100% chemical efficiency during each step can affect overall target product purity.

Merrifield Peptide Synthesis

Pioneering work conducted by Bruce Merrifield saw the introduction of an insoluble solid support to peptide synthesis (**Figure 11**).[166–168] This mode of fabrication is known as solid phase peptide synthesis (SPPS) and provided an improved ability to grow a peptide using a solid resin, thus helping to minimise loss during each reaction step. Additionally, the premise of an orthogonal protecting system was introduced to amino acids that carry more than two reactive moieties. These groups are subsequently deprotected using different independent chemical mechanisms. The insoluble solid support resembles tiny beads which are made from plastic such as polystyrene and are used due their tolerance towards SPPS conditions. Moreover, the resin helps to expedite the separation of excess solvents and solution phase reagents from materials bound to the resin, and therefore facilitating product purity.

To couple the first amino acid to the resin, there is a chemical motif exploited as a linker. For example, (chloromethyl)polystyrene beads used in Merrifield SPPS utilises a chloromethyl handle that can attach the primary amino acid by alkylating its

corresponding carboxy group (**Figure 11**).[166] To aid the linkage of amino acid to resin, reactive groups such as the α-amine must be protected. Reactivity masking groups such as tertiary butoxy (^{t}Boc) esters have been successfully used in Merrifield SPPS for this purpose to prevent reactive interference, and hence allow only the carboxy group to be exposed for connection to the solid support (**Figure 11**). For trifunctional amino acids containing reactive side chains, masking reactivity is acquired by employing benzyl-based protecting groups[169,170] The carboxy group can be activated by using a non-nucleophilic bulky amine such as triethyl amine for deprotonation (**Figure 11**). This increases the nucleophilicity of the carboxylate motif of the incoming amino acid and resulting in an S_N2 substitution leading to the dissociation of the chloride anion, and alkylation of the first carboxy group.[166] After securing the first amino acid to the solid support, a peptide can be developed by following an autonomous regime of ^{t}Boc deprotection and peptide bond formation (**Figure 11**). To successfully remove the ^{t}Boc ester from α-amine, application of neat trifluoroacetic acid (TFA) can be used, at the same time, leaving benzyl-based protecting groups attached to reactive side chains undeterred.[169,170] Once the ^{t}Boc protecting group is removed, the primary amine is exposed and ready for generating peptide bonds with a second incoming ^{t}Boc protected amino acid. The carboxy group of the second amino acid is converted into an active ester by using a combination of reagents including a tertiary amine (*e.g* triethyl amine) and dicyclohexylcarbodiimide (DCC). Deprotonation of the amino acid carboxy group facilitates active ester formation with DCC and following activation, a peptide bond can be formed between amino acids on resin (**Figure 11**). This process of deprotection and coupling can be repeated until the desired full-length peptide sequence is developed on resin.

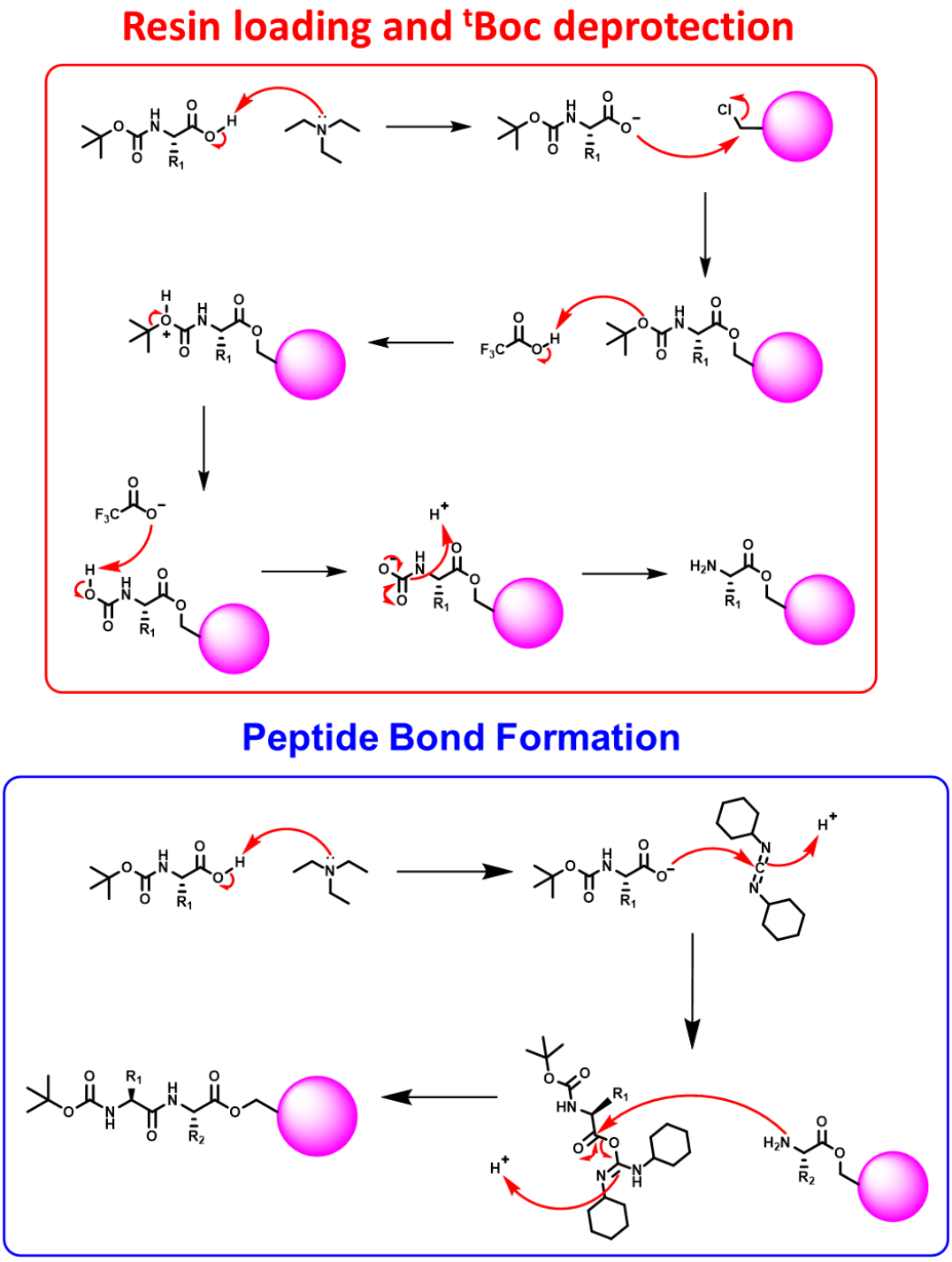

Figure 10 - The chemical mechanisms behind resin loading, tBoc deprotection and peptide bond formation via activated ester.

The final stage of Merrifield SPPS is the complete cleavage of the peptide from solid support and, simultaneous deprotection of benzyl-based protecting groups from reactive side chains. Anhydrous hydrofluoric acid (HF) is used for successfully disconnecting the peptide from all attachments. This synthetic method has been used with great success for producing synthetic peptides[171] and retains utility for assembly of peptides with base sensitive segments such as depsipeptides and minimising peptide aggregation.[172] However, there are dwindling numbers of practitioners and newcomers exploiting this method due the use of highly toxic HF in expensive specialised equipment lined with polytetrafluoroethylene.[170]

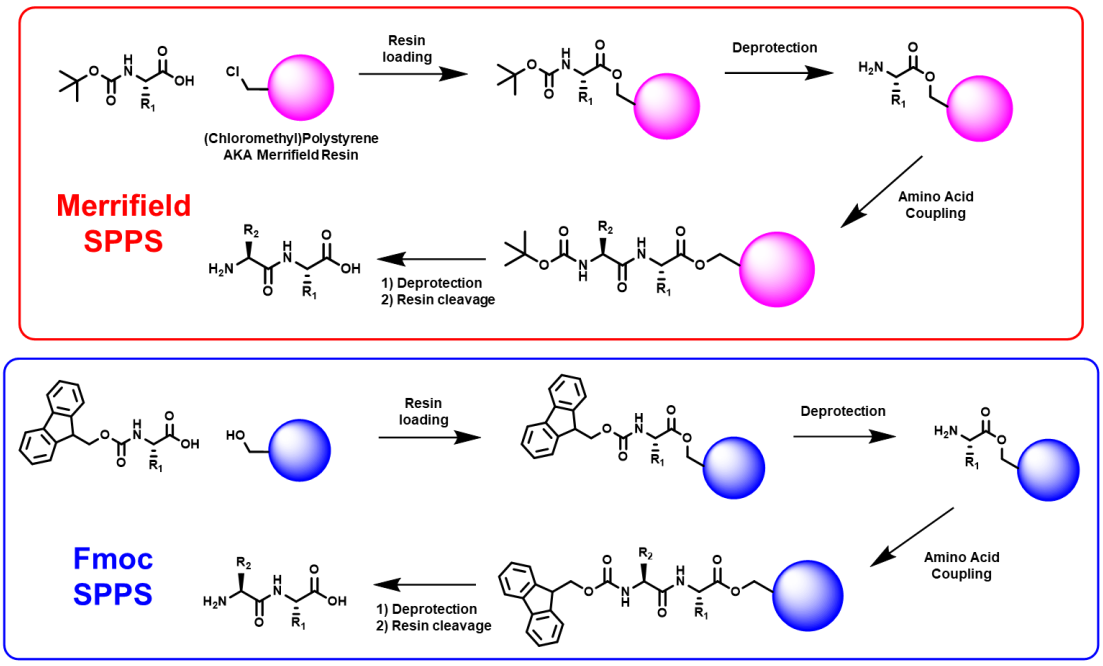

Figure 10 - Outline of Merrifield SPPS procedure compared to Fmoc SPPS protocol.

In addition to the expense of using HF, it is also problematic to handle and dispose. Merrifield SPPS also falls short due to the use of (chloromethyl)polystyrene as a resin. For the synthesis of long peptide sequences, it was found to be unsuitable because of inconsequential acid stability of the benzyl-ester linkage anchoring the peptide to resin. Low acid stability of this resin would result in unwanted side reactions.[170]

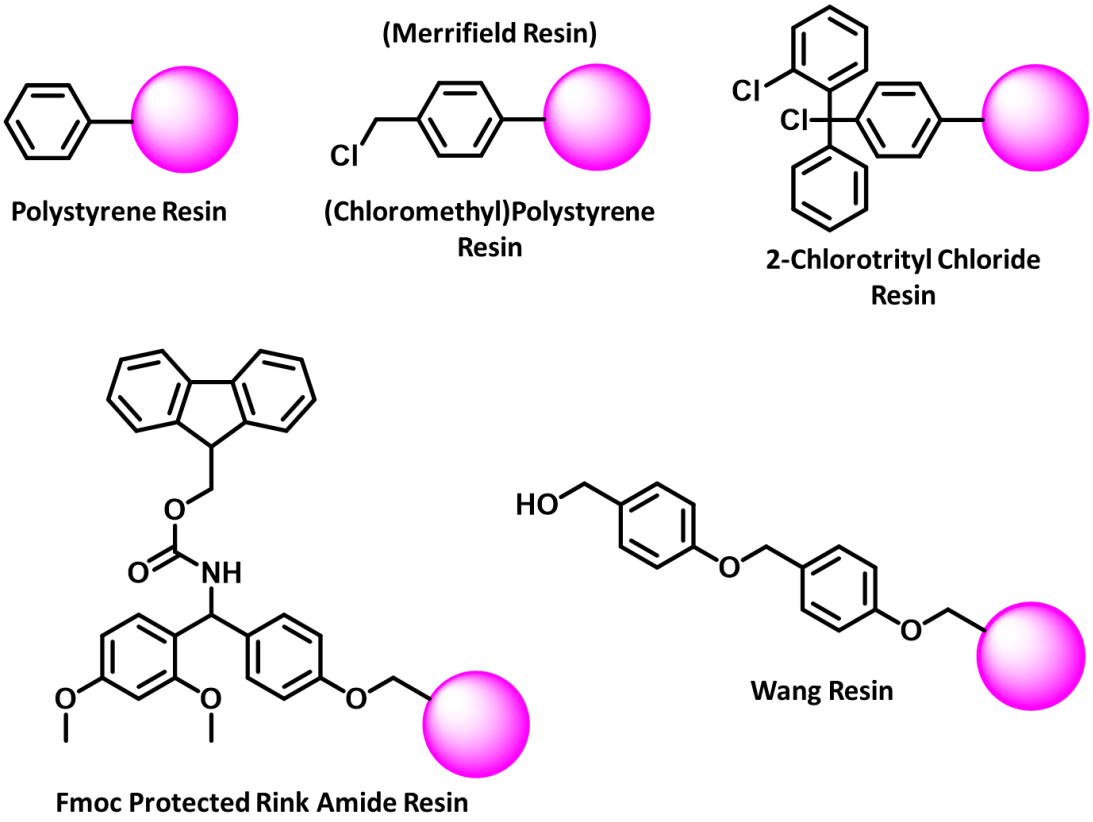

Figure 11 - Structure of Polystyrene, (chloromethyl)polystyrene and commonly used SPPS resins.

Alternative Resins to Merrifield Method

Alternative resins that have been implemented include Rink amide and Wang resins (**Figure 12 and Figure 13**) which have both demonstrated utility as acid tolerant supports, both better suited for making long sequences. However, following synthesis of a peptide using Rink amide resin, cleavage will result in a *C*-terminal amide, rather than a *C*-terminal carboxy group (**Figure 12**). This is because the chemical motif exploited as a handle for securing the initial amino acid is a secondary amine, situated between a pair of π-rings which help stabilise a secondary carbocation *via* resonance following peptide cleavage (**Figure 14**). The secondary amine acts as a Lewis base performing nucleophilic attack on an activated ester of an incoming amino acid, resulting in the formation of a peptide bond.

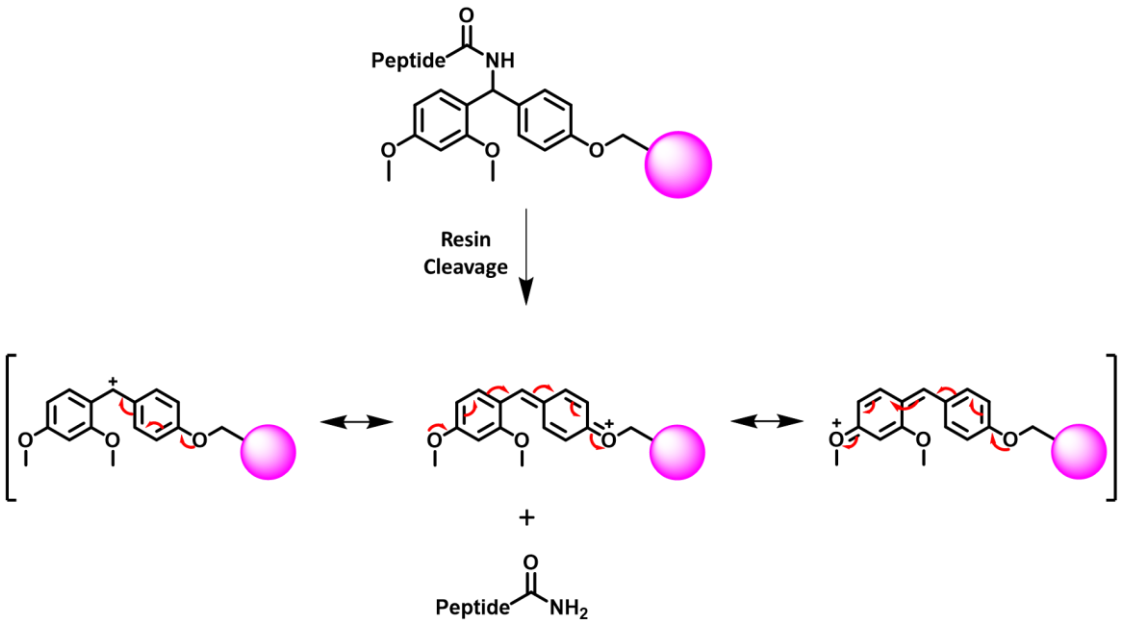

Figure 12 - Resonance stabilisation of secondary carbocation following cleavage of peptide from Rink amide resin.

Deprotection from either resin requires TFA to help liberate the target peptide from its support and this process can take a minimum of 2 – 3 hours for completion. In the presence of reactive side chains and their protecting groups, TFA can be supplemented with scavenger molecules to prevent unwanted re-attachments or side reactions. There are other solid supports known as hyperacid labile supports. An example of this type of resin is 2-chlorotrityl chloride (**Figure 13**) which can be separated from a peptide by using low percentage volume TFA (1 – 50%) in organic solvent such as dichloromethane. Alternatively, neat TFA with appropriate scavengers can be used to decrease deprotection time required to obtain a synthetic peptide. This can be done as quickly as 10 minutes; however, this depends on the type of sequence being developed. For instance, hyperacid labile protecting groups such as methyl trityl and trityl (**Figure 14**), which are used for masking lysine and cysteine side chain reactivity, cannot be selectively removed without also detaching a peptide from resin. This is due to the similar hyperacid sensitivity of both protecting groups and resin. Therefore, for this type of application Rink amide and Wang resins are more appropriate supports.

Alternatives Side Chain Protecting Groups to Merrifield Method

Similarly, the type of side chain protecting group has changed from benzyl-based variety. Merrifield SPPS used a ^{t}Boc deprotection regime applying TFA to expose the α-amine, whilst preserving benzyl-based protecting groups and attachment to the resin. Furthermore, solid support cleavage protocol employing anhydrous HF was used to separate benzyl-based protecting groups, at the same time as separating peptide from resin. There is now more focus on using side chain masking groups that can be removed without HF, but instead can be discharged by using more acidic chemicals such as TFA that also function to release peptide from resin and, provide a milder chemical route for producing peptides. For example, side chain protecting groups containing a 3^{o} carbon such as trityl, tertiary butyl (^{t}Bu) and ^{t}Boc (**Figure 14**) can be employed due to their ability to release a tertiary carbocation stabilised *via* hyperconjugation, upon treatment with TFA. There are other examples of TFA labile protecting groups that do not contain a tertiary carbon, but instead possess a sulphate group that can also be liberated *via* TFA.

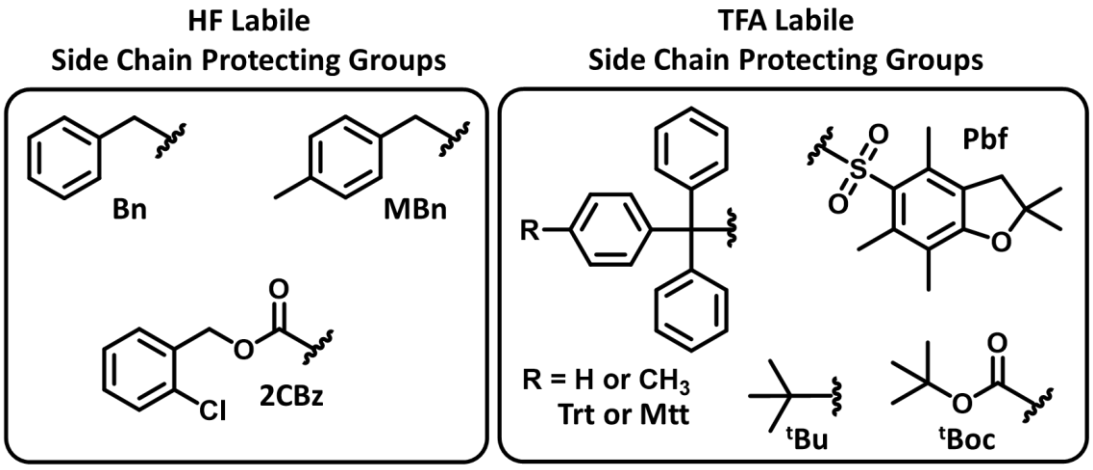

Figure 14 - Examples of side chain protecting groups cleaved using HF, and TFA labile reactivity masking groups.

Fmoc Peptide Synthesis

Further SPPS developments have moved towards milder protocols for α-amine deprotection. For instance, ^{t}Boc esters were swapped for tertiary butyl (^{t}Bu) groups due to their higher acid sensitivity meaning that lower percentage volumes of TFA (1%) were required for removal. However, despite protocol alterations a possibility for accidental side chain deprotection might occur during acid reliant ^{t}Bu excision. This may result in a rise of unwanted side products that can be prominent for long peptide synthesis. As a substitute, the α-amine can be temporarily shielded with a fluoronylmethyloxycarbonyl (Fmoc) group that can be selectively removed using bases such as piperidine. This is advantageous for SPPS because removal of base labile Fmoc will not harm the fortification of reactive side chains and, likewise selective removal of acid sensitive side chain protecting groups will not affect α-amine safeguarding provided by Fmoc. Therefore, this mode of protecting group orthogonality can further prevent unwanted side reactions occurring, and thus contribute increased focus towards synthesis of a target peptide.

2.1.3 Sold Phase Peptide Synthesis of Modified Pterin Tags

Synthesis of folate and pteroate labelled peptides began on a 2-chlorotrityl chloride resin (**Scheme 2** and **Figure 13**). Fluorenylmethyloxy carbonyl protected glycine (Fmoc-Gly-OH, *Step 1* in **Scheme 2**) was the first amino acid used to coat the resin. Initial reaction was given 3 hours and a mixture of dichloromethane : methanol : diisopropylethylamine (DCM : MeOH : DIPEA) was used to quench remaining unreacted sites on the resin. A cycle of Fmoc deprotection accompanied by subsequent amino acid coupling (**Scheme 2 –** *Step 2*) followed completing the inceptive PEG_9 capped five amino acid chain (*i.e.* linker peptide).

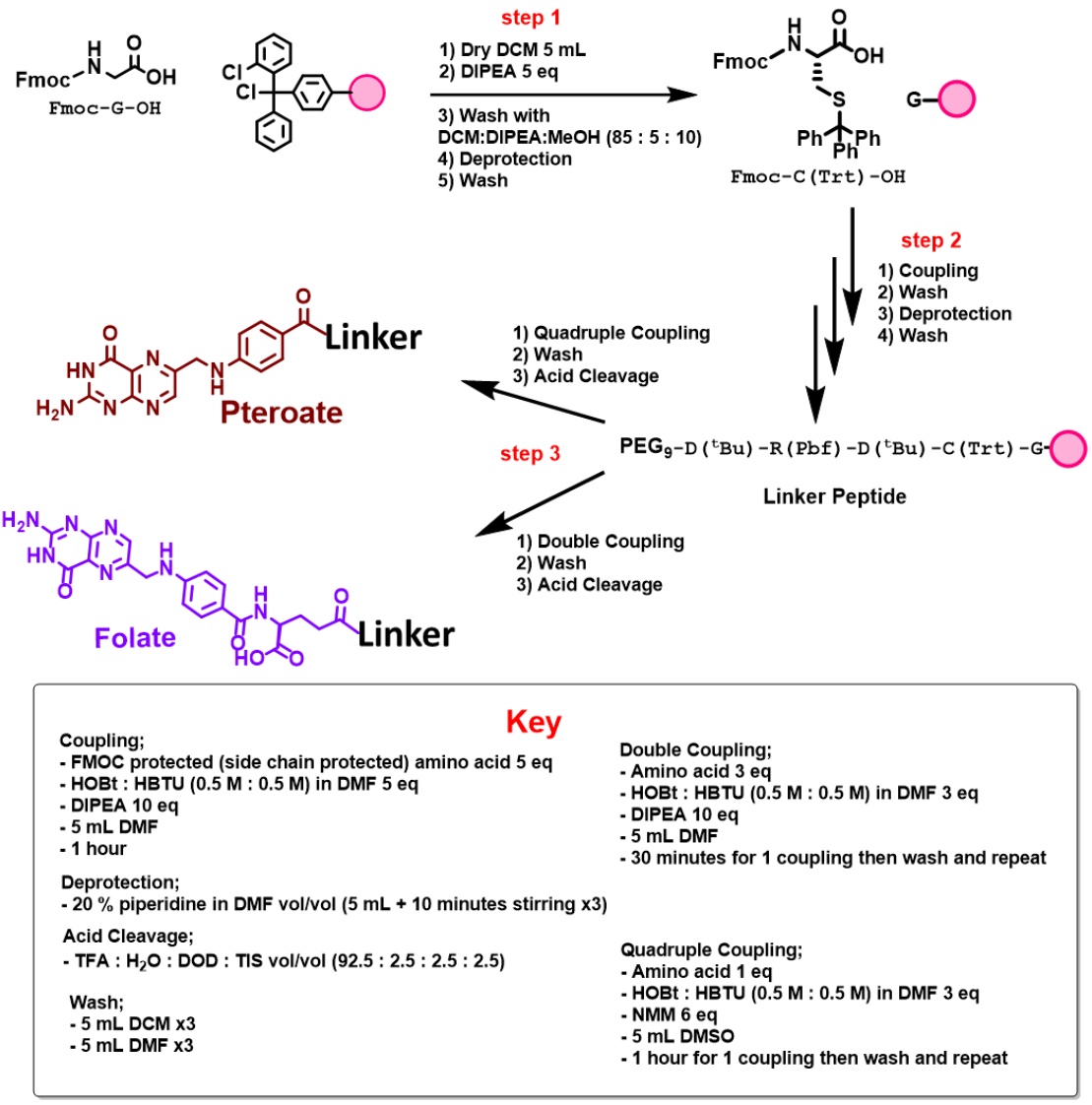

Scheme 2 - Fmoc SPPS scheme showing reactions encapsulating the synthetic route followed for Folate tagged peptide A and pteroate tagged peptide B (Scheme 1).

Peptide coated resin (**Scheme 2** – *Step* 3) was split into half for production of two peptide sequences (*i.e.* folate- and pteroate-labelled). Pteroic acid coupling was challenging due to inherent low solubility, therefore, quadruple coupling protocol was developed applying *N*-methyl morpholine (NMM) as base and dimethyl sulfoxide (DMSO) as solvent for synthesis.[173] The four successive cycles of pteroic acid coupling was performed using small quantities (*e.g.* ≤ 1 eq). This was due to its low organic solvent solubility causing issues such as reaction vessel blockage, and because of this, incomplete peptide bond formation. Small mass quantities did not cause reaction vessel blockages, and therefore, were easier wash off resin. In addition to this, four peptide coupling cycles was found to successfully saturate all *N*-terminal α-amines. Addition of folic acid was comparatively straightforward due to the presence of the glutamate tail improving its organic solvent solubility; hence, folate was double coupled using a mixture of HOBt : HBTU in DMF with an excess of DIPEA as base and DMSO as solvent**.** Both resins were subjected to acid deprotection using 92.5% trifluoroacetic acid (TFA) and scavengers (3,6-dioxa-1,8-octanedithiol, water and triisopropyl silane **Scheme 2** – *Step 3*) total 7.5% $^{V}/_{V}$ removing solid resin and amino acid side chain protecting groups. A solution containing peptide was diluted with cold diethyl ether to aid precipitation yielding crude pellets. Liquid chromatography mass spectrometry (LC/MS) had revealed contaminations present in both pellets and, consequently, both required isolation. Method of seperation used was high performance liquid chromatography (HPLC). Solvent systems utilised in isolation of both peptides were acetonitrile and 10 mM ammonium bicarbonate (pH 8) and the gradient used was 1 – 60% acetonitrile in 60 minutes. Folate-labelled peptide eluted with a retention time of 20 minutes from HPLC and its corresponding fraction was analysed *via* LC/MS. Two peaks belonging to folate-labelled peptide was identified. The observed mass to charge ratios were 1133.70 $[M+H]^+$ and 567.29 $[M+2H]^{2+}$ (**Figure 16**) and these values matched the calculated $[M+H]^+$ and $[M+2H]^{2+}$ (1133.12 and 567.56 respectively). The peptide coupling reagents used here could not discriminate the carboxyl groups of the glutamate group and, hence, two structural isomers were obtained.[156] However, peptide coupling to γ- or α-carboxyl group makes no difference for binding to FR-α.[156] Pteroate-labelled peptide had eluted with a retention time of 25 minutes during HPLC isolation and the corresponding fraction was analysed using LC/MS. Mass to charge ratios observed were 1004.59 $[M+H]^+$ and 502.73 $[M+2H]^{2+}$ (**Figure 17**) and these values matched the calculated $[M+H]^+$ and $[M+2H]^{2+}$ (1004 and 503 respectively).

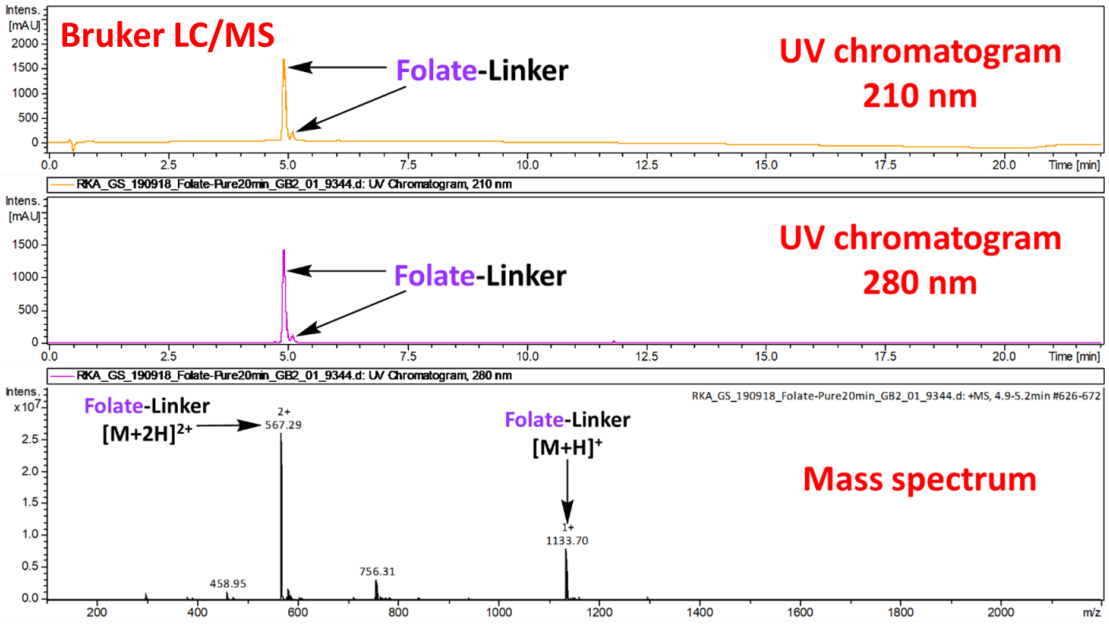

MS Method = Electrospray Ionisation

Gradient

1 – 97% CH_3CN in 30 minutes

Solvent Systems

dH_2O (+ 0.1% $^{V}/_{V}$ formate)

CH_3CN (+ 0.1% $^{V}/_{V}$ formate)

Flow Rate = 500 µL min^{-1}

Injection Volume = 5 µL

C_{18} Column

Figure 13 - Chromatographic data and mass spectrum corresponding to folate labelled peptide.

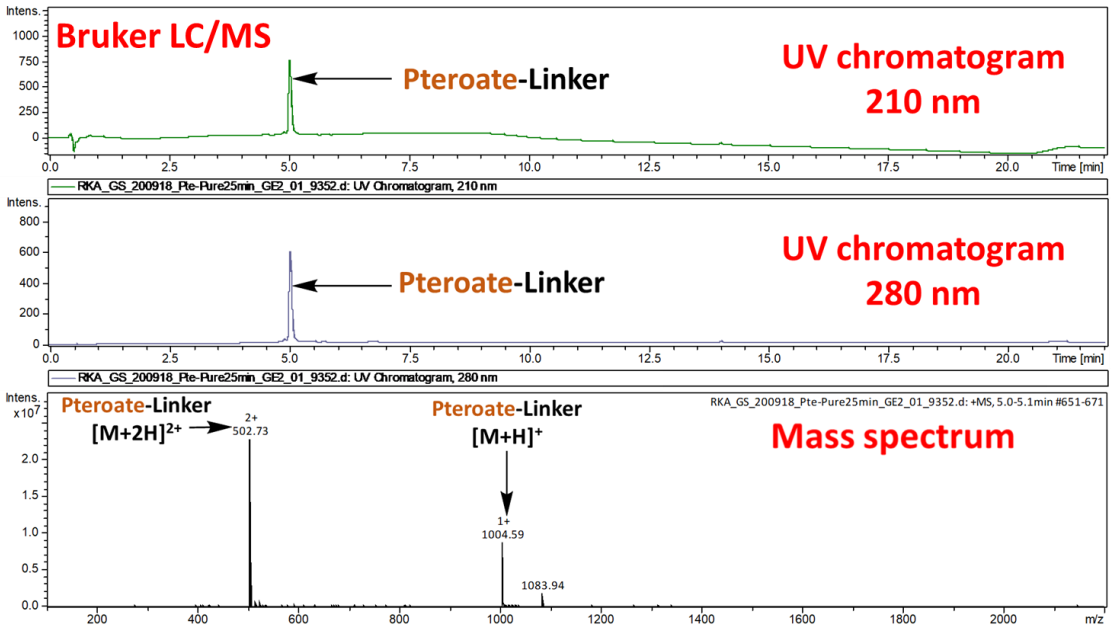

MS Method = Electrospray Ionisation

Gradient

1 – 97% CH_3CN in 30 minutes

Solvent Systems

dH_2O (+ 0.1% $^{V}/_{V}$ formate)

CH_3CN (+ 0.1% $^{V}/_{V}$ formate)

Flow Rate = 500 µL min^{-1}

Injection Volume = 10 µL

C_{18} Column

Figure 14 - Chromatographic data and mass spectrum corresponding to pteroate labelled peptide.

2.1.4 Production of Modified Green Fluorescent Proteins

Three sfGFP constructs were produced, two conjugates were made including folate and pteroate peptides (**Scheme 1** – **A** and **B**). The fluorescence of GFP is derived from the formation of its chromophore. This is through a series of reactions involving cyclisation, dehydration and oxidation of a tripeptide sequence (**Figure 17** – `SYG`). The gene of sfGFP was inserted into a *pET-28a* vector for gene expression. *E. coli* strain BL21(DE3) containing the target gene was selectively cultured using lysogeny broth (LB) media that contained kanamycin sulphate (50 mg L^{-1}) and *gfp* expression was induced *via* IPTG (120 mg L^{-1}). The harvested cells were subjected to sonication and centrifugation providing a supernatant containing sfGFP that was treated with excess iodoacetamide for 3 hours. This was to cap solvent exposed cysteine preventing sfGFP dimerization which occurs due to the absence of reducing agents in buffer solution, and thus can be used in cell tests to demonstrate the importance for folate labelled modification to access FR-α. After incubation, supernatant containing sfGFP, containing a his_6-tag was injected onto an affinity column containing nickel nitrilotriacetic acid (Ni^{2+} NTA) to remove host proteins from *E. coli*. Upon concentration by use of a spin column, sfGFP was collected and then injected onto a BioRad Next Generation Chromatography system connected to a HiLoad 26/600 superdex 75 pg (Cytiva) size exclusion column (cross-linked agarose and dextran, 8.6 µm bead size) for isolation using an isocratic gradient. The buffer solution applied for this FPLC isolation was phosphate buffered saline (pH 7.4). Fractions corresponding to acetamide capped sfGFP were collected and analysed by high resolution mass spectrometry. Mass to charge expected for this species was 26,963.0 $^{M}/_{Z}$ and the mass to charge observed was 26962.5 $^{M}/_{Z}$ (**Figure 18**).

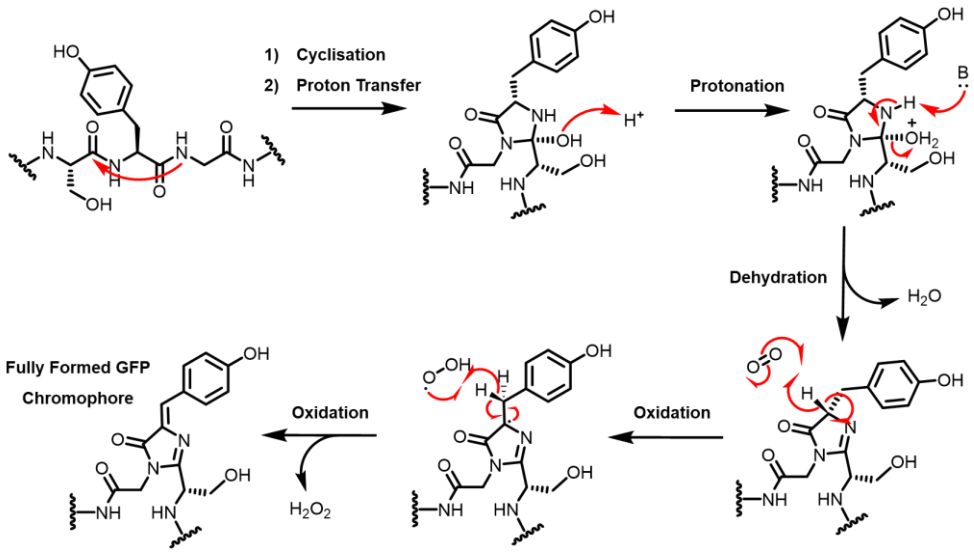

Figure 17 – Chemical mechanism of GFP chromophore formation.

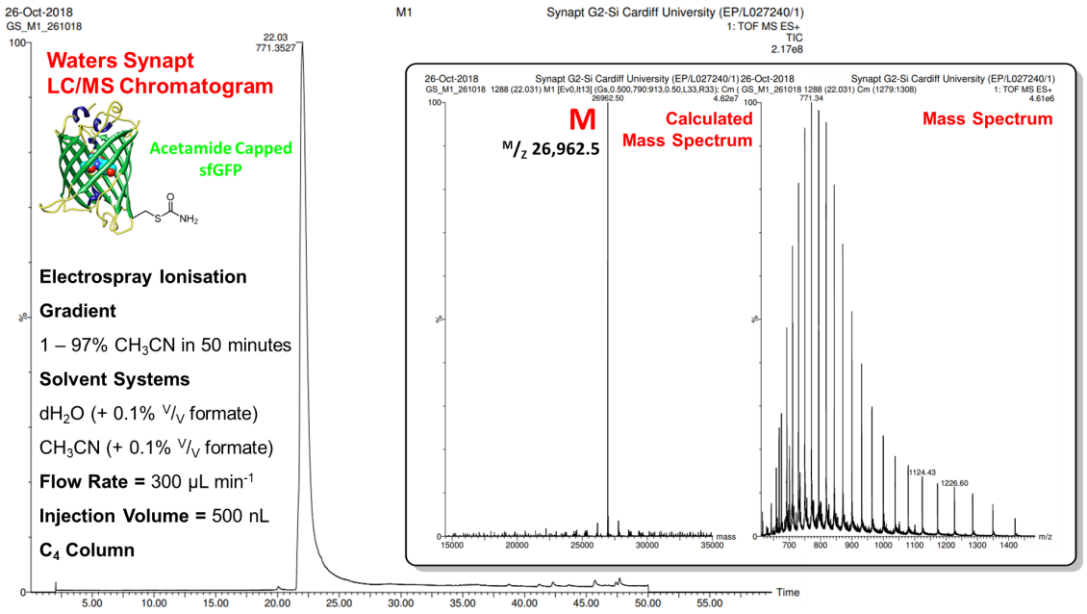

Figure 18 - Acetamide capped sfGFP chromatogram (top) and corresponding mass spectrum (bottom).

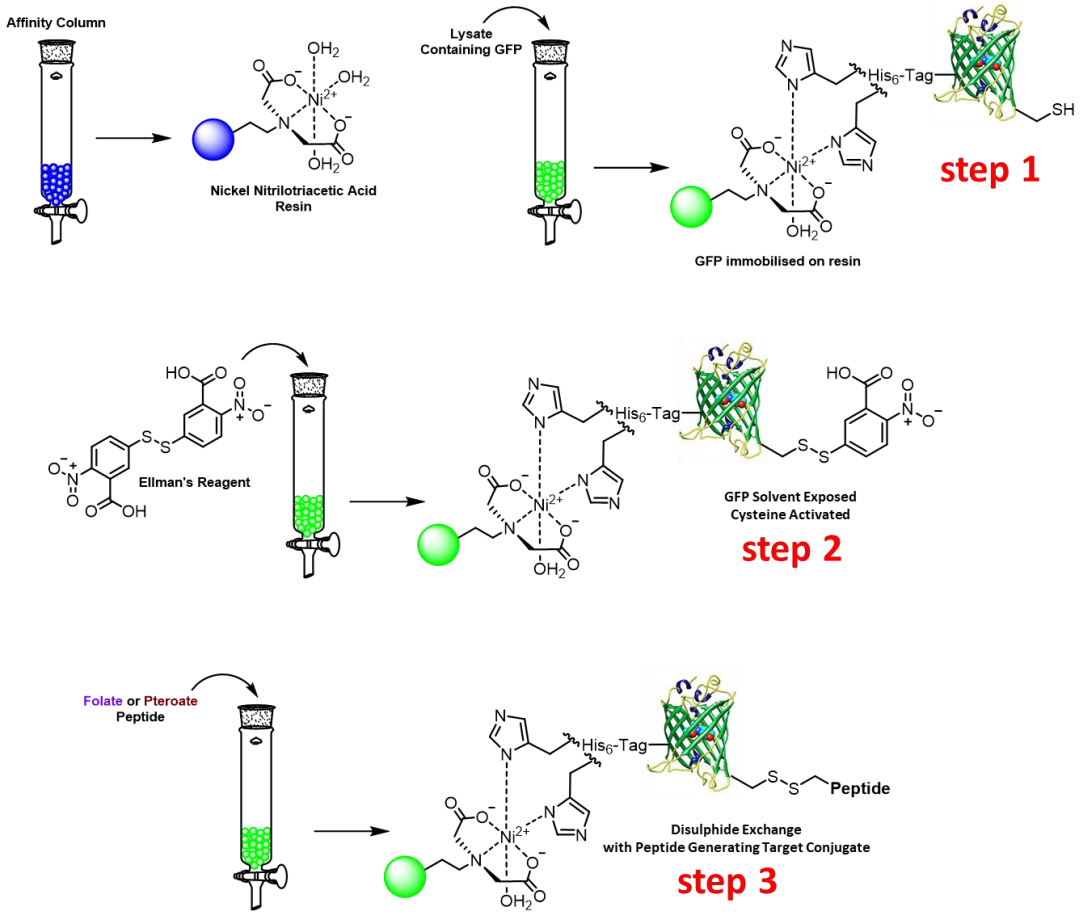

Scheme 3 - Site selective chemical modification of sfGFP via immobilisation on nickel resin.

Folate labelled peptide (**Scheme 1** – Peptide A) was conjugated with sfGFP *via* the same affinity column, but this time using Ellman's reagent for thiol activation on resin (**Scheme 3**). The collected eluent was injected on size exclusion column for three individual runs separating sfGFP dimer from modified sfGFP construct. This was done due to the poor separation between the monomeric target sfGFP conjugate and the sfGFP dimer. A sample was analysed by high resolution mass spectrometry and mass to charge expected for this species was 28,037.0 $^{M}/_{Z}$. Mass to charge observed was 28,036.0 $^{M}/_{Z}$ (**Figure 19**). Pteroate labelled peptide (**Scheme 1** – Peptide B) was conjugated to sfGFP using the same conjugation method (**Scheme 3**) and analysed by high resolution mass spectrometry, however, a β-mercaptoethanol adduct was found to co-elute. The column used for targeting His_6 tagged protein was cleaned with 20% β-mercaptoethanol ($^{V}/_{V}$) before isolation. Consequently, β-mercaptoethanol was present on the column comprised of Ni^{2+} NTA resin during the conjugation procedure. Nonetheless, mass to charge expected for this species was 27,906.0 $^{M}/_{Z}$ and the mass to charge observed was 27,905.0 $^{M}/_{Z}$ (**Figure 20**). Despite the minor contamination of the β-mercaptoethanol adduct, this sample was used for cell culture studies due to the majority species being the target conjugate.

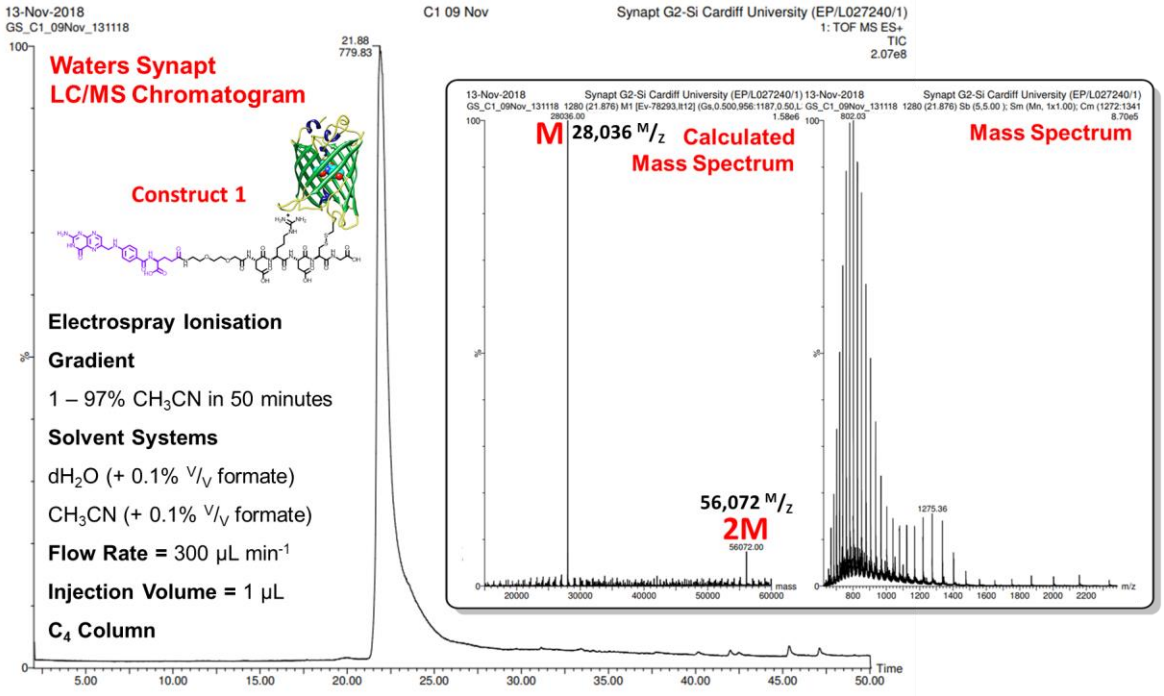

Figure 19 - Folate labelled sfGFP construct chromatogram and corresponding mass spectrum.

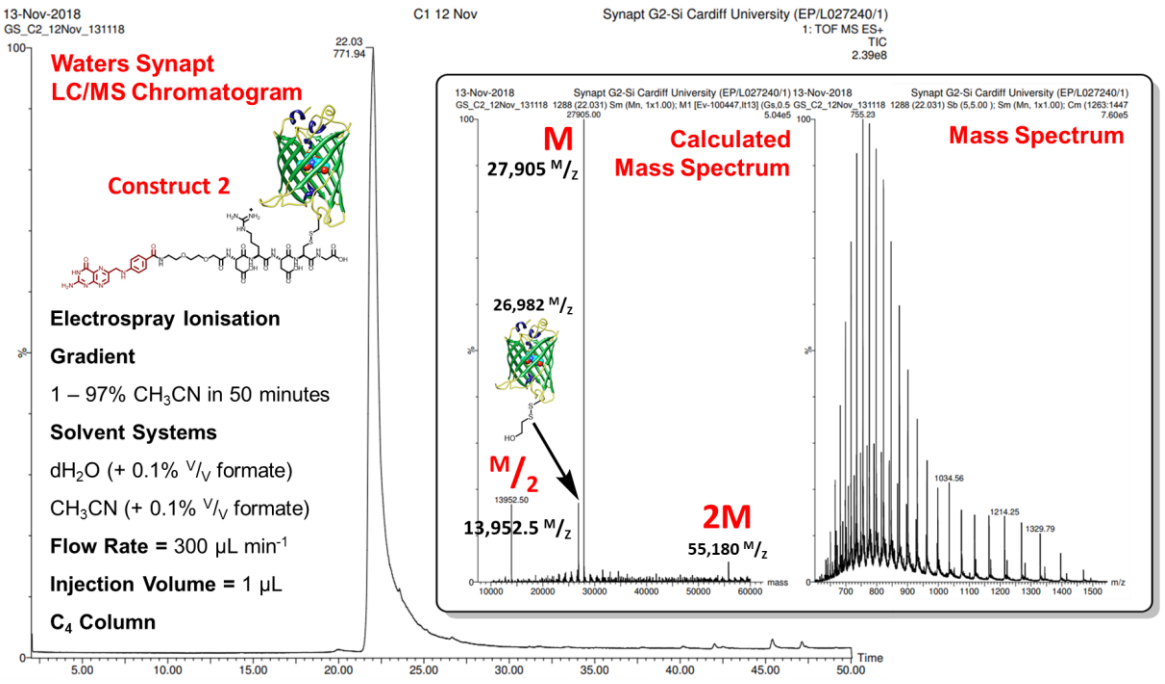

Figure 20 - Pteroate labelled sfGFP construct chromatogram and corresponding mass spectrum.

2.1.5 Summary of Modified sfGFPs

Constructs based on sfGFP containing folate and Pteroate labels through a disulphide bridge between a short PEG_9-peptide and solvent exposed cysteine (**Scheme 4 - constructs 1 and 2)** were established. These conjugates were assembled to investigate the uptake of protein by malignancies overexpressing the *folr1* gene. A control that does not possess a pterin label (**acetamide capped sfGFP Scheme 4**) was also generated to demonstrate the role of folate to initiate cellular uptake *via* FR-α. In the absence of folate moiety, sfGFP is anticipated to be unresponsive towards cells comprised of FR-α, while the constructs containing folate and pteroate are expected to interact with FR-α. The difference between folate and pteroate labelled sfGFP should reveal the importance of the glutamate tail in the binding of folate to FR-α which is known to alter the affinity.

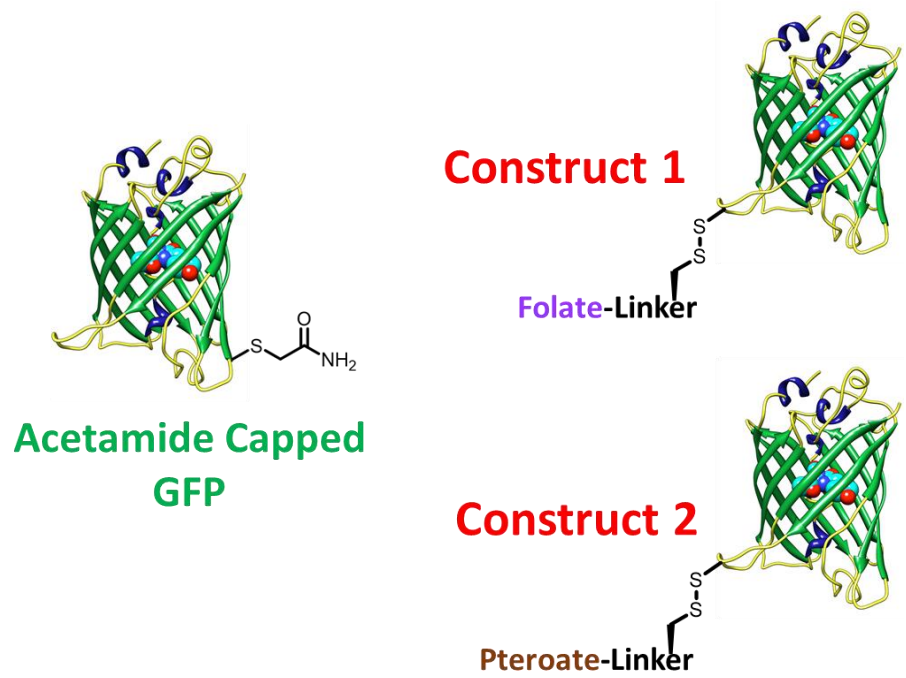

Scheme 4 - Structures of sfGFP conjugates.

2.1.6 Mammalian Cell Culture Experiments

Each sfGFP construct was first examined for uptake within the KB cell line which overproduces FR-α[174] by fluorescence activated cell sorting (FACS). KB cells are derived from epithelial cervical cancer cells that utilise human papilloma virus-18 E6 and E7 proteins for inhibition of tumour suppressor proteins to allow for indefinite cell growth. This technique was used to measure a cells fluorescence intensity after

sorting into droplets, but cannot identify where a fluorescent macromolecule is located within a cell (*e.g.* cell membrane, cytosol or endosome). Despite this limitation, FACS could identify constructs that bind best to FR-α by fluorescence intensity.

Fluorescence Activated Cell Sorting

Cell Uptake Assessment

FACS experiments were performed for folate labelled, pteroate labelled and acetamide capped sfGFP constructs (**Scheme 4**) in the presence and absence of free folic acid. Two cell lines were chosen; FR-α overproducing KB cancer cells and non-cancerous HEK293, which are FR-α negative.[175,176] The number of FR-α can be determined from the KB cells by techniques such as Western Blot. However, due to the absence of FR-α in HEK293 cells and vast overexpression in KB cells this is not necessary. This is due to the purpose of this study which was to demonstrate improved cell target specificity of GFP. The KB cells were maintained in folic acid depleted RPMI media supplemented with 10% ($^{V}/_{V}$) fetal bovine serum (FBS) at 37°C in a 5 % CO_2/95% air humidified incubator. HEK293 cells were grown in the same way but instead with DMEM media containing glutamax supplement with 10% ($^{V}/_{V}$) FBS. KB cells and HEK293 cells were grown to confluency (1.0 x 10^6 cells) and suspended in 5 mL of folic acid depleted RPMI media without FBS. From the suspensions, 500 µL was plated into 24 well-plates at a concentration of 2.0 x 10^5 cells mL^{-1}. These cells were placed into a humidified incubator at 37°C in a 5% CO_2/95% for 24 hours. Following overnight incubation, culture media was removed from the cells and media containing sfGFP constructs was introduced. Cells were incubated for one hour at 37°C in a 5% CO_2/95 % air in a humidified incubator for uptake. Four different concentrations of constructs 1 and 2 (**1 nM, 10 nM, 100 nM and 1 µM – Figure 21**) were applied to KB cells for direct comparison. It was found that both folate and pteroate labelled sfGFP treated KB cells displayed increased fluorescence (**Figure 21**) indicating uptake. At 1 nM the relative mean fluorescence intensity appears to be marginally higher for the folate labelled construct in comparison to the background fluorescence produced by KB cells that had not been treated with protein. With further addition of the folate construct at 10, 100 and 1000 nM, cellular fluorescence and uptake was significantly increased. For the same concentrations of pteroate labelled construct fluorescence was reduced in KB cells compared to the folate construct, although it was still above the background fluorescence of cells alone for all concentrations apart from at 1 nM. These results suggest folate labelling is better for cellular uptake compared to pteroate (*i.e* construct

1 > construct 2), possibly due to the higher affinity for FR-α.[177] This indicates that the glutamate tail of folate significantly enhances the binding interaction of the sfGFP constructs with FR-α, although it is not a critical requirement for binding; the pteroate moiety is essential for some affinity to the receptor. Together this clearly demonstrates that by labelling protein constructs with folate or pteroate uptake can be achieved in FR-α containing KB cells. Nanomolar concentrations were sufficient for uptake of sfGFP constructs due to the high affinity of folic acid for FR-α, meaning that this method is highly sensitive for introducing therapeutic polypeptides.[58,158,178]

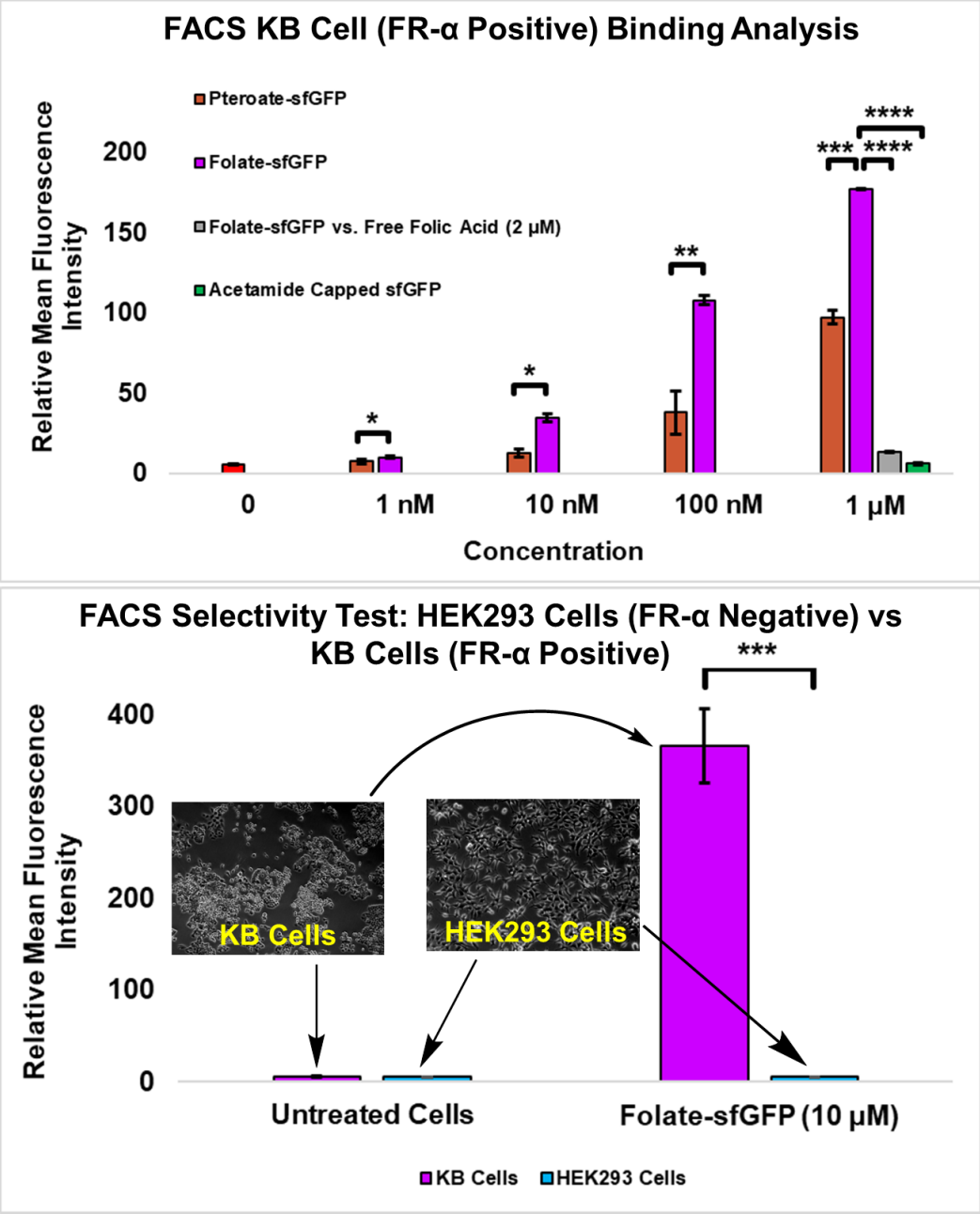

Figure 20 - sfGFP construct results on malignant KB cells and non-cancerous HEK293 cells from FACS.

Folic Acid Competitive Inhibition

Next construct 1 was subjected to folic acid competitive inhibition experiment on KB cells, as well as testing on HEK293 cells at 10 µM (**Figure 21**). This was to demonstrate that uptake of folate tagged sfGFP was directed by the folate moiety and dependent on free FR-α. Construct 1 was applied to KB cells at 1 µM concentration in the presence of RPMI media containing 2 µM folic acid. Free folic acid containing media inhibited most of the uptake of construct 1. Cellular fluorescence obtained was comparable to uptake experiments performed at 1 nM in the absence of folic acid suggesting a thousand-fold retardation in uptake due to competition for FR-α. Furthermore, folic acid inhibition provided a significant difference when compared to the fluorescence intensity generated by construct 1 in the absence of free folate, and thus suggesting the mechanism of uptake is *via* FR-α.

Additional Cell Uptake Assessment

Experiments performed on FR-α negative HEK293 cells[175] show that construct 1 was unable to initiate cellular interaction due to lack of fluorescence (bottom – **Figure 21**). This result was directly compared to construct 1 applied at the same concentration on KB cells and the difference in fluorescence was profound. The results from HEK293 were comparable to acetamide capped sfGFP treatment (10 µM) on KB cells which produced a similar result showing no cellular interaction. This demonstrates that by targeting FR-α uptake of sfGFP can be achieved. Therefore, a non-toxic large polypeptide like sfGFP can be swapped for a toxic polypeptide for selectively killing cancer cells. Large polypeptides are a potential candidate, however, issues associated with endosome escape coupled with diminishing efficacy due to late endosome degradation will require installation of cell penetrating peptides to help prevent this. On the other hand, small cytotoxic polypeptides can be exploited due to their superior ability to access the cells interior beyond the endosome.

Cell Titre Blue Cell Viability

Each of the sfGFP constructs were subjected to tests *via* cell titre blue cell viability experiments to verify toxicity towards malignant cells during a 24-hour incubation period. The cell titre blue cell viability assay utilises resozurin which is reduced by diaphorase enzymes into highly fluorescent resorufin.[179] This redox process is associated with the metabolic activity of cells and is indicative of cell viability. The cells used in these assays were KB cells and they were grown to confluency (1.3 x 10^5 cells mL^{-1}). The cell suspension was plated in triplicates at a volume of 100 µL into a 96 well plate and given 24 hours to attach to the wells. Following this, media was replaced with 100 µL of each control at 10 µM in culture media and provided with 24 hours to incubate. After the final incubation period, the plates were examined for cell viability using a Perkin Elmer Victor X5 multimode plate reader.

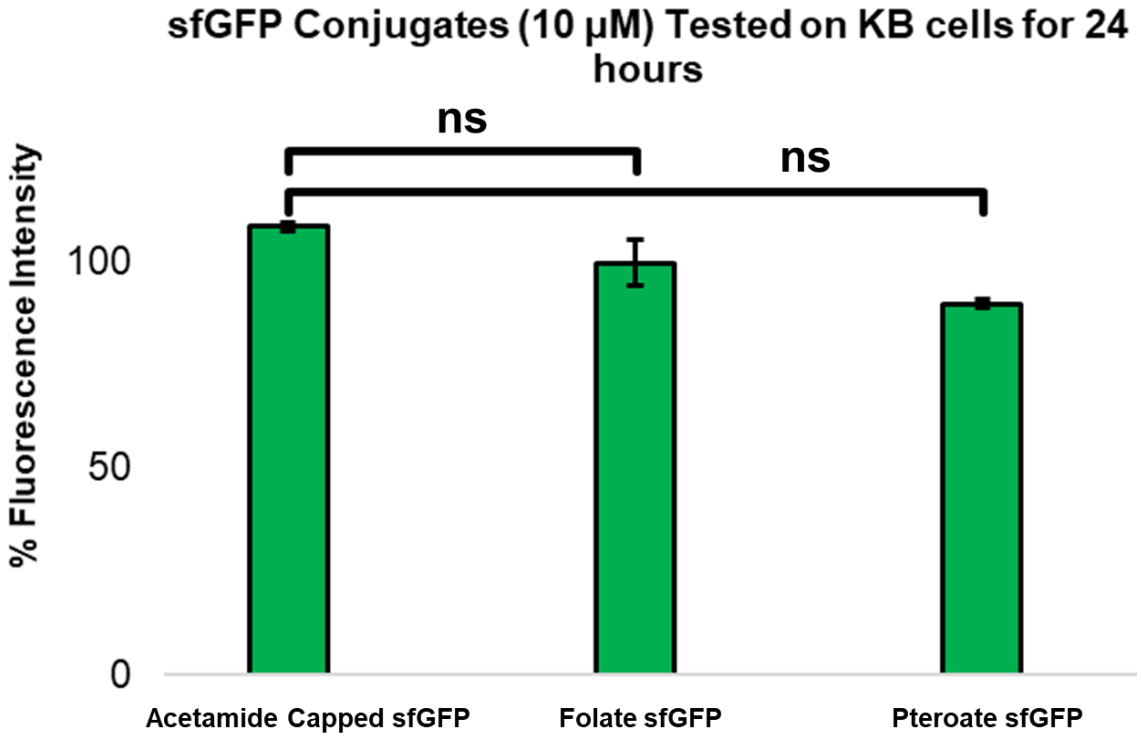

Figure 15 - KB cell viability after 24-hour incubation with sfGFP constructs.

It was found that each of sfGFP conjugates tested had demonstrated negligible effect on the viability of the malignant cells as suggested by the resorufin fluorescence recorded (**Figure 22**). Both pterin labelled proteins were found to have a non-significant difference in viability percentage when compared to acetamide capped sfGFP, which was shown to have no ability to interact with KB cells in prior experiments (**Figure 21**). This data combined with the FACS data indicate that the sfGFP controls behaved as planned.

Chapter 3: CPPs for Endosome Escape of Large Polypeptides

3.1 Introduction

In this chapter the goal was to develop a folic acid labelled CPP linked to GFP. Chapter two had shown that folate labelling of sfGFP provided characteristics such as binding to FR-α at low concentrations and cell specificity (**Figure 21**). The next step was to investigate the effect of swapping a non-CPP sequence (**Scheme 1** – DRDCG) for a CPP. Folate would provide cell targeting and was planned for coupling with a CPP for conjugation to GFP. This conjugate was destined for testing on KB cells and HEK293 cells to understand its ability to selectively access the cell cytosol through FR-α mediated endocytosis. Once established, GFP was going to be substituted for a cytotoxic protein and further experiments would follow to see if a protein-based conjugate would be capable of selectively killing cancer cells.

3.2 Cell Membrane

3.2.1 Composition

Through millions of years of evolution, eukaryotic organisms have developed cell membranes designed for protection, compartmentalisation, and selective uptake of essential nutrients.[180,181] Primarily made of phospholipids, these amphipathic films provide the strength and fluidity needed for survival.[180] Each phospholipid contains a hydrophilic phosphate head that attracts water and a hydrophobic fatty acid tail repelling water. Consequently, they form a membrane bilayer by pairing up tail to tail *via* hydrophobic interactions extending across the cell forming a barrier to external environments[180] (**Figure 23**). In combination with phospholipids are negatively charged membrane components such as glycolipids and glycoproteins.[182] The potential of the cell membrane is derived from the presence of chemical groups such as sulphates, carboxylates and phosphates giving the surface membrane a net negative charge.[183] Each constituent is in constant flux and is persistently moving. This allows for the exchange of materials from the intracellular space to the extracellular domain and *vice versa*[184] (fluid mosaic model[185] - **Figure 23**).

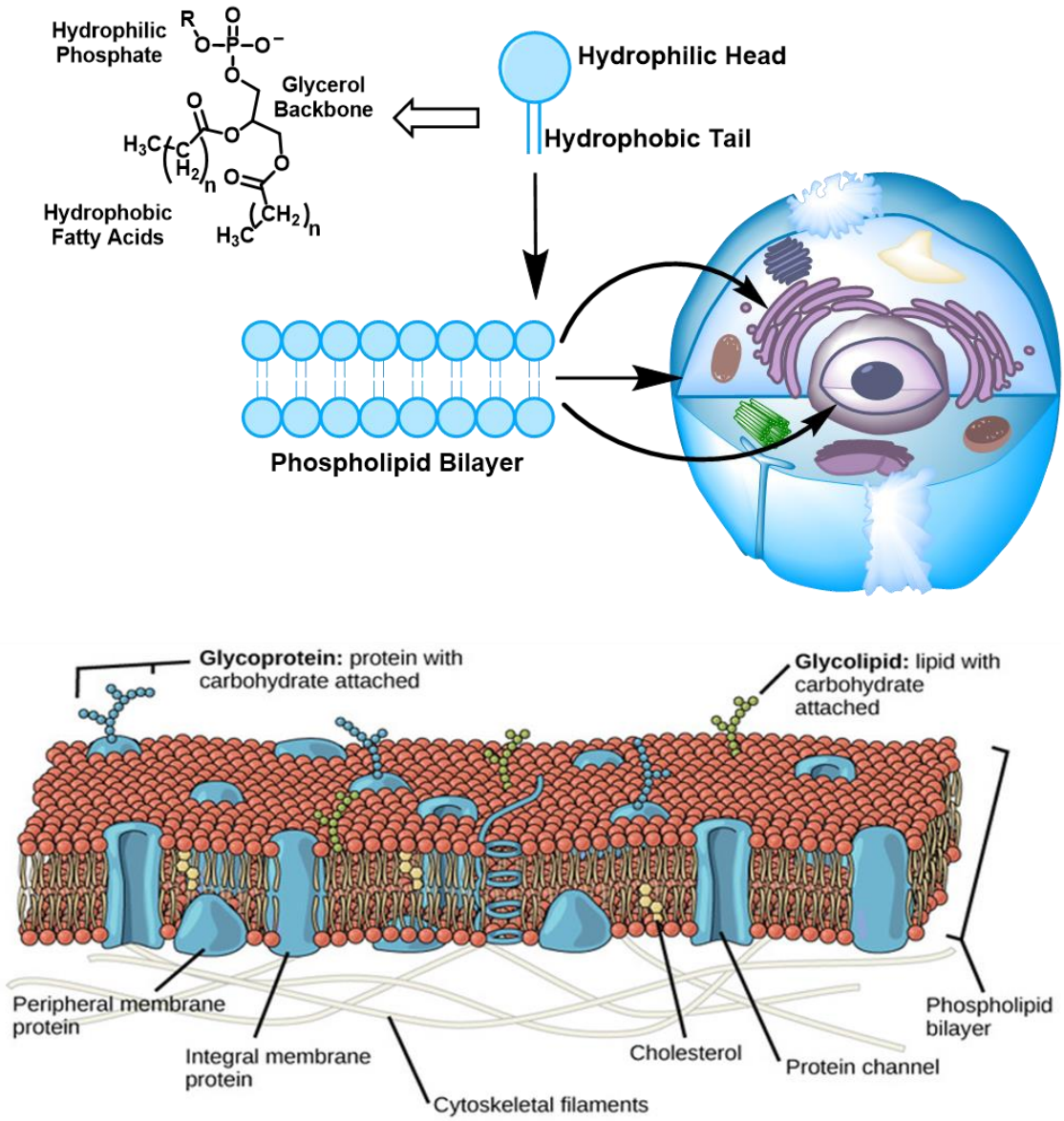

Figure 23 - Phospholipid bilayer (top) and fluid mosaic model[185] (bottom).

3.2.2 Cell Penetrating Peptide Mediated Uptake

The route of cellular internalisation taken by CPPs is governed by chemical composition which influences membrane interaction (**Figure 24**). This topic was visited in chapter one in further detail (please see 1.3.2 - CPP Chemical Properties and Membrane Interaction). Translocation mechanisms refer to the direct movement of CPPs from the extracellular milieu into the intracellular environment. This can be sub-categorised into multiple types of activity which have been discovered to occur at low temperature (4°C) in cell culture experiments, under which energy-dependent biomolecular processes are halted (**Figure 24 – direct penetration pathways**).[186] Hydrophobic sequences typically operate *via* this mode of transport. This is supported by studies utilising cationic oligoarginines and increasing its hydrophobicity using pyrenebutyrate as a hydrophobic and anionic counterion. Research suggests that upon decreasing hydrophilicity of oligoarginines direct translocation is promoted.[187] Lipophilic side chains interact with non-polar sections of the membrane initiating processes such as inverted micelle formation.

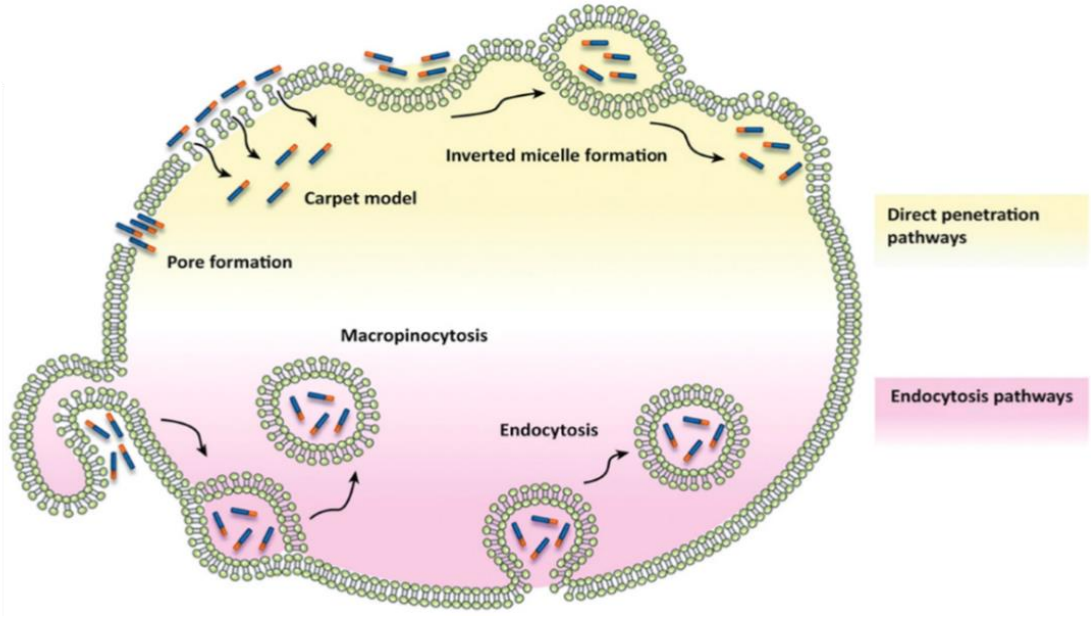

Figure 24 - Endocytosis and direct penetration pathways mediated by CPPs.[186]

It has been shown that addition of CPP to a cargo can induce energy-dependent endocytosis[124,188–190] using adenosine triphosphate (ATP) to power the polymerisation of ATPases such as globular actin and related mimics (**Figure 24**).[186] These processes are initiated by a stimulus which is derived from the binding of a ligand such as a CPP containing charged residues. For example, cationic CPPs such as TAT and amphipathic CPPs such as xentry are known to bind onto negatively charged membrane components. TAT interacts with sulphate groups belonging to an endocytic receptor known as heparan sulphate proteoglycans (HSPG). Similarly, xentry interacts with sulphate groups belonging to syndecan-4 receptors.[126] This stimulus propagates a physiological response, resulting in endocytic trafficking of a region of the cell membrane comprised of CPP-receptor complex.

3.2.3 Transactivator of Transcription (TAT)

The first CPP of interest was TAT derived from the HIV1 virus and is used for promoting trans-activation of its corresponding viral promoter.[113] A derivatised variation of the TAT sequence (RRRGRKKRR) used by Christian Hackenburger was employed for the delivery of large molecules like proteins[192] and was discovered to have enhanced cell penetrating properties when cyclised due to a more rigid structure.[191] TAT sequences can initiate uptake by interacting with heparan sulphate proteoglycans which have upregulated production in cancer cells. However, expression of its corresponding gene sequence is ubiquitous amongst normal cells and malignant cells, and hence TAT does not have an intrinsic method of discriminating cells.

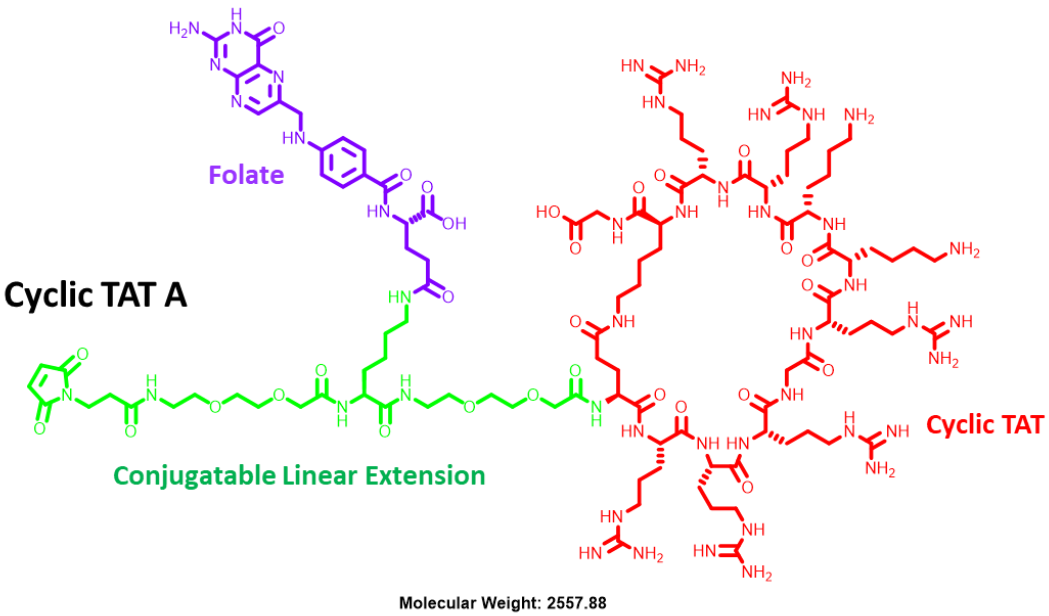

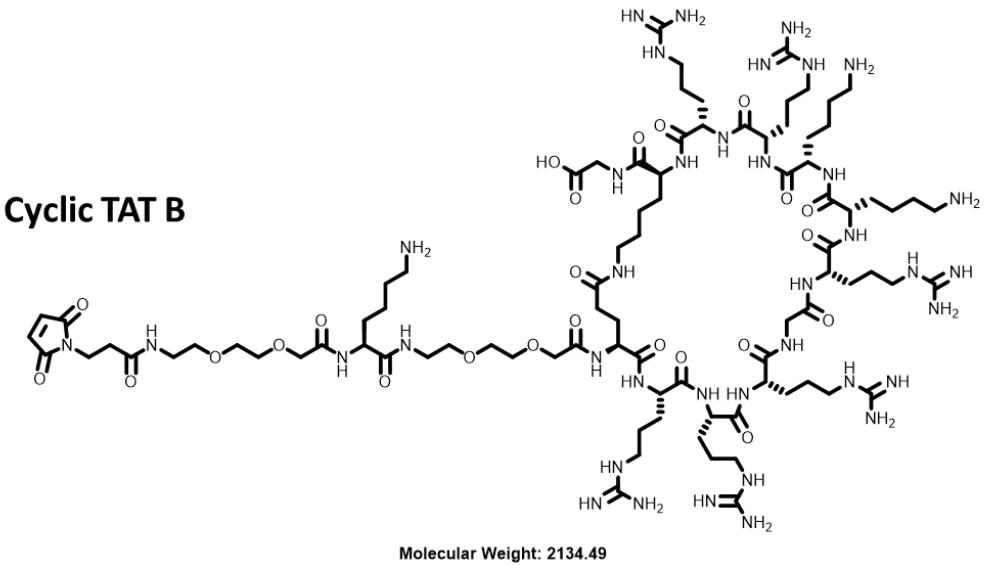

Scheme 5 - Structures of cyclised TAT sequences[191] for synthesis

Synthesis of TAT Variants

Cyclic TAT

Synthesis of a modified variation incorporating folic acid for cell targeting was planned *via* a manual Fmoc SPPS approach (**Scheme 5** – Cyclic TAT A). This modified TAT would incorporate an *N*-terminal linker system based on a maleimide for easy and selective conjugation to the solvent exposed cysteine of sfGFP. Disulphide bridge conjugation used in the production of constructs 1 and 2 (**Scheme 3**) was difficult due to the propensity of sfGFP to generate dimers *via* disulphide bridge. This resulted in

overlap of monomeric target conjugates with dimeric sfGFPs in size exclusion column and required three attempts for full isolation (*e.g.* constructs 1 and 2 – **Scheme 4**). For this reason, a maleimide was used instead for site selective protein labelling to avoid complications. The folic acid motif would also be incorporated into the *N*-terminal portion of the modified sequence to provide enhanced cell targeting of the peptide. Once completed, the sequence was planned for attachment to sfGFP, and a variation of the same sequence without folic acid was also planned for assembly and comparison (**Scheme 5** – Cyclic TAT B). The premise of this work was that folic acid would facilitate the movement of the entire conjugate towards FR-α and initiate receptor mediated endocytosis. Once the modified GFP was endocytosed, TAT can interact with the inner cell membrane of the vesicle from the intra-endosomal environment and potentiate entry to the cytosol. Off-site activity would likely occur, for instance, interaction of TAT with its receptor before folate interaction with FR-α. This would lead to a lack of cell discrimination due to the abundance of heparan-sulphate proteoglycans amongst cancerous and non-cancerous cells,[122] despite their upregulated production in malign cells.[192,193] Mammalian cell culture experiments were planned to investigate this potential off-site activity *via* free folic acid competitive inhibition assays and using FR-α negative cells, such as HEK293.[175] Results obtained would have been compared to studies on FR-α positive cells to find appropriate working concentrations of conjugate, whereby the desired characteristics of cell targeting, and endosome escape were found. Once these conditions were established, GFP was going to be swapped in preference for another large polypeptide with cytotoxic properties such as a type I ribosome inactivating protein.[91] Cyclic TAT was synthesised using a manual Fmoc SPPS approach (**Scheme 6**). Multiple challenges were encountered during synthesis that required troubleshooting. Initially, construction of cyclic TAT started with a glutamate next to a glycine (**Figure 25 – Original Planned Sequence**). However, it was discovered late in synthesis of the initial sequence that proximity of the amino acids lead to formation of an glutarimide group.[194] This was identified *via* high resolution mass spectrometry (**Figure 26**), and because of this, the positions of lysine and glutamate were swapped to avoid this problem (**Figure 25 – Revised Sequence**).

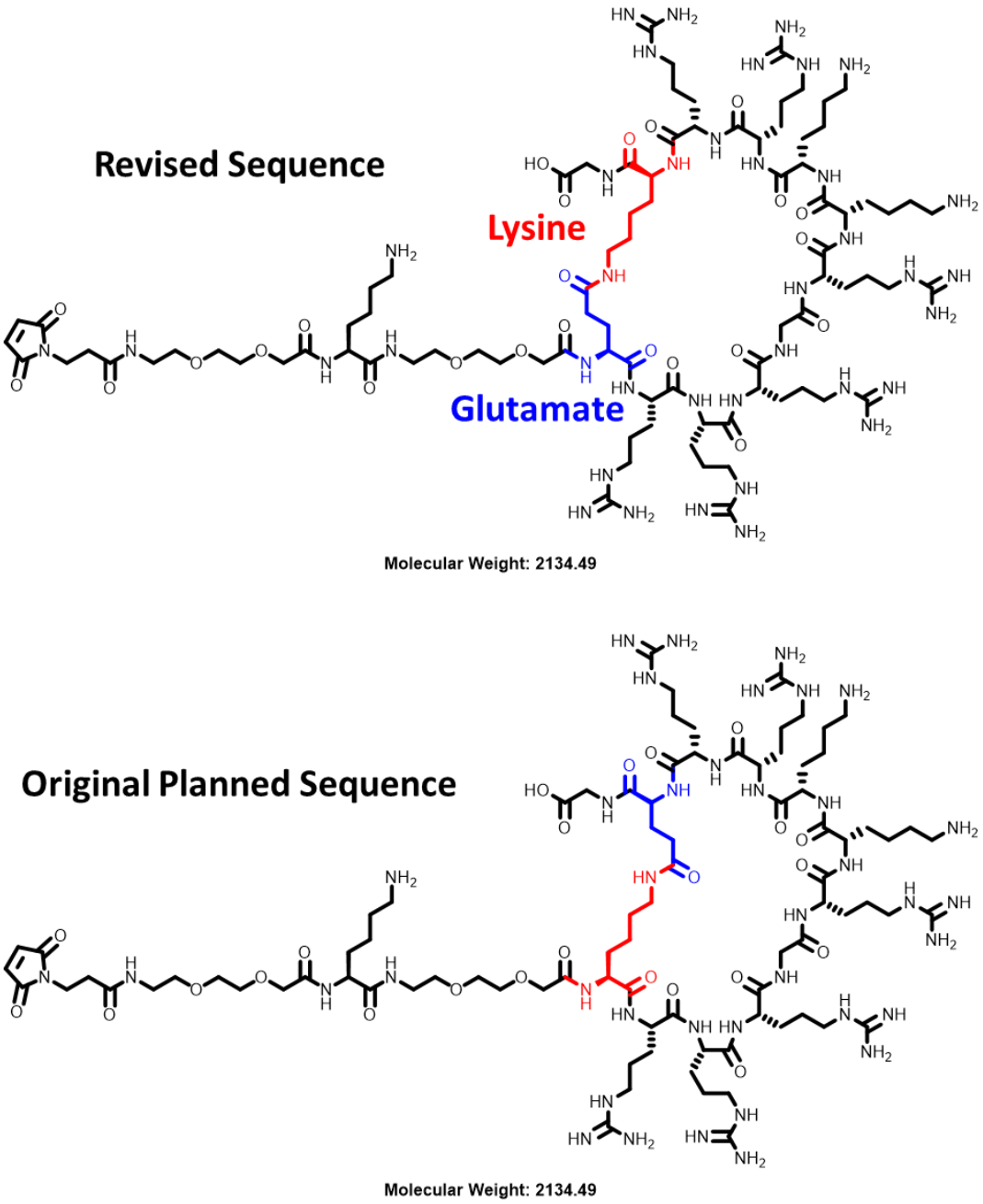

Figure 25 - Modified cyclic TAT design comparison.

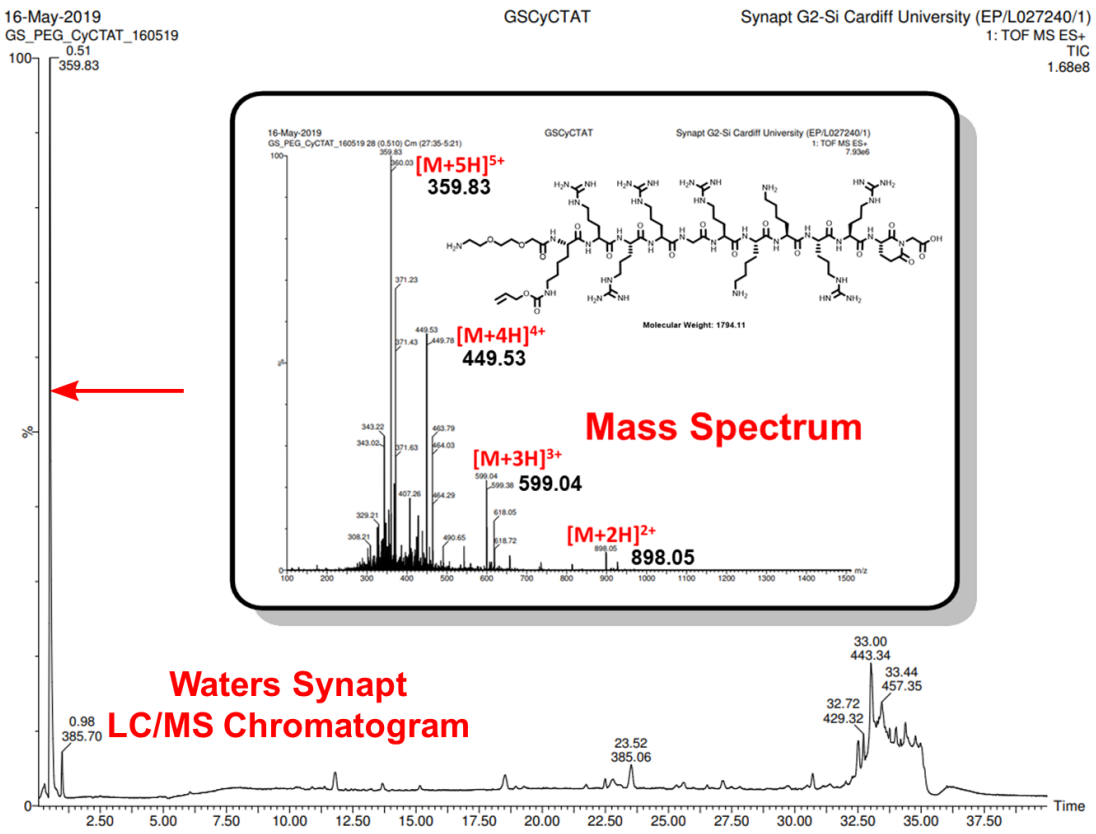

MS Method = Electrospray Ionisation	**Solvent Systems**	**Flow Rate =** 300 µL min^{-1}
Gradient	dH_2O (+ 0.1% $^{V}/_{V}$ formate)	**Injection Volume =** 1 µL
3 – 97% CH_3CN in 40 minutes	CH_3CN (+ 0.1% $^{V}/_{V}$ formate)	**C_8 Column**

Figure 26 - High resolution mass spectrometry of linear sequence comprised of *C*-terminal glutarimide formation from unwanted side-reaction between adjacent glutamate and glycine.

After adjustments were made, production of linear sequence and subsequent alloc and allyl deprotection (**Scheme 6**) was successful. However, inceptive efforts to generate an isopeptide bond for cyclisation was unsuccessful. Failed efforts to cyclise TAT on resin involved using a mixture of HOBt : HBTU (0.5 M : 0.5 M) in DMF and PyBOP respectively. Successful isopeptide bond formation was achieved by using HATU (**Scheme 6** – Step 2).

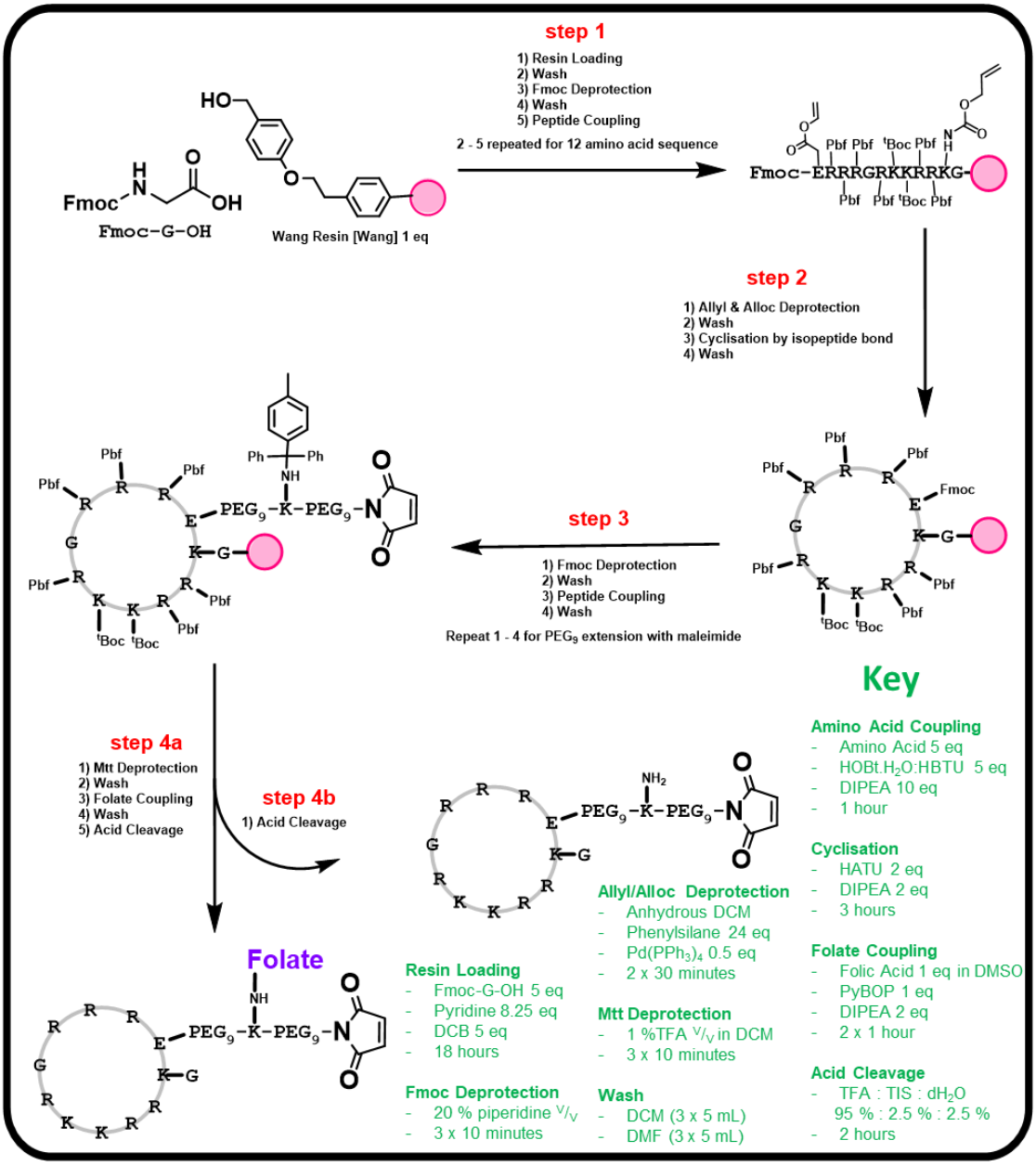

Scheme 6 - Modified cyclic TAT synthetic route.

The next step was to add a linear extension made of a lysine protected with a *4*-methyltrityl (Mtt) group culminating with an *N*-terminal maleimide (**Scheme 6** – Step 3). Mtt provided a route of chemo-selective deprotection due to its hypersensitivity to acidic conditions. This resulted in exposure of the primary amine on the lysine side chain which was exploited for attempted folic acid labelling (**Step 4a Folate Labelling - Scheme 6**). Multiple conditions were set out to form an isopeptide bond between folic acid and the exposed lysine side chain, However, folate labelling was not

successful. Despite labelling failure, one half of resin containing peptide was used for resin cleavage (**Step 4b - Scheme 6**). Cyclic TAT was then isolated by HPLC using solvent systems such as deionised water and acetonitrile both comprised of 0.1% $^{v}/_{v}$ TFA with a C_{18} ACE semi-preparation scale column. Target peptide eluted with a retention time of 15.5 minutes using a gradient of 10 - 45% CH_3CN in 35 minutes. This was analysed using an Agilent LC/MS. The observed mass to charge ratios ($^{M}/_{Z}$) were 356.7, 427.9, 534.5 and 712.4. (**Figure 27**). All values matched calculated $[M+6H]^{6+}$, $[M+5H]^{5+}$, $[M+4H]^{4+}$ and $[M+3H]^{3+}$ charge states (356.7, 427.9, 534.6 and 712.5 respectively).

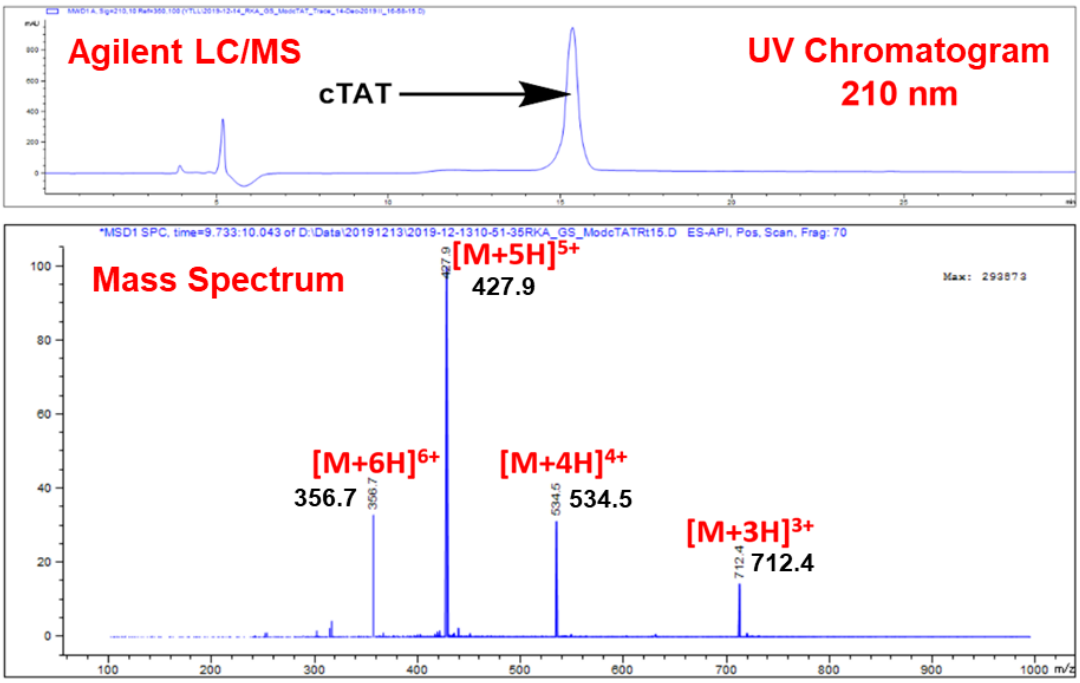

MS Method = Electrospray Ionisation	**Solvent Systems**	**Flow Rate =** 300 µL min^{-1}
Gradient	dH_2O (+ 0.1% $^{V}/_{V}$ formate)	**Injection Volume =** 5 µL
1 – 30% CH_3CN in 30 minutes	CH_3CN (+ 0.1% $^{V}/_{V}$ formate)	**C_{18} Column**

Figure 27 - LC/MS data of isolated cyclic TAT (Scheme 5 Cyclic TAT B).

Despite success in isolating cyclic TAT (**Scheme 5 –** Cyclic TAT B), this peptide was obtained in negligible quantities only visible by LC/MS (**Figure 27**). Due to the complicated nature of producing both cyclic TAT sequences (**Scheme 5**) a simplified alternative was planned (**Scheme 7**).

Linear TAT for OaAEP1 Mediated Cyclisation

A TAT derivative was synthesised as a linear sequence with an *N*-terminal folate and *C*-terminal maleimide. In addition to the maleimide, a glycine-leucine dipeptide component would be installed on the *N*-terminal region of the peptide. The premise behind this design was to combine GFP with TAT through an extrinsic exo-cyclisation route facilitated by an enzyme (**Scheme 8**), instead of the preliminary intrinsic endo-cyclisation of the peptide *via* isopeptide bond (**Scheme 6** – Step 3). A variation of GFP comprised of an NCL loop (eGFP) was used as the protein scaffold and asparaginyl endopeptidase (OaAEP1) was planned to expedite this process. OaAEP1 would expose the asparagine residue of the eGFP NCL loop for coupling with the glycine from the GL portion of TAT (**Scheme 7**).

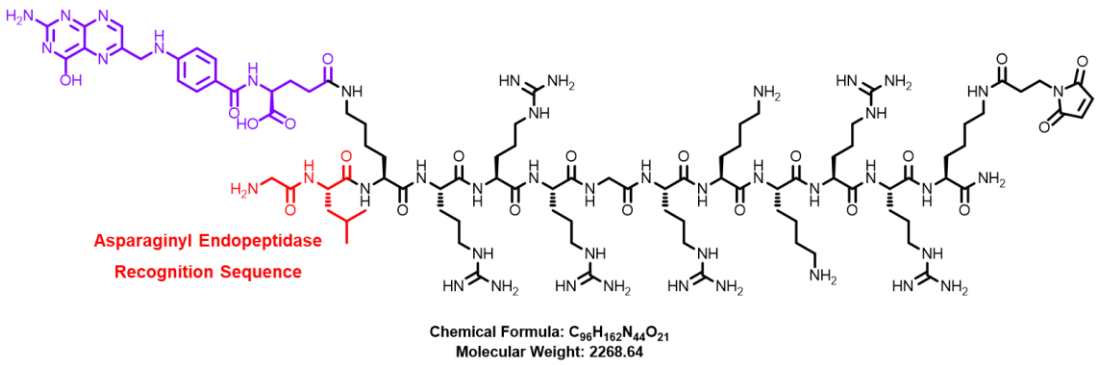

Scheme 7 - Planned structure for folate labelled TAT for enzyme mediated exo-cyclisation.

OaAEP1

Asparaginyl endopeptidases including OaAEP1 are derived from plants such as *Oldenlandia affinis.*[195] They are a type of protease that utilises a cysteine residue for enzymatic activity. This enzyme exploits a *C*-terminal recognition motif (*i.e.* NGL – **Scheme 8**) for cleavage to expose an asparagine for intermolecular or intramolecular (**Scheme 8**) ligation with an *N*-terminal GL sequence (**Scheme 7** and **8**).[195] In addition to NGL, OaAEP1 can recognise NCL as a substrate,[196] and thus OaAEP1 was planned for mediating conjugation of folate labelled TAT (**Scheme 7**) into the loop of an eGFP mutant comprised of an NCL loop (**Scheme 9**). OaAEP1 would mediate NCL cleavage (step 1 – **Scheme 9**), and subsequent intramolecular ligation of an *N*-terminal glycine to an exposed asparagine. The modified folate TAT was synthesised with a *C*-terminal maleimide, and this was intended for connection to the free cysteine residue (step 2 – **Scheme 9**).

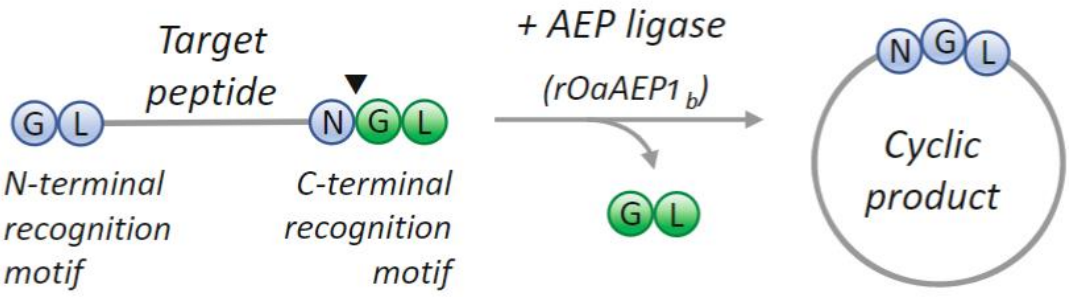

Scheme 8 - Illustration of the cyclisation conjugation of Oldenlandia affinis asparaginyl endopeptidase on a linear peptide comprised of an NGL recognition motif[195]

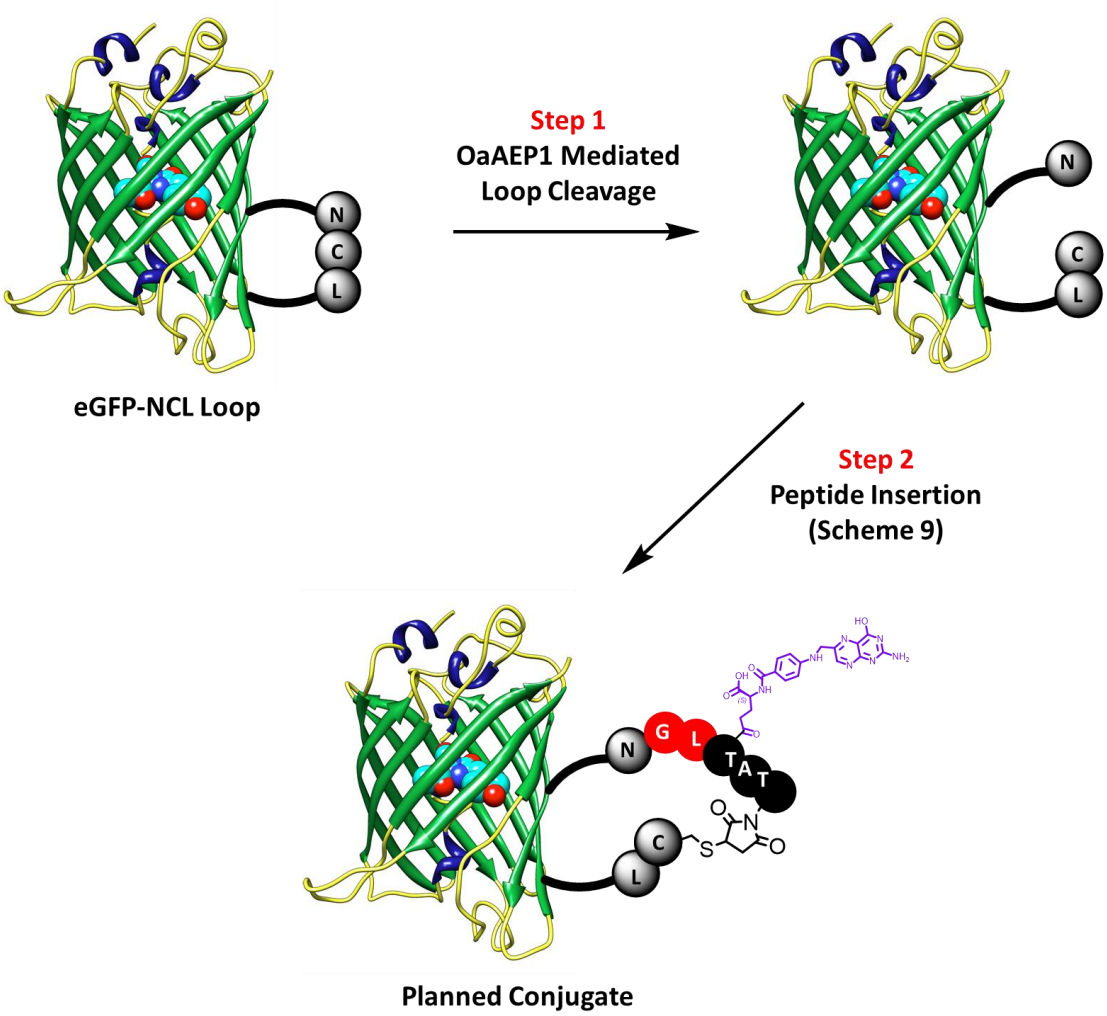

Scheme 9 - Plan for exo-cyclisation of eGFP + folate labelled TAT (Scheme 8) mediated by OaAEP1.

Folate labelled TAT (**Scheme 7**) was assembled using a combination of automated SPPS and manual SPPS (**Scheme 10**). A CEM automated peptide synthesiser was exploited for generating the full linear sequence (**Scheme 10**). A manual approach was needed for removal of orthogonal protecting groups such as Mtt and alloc ester, as well as folic acid and maleimide labelling *via* peptide bond formation.

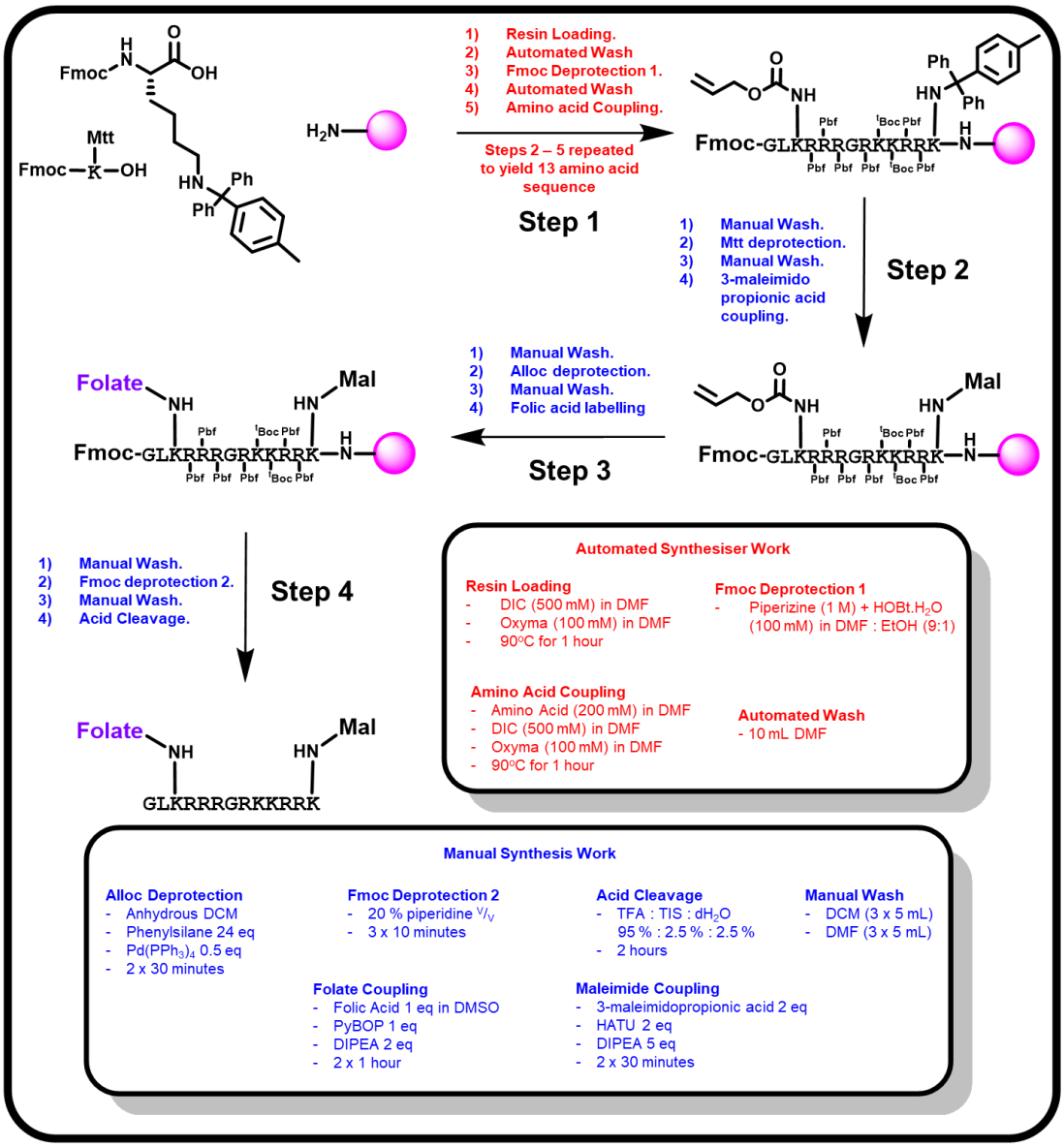

Scheme 10 - Synthetic route of folate labelled TAT (Scheme 7) for OaAEP1 mediated exo-cyclisation to eGFP.

After following the synthetic pathway, crude peptide was processed *via* HPLC using a solvent system made of deionised water and acetonitrile containing 0.1% ($^{V}/_{V}$) TFA. A semi-preparation scale C_{18} ACE column was used for separation, and this was connected to an Agilent HPLC pump. A gradient of 10 – 45% acetonitrile over 35 minutes was used for isolation of the target sequence. The peptide of interest was isolated with minor contaminants including a single arginine deletion and was characterised *via* an Agilent LC/MS (**Figure 28**). Mass to charge ratios observed were

379.1 $[M+6H]^{6+}$, 454.7 $[M+5H]^{5+}$, 568.1 $[M+4H]^{4+}$ and 757.1 $[M+3H]^{3+}$ (**Figure 28**) and these values matched the calculated $[M+6H]^{6+}$, $[M+5H]^{5+}$, $[M+4H]^{4+}$ and $[M+3H]^{3+}$ charged states (379.1, 454.7, 568.2, 757.2 respectively). In addition to the observed charge state species, salt and HCl adducts were also found. Visible, but negligible amounts of isolated peptide were obtained.

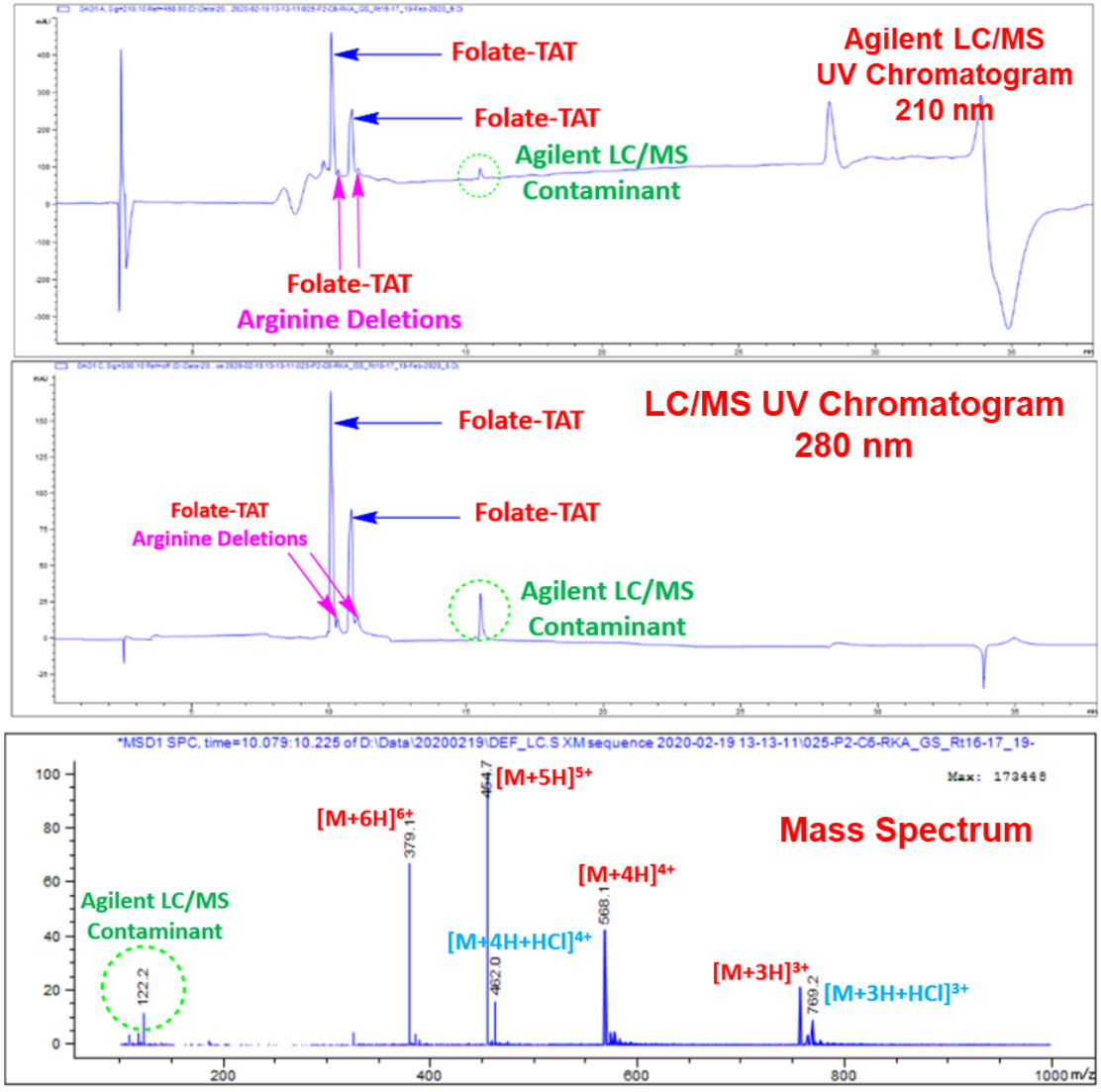

MS Method = Electrospray Ionisation

Gradient

1 – 30% CH_3CN in 30 minutes

Solvent Systems

dH_2O (+ 0.1% $^{V}/_{V}$ formate)

CH_3CN (+ 0.1% $^{V}/_{V}$ formate)

Flow Rate = 300 µL min^{-1}

Injection Volume = 1 µL

C_{18} Column

Figure 28 - Folate-TAT (Scheme 7) HPLC fraction LC/MS Data.

Alongside the isolation of folate labelled TAT, OaAEP1 was isolated in preference to eGFP to establish exo-cyclisation conditions. The Luk research group provided SHuffle T7 *E. coli* strain transformed with the *ooaep1* gene. These cells were introduced to LB media incorporating kanamycin (50 mg L^{-1}) and left to incubate at 37°C for 4 hours to reach an optical density (OD_{600}) of 0.7 (UV measurement at 600 nm). At this point IPTG (120 mg L^{-1}) was added to induce gene expression at 16°C for 20 hours. Target protein OaAEP1 was isolated using a combination of affinity (Ni^{2+}-NTA) and size exclusion chromatography.

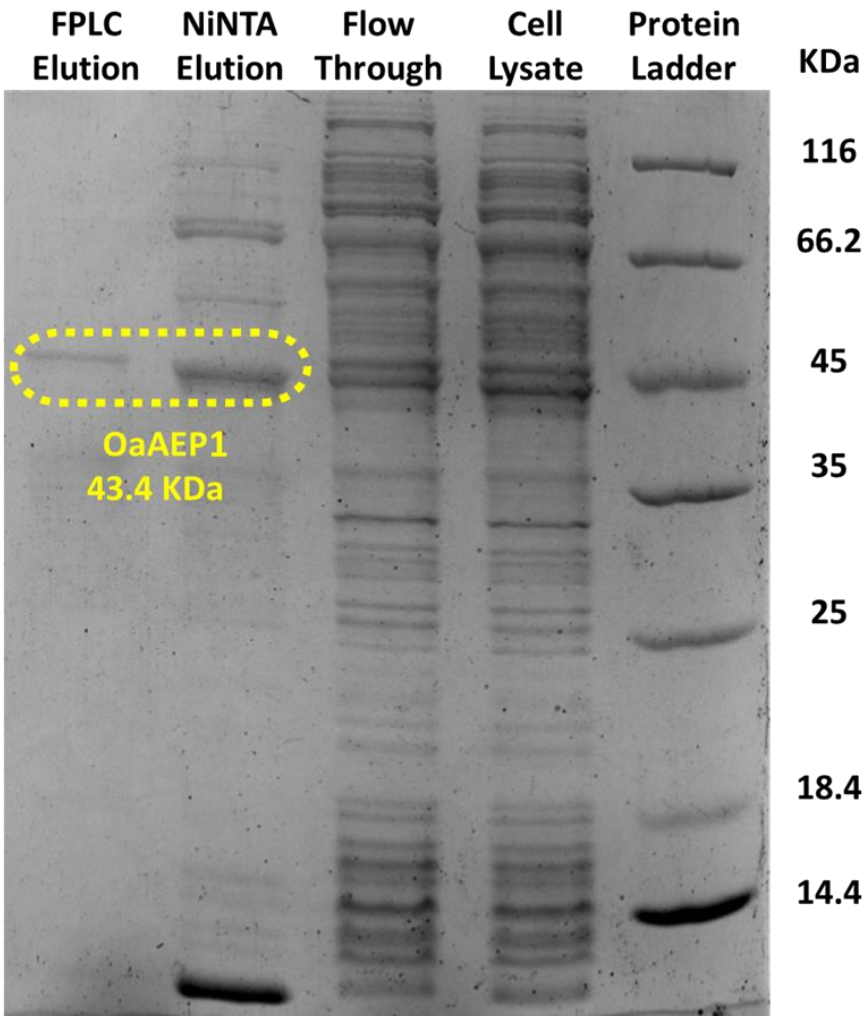

Figure 29 - SDS-PAGE comprised of samples taken during the OaAEP1 isolation procedure.

FPLC eluate containing OaAEP1 was collected and processed by SDS-PAGE (**Figure 29**). A faint band residing at approximately 45 kDa was observed and correlated with the expected molecular weight of 43.4 kDa.[196] A portion of this sample was analysed using Waters synapt LC/MS. However, due to the lack of specificity of the enzymes intrinsic protease activity, the sample was digested resulting in multiple truncations, nonetheless, this sample was used in test reactions on a model peptide (GLPVSTKPVATRNGL) to establish asparaginyl endopeptidase activity and conditions that can be applied to eGFP-NCL and folate labelled TAT for exo-cyclic conjugation. Multiple test conditions were attempted with the model peptide and all displayed asparaginyl endopeptidase activity, and the best-established conditions were found at pH 5.5 with an enzyme to peptide ratio of 1:1000. However, despite success in cyclising the model sequence, there was a portion of peptide that remained linear (**Figure 30**).

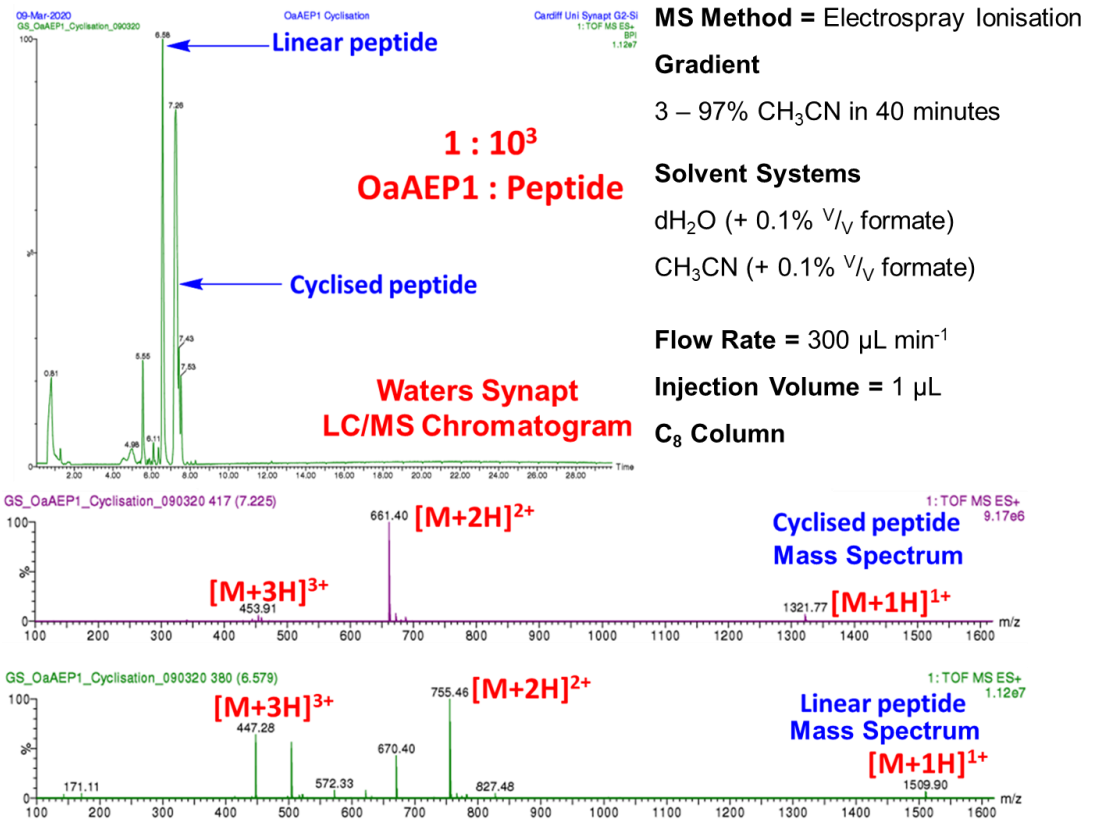

Figure 30 - OaAEP1 cyclisation of linear model peptide (GLPVSTKPVATRNGL) LC/MS.

Due to the complications associated with peptide synthesis (*e.g.* folate labelling of **Scheme 5** and arginine deletions from **Scheme 7**), along with difficulties of establishing enzyme driven exo-cyclisation processes reaching completion, a further research plan adjustment was made centred around the CPP of interest. This revised strategy placed focus on a CPP that is known to have noteworthy cell penetrating activity in a linear conformation, thereby, irradicating difficulties such as cyclisation and enzyme catalysis.

3.2.4 Aurein-1.2

The new sequence of interest was aurein-1.2 (**Scheme 11** – GLFDIIKKIAESF) which is a peptide derived from the skin secretions of *Litoria* genus of Australian bell frogs.[131,143–145] This peptide was used for providing an endosomal escape pathway[96] for supercharged GFP comprised of an additional +36 charged from basic amino acid residues. This protein was prone to entrapment inside of endosomes.[93,96] Despite enhancing cytosolic entry of protein, the membrane component that was targeted is ubiquitously produced among cancerous and non-malignant cells.[197] Therefore, folic acid was planned for connection to aurein-1.2 to enhance cell discrimination and facilitate delivery of sfGFP into malignant cells that mass produce FR-α.

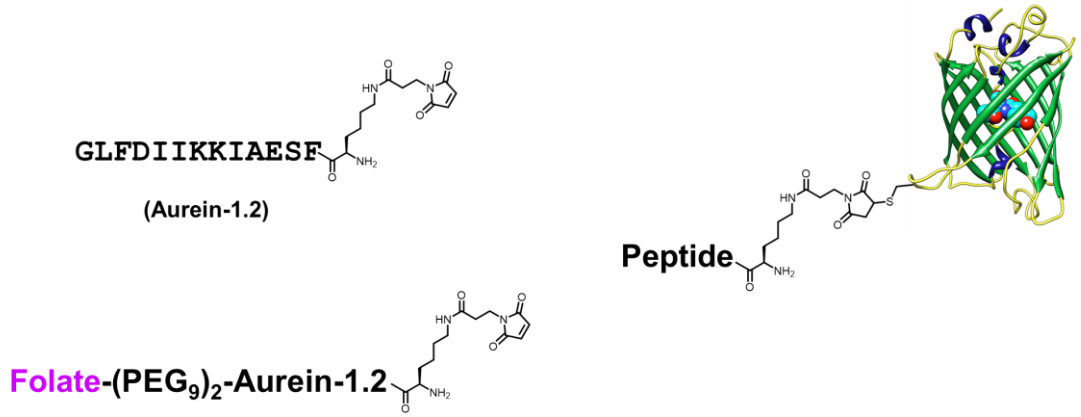

Scheme 11 - Modified sequences based on aurein-1.2 (GLFDIIKKIAESF) connected to sfGFP.

Synthesis of Aurein-1.2 Variants

Non-Folate Labelled Sequence

Aurein-1.2 peptides (**Scheme 11**) were made using Fmoc SPPS approach[170] and utilising a CEM peptide synthesiser to produce sequences for route 1 and 2 (**Scheme 12**). Aurein-1.2 with a *C*-terminal maleimide was produced *via* route 1 and was easily generated requiring minimal troubleshooting. Following automated synthesis, peptide bound resin required mtt deprotection for chemo-selective exposure of the *C*-terminal lysine residue, which was used for peptide bond formation with *3*-maleimidopropionic acid, and thus yielding the finished sequence on resin. The resin, *N*-terminal ^{t}Boc and side chain protecting groups were all removed using an acid cleavage cocktail comprised of 95% TFA and 5% scavengers $^{V}/_{V}$. Target peptide was isolated from its crude mixture using a Shimadzu preparation scale C_{18} reverse phase column connected to a Shimadzu preparation scale HPLC pump. The gradient applied was 40 - 60% acetonitrile (+ 0.1% $^{V}/_{V}$ TFA) with a flow rate of 10 mL min^{-1} in 25 minutes and the isolated fraction was analysed by Agilent LC/MS. The observed mass to charge ratios ($^{M}/_{Z}$) were 880.6 and 587.2 and both values matched the calculated $[M+2H]^{2+}$ and $[M+3H]^{3+}$ charged states (880.54 and 587.36 respectively (**Figure 31**).

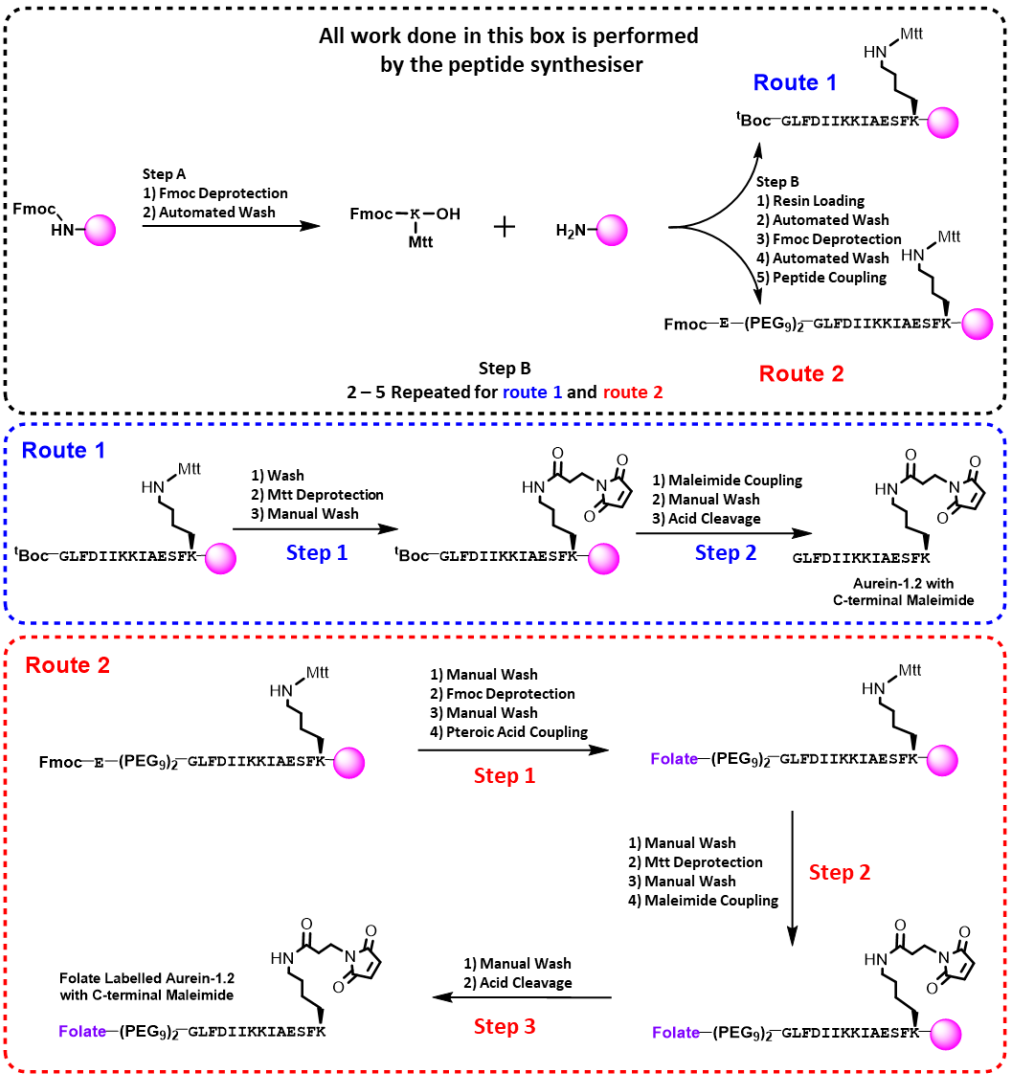

Key

Resin Loading
- Rink Amide Resin
- Fmoc-Lys(Mtt)-OH (200 mM in DMF)
- DIC (500 mM in DMF)
- Oxyma (100 mM in DMF)
- 90°C for 1 hour

Peptide Coupling
- Fmoc and side chain protected amino acid (200 mM in DMF)
- DIC (500 mM in DMF)
- Oxyma (100 mM in DMF)
- 90°C for 1 hour
- 25°C for 2 x 1 hour only for arginine

Maleimide Coupling
- 3-Maleimido Propionic Acid in DMF 2 eq
- HATU 2 eq
- DIPEA 5 eq
- 2 x 30 minutes

Fmoc Deprotection
- Piperidine 20 % $^{v}/_{v}$ in DMF 5 mL
- 3 x 10 minutes

Pteroic Acid Labelling
- Pteroic Acid 1.1 eq in DMSO
- HATU 2 eq
- NMM 5 eq
- 4 x 30 minutes

Acid Cleavage
- TFA (95 % : 2.5 % : 2.5 %)

Manual Wash
- 3 x 5 mL DCM
- 3 x 5 mL DMF

Automated Wash
- 10 mL DMF

Mtt Deprotection
- 1 % TFA $^{v}/_{v}$ in DCM
- 3 x 30 minutes

Scheme 12 - Synthetic pathway for producing peptides based on aurein-1.2.

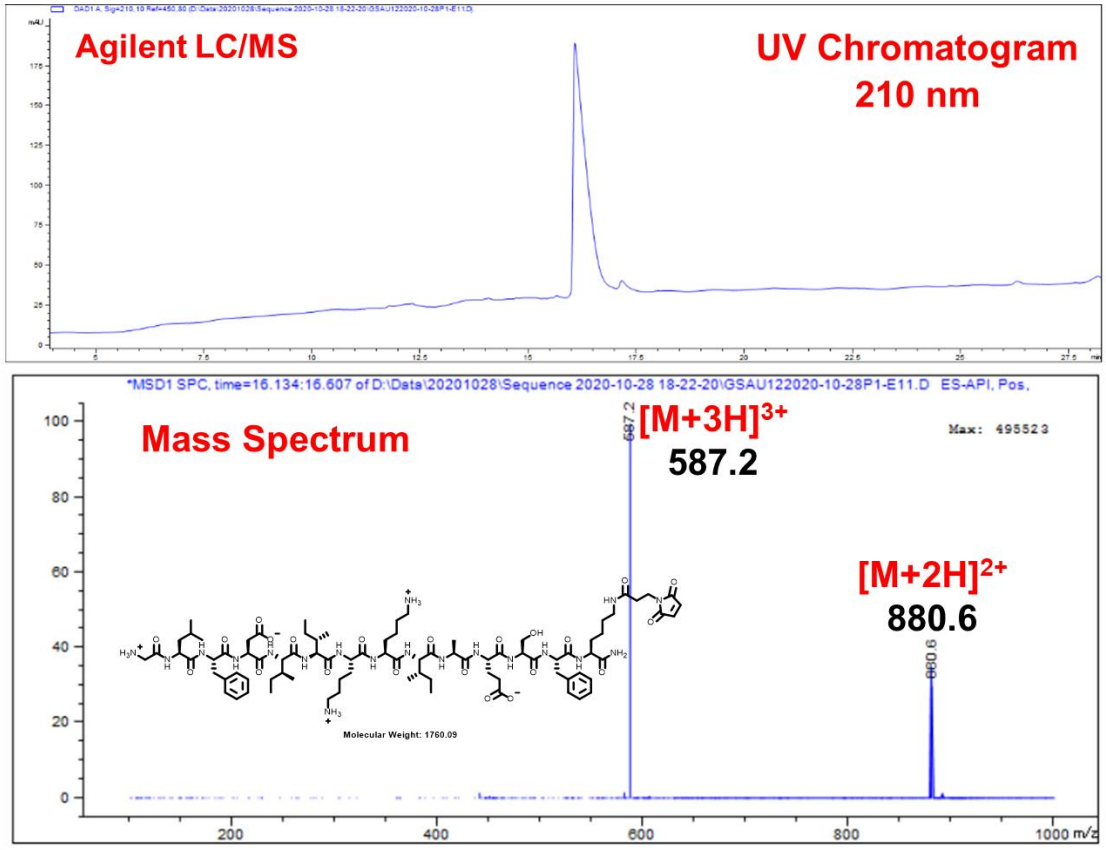

MS Method = Electrospray Ionisation

Gradient

30 - 60% CH_3CN in 30 minutes

Solvent Systems

dH_2O (+ 0.1% $^{V}/_{V}$ formate)

CH_3CN (+ 0.1% $^{V}/_{V}$ formate)

Flow Rate = 300 µL min^{-1}

Injection Volume = 10 µL

C_{18} Column

Figure 31 - LC/MS data of isolated aurein-1.2 obtained by route 1 (scheme 12).

Folate Labelled Sequence

Folate labelled aurein-1.2 was produced *via* route 2 (**Scheme 12**) and was assembled using a similar reaction scheme compared to aurein-1.2. However, the N-terminus of the peptide sequence was extended using Fmoc protected glycine, rather than ^{t}Boc protected variant used to cap aurein-1.2 (**Scheme 12**). This granted further addition of amino acids to the N-terminus such a two PEG_9 spacers and α-carboxy protected glutamate (**Scheme 12 – Route 2, Step 1**). The *N*-terminal glutamate was coupled with pteroic acid through a peptide bond to yield a folic acid motif. This segmental route of folic acid capping was performed because whole folate addition was found to be a sequence dependent problem. It was likely on resin aggregation and steric hinderance contributed towards poor peptide bond formation when using whole folic acid. This problem was solved through the use of two PEG_9 spacers and addition of smaller segments (*i.e.* first glutamate and then pteroate) that would culminate in the desired folate label (**Scheme 12**). Although this route of folate labelling aurein-1.2 was successful, addition of pteroic acid to glutamate required 10 coupling cycles to fully saturate the N-terminus, and thus, generated a large amount of waste. Nonetheless, the peptide of interest was complete and cleaved from its resin and side chain protecting groups using 95% TFA and 5% scavenger's $^{V}/_{V}$ to obtain the crude mixture. Folate labelled aurein-1.2 was isolated using a semi-preparative scale C_{18}-ACE column connected to an Agilent Infinity pump. The gradient used for isolation was 55 – 65% acetonitrile (+ 0.1% $^{V}/_{V}$ TFA) with a flow rate of 3 mL min^{-1} in 25 minutes. A total of 14 individual HPLC runs were performed to isolate the peptide of interest from its crude mixture. Small injection volumes (*e.g.* 200 µL) were applied to each run in order to minimise UV detector saturation and peptide truncation overlap. Isolated fractions were collected and analysed by Waters synapt LC/MS. The observed mass to charge ratios ($^{M}/_{Z}$) were 1237.14, 825.10 and 619.20 (**Figure 32**) and these values matched the calculated $[M+2H]^{2+}$, $[M+3H]^{3+}$ and $[M+4H]^{4+}$ charged states (1237.40, 825.26 and 619.20 respectively). Due to the difficulties faced in synthesis and isolation of this sequence, which garnered little peptide (*e.g.* 2 mg), aurein-1.2 not bearing folic acid was used for initial attempts at sfGFP labelling.

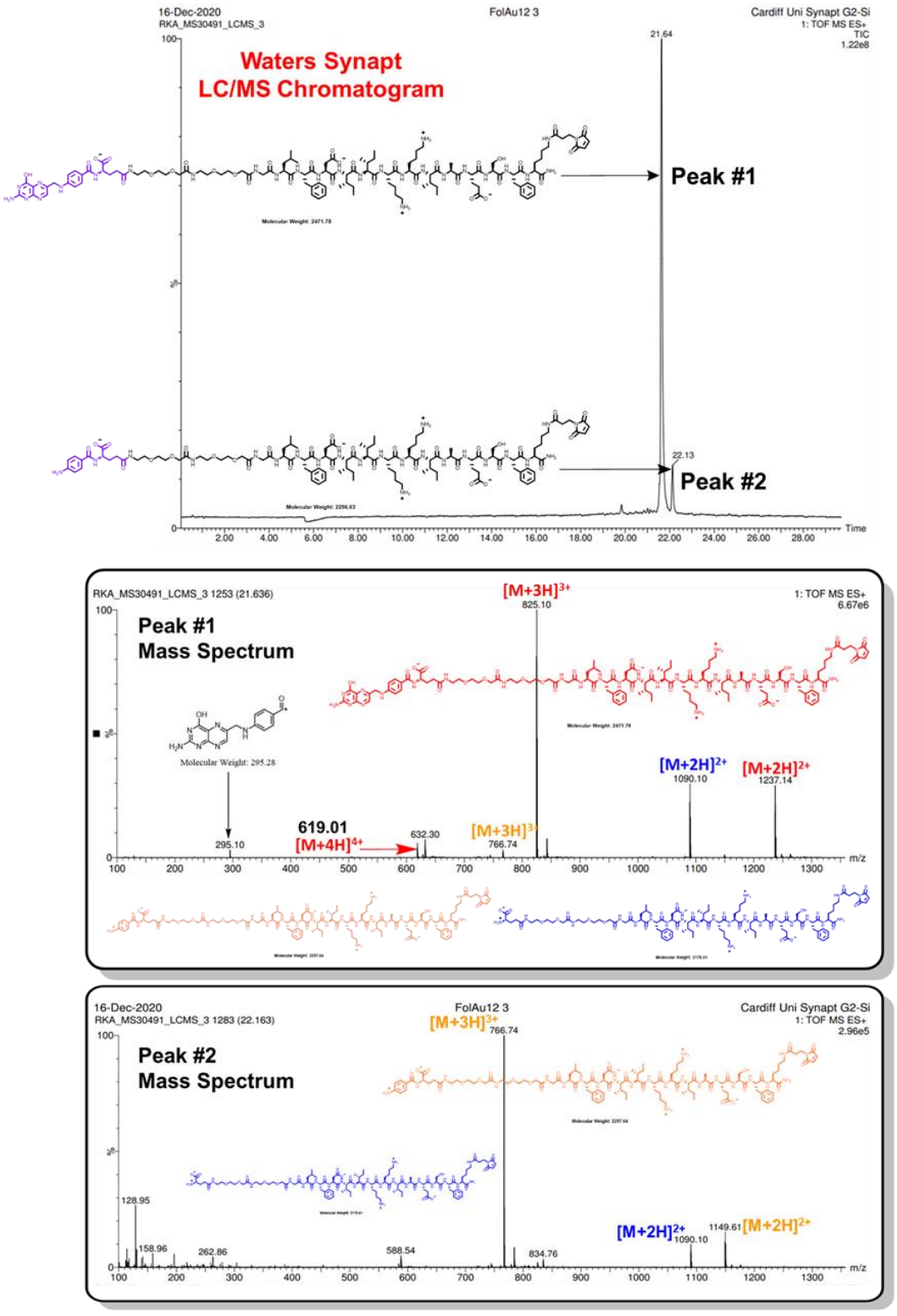

Electrospray Ionisation	**Solvent Systems**	**Flow Rate =** 300 µL min^{-1}
Gradient	dH_2O (+ 0.1% $^{V}/_{V}$ formate)	**Injection Volume =** 1 µL
3 – 97% CH_3CN in 40 minutes	CH_3CN (+ 0.1% $^{V}/_{V}$ formate)	**C_8 Column**

Figure 32 - LC/MS data of isolated folate labelled aurein-1.2 obtained by route 2 (Scheme 12).

3.2.4.1.3 Attempted Aurein-1.2 Labelling of sfGFP

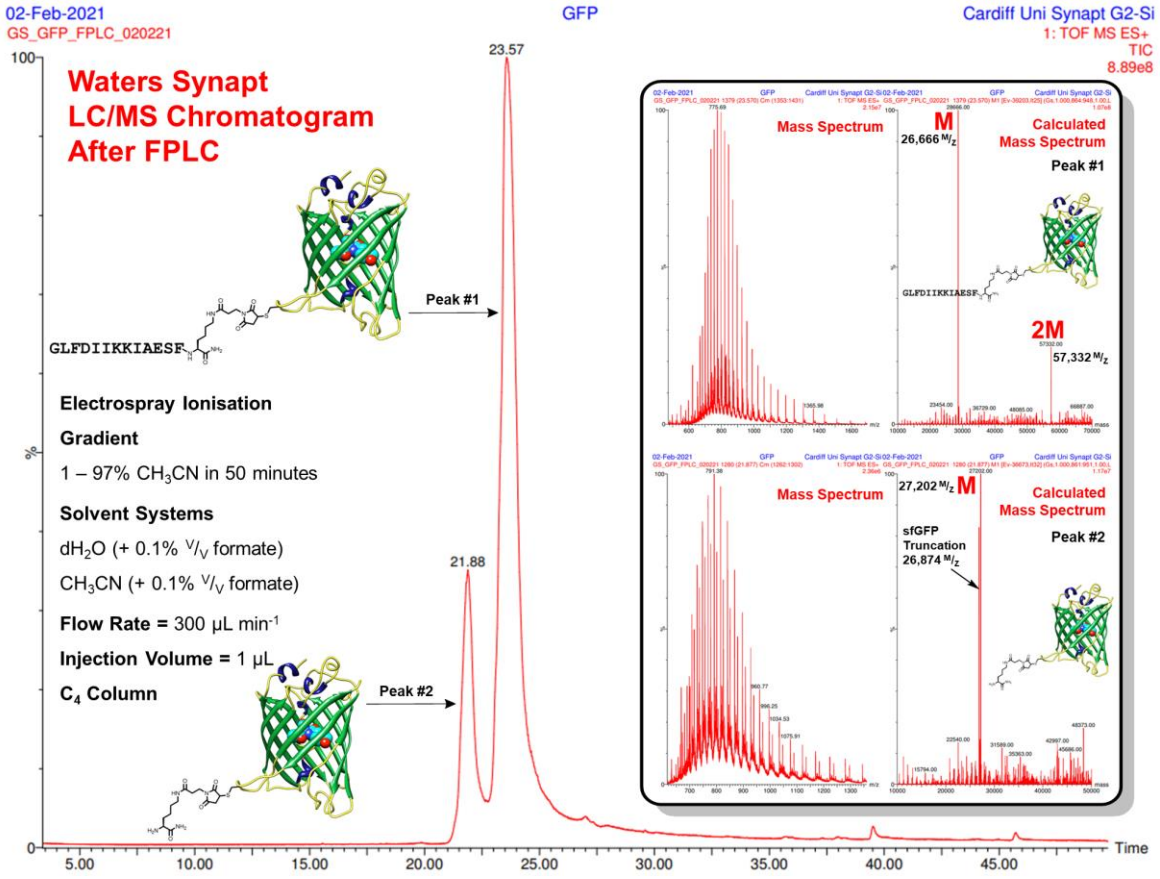

Figure 33 - LC/MS data of FPLC isolated aurein-1.2 labelled sfGFP.

Initial efforts made in connecting aurein-1.2 to sfGFP *via* cysteine thiol alkylation were unsuccessful due to the hydrophobic nature of the sequence. During the inceptive attempt at aurein-1.2 Michael addition, sfGFP linked to Ni^{2+} column by His_6-tag was eluted using a high imidazole concentration buffer (250 mM - pH 7.5). The eluate containing sfGFP was added dropwise from the Ni^{2+} column into a 50 mL falcon tube containing aurein-1.2 in solid form (10 mg). However, aurein-1.2 was insoluble to the buffer applied, and thus, additives like acetonitrile were added in small quantities (100 µL) to solubilise the peptide without damaging sfGFP. This attempt was not successful and did not produce enough aurein-1.2 labelled sfGFP. During the second attempt at Michael addition, aurein-1.2 was solubilised in acetonitrile (10 mg in 100 µL) before introduction to affinity column eluate containing sfGFP. This attempt proved to be successful, despite the presence of dimerised sfGFP found in the conjugation mixture, but due to the molecular weight differences, size exclusion chromatography was plausible for separating and isolating the target conjugate. For the isolation process a PBS buffer (pH 7.4) was used. Fractions relating to the target

protein were collected and analysed *via* water synapt LC/MS (**Figure 33**). The observed calculated molecular weight of the target conjugate was 28,666 $^{M}/_{Z}$ and this was close to the anticipated value of 28,664 $^{M}/_{Z}$ which corresponds to a percentage error of 0.007% (70 ppm). Despite the marginal difference in molecular weight value, the observed calculated mass is within the acceptable error range of ± 0.01%.[198] However, during the isolation of the target conjugate, a portion of protein suffered from self-cleavage of the endosome escape peptide (*e.g.* aurein-1.2 – GLFDIIKKIAESF), and thus, producing an unwanted by-product and its corresponding truncation. Degradation of the target conjugate appeared to be promoted by the substitution of high imidazole salt buffer for PBS (*i.e.* absence of imidazole in PBS). This caused a decrease in hydrogen bond donors that were initially present to stabilise aurein-1.2 labelled sfGFP during Michael addition. Due to the construct's stable behaviour in high imidazole buffer, and lack of stability in PBS, it is likely the same degradation pathway would commence in cell culture media. In view of positive results such as the ease of aurein-1.2 synthesis and maleimide labelling of thiols, versus negative results such as folic acid labelling *via* SPPS and lack of stability of sfGFP constructs, a different research route was explored. Considering the anticancer properties of aurein-1.2,[131,199] a cytotoxic peptide delivery route was developed. Aurein-1.2 was synthesised as a native sequence, and with a folate label. Both were studied *in vitro* for changes in sequence behaviour. For folic acid variants, *N*-terminal maleimide adaptations were applied to create cytotoxic peptides for Michael addition to previously synthesised folates containing a *C*-terminal cysteine (**Scheme 1** and **Figure 16**). Experiments performed beforehand had demonstrated that folate labelling provided sfGFP with the ability to interact with FR-α in select cells (**Figure 21**).

Chapter 4: Small Cytotoxic Polypeptide Conjugates

4.1 Introduction

In chapter two, sfGFPs bearing pterin adaptations such as folate were created (**Scheme 4**) and tested on mammalian cells (**Figure 21**). The results produced had demonstrated that a folic acid motif can enhance cellular uptake and specificity of sfGFP. Following on from this work, attempts were made in chapter three at synthesising a substitution peptide comprised of a CPP capped with folic acid (**Scheme 6, 10 and 12**) which were planned for conjugation to GFP (*i.e.* sfGFP and eGFP), and thus, providing a large fluorescent polypeptide with cell targeting and membrane permeability. It was postulated that this system would allow for active uptake of GFP *via* FR-α. In addition to this activity, the CPP would facilitate endosome escape of GFP which is known to suffer from vesicular entrapement.[57,62] Despite efforts made to produce a modified CPP, construction of a conjugate was unsuccessful due to degradation of the endosome escape tool in media mimicking physiological conditions (**Figure 33**). Because of these results, an altered research route was followed in this chapter whereby GFP was substituted for a natural cytotoxic peptide that does not require a CPP for cytosolic entry, instead of a protein which was originally the plan. In this chapter the peptides of interest were aurein-1.2 and Bid-BH3 which are both known to potentiate mechanisms of cell death previously discussed in chapter one (see 1.3.2 - Necrosis and Apoptosis). These peptides were synthesised as native sequences and as derivatives comprised of the same folic acid label used in chapter two for tagging sfGFP (**Figure 16** and **19**) and tested on mammalian cells (**Figure 21**).

4.2 Aurein-1.2

4.2.1 Synthesis of Aurein-1.2 Variants

Non-Folate Labelled

The first small cytotoxic polypeptide of interest was aurein-1.2. Previously, a modified analogue was generated containing a *C*-terminal maleimide and was found to be easily synthesised (**Scheme 12** – Route 1 and **Figure 31**). In this case, aurein-1.2 native sequence (GLFDIIKKIAESF) was produced using a CEM automated peptide synthesiser (**Scheme 13**). The crude mixture was severed from its resin using an acid cleavage cocktail comprised of 95% TFA and 5% scvanagers $^{V}/_{V}$. Soon after the target sequence was isolated using a Shimadzu preparation scale C_{18} HPLC column connected to a Shimadzu pump. Solvent system applied was acetonitrile and deionised water containing 0.1% $^{V}/_{V}$ TFA. The gradient was 40 – 60% acetonitrile over 20 minutes with a flow rate of 10 mL min^{-1}.

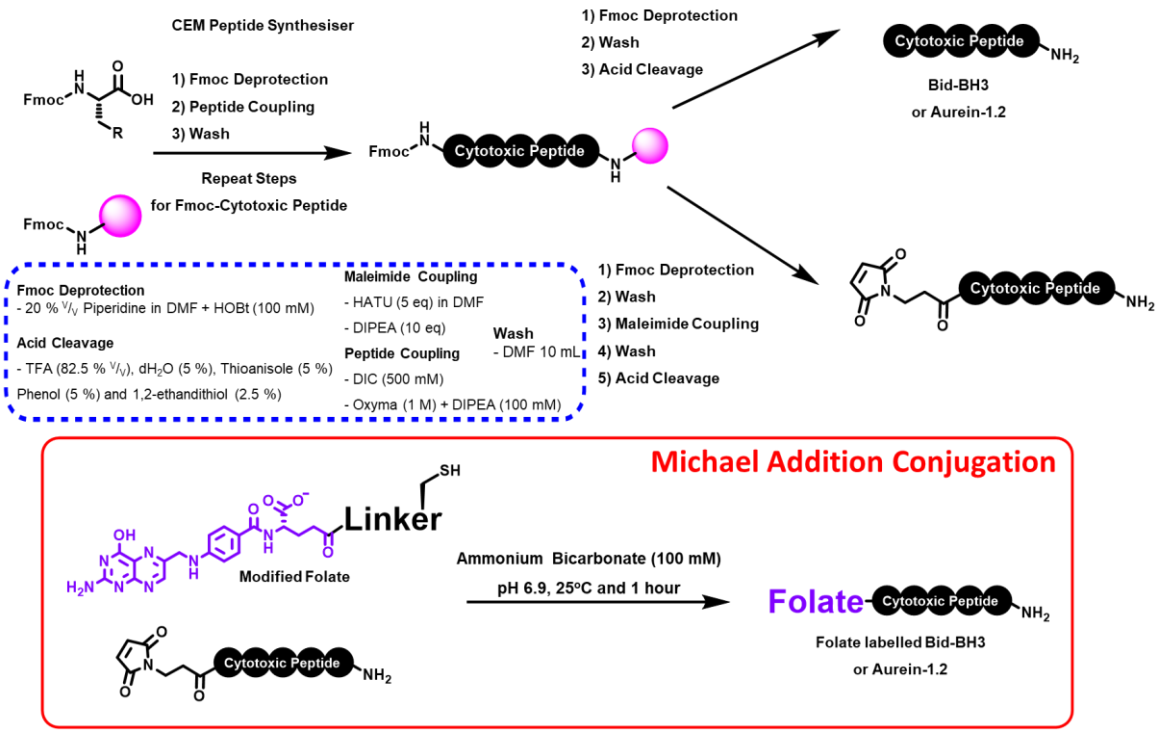

Scheme 13 - Construction of native cytotoxic peptides and folate labelled analogues.

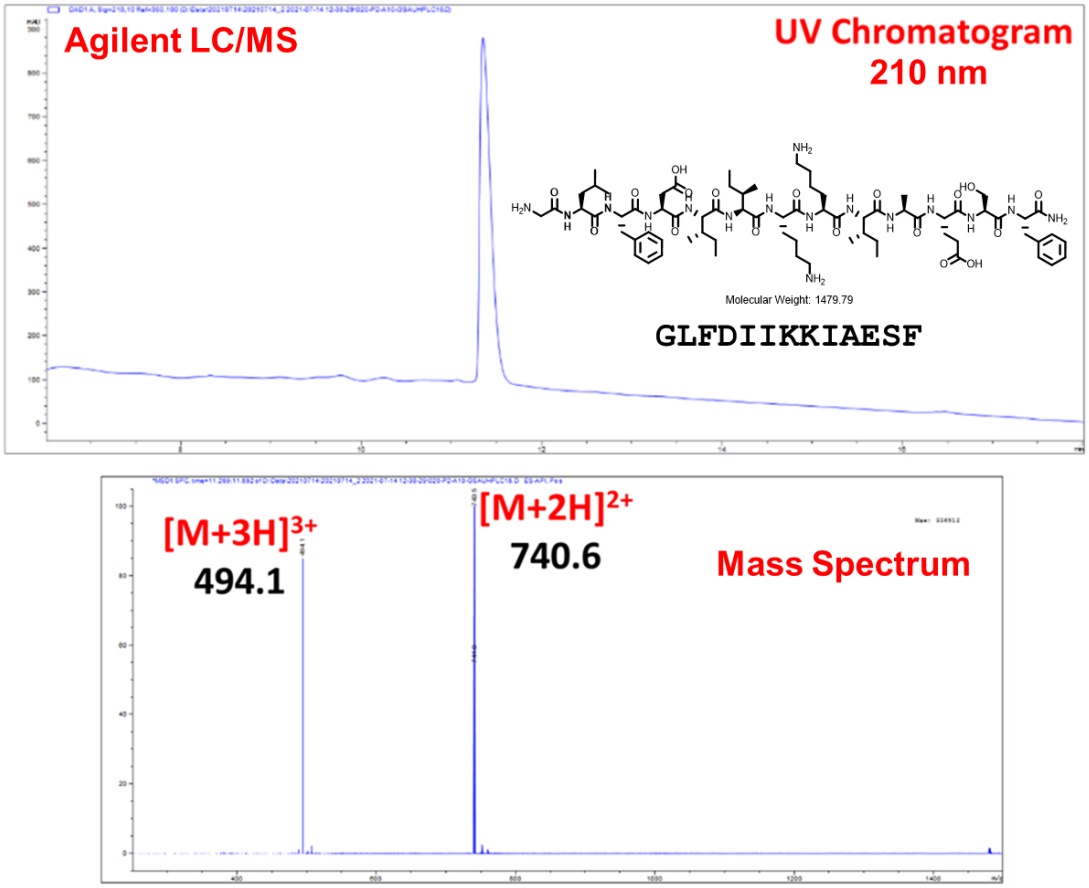

MS Method = Electrospray Ionisation	**Solvent Systems**	**Flow Rate =** 300 µL min^{-1}
Gradient	dH_2O (+ 0.1% $^{V}/_{V}$ formate)	**Injection Volume =** 5 µL
30 - 60% CH_3CN in 30 minutes	CH_3CN (+ 0.1% $^{V}/_{V}$ formate)	**C_{18} Column**

Figure 34 - LC/MS data of HPLC isolated aurein-1.2 (GLFDIIKKIAESF).

Fractions containing aurein-1.2 were analysed using an Agilent LC/MS (**Figure 34**) and the observed $^{M}/_{Z}$ values were 740.6 and 494.1 and these values line up with the expected calculated values corresponding to $[M+2H]^{2+}$ and $[M+3H]^{3+}$ (740.9 and 494.3 respectively).

Folate Labelled

Following production aurein-1.2, a derivative comprised of an *N*-terminal maleimide was constructed for the purpose of Michael addition conjugation to a folic acid tag (**Scheme 13**). A modified folate previously made for sfGFP conjugation (**Figure 16**) was utilised for connection to maleimide labelled aurein-1.2 by exploiting its *C*-terminal cysteine, and this was performed under mild conditions (*i.e.* ammonium bicarbonate buffer pH 6.9, 25°C for 1 hour – **Scheme 13**). This crude Michael addition mixture was freeze dried to remove volatile buffer, and thereafter, processed *via* HPLC under the same conditions used to isolate the native aurein-1.2 sequence. Fractions corresponding to the folate labelled aurein-1.2 were collected and analysed by a Waters synapt LC/MS (**Figure 35**). The observed $^{M}/_{Z}$ values were 691.83, 922.10 and 1382.64, and these figures matched the calculated $[M+4H]^{4+}$, $[M+3H]^{3+}$ and $[M+2H]^{2+}$ values (692.01, 922.34 and 1383.02 respectively). In addition to these $^{M}/_{Z}$ values, unrelated Waters synapt contaminations were found (*i.e.* $^{M}/_{Z}$ 825.14 and 863.75). These contaminants had been found to reside on the Water synapt C_8 LC/MS column. This same HPLC isolate was analysed *via* an Agilent LC/MS and these contaminant species were absent, and thus, present no issues with the HPLC isolated sample which was freeze dried and prepared for testing on mammalian cells.

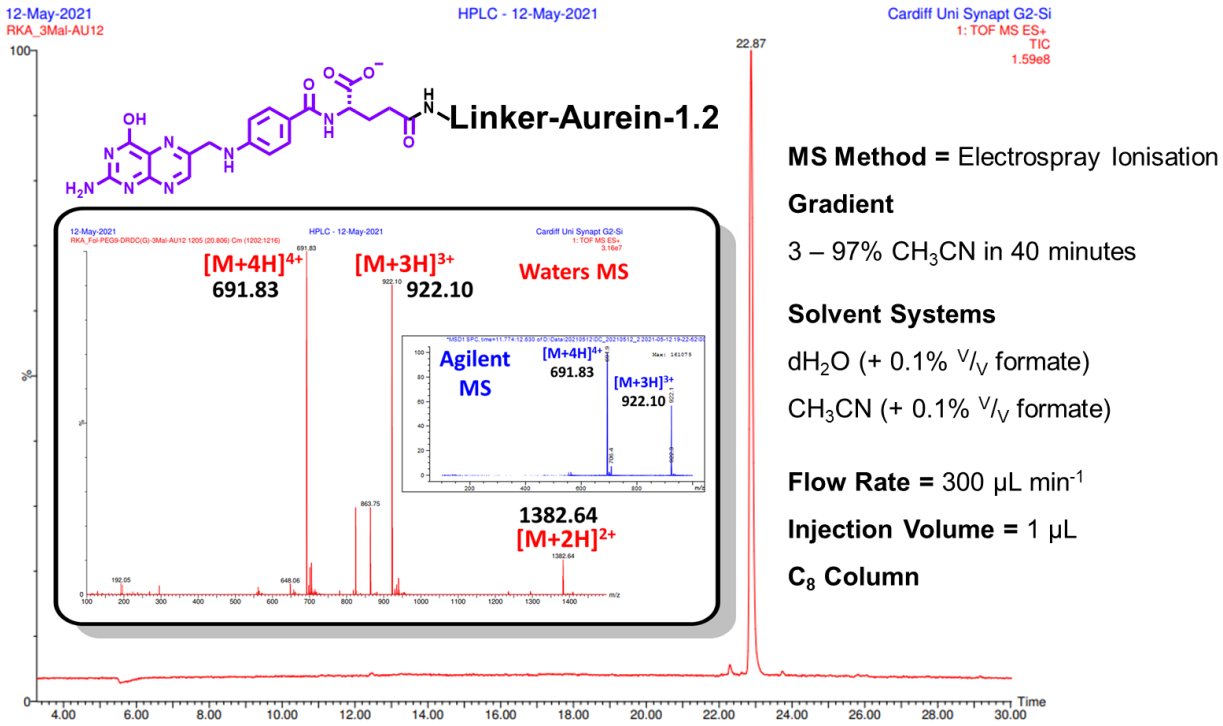

Figure 35 - LC/MS data of HPLC isolated folate labelled aurein-1.2.

4.2.2 Mammalian Cell Culture Experiments

KB cells were chosen as the model malignant system that overproduces FR-α when deprived of free folic acid in folate depleted media, and is therefore, considered FR-α positive under such conditions. On the other hand, a non-malignant cell line considered to be FR-α negative such as HEK293[175,176] was selected as a comparison mammalian system. Both cell lines had been previously used in studies looking at interaction of folate labelled sfGFPs on both cell lines using FACS (**Figure 21**). For testing the activity of folate labelled aurein-1.2 against native aurein-1.2, cell titre blue cell viability assay was used to probe the percentage fluorescence intensity of resorufin, which is directly proportional to the viability of a cell population. Folate labelled aurein-1.2 was tested down to a minimum of 10 nM due to the ability of the folic acid tag granting sfGFP the ability to access FR-α, as found in prior work (**Figure 21**).

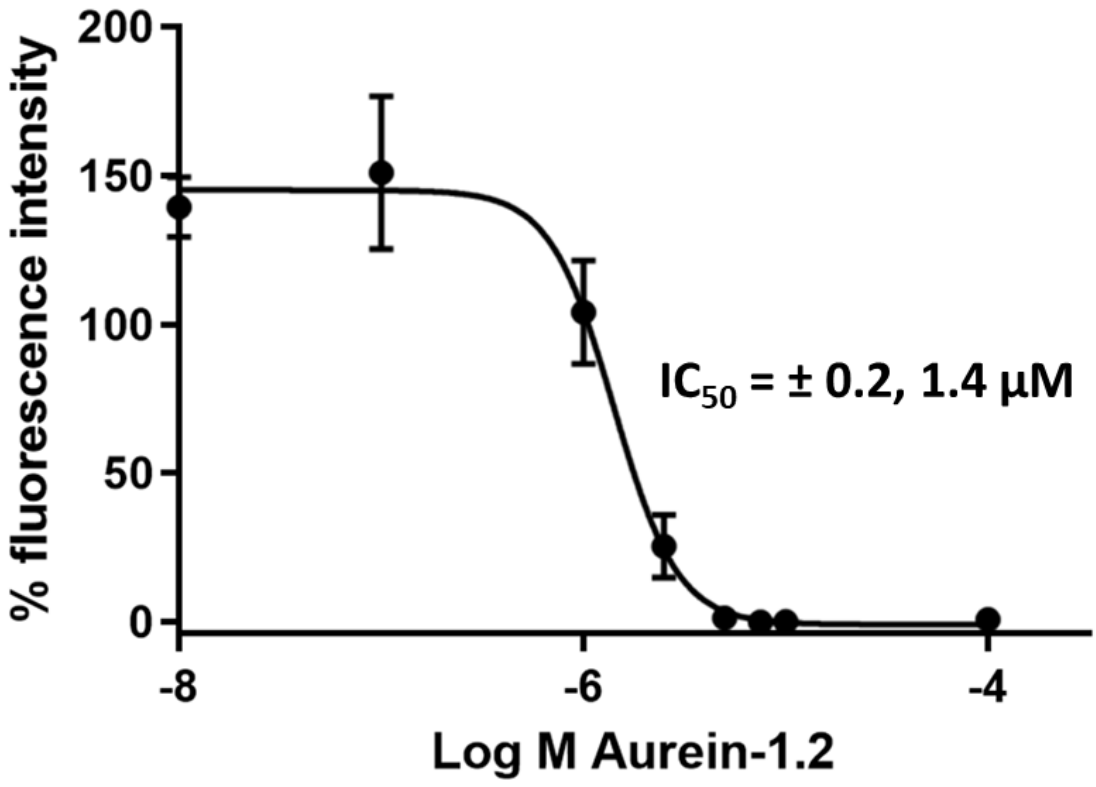

Figure 36 - Aurein-1.2 IC_{50} curve produced from 24-hour incubation on KB cells.

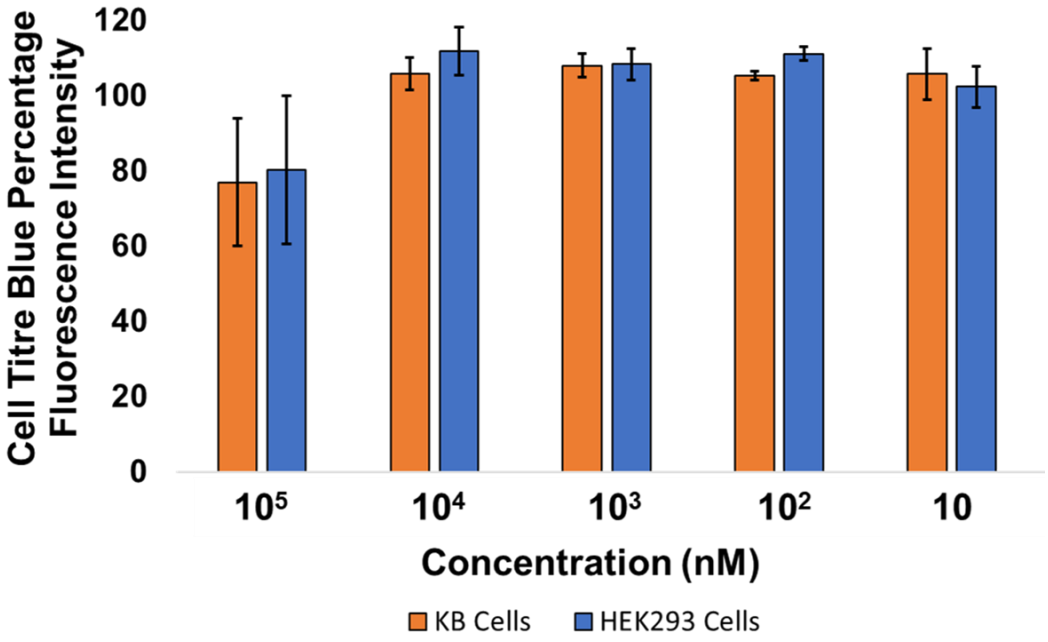

Figure 37 - Folate labelled aurein-1.2 on KB cells and HEK293 cells for 24-hour incubation and cell titre blue cell viability assay used to determine toxicity.

Native aurein-1.2 was tested on KB cells for a 24-hour duration (**Figure 36**), and a corresponding IC_{50} curve was generated providing a value of 1.4 μM which was comparable to values documented in previous research.[129,131] Following this test, folate labelled aurein-1.2 was examined during a 24-hour time frame on cancerous FR-α positive KB cells and non-cancerous FR-α negative HEK293 cells[175,176] side by side for a direct comparison (**Figure 37**). It was discovered that the addition of the folic acid tag to aurein-1.2 rendered the polypeptide non-toxic, and this was likely due to a change in cellular uptake adopted by the modified sequence. Aurein-1.2 was found to initiate cell death by damaging charged membranes, and thus mediate cell death by membrane lysis. It was thought that the folate motif would direct aurein-1.2 towards malign cells, and away from non-cancerous cells, and therefore, only interact with and damage charged malignant cell membranes. However, the inclusion of a folic acid targeting moiety was likely to have redirected the route travelled by the peptide, whereby, the sequence no longer interacted with charged cell membranes. Instead, the modified sequence binds to FR-α and participated in a receptor mediated endocytosis. Because of these results, a peptide with a different primary mechanism of cell death was conjured for combination with a folate tag.

4.3 Bid-BH3

4.3.1 Synthesis of Bid-BH3 Variants

Alternatively, a pro-apoptotic peptide sequence known as Bid-BH3 (EDIIRNIARHLAQVGDSMDR), originating from proteins responsible for initiating intrinsic apoptosis was synthesised in its native sequence, as well as a modified variation containing an *N*-terminal maleimide (**Scheme 13**) destined for Michael addition with the synthetic folate comprised of a *C*-terminal cysteine (**Figure 16**).

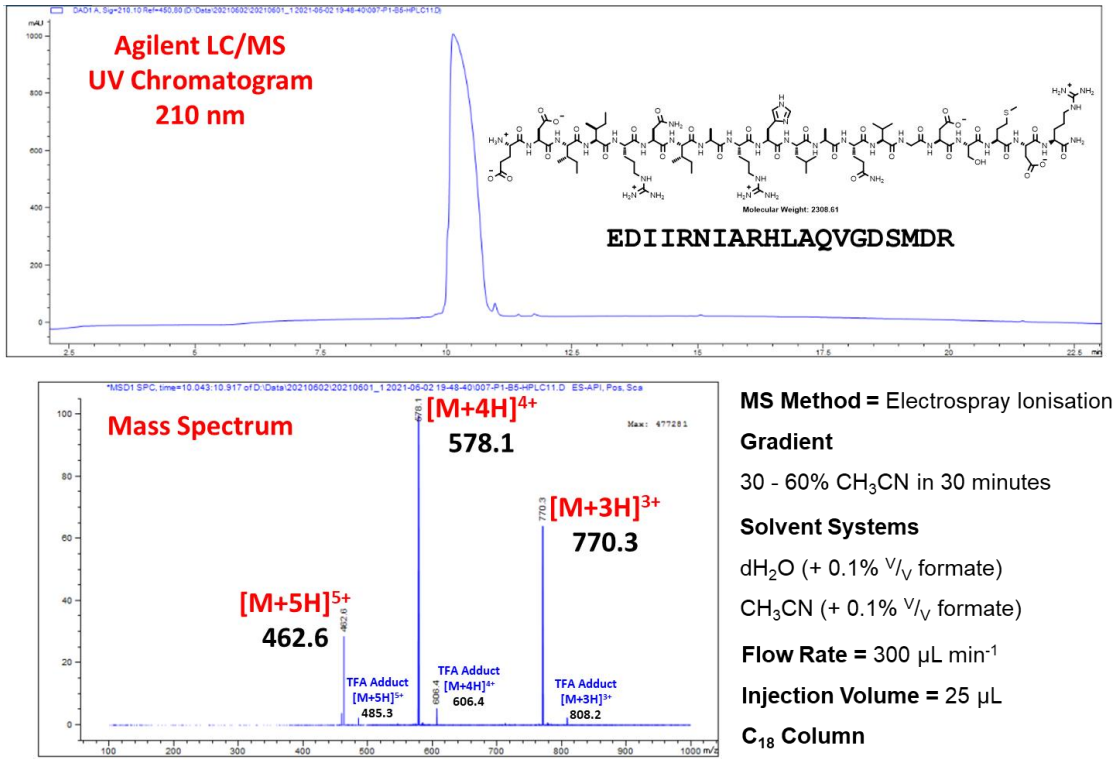

Figure 38 - LC/MS data of HPLC isolated Bid-BH3 (EDIIRNIARHLAQVGDSMDR).

Non-Folate Labelled

Synthesis of Bid-BH3 was carried out using a CEM peptide synthesiser, in the same way production of aurein-1.2 was implemented (**Scheme 13**). Bid-BH3 was stripped from its side chain protecting groups and resin using reagent K as an acid cleavage cocktail. The corresponding crude was subjected to HPLC isolation using a Shimadzu preparation scale C_{18} HPLC column and Shimadzu pump. The solvent system used was acetonitrile and deionised water (+ 0.1% TFA $^{V}/_{V}$) and the gradient selected for this process was 20 – 80% acetonitrile in 60 minutes and the flow rate was 10 mL min^{-1}. Fractions containing the peptide of interest were analysed using an Agilent LC/MS (**Figure 38**) and the observed $^{M}/_{Z}$ were 462.6, 578.1 and 770.3. These values match up closely with the anticipated values of 462.7, 578.2 and 770.5 ($[M+5H]^{5+}$, $[M+4H]^{4+}$ and $[M+3H]^{3+}$ respectively). In addition to the target peptide, a TFA adduct of Bid-BH3 was detected in the HPLC isolated fraction (**Figure 38** – Mass Spectrum $^{M}/_{Z}$ 606.4 $[M+4H]^{4+}$).

Folate Labelled

To accompany the production of native Bid-BH3, an *N*-terminal maleimide derivative was produced, and this was prepared for Michael addition to the same modified folate used for sfGFP and aurein-1.2 conjugation (**Scheme 4** and **13**). Reaction conditions for thiol alkylation were the same as those used for connecting the folic acid tag to maleimide labelled aurein-1.2. The crude material comprised of folate linked to Bid-BH3 was processed *via* HPLC separation, whereby the same equipment and conditions used for obtaining Bid-BH3 was applied to acquire the folic acid conjugated variant. HPLC fractions containing the target sequence were analysed using a Waters synapt LC/MS (**Figure 39**). Observed $^{M}/_{Z}$ values generated were 599.45, 719,14, 898.90 and 1198.20, and these values compared well with the calculated charge states of 599.48, 719.17, 898.72 and 1198.00 ($[M+6H]^{6+}$, $[M+5H]^{5+}$, $[M+4H]^{4+}$, $[M+3H]^{3+}$ respectively). Following the successful isolation of native Bid-BH3 and folate labelled Bid-BH3, both sequences were planned for testing on mammalian cells.

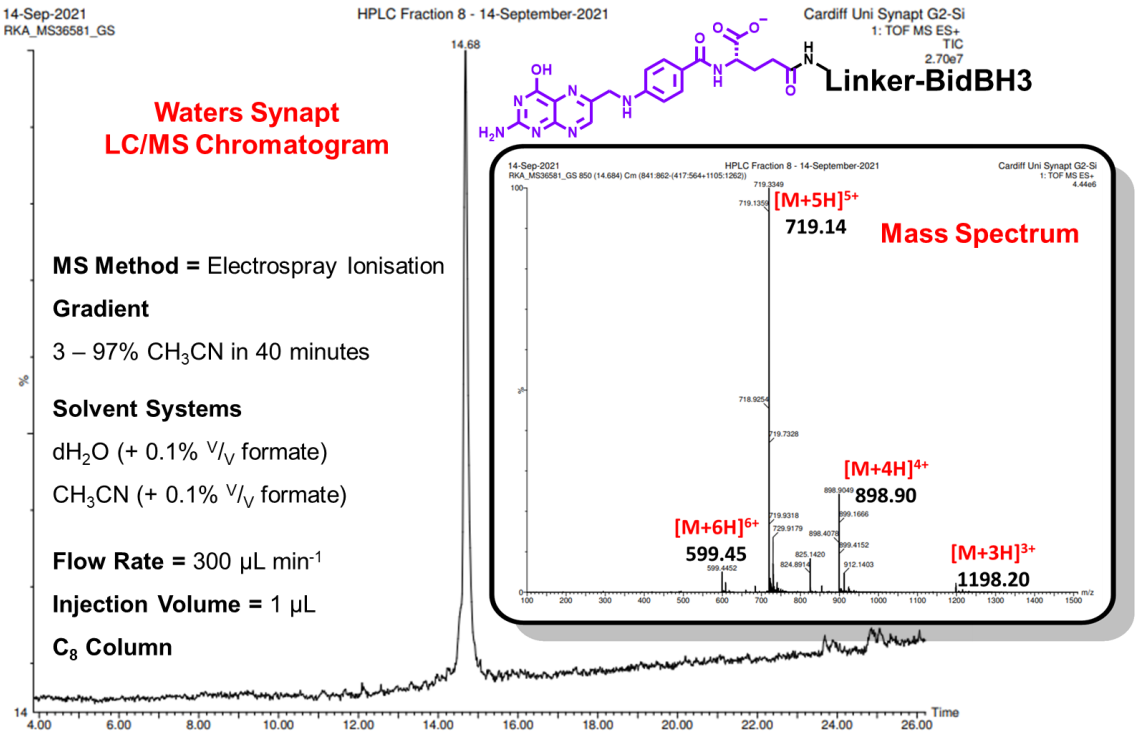

Figure 39 - LC/MS data of HPLC isolated folate labelled Bid-BH3.

4.3.2 Mammalian Cell Culture Experiments

Cell Uptake Assessment using Cell Titre Blue

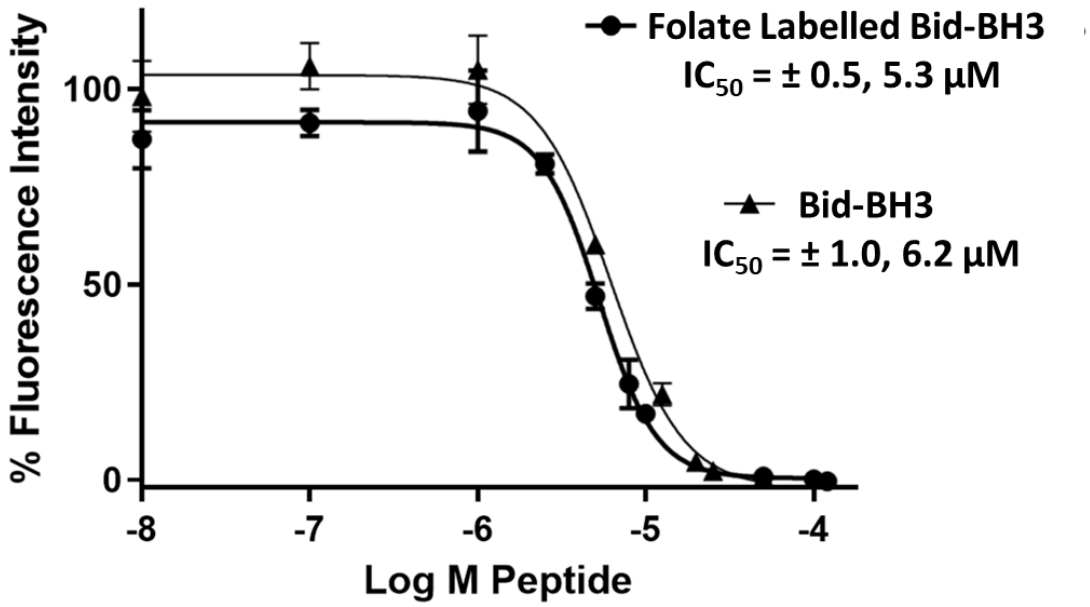

Figure 40 - Folate labelled Bid-BH3 tested against native Bid-BH3 on KB cells for 24-hour incubation.

Folate tagged Bid-BH3 and its native sequence were tested side by side on a single colony of KB cells during a 24-hour incubation period in media depleted of folic acid. Cell titre blue assay was used to investigate the activity of both peptides over a range of concentrations varied from 10 nM and upward (**Figure 40**). From the incubation studies it was discovered that folate labelling Bid-BH3 did not significantly improve cytotoxicity. However, when comparing the result of this study to that performed with a peptide such as aurein-1.2 and its folate tagged derivative, it was evident that the primary mode of cell death was important in selecting a cytotoxic peptide. For sequences that initiate cell death from membrane lysis like aurein-1.2, folate labelling had removed cell killing abilities (**Figure 37**). On the other hand, for a peptide like Bid-BH3 which promotes intrinsic apoptosis, folate labelling did not remove cytotoxicity.

Folic Acid Competitive Inhibition and Comparison with Non-Cancerous Cells

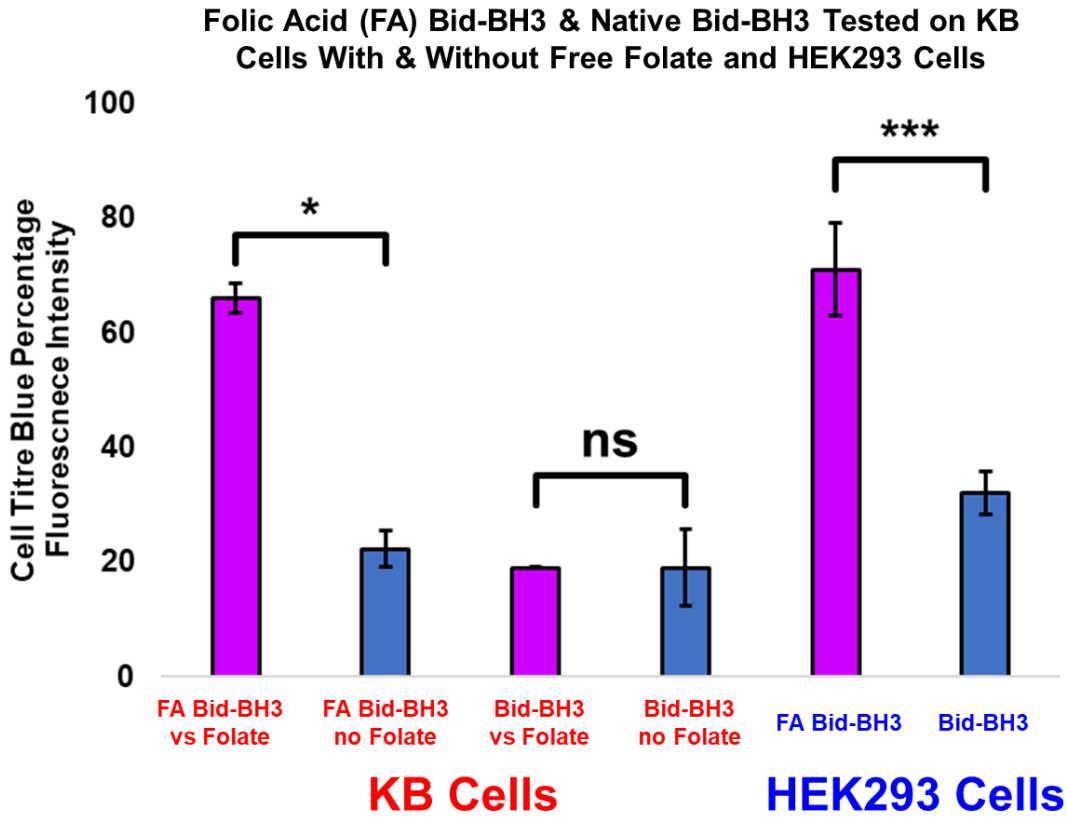

Figure 41 - Folate labelled Bid-BH3 vs native Bid-BH3 (both 5 μM) during 24-hour incubations on KB cells in media containing folic acid and media not containing folic acid, and HEK293 cells (right).

Follow up examinations of the Bid-BH3 peptides were performed at 5 μM (**Figure 41**). Both peptides were examined *via* free folic acid competitive inhibition experiments in media comprised of 9 μM folic acid over 24 hours. To supplement this study, a concurrent 24-hour cell viability test was performed in media depleted of folic acid using the same colony of KB cells (**Figure 41**). Cell titre blue cell viability assay was employed to deduce percentage fluorescence intensity of resorufin from the tested cells. Results from the folic acid inhibition experiments show a significant difference for the folate labelled Bid-BH3 when compared to the native Bid-BH3. In the absence of free folic acid in media, both sequences demonstrated similar toxicity towards KB cells. This result agrees with previous findings made from 24-hour incubation study (**Figure 40**), whereby, both Bid-BH3 peptides had comparable cytotoxicity towards KB cells. However, when free folic acid (9 μM) was introduced, a difference in cytotoxicity was discovered. Addition of free folate in media had no significant effect on the cytotoxicity of native Bid-BH3. However, a pronounced decrease in cytotoxic activity was observed for folate tagged Bid-BH3. This suggests that folic acid was blocking folate Bid-BH3 from accessing FR-α for endocytic uptake, which results in an increased viability of the cell population. Nevertheless, approximately one third of the cancer cells had died and this was likely caused by some folate Bid-BH3 outcompeting free folic acid for interacting with FR-α. This phenomenon was observed in prior competitive inhibitions experiments *via* FACS using folate labelled sfGFPs (**Figure 21**). Moreover, off site activity mediated by the cytotoxic peptide was likely causing unwanted cell death. An attempt was made to investigate this issue, HEK293 cells which were used in prior experiments as a FR-α negative cell line[175,176] (**Figure 21**), was employed again for the same purpose. Bid-BH3 peptides were tested side by side at 5 μM on these non-cancerous cells for 24-hours (**Figure 41 – Right**). Results obtained from these cells mirror the results generated from the folic acid inhibition tests, therefore, suggesting that off-site activity was likely to have mediated cell death in the absence of FR-α.

Chapter 5: Conclusions and Future Work

The addition of a folic acid tag (**Scheme 1** and **Figure 19**) was shown to be effective at altering the behaviour and targeting ability of polypeptides. For example, sfGFP was previously unable to interact with FR-α on KB cells before folic acid modification. However, after folic acid labelling, sfGFP was granted the ability to bind at concentrations as low as 10 nM according to FACS results (**Figure 21**). Changes to natural cell killing properties were observed in small cytotoxic peptides such as aurein-1.2 and Bid-BH3. Folate labelled aurein-1.2 was rendered non-toxic compared to its native sequence (**Figure 36** and **37**) which is known to initiate cell death by targeting and damaging charged membranes. Folic acid modification had likely re-routed aurein-1.2 away from its intended target and towards FR-α for endocytosis. To accompany this study, another sequence with a different cell killing mechanism was examined. Bid-BH3 which is known to facilitate intrinsic apoptosis, was labelled with folic acid and found to be equally as toxic as its native sequence (**Figure 40**). Folic acid competitive inhibitions assays performed with both Bid-BH3 peptides (*e.g.* folate labelled and native sequence) highlighted a pronounced difference in cell viability (**Figure 41**). Free folate actively blocked folate Bid-BH3 from accessing FR-α, however, this competitive inhibition experiment would show that approximately one third of the cell population was dead. This was likely caused by some folate Bid-BH3 binding to FR-α despite the presence of the higher affinity folic acid, or membrane permeation of the modified Bid-BH3 sequence had caused offsite activity, and thus, circumvent FR-α endocytosis. An additional study was performed on HEK293 cells, and an identical result was obtained whereby approximately one third of cells had died. These results combined show that folic acid labelling can direct large and small polypeptides towards FR-α, as demonstrated by FACS (**Figure 21**) and cell titre blue cell viability assay results (**Figure 36** – **41**). Interaction with FR-α is the dominant interaction mechanism of large and small polypeptides modified with folic acid. Additionally, for attempting to selectively destroy cancer cells, the mechanism of cell death, and henceforth, biological target of cytotoxic peptide is important. An issue highlighted with these examinations (**Figure 40** and **41**) is that peptides like Bid-BH3 before folic acid modification is toxic. An ideal cargo is one which is non-toxic before folic acid modification and possesses no ability to move past the cell membrane. The original premise of this research study was to employ large cytotoxic polypeptides for selective delivery into cancer cells *via* FR-α and mediate cell death. Potential candidates that can be exploited for this work are large molecular weight species like type I ribosome inactivating proteins such as momordin.[91,156] Previous research had demonstrated that these proteins lack sufficient cell killing ability without a route of entry, and even after folic acid modification, momordin based conjugates suffered

from endosome entrapment due to their large size and charge.[91,156] Efforts had been made to synthesise CPP sequences comprised of folic acid and a maleimide for Michael addition conjugation to sfGFP (**Scheme 6**, **10** and **12**). It was thought the modified CPP with folate would guide a protein cargo towards cells overproducing FR-α and highjack the corresponding endocytic pathway. Once the desired construct was trafficked into the cell the conjugate would utilise the CPP for translocation into the cytosolic space, and therefore, allow the protein to mediate its biological activity. Synthesis and isolation of these modified folates (**Figure 28** and **32**) was difficult due to peptide truncations and other co-eluting species isolated alongside the target peptide *via* HPLC. Despite these difficulties involving folic acid peptide bond formation on resin, an alternative synthetic strategy could be adopted for future work, whereby, folate can be installed onto a CPP like aurein-1.2 on the N-terminus which was previously performed (**Scheme 13** and **Figure 32**) and a hydrazide can be connected to the *C*-terminus of the peptide for native chemical ligation to a protein (**Scheme 14**).[200]

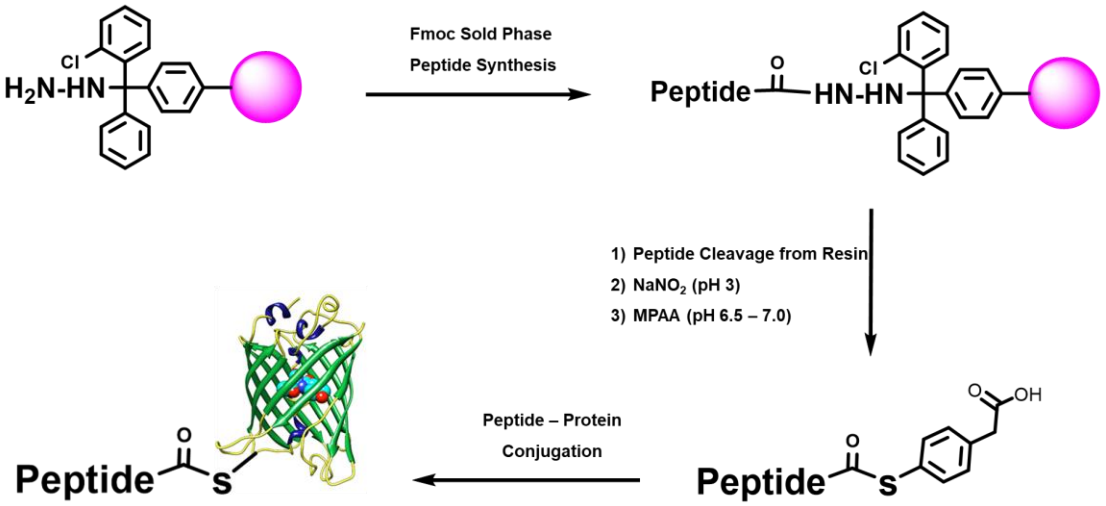

Scheme 14 - Utilising native chemical ligation for labelling a protein with a CPP.

Aside from further CPP synthesis, a protein comprised of a folate label can be used to exploit FR-α mediated endocytosis (**Figure 21**). Issues such as vesicular entrapment remain, however, methods involving light activated magnetic proteins, that when dimerised can induce lysosome and mitochondrial membrane fusion. This process can be exploited to aid selective delivery of a protein into specific cellular compartments.[100] Folate labelled sfGFP can be used to visualise such a process *via* con-focal microscopy to see the location of green fluorescence, and once this system is established, sfGFP can be substituted for a protein such as momordin, which is toxic when it has moved past a biological membrane. Therefore, this system has potential to induce apoptosis by destroying mitochondrial ribosomes. In addition to this route of research, transcription factors can be labelled with folate and used for targeting and delivery to induce effects other than cell death such as changes to cell characteristics such as proliferation and size.[201,202]

Chapter 6: Materials and Methods

6.1 Organic Chemical Synthesis of Peptides

A catalogue of peptide sequences, capped with and without pterins such as folic acid were produced using a combination of manual and automated synthetic techniques. In this chapter the materials (chemicals and apparatus) and methods (*e.g.* SPPS, HPLC and LC/MS) used to generate these peptides will be discussed.

6.1.1 Manual Solid Phase Peptide Synthesis of Pterin Labelled Peptides

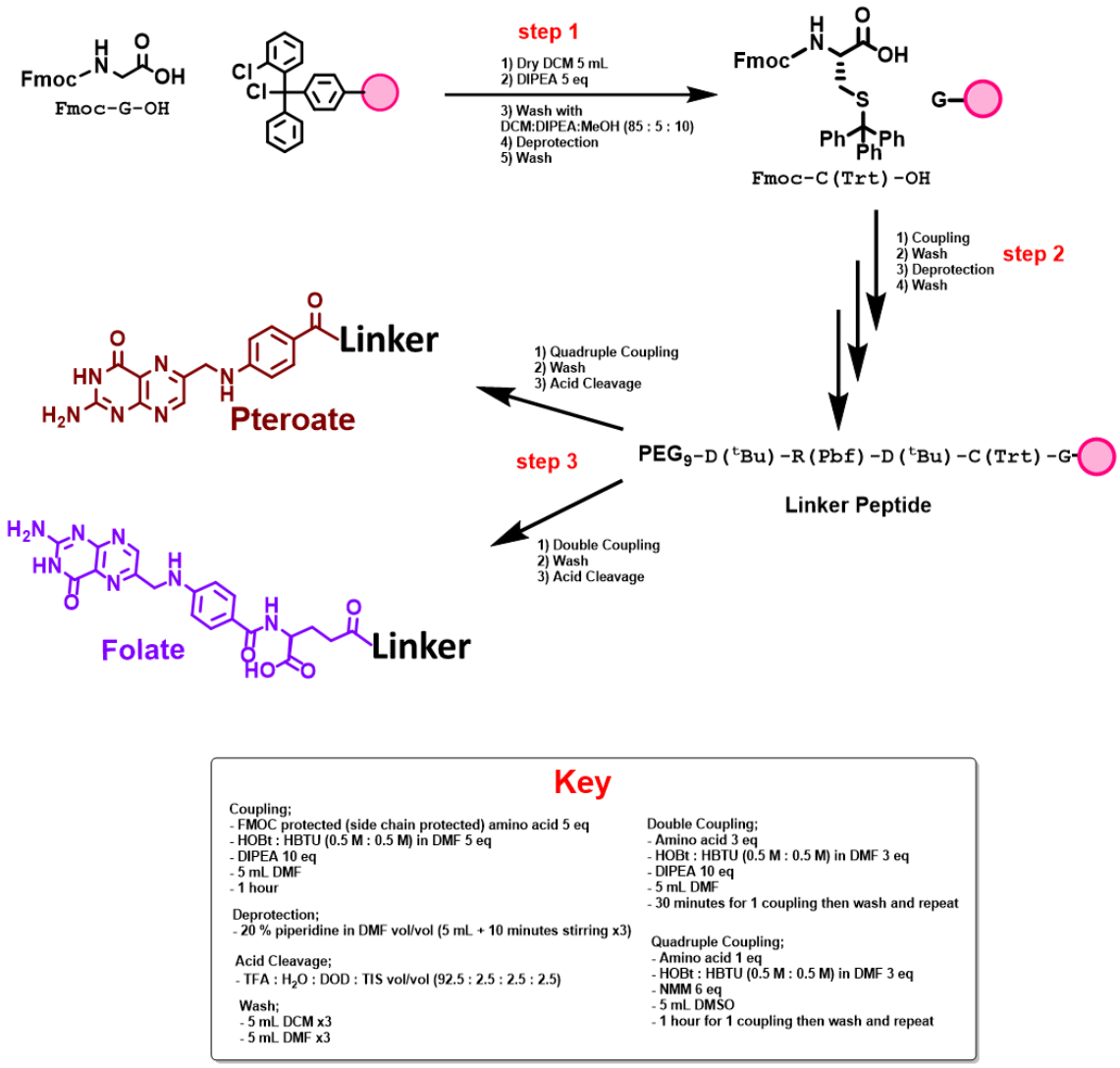

Key

Coupling;
- FMOC protected (side chain protected) amino acid 5 eq
- HOBt : HBTU (0.5 M : 0.5 M) in DMF 5 eq
- DIPEA 10 eq
- 5 mL DMF
- 1 hour

Deprotection;
- 20 % piperidine in DMF vol/vol (5 mL + 10 minutes stirring x3)

Acid Cleavage;
- TFA : H_2O : DOD : TIS vol/vol (92.5 : 2.5 : 2.5 : 2.5)

Wash;
- 5 mL DCM x3
- 5 mL DMF x3

Double Coupling;
- Amino acid 3 eq
- HOBt : HBTU (0.5 M : 0.5 M) in DMF 3 eq
- DIPEA 10 eq
- 5 mL DMF
- 30 minutes for 1 coupling then wash and repeat

Quadruple Coupling;
- Amino acid 1 eq
- HOBt : HBTU (0.5 M : 0.5 M) in DMF 3 eq
- NMM 6 eq
- 5 mL DMSO
- 1 hour for 1 coupling then wash and repeat

Scheme 15 - Fmoc SPPS scheme showing reactions encapsulating the synthetic route followed for Folate tagged peptide A and pteroate tagged peptide B (Scheme 1).

Resin Coupling and First Fmoc Deprotection

Scheme 2, Step 1

Dry DCM was prepared by addition of $MgSO_4$ to DCM and provided 15 minutes to remove water making this solvent sufficiently dry for purpose. $MgSO_4$ was filtered *via* funnel and filter paper to separate anhydrous DCM into a conical flask. This dry solvent (5 mL) was used in conjunction with DIPEA to solubilise Fmoc-Gly-OH. The mixture was then added to a Kenesis polypropylene syringe filter filled with 2-chlorotrityl chloride resin (loading = 1.32 mmol g^{-1}) and was left to stir for four hours. After this time, the reaction mixture was connected to a filtration pump (20 mbar) to remove solution phase materials. The resin was washed with a solution of DCM, DIPEA and methanol (85% : 5% : 10% $^{V}/_{V}$) followed by washes with DCM (5 mL x 3) and DMF (3 x 5 mL). A mixture of 20% piperidine $^{V}/_{V}$ in DMF (5 mL) was used for removing the Fmoc protecting group in three 10-minute cycles, and thus, exposing the α-amine of glycine for peptide bond formation.

Chemical	Company	Lot #	Mass	Volume	Mol	Eq
Fmoc-Gly-OH	Cambridge Reagents	AG771160216	120 mg	NA	0.4 mmol	2
DIPEA		AG10251525	NA	280 µL	1.6 mmol	8
2-Chlorotrityl Chloride Resin	Novabiochem	S7423817	150 mg	NA	0.2 mmol	1
$MgSO_4$	Fisher Scientific	1865567	5 g	NA		
DCM		1862579	NA	4 x 5 mL	NA	
Methanol		2029545		NA		
Piperidine	Alfa Aesar	10209545		3 x 1 mL		
DMF	Acros Organics	1854072		3 x 4 mL, & 3 x 5 mL		

Table 3 - Chemicals and quantities used for 2-chlorotrityl chloride resin loading and Fmoc deprotection.

Amino Acid Coupling and Fmoc Deprotection Cycles

Scheme 2, Step 2

Fmoc protected amino acid was solubilised in a combination of DIPEA in DMF and added to a Kenesis polypropylene syringe filter filled with amino acid bound resin. This suspension was homogenised by stirring, and a solution comprised of HBTU/HOBt (0.5 M : 0.5 M) in DMF was added to initiate peptide bond formation. This reaction mixture was given one hour before the solution was separated from resin *via* vacuum filtration using a 20-mbar pump. Solvents such as DCM and DMF were used to wash the resin before subjecting it to 20% piperidine $^{V}/_{V}$ in DMF for three 10 minutes cycles. Additional washes were performed using DCM and DMF to ensure all piperidine was removed, and the next Fmoc protected amino acid was prepared for the same peptide bond formation procedure. This cycle of amino acid coupling and Fmoc deprotection was repeated until the first five amino acids were connected, with the *N*-terminal α-amine exposed for Fmoc-PEG_9-OH addition.

Chemical	Company	Lot #	Mass	Volume	Mol	Eq
Fmoc-Cys(trt)-OH	AGCT Bioproducts	AG11031135202	586 mg	NA	1.0 mmol	5
Fmoc-Arg(Pbf)-OH	Cambridge Reagents	AG00132160725	650 mg			
Fmoc-Asp(^{t}Bu)-OH		AG00174160417	2 x 412 mg			
HBTU		AGA00801171228	NA	10 mL		
HOBt		AG805160322				
DIPEA		AG10251525		871 µL	5.0 mmol	25
Piperidine	Alfa Aesar	10209545		3 mL	NA	
DMF	Acros Organics	1854072		10 mL		
DCM	Fisher Scientific	1862579		15 mL		

Table 4 - Chemicals and quantities used for amino acid coupling and Fmoc deprotection cycles.

PEG_9 Addition

Scheme 2, Step 2

Addition of Fmoc protected PEG_9 and removal the α-amine Fmoc group was performed using an identical procedure employed for connecting the first five amino acids (**see Scheme 2, Steps 2**).

Chemical	Company	Lot #	Mass	Volume	Mol	Eq
Fmoc-PEG_9-OH	Apollo scientific	A5474276	385 mg	NA	1.0 mmol	5
HBTU	Cambridge Reagents	AGA00801171228	NA	10 mL	1.1 mmol	5.1
HOBt		AG805160322				
DIPEA		AG10251525		871 µL	5.0 mmol	25
Piperidine	Alfa Aesar	10209545		3 mL	NA	
DMF	Acros Organics	1854072		10 mL		
DCM	Fisher Scientific	1862579		15 mL		

Table 5 - Chemicals and quantities used for PEG_9 coupling of DRDCG.

Pteroic Acid Coupling

Scheme 2, Step 3

To a glass vial containing a magnetic stirrer bar, pteroic acid was added into a mixture of DMSO with NMM and HOBt.H_2O : HBTU (0.5 M : 0.5 M in DMF). This mixture was given 5 minutes to stir vigorously over a magnetic hot plate at room temperature, and thus, allowing for the maximum quantity of pteroate to solubilise. This was then added into a polypropylene syringe filter containing peptide bound resin and was given 1 hour for peptide bond formation. After 60 minutes, solution was filtered *via* vacuum pump (20 mbar) and the resin was thouroughly washed with organic solvents (DMSO 3 x 5 mL, DCM 3 x 5 mL and DMF 3 x 5 mL) before three additional repeat cycles of pteroic acid coupling was performed. Overall, pteroate was quadruple coupled onto the N-terminus of the peptide due to its lack of organic solvent solubility. A final organic solvent wash was performed (DMSO 3 x 5 mL, DCM 3 x 5 mL and DMF 3 x 5 mL) before subjecting the resin to acid cleavage protocol.

Chemical	Company	Lot #	Mass	Volume	Mol	Eq
Pteroic Acid	Apollo scientific	AS477835	82 mg	NA	0.3 mmol	3
HBTU	Cambridge Reagents	AGA00801171228	NA	1.58 mL	0.9 mmol	9
HOBt.H_2O		AG805160322				
NMM	Sigma Aldrich	DR10526CR	160 mg	174 µL	1.8 mmol	18
DMSO	Alfa Aesar	10197581	NA	4 mL	NA	
DCM	Fisher Scientific	1862579	NA		NA	
DMF		1854072				

Table 6 - Chemicals and quantities used for pteroic acid coupling of PEG_9-DRDCG.

Acid Cleavage

Scheme 2, Step 3

A solution of 92.5% TFA, 2.5% DOD, 2.5% dH_2O and 2.5% TIS $^{V}/_{V}$ (4 mL) was prepared and added to the resin for peptide deprotection, and this was given 1 hour. After time, a yellow solution evolved and was transferred drop wise from the polypropylene filter into a 50 mL falcon tube filled with cold diethyl ether (40 mL). This produced a yellow flocculate which was subjected to centrifugation (Centrifuge-5810 – 4000 rpm, 4°C, 2 minutes) yielding a pale-yellow pellet. Diethyl ether was removed *via* decantation and a gentle stream of nitrogen was used to dry the crude peptide.

Chemical	Company	Lot #	Mass	Volume	Mol	Eq
TFA	Fluorochem	FCB009271	NA	3.7 mL	NA	
dH_2O	NA			100 µL		
DOD	Sigma Aldrich	03607AJ				
TIS	Acros Organics	A0357983		100 µL		
Diethyl Ether	Fisher Scientific	1852837		40 mL		

Table 7 - Chemicals and quantities for acid cleavage of pteroate capped PEG_9-DRDCG.

HPLC Isolation

Bicarbonate (10 mM) buffer solution was prepared by adding ammonium bicarbonate to a Schott bottle filled with 1 L of dH_2O. This buffer solution and a bottle of acetonitrile (2.5 L) were connected to a preparation scale dionex HPLC pump which was connected to a supelcosil™ PLC-18 column (dimensions 25 cm x 21.2 mm, 12 µm particle size) and a 5 mL loop. A gradient was selected (1 - 60% acetonitrile in 60 minutes), flow rate was set to 10 mL min^{-1} and the column pressure during the isolation procedure was 44 bar. Target peptide was collected manually and had eluted with a retention time of 25 minutes. The fraction containing the isolated analyte of interest was analysed using a bruker LC-MS.

$^{M}/_{Z}$ = 1004.6 [M+1] and 502.8 [M+2]

R_t = 25 minutes

Chemical	Company	Lot #	Mass	Volume	Mol	Eq
NH_4HCO_3	Acros Organics	A0383847	790 mg	NA	10 mmol	NA
CH_3CN	Fisher Scientific	1851873	NA	2.5 L	NA	
H_2O	NA			1 L		

Table 8 - Chemicals used for HPLC isolation of pteroate capped PEG9-DRDCG.

Folic Acid Coupling

Scheme 2, Step 3

To a glass vial containing a magnetic stirrer bar, folic acid was added into a mixture of DMSO with DIPEA and HOBt : HBTU (0.5 M : 0.5 M in DMF). This mixture was given 5 minutes to stir vigorously over a magnetic hot plate at room temperature, and thus, fully solubilising folate into the organic solvent. This was then added into a polypropylene syringe filter containing peptide bound resin and was given 1 hour for peptide bond formation. After 60 minutes, solution was filtered *via* vacuum pump (20 mbar) and the resin was thouroughly washed with organic solvents (DMSO 3 x 5 mL, DCM 3 x 5 mL and DMF 3 x 5 mL) before one additional repeat cycle of folic acid coupling was performed. Once folic acid double coupling was complete, the resin was washed with organic solvent before performing acid cleavage (DMSO 3 x 5 mL, DCM 3 x 5 mL and DMF 3 x 5 mL).

Chemical	Company	Lot #	Mass	Volume	Mol	Eq
Folic Acid	Apollo Scientific	AS455409	88 mg	NA	0.2 mmol	2
$HOBt.H_2O$	Cambridge Reagents	AG805160322	NA	400 µL		
HBTU		AGA00801171228				
DIPEA		AG10251525		200 µL	1.0 mmol	10
DMSO	Alfa Aesar	10197581		5 mL	NA	
DCM	Fisher Scientific	1862579		NA		
DMF		1854072				

Table 9 - Chemicals and quantities used for folic acid coupling of PEG_9-DRDCG.

Acid Cleavage

Scheme 2, Step 3

Resin and side chain protecting group cleavage protocol applied was identical to the prior procedure followed. Please see 6.1.1 - acid cleavage for detail.

Chemical	Company	Lot #	Mass	Volume	Mol	Eq
TFA	Fluorochem	FCB009271	NA	3.7 mL	NA	
dH_2O	NA					
DOD	Sigma Aldrich	SHBH9681		100 µL		
TIS	Acros Organics	A0389936		100 µL		
Diethyl Ether	Fisher Scientific	1852837		1 mL		

Table 10 - Chemicals and quantities for acid cleavage of folate capped PEG_9-DRDCG.

HPLC Isolation

Preparation scale HPLC isolation protocol applied for obtaining folate labelled peptide was identical to the prior procedure followed. Please see 6.1.1 - HPLC Isolation for detail.

$^{M}/_{Z}$ = 1133.8 $[M+H]^+$ and 567.3 $[M+2H]^{2+}$

R_t = 20 – 22 minutes

Chemical	Company	Lot #	Mass	Volume	Mol	Eq
NH_4HCO_3	Acros Organics	A0383847	790 mg	NA	10 mmol	NA
CH_3CN	Fisher Scientific	1851873	NA	2.5 L	NA	
dH_2O	NA			1 L		

Table 11 - Chemicals used for HPLC isolation of folate capped PEG_9-DRDCG.

6.1.2 Manual Solid Phase Peptide Synthesis of Cyclic TAT

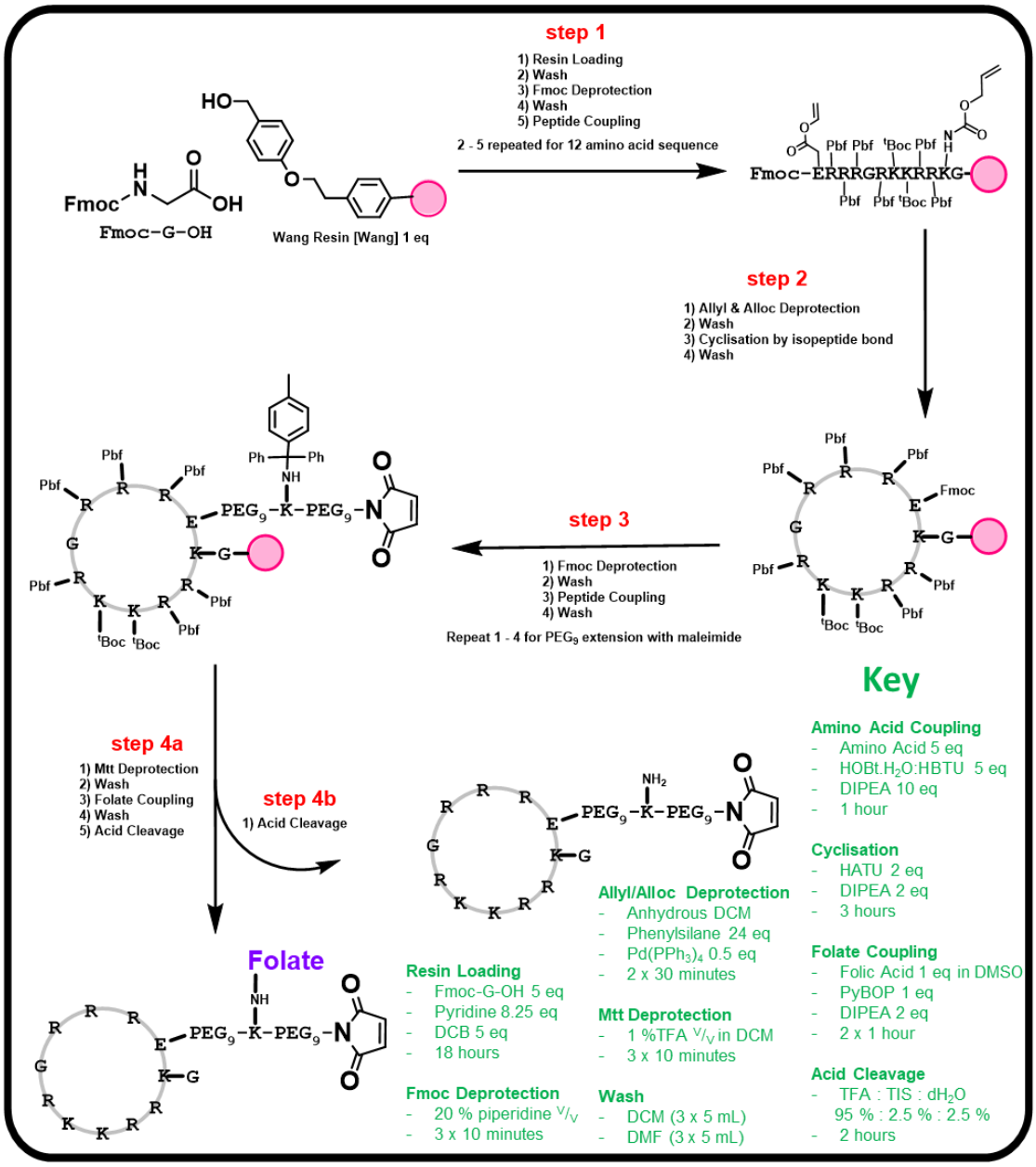

Scheme 16 - Modified cyclic TAT synthetic route.

Resin Coupling

Scheme 6, Step 1 (1 – 2)

Wang resin was placed in a Kenesis polypropylene syringe filter containing a magnetic stirrer bar and suspended over a magnetic hot plate. DMF (10 mL) was added to swell the resin, and the stirrer bar was used to homogenise the suspension by switching on the magnetic hot plate without heating. To the swirling suspension, a mixture comprised of Fmoc-Gly-OH solubilised in DMF and pyridine was introduced, followed by DCB. The reaction system was provided with 18 hours to mix before the solution was drained *via* vacuum filtration (20 mbar) and additional washes with DCM (3 x 5 mL) and DMF (3 x 5 mL) were applied to clean the resin.

Chemical	Company	Lot #	Mass	Volume	Mol	Eq
Wang Resin (200 – 400 mesh) 0.6 – 1.0 mmol g^{-1}	Sigma Aldrich	BCBW8903	300 mg	NA	0.3 mmol	1
Fmoc-Gly-OH	Fluorochem	FCB024870	446 mg		1.5 mmol	5
2,6-Dichlorobenzoyl Chloride (DCB)	Sigma Aldrich	EQ 02514JZ	NA	215 µL	1.5 mmol	5
Pyridine	Acros Organics	1706304		200 µL	2.48 mmol	8.25
DMF	Fisher Scientific	1994431		10 mL, 3 x 5 mL	NA	
DCM		1862579		3 x 5 mL		

Table 12 - Chemicals and quantities used for Wang resin loading.

Amino Acid Coupling and Fmoc Deprotection Cycles

Scheme 6, Step 1 (3 – 5)

Fmoc protected amino acid (2.5 eq) was solubilised in a combination of DIPEA (25 eq) in DMF and added to a Kenesis polypropylene syringe filter filled with resin. This suspension was homogenised by stirring, and a solution comprised of HBTU/HOBt (0.5 M : 0.5 M) in DMF (5.2 eq) was added to initiate peptide bond formation. This reaction mixture was given one hour before the solution was separated from resin *via* vacuum filtration using a 20-mbar pump. Solvents such as DCM (3 x 5 mL) and DMF (3 x 5 mL) were used to wash the resin before subjecting it to 20% piperidine $^{V}/_{V}$ in DMF for three 10-minute cycles (3 x 5 mL). Additional washes were performed using DCM and DMF to ensure all piperidine was removed, and the next Fmoc protected amino acid was prepared for the same peptide bond formation procedure. This cycle of amino acid coupling and Fmoc deprotection would be repeated to generate the desired 12 amino acid peptide on resin.

Chemical	Company	Lot #	Mass	Volume	Mol	Eq
Fmoc-Lys(Alloc)-OH	Fluorochem	FCC21343	339.5 mg	NA	0.75 mmol	2.5
Fmoc-Glu(O'All)-OH		FCC2009651	307 mg			
Fmoc-Arg(Pbf)-OH		FCB076776	486.5 mg			
Fmoc-D-Arg(Pbf)-OH		FCC2010055	486.5 mg			
Fmoc-D-Lys-(^{t}Boc)-OH		140430	351.5 mg			
HOBt.H_2O		FCB046763	NA	3.12 mL	1.56 mmol	5.2
HBTU		FC13052124				
DIPEA		FCB086379		1.31 mL	7.5 mmol	25
Fmoc-Lys-(^{t}Boc)-OH	Sigma Aldrich	BCB40540		NA	0.75 mmol	2.5
Fmoc-Gly-OH		BCBW7470				
Piperidine		STBH7898		NA		
DMF	Fisher Scientific	1994431				
DCM		1998076				

Table 13 - Chemicals and quantities for amino acid coupling and Fmoc deprotection cycles to assemble modified TAT sequence.

Allyl and Alloc Ester Deprotection

Scheme 6, Step 2 (1 – 2)

Peptide bound resin was removed from the Kenesis polypropylene syringe filter and placed into a cleaned and dried 100 mL glass round bottom flask with a magnetic stirrer bar. This apparatus was held above a magnetic hot plate *via* clamp and stand. A rubber septum was used to seal the neck of the flask and a vacuum pump (20 mbar) was used to remove air from the flask. Argon was added to the flask by using a balloon connected to a needle which was used to pierce the rubber septum, maintaining its airtight seal. Anhydrous DCM was introduced to the resin and given 5 minutes to swell/stir. Phenylsilane was added to the suspension, followed by $Pd(PPh_3)_4$ solubilised in anhydrous DCM. The reaction flask was covered in foil to prevent light induced side reactions and provided with 30 minutes before a second repeat cycle was performed. Resin washes with DMF and DCM were performed between cycles whereby the resin was reintroduced temporarily into a polypropylene syringe filter, and a vacuum pump (20 mbar) was used to remove unwanted material.

Chemical	Company	Lot #	Mass	Volume	Mol	Eq
$Pd(PPh_3)_4$	Sigma Aldrich	SHBB5334V	173 mg	NA	0.15 mmol	0.5
Phenylsilane	Fluorochem	FCB030491	NA	887 µL	7.2 mmol	24
Anhydrous DCM	Acros Organics	1998076		NA		
DMF	Fisher Scientific	1994431				

Table 14 - Chemicals and quantities used for allyl and alloc ester deprotection of *N*-terminal glutamate, and *C*-terminal lysine added to TAT.

On Resin Intramolecular Peptide Cyclisation

Scheme 6, Step 2 (3 – 4)

Following the removal of orthogonal protecting groups, the resin was reintroduced to a Kenesis polypropylene syringe filter. A magnetic stirrer bar was placed into the syringe filter along with the resin and this system was suspended above a magnetic hot plate. DMF was used to swell the resin, whilst the stirrer bar homogenised the suspension. A mixture of HATU solubilised in DMF and DIPEA was introduced to the suspension and this reaction system was provided with 2.5 hours for completion. After sufficient time for peptide cyclisation had passed, the resin was washed with organic solvents (DCM 3 x 5 mL and DMF 3 x 5 mL).

<table>
<tr><th>Chemical</th><th>Company</th><th>Lot #</th><th>Mass</th><th>Volume</th><th>Mol</th><th>Eq</th></tr>
<tr><td>HATU</td><td rowspan="2">Fluorochem</td><td>FCB084736</td><td>114 mg</td><td>NA</td><td rowspan="2">0.3 mmol</td><td rowspan="2">1</td></tr>
<tr><td>DIPEA</td><td>FCB086379</td><td rowspan="3">NA</td><td>52 µL</td></tr>
<tr><td>DMF</td><td rowspan="2">Fisher Scientific</td><td>1994431</td><td rowspan="2">NA</td><td rowspan="2">NA</td></tr>
<tr><td>DCM</td><td>1862579</td></tr>
</table>

Table 15 - Chemicals and quantities used for on resin intramolecular peptide cyclisation of TAT.

Conjugatable Linear Extension and Final Fmoc Deprotection Reactions

Scheme 6, Step 3 (1 – 4)

Addition of Fmoc protected PEG_9, Fmoc-Lys(Mtt)-OH and *3*-maleimidopropionic acid, as well as Fmoc deprotection was performed using an identical procedure to that applied for connecting the first 12 amino acids (**see Scheme 6, Step 1, 3 – 5**).

Chemical	Company	Lot #	Mass	Volume	Mol	Eq
3-Maleimidopropionic acid	Fluorochem	FCC2010214	127 mg	NA	0.75 mmol	2.5
Fmoc-Lys(Mtt)-OH		FCB060379	469 mg			
Fmoc-PEG_9-OH		FCB065818	289 mg			
$HOBt.H_2O$		FCB046763	NA	1.5 mL		
HBTU		FC13052124				
DIPEA	Sigma Aldrich	STBH5467		653 µL	3.75 mmol	12.5
Piperidine		STBH7898		NA		
DMF	Fisher Scientific	1994431		NA		
DCM		1998076				

Table 16 - Chemicals and quantities used for addition of conjugatable linear extension to cyclic TAT and Fmoc deprotection.

Acid Cleavage

Scheme 6, Step 4a 5 and Step 4b

Resin and side chain protecting group cleavage protocol applied was identical to the prior procedure followed. Please see 6.1.1 - acid cleavage for detail.

Chemical	Company	Lot #	Mass	Volume	Mol	Eq
TFA	Fluorochem	FCB009271	NA	3.8 mL	NA	
dH_2O	NA			100 µL		
TIS	Acros Organics	A0389936		100 µL		
Diethyl Ether	Fisher Scientific	1852837		40 mL		

Table 17 - Chemicals and quantities used for acid cleavage of modified cyclic TAT.

HPLC Isolation

Deionised water and HPLC grade acetonitrile were both added to Schott bottles (2 L) and treated with 0.1% $^{V}/_{V}$ TFA. Both solutions were connected to a semi-preparation scale Agilent infinity HPLC pump, which had an analytical scale ACE C_{18} column attached with 5 mL loop. A gradient was selected (10 - 45% acetonitrile in 35 minutes). The crude sample was dissolved in 1 mL of solution (10% acetonitrile $^{V}/_{V}$) and injected into a 5 mL loop linked to the column. Fractions were collected manually, and those containing the target peptide were found to have a retention time of 11 minutes. Isolated samples were analysed using an Agilent LC/MS for characterisation.

$^{M}/_{Z}$ = 712.4 $[M+3H]^{3+}$, 534.5 $[M+4H]^{4+}$, 427.9 $[M+5H]^{5+}$ & 356.7 $[M+6H]^{6+}$

R_t = 12 minutes

Chemical	Company	Lot #	Mass	Volume	Mol	Eq
TFA	Acros Organics	A0384182	NA	4.0 mL	NA	
CH_3CN	Fisher Scientific	1996666		2.0 L		
dH_2O	NA					

Table 18 - Chemicals used for HPLC isolation of modified cyclic TAT.

6.1.3 Synthesis of Linear Folate-TAT for OaAEP1 Conjugation

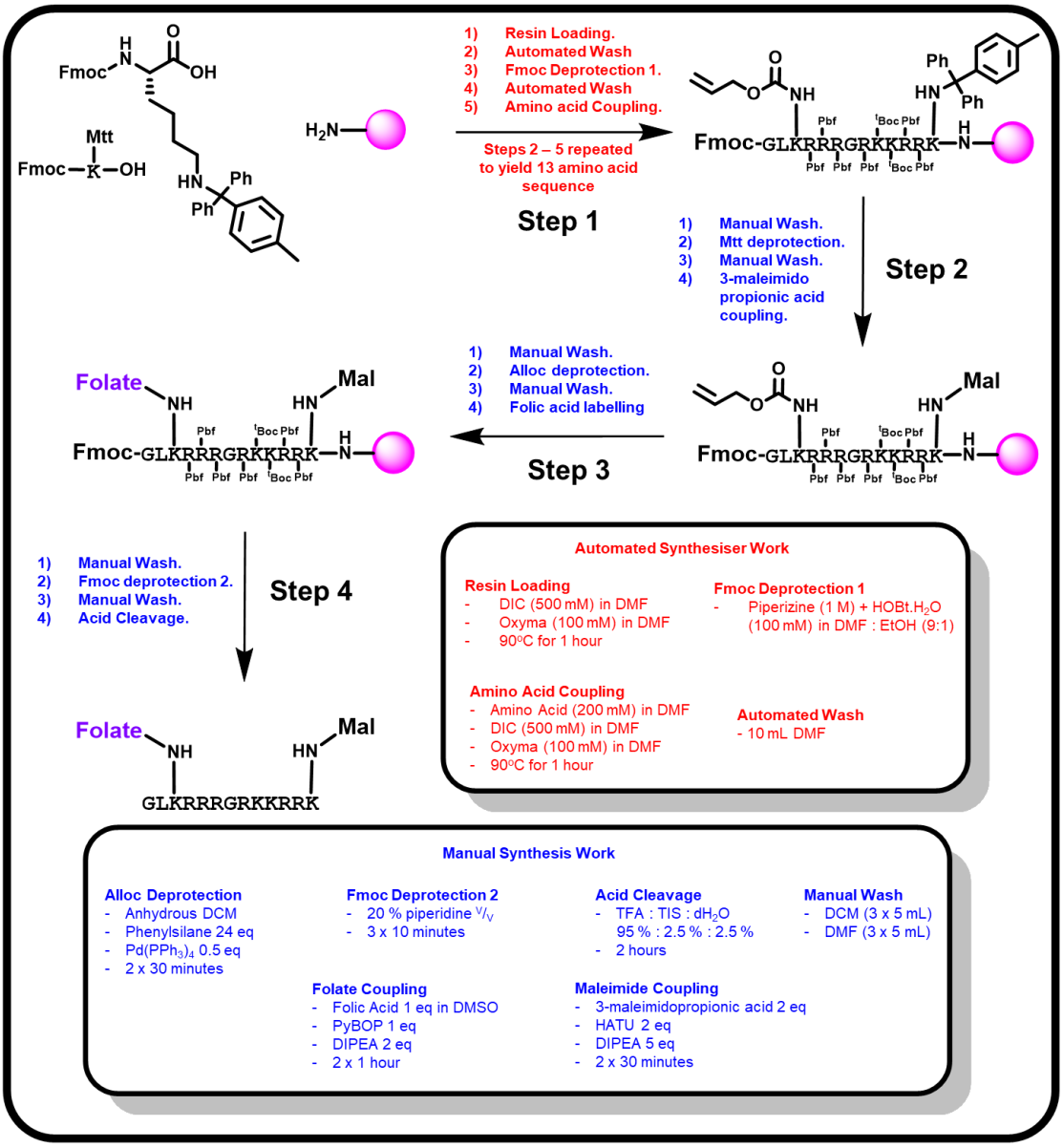

Scheme 17 - Synthetic route of folate labelled TAT (Scheme 7) for OaAEP1 mediated exo-cyclisation to eGFP.

Automated Solid Phase Peptide Synthesis

Scheme 10, Step 1

CEM Liberty Blue peptide synthesiser was employed to produce a linear modified TAT. A programmed sequence was created using the corresponding Liberty Blue software linked to the synthesiser. The scale of synthesis was set to 50 µmole, and the quantity of all reagents and Rink amide resin needed for producing the peptide were scaled accordingly. All amino acid solutions were prepared in appropriate 50 mL falcon tubes with each solution containing 200 mM amino acid solubilised in DMF. Deprotection mixture (1 M piperazine in 9:1 DMF: ethanol + 100 mM HOBt) and activation mixtures (500 mM DIC and 1 M oxyma) were prepared in Schott bottles that were connected to the peptide synthesiser. Pressure from a nitrogen cylinder was introduced into the peptide synthesiser (25 psi) and synthesis had started with Fmoc deprotection of the Rink amide resin by introducing 10 mL of deprotection mixture into the reaction chamber. This would be heated to 75^{o}C *via* microwave irradiation for 10 minutes, and thus, exposing the secondary amine of the resin. Following this, a 5-minute wash cycle of 10 mL of DMF was used to remove left over deprotection mixture from the chamber, therefore setting up the resin for amino acid coupling. A combination of activation mixtures and Fmoc amino acid were placed into the synthesis chamber and heated to 90^{o}C for a pair of 30-minute repeat cycles for peptide bond formation. After programmed time had passed, a wash cycle of 10 mL DMF had washed away excess Fmoc amino acid and activation mixtures, and a deprotection cycle was used to disconnect the Fmoc group of the attached amino acid exposing the *N*-terminal α-amine for further coupling with another amino acid. This cycle of peptide bond formation and Fmoc deprotection would continue until the desired peptide sequence was complete.

Chemical	Company	Lot #	Mass	DMF Volume
Fmoc-D-Arg(Pbf)-OH	Fluorochem	FCC2010055	1.43 g	11 mL
Fmoc-L-Arg(Pbf)-OH		FCC2011555	720 mg	5.5 mL
Fmoc-D-Lys(^{t}Boc)-OH		140430	300 mg	3.1 mL
Fmoc-Lys(Alloc)-OH		FCC21343	290 mg	
Fmoc-Lys(Mtt)-OH		FCB060379	390 mg	
Fmoc-Gly-OH		FCC26269	370 mg	6.1 mL
Fmoc-Leu-OH		FCC26151	220 mg	3.1 mL
DIC		FCB099914	9.5 g	150 mL
Oxyma		FCB106481	21.3 g	
Fmoc-L-Lys(^{t}Boc)-OH	Sigma Aldrich	BCB40540	300 mg	3.1 mL
Piperazine	Acros Organics	A0385026	43.1 g	500 mL
HOBt.H_2O	Cambridge Reagents	AG805160322	7.7 g	
DMF	Fisher Scientific	1994431	NA	
Ethanol		2197980		

Table 19 - Chemicals and quantities used for automated SPPS of linear TAT comprised of *N*-terminal alloc ester protected lysine, and *C*-terminal mtt protected lysine.

Manual Solid Phase Peptide Synthesis

4-Methyl Trityl Deprotection (MTT)

Scheme 10, Step 2 (1 – 2)

A solution comprised of DCM treated with 1% TFA $^{V}/_{V}$ was added to a polypropylene syringe filter containing resin and a stirrer bar, and this was held over a magnetic hot plate. The suspension was provided with 30 minutes to stir at room temperature before vacuum filtration (20 mbar) and washes with organic solvents (DCM 3 x 5 mL and DMF 3 x 5 mL) were employed to remove unwanted soluble materials. This process would be repeated twice more for chemo-selective deprotection of Mtt protecting group.

Chemical	Company	Lot #	Mass	Volume	Mol	Eq
TFA	Fluorochem	FCB078391	NA	100 µL	NA	
DCM	Fisher Scientific	1998076		9.9 mL		
DMF		1994431		NA		

Table 20 - Chemicals and quantities used for mtt deprotection of *C*-terminal lysine added to linear TAT.

3-Maleimido Propionic Acid Coupling

Scheme 10, Step 2 (3 – 4)

A mixture of *3*-maleimido propionic acid solubilised in DMF and DIPEA was added to a polypropylene syringe filter containing peptide bound resin. This reaction mixture was given 30 minutes before the solution was separated from resin *via* vacuum filtration (20 mbar) and washed with DCM (3 x 5 mL) and DMF (3 x 5 mL). A second repeat cycle of amino acid coupling and organic solvent wash was performed.

Chemical	Company	Lot #	Mass	Volume	Mol	Eq
3-maleimido propionic acid	Fluorochem	FCC2010214	102 mg	NA	0.6 mmol	2
HATU		FCB084736	239 mg		0.63 mmol	2.1
DIPEA		FCB086379	NA	523 µL	3 mmol	10
DMF	Fisher Scientific	1994431		NA		
DCM		1998076				

Table 21 - Chemicals and quantities used for *3*-maleimidopropionic acid coupling of linear TAT *C*-terminus.

Alloc Ester Deprotection

Scheme 10, Step 3 (1 – 2)

Removal of the alloc ester group was performed using an identical procedure to that applied for exposing lysine and glutamate side chains for the construction of cyclic TAT (see 6.1.2 - Allyl and Alloc Ester Deprotection).

Chemical	Company	Lot #	Mass	Volume	Mol	Eq
$Pd(PPh_3)_4$	Fluorochem	FCB087066	174 mg	NA	0.075 mmol	0.25
Phenylsilane		FCB083483		887 µL	7.2 mmol	24
Anhydrous DCM	Acros Organics	1998076	NA		NA	
DMF	Fisher Scientific	1994431				

Table 22 - Chemicals and quantities used for deprotection of alloc ester protecting group on N-terminus of linear TAT.

Folate Labelling

Scheme 10, Step 3 (3 – 4)

Addition of folic acid was performed using an identical procedure to that applied for labelling PEG_9-DRDCG peptide tag (see 6.1.1 - Folic Acid Coupling). Fmoc deprotection involved application of 20% piperidine $^{V}/_{V}$ in DMF for three 10-minute cycles at room temperature, including intermittent organic solvent washes (DCM 3 x 5 mL and DMF 3 x 5 mL) in-between cycles to remove unwanted soluble materials from resin.

Chemical	Company	Lot #	Mass	Volume	Mol	Eq
Folic Acid	Carbosynth	Batch Number: FF024031901	22 mg	NA	0.05 mmol	0.2
$HOBt.H_2O$	Fluorochem	FCB046763	8 mg			
HBTU		FC13052124	19 mg			
DIPEA		FCB086379	NA	44 µL	0.25 mmol	0.8
DMSO		FCB046560		5 mL	NA	
Piperidine	Sigma Aldrich	STBH7898		3 mL		
DCM	Fisher Scientific	1998076		NA		
DMF		1994431				

Table 23 - Chemicals and quantities used for Fmoc deprotecting and folic acid coupling of linear TAT.

Acid Cleavage

Resin and side chain protecting group cleavage protocol applied was identical to the prior procedure followed (see 6.1.1 - acid cleavage).

Chemical	Company	Lot #	Mass	Volume	Mol	Eq
TFA	Fluorochem	FCB009271	NA	3.8 mL	NA	
dH_2O	NA			100 µL		
TIS	Acros Organics	A0389936		100 µL		
Diethyl Ether	Fisher Scientific	1852837		40 mL		

Table 24 - Chemicals and quantities used for acid cleavage of linear TAT comprised of *N*-terminal folate and *C*-terminal maleimide.

HPLC Isolation

Semi-preparation scale HPLC isolation protocol applied for obtaining linear folate labelled TAT with *C*-terminal maleimide was identical to the prior procedure followed for cyclic TAT. Please see 6.1.2 - HPLC Isolation for detail.

$^{M}/_{Z}$ = 769.2 $[M+3H]^{3+}$, 568.1 $[M+4H]^{4+}$, 454.7 $[M+5H]^{5+}$ and 379.1 $[M+6H]^{6+}$

R_t = 16 - 17 minutes

Chemical	Company	Lot #	Mass	Volume	Mol	Eq
TFA	Fluorochem	FCB078391	NA	4 mL	NA	
CH_3CN	Fisher Scientific	1996666		2 L		
dH_2O	NA					

Table 25 - Chemicals used for HPLC isolation of linear TAT comprised of *N*-terminal folate and *C*-terminal maleimide.

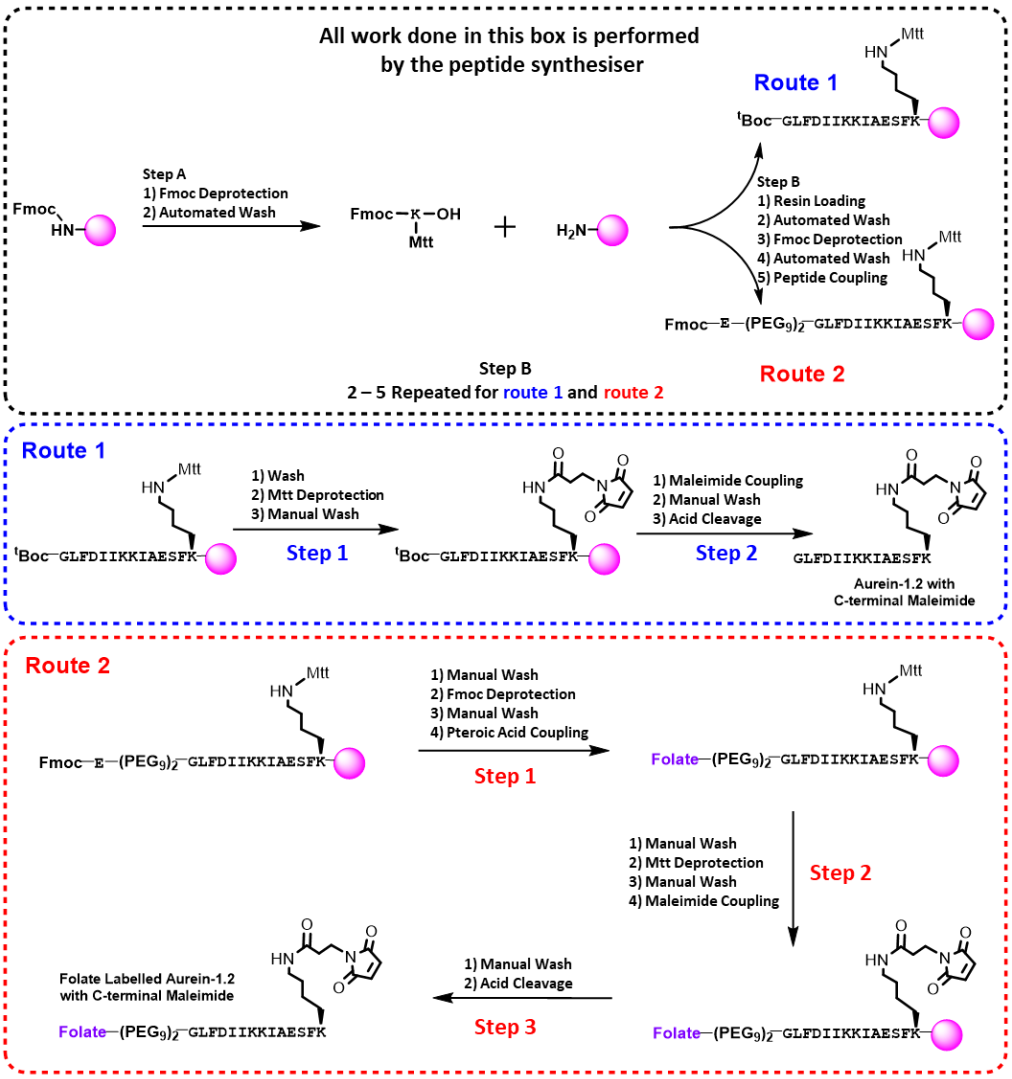

Key

Resin Loading
- Rink Amide Resin
- Fmoc-Lys(Mtt)-OH (200 mM in DMF)
- DIC (500 mM in DMF)
- Oxyma (100 mM in DMF)
- 90°C for 1 hour

Peptide Coupling
- Fmoc and side chain protected amino acid (200 mM in DMF)
- DIC (500 mM in DMF)
- Oxyma (100 mM in DMF)
- 90°C for 1 hour
- 25°C for 2 x 1 hour only for arginine

Maleimide Coupling
- 3-Maleimido Propionic Acid in DMF 2 eq
- HATU 2 eq
- DIPEA 5 eq
- 2 x 30 minutes

Fmoc Deprotection
- Piperidine 20 % $^{v}/_{v}$ in DMF 5 mL
- 3 x 10 minutes

Pteroic Acid Labelling
- Pteroic Acid 1.1 eq in DMSO
- HATU 2 eq
- NMM 5 eq
- 4 x 30 minutes

Acid Cleavage
- TFA (95 % : 2.5 % : 2.5 %)

Manual Wash
- 3 x 5 mL DCM
- 3 x 5 mL DMF

Automated Wash
- 10 mL DMF

Mtt Deprotection
- 1 % TFA $^{v}/_{v}$ in DCM
- 3 x 30 minutes

Scheme 18 - Synthetic pathway for producing peptides based on aurein-1.2.

6.1.4 Aurein-1.2 with *C*-terminal Maleimide

Automated Solid Phase Peptide Synthesis

Scheme 12, Step A and B

Automated solid phase peptide synthesis protocol applied to produce aurein-1.2 labelled with a *C*-terminal Mtt protected lysine was identical to the prior procedure followed (see 6.1.3 - Automated Solid Phase Peptide Synthesis). The only notable difference in procedure was the scale of synthesis which was 100 µmole

Chemical	Company	Lot #	Mass	DMF Volume
DIC	Fluorochem	FCB099914	9.5 g	150 mL
Oxyma		FCB106481	21.3 g	
Fmoc-Ala-OH		FCC2009850	180 mg	2.8 mL
Fmoc-Lys(Mtt)-OH		FCB094528	240 mg	
Fmoc-Glu(^{t}Bu)-OH		FCB061859		
^{t}Boc-Gly-OH		FCC32924	100 mg	
Fmoc-Ile-OH		FCC3119988	1.17 g	16.5 mL
Fmoc-Leu-OH		FCC26151	400 mg	5.5 mL
Fmoc-L-Lys(^{t}Boc)-OH		FCB079060	520 mg	
Fmoc-Phe-OH	Sigma Aldrich	BCBV7517	430 mg	
Fmoc-Ser(^{t}Bu)-OH		BCBW0235	220 mg	2.8 mL
Fmoc-Asp(^{t}Bu)-OH		BCBX0738	240 mg	
Piperazine	Acros Organics	A0385026	43.1 g	500 mL
HOBt.H_2O	Cambridge Reagents	AG805160322	7.7 g	
DMF	Fisher Scientific	1994431	NA	

Table 26 - Chemicals and quantities used for automated SPPS of aurein-1.2 with *C*-terminal mtt protected lysine.

Manual Solid Phase Peptide Synthesis

4-MethylTrityl Deprotection

Scheme 12, Route 1 (Step1)

Chemo-selective deprotection of *4*-methyl trityl protecting group protocol applied was identical to the prior procedure followed. Please see 6.1.3 - *4*-methyl trityl deprotection for detail.

Chemical	Company	Lot #	Mass	Volume	Mol	Eq
TFA	Fluorochem	FCB078391	NA	100 µL	NA	
DCM	Fisher Scientific	1998076		9.9 mL		
DMF		1994431		NA		

Table 27 - Chemicals and quantities used for mtt deprotection of *C*-terminal lysine added onto aurein-1.2.

3-Maleimido Propionic Acid Coupling

Scheme 12, Route 1, Step 2 (1 – 2)

Addition of peptide bond formation of *3*-maleimido propionic acid with amino acid on resin procedure used was identical to the prior protocol followed. Please see 6.1.3 - *3*-maleimido propionic acid coupling for detail.

Chemical	Company	Lot #	Mass	Volume	Mol	Eq
3-maleimidopropionic acid	Fluorochem	FCC2010214	85 mg	NA	0.5 mmol	5
HATU		FCB084736	194 mg		0.51 mmol	5.1
DIPEA		FCB086379	NA	174 µL	1.0 mmol	10
DMF	Fisher Scientific	1994431		NA		
DCM		1998076				

Table 28 - Chemicals and quantities used for *3*-maleimidopropionic acid coupling of *C*-terminal lysine added to aurein-1.2.

Acid Cleavage

Scheme 12, Route 1 (3)

Resin and side chain protecting group cleavage protocol applied was identical to the prior procedure followed. Please see 6.1.1 - acid cleavage for detail.

Chemical	Company	Lot #	Mass	Volume	Mol	Eq
TFA	Fluorochem	FCB009271	NA	3.8 mL	NA	
dH_2O	NA			100 µL		
TIS	Acros Organics	A0389936		100 µL		
Diethyl Ether	Fisher Scientific	1852837		1 mL		

Table 29 - Chemicals and quantities used for acid cleavage of aurein-1.2 with *C*-terminal maleimide.

HPLC Isolation

Deionised water and HPLC grade acetonitrile were both added to Schott bottles (2 L) and treated with 0.1% $^{V}/_{V}$ TFA. Both solutions were connected to a preparation scale Shimadzu HPLC pump, which had a preparation scale C_{18} column attached with 5 mL loop. A gradient was selected (35 - 75% acetonitrile in 40 minutes). The crude sample was dissolved in 2 mL of solution (35% acetonitrile $^{V}/_{V}$) and injected into a 5 mL loop linked to the column. Fractions were collected using an automated fraction collector, and those containing the target peptide were found to have a retention time of 11 minutes. Isolated samples were analysed using an Agilent LC/MS for characterisation.

$^{M}/_{Z}$ = 880.6 $[M+2H]^{2+}$ and 587.2 $[M+3H]^{3+}$

R_t = 10 - 11 minutes

Chemical	Company	Lot #	Mass	Volume	Mol	Eq
TFA	Fluorochem	FCB078391	NA	4.0 mL	NA	
CH_3CN	Fisher Scientific	2063488		2.0 L		
dH_2O	NA					

Table 30 - Chemicals used for HPLC isolation of modified aurein-1.2 with *C*-terminal maleimide.

6.1.5 Folate Labelled Aurein-1.2 with *C*-terminal Maleimide

Automated Solid Phase Peptide Synthesis

Scheme 12, Step A and B

Automated solid phase peptide synthesis protocol applied to produce aurein-1.2 labelled with a *C*-terminal Mtt protected lysine, and *N*-terminal linear extension comprised of two PEG_9 spacers ending with a glutamate was identical to the prior procedure followed (see 6.1.3 - Automated Solid Phase Peptide Synthesis). Notable differences applied to this procedure was the scale of synthesis, which was 100 µmole, the deprotection solution was switched to 20% piperidine in DMF $^{V}/_{V}$ and addition of DIPEA (100 mM) into oxyma solution.

Chemical	Company	Lot #	Mass	DMF Volume
DIC	Fluorochem	FCB099914	9.5 g	150 mL
Oxyma		FCB106481	21.3 g	
DIPEA		FCB086379	1.94 g = 1.44 mL	
Fmoc-Ala-OH		FCC2009850	180 mg	2.8 mL
Fmoc-Lys(Mtt)-OH		FCB094528	350 mg	
Fmoc-Glu(^{t}Bu)-OH		FCB061859	240 mg	
Fmoc-Glu-O^{t}Bu		FCC200874		
Fmoc-Ile-OH		FCC3119988	1.17 g	16.5 mL
Fmoc-Leu-OH		FCC26151	400 mg	5.5 mL
Fmoc-PEG$_9$-OH		FCB097749	430 mg	
Fmoc-L-Lys(^{t}Boc)-OH		FCB079060	520 mg	
Fmoc-Phe-OH	Sigma Aldrich	BCBV7517	430 mg	
Fmoc-Asp(^{t}Bu)-OH		BCBX0738	240 mg	2.8 mL
Fmoc-Ser(^{t}Bu)-OH		BCBW0235	220 mg	
Piperidine		STBH7898	116 g = 100 mL	500 mL
HOBt.H$_2$O	Cambridge Reagents	AG805160322	7.7 g	
DMF	Fisher Scientific	1994431	NA	

Table 31 - Chemicals and quantities used for automated SPPS of *N*-terminal Fmoc protected aurein-1.2 modified with *C*-terminal mtt protected lysine.

Manual Solid Phase Peptide Synthesis

Pteroic Acid Labelling

Scheme 12, Route 2 (Step 1 – 4)

Peptide bound to resin was taken from the reaction vessel of the peptide synthesiser and placed into a Kenesis polypropylene syringe filter, along with a magnetic stirrer bar for manual synthesis. This system was held over a magnetic hot plate *via* clamp and stand for room temperature stirring. The resin was washed with organic solvents (DCM 3 x 5 mL and DMF 3 x 5 mL) and then subjected to three cycles of 10-minute deprotection reactions using 20% piperidine in DMF $^{V}/_{V}$ (3 x 5 mL) with intermittent organic solvent washes, and thus, setting up the resin for pteroic acid coupling.

Pteroic acid labelling protocol applied was mostly identical to the prior procedure followed. Please see 6.1.1 - pteroic acid coupling for detail. The only significant difference for this procedure was the 10 individual pteroic acid coupling cycles required to create the final folic acid motif.

Chemical	Company	Lot #	Mass	Volume	Mol	Eq
Pteroic Acid	Fluorochem	FCC3147916	63 mg	NA	0.2 mmol	2
HATU		FCB084736	80 mg		0.21 mmol	2.1
DMSO		FCB098590	NA			
NMM	Sigma Aldrich	DR10526CR	NA	220 µL	2.0 mmol	10
Piperidine		STBH7898		3 mL	NA	
DMF	Fisher Scientific	1994431		NA		
DCM		1998076				

Table 32 - Chemicals and quantities used for pteroic acid coupling of aurein-1.2 with *N*-terminal glutamate.

4-Methyl Trityl Deprotection

Scheme 12, Route 2 (Step 1- 2)

Chemo-selective deprotection of *4*-methyl trityl group was identical to the prior procedure followed. Please see 6.1.4 - *4*-methyltrityl deprotection for detail.

Chemical	Company	Lot #	Mass	Volume	Mol	Eq
TFA	Fluorochem	FCB078391	NA	100 µL	NA	
DCM	Fisher Scientific	1998076		9.9 mL		
DMF		1994431		NA		

Table 33 - Chemicals and quantities used for mtt deprotection *of C*-terminal lysine on modified aurein-1.2

3-Maleimido Propionic Acid Coupling

Scheme 12, Route 2 (Step 3 – 4)

Addition of *3*-maleimido propionic acid *via* peptide bond formation procedure used was identical to the prior protocol followed. Please see 6.1.4 - *3*-maleimido propionic acid coupling for detail.

Chemical	Company	Lot #	Mass	Volume	Mol	Eq
3-maleimidopropionic acid	Fluorochem	FCC2010214	85 mg	NA	0.5 mmol	5
HATU		FCB084736	194 mg		0.51 mmol	5.1
DIPEA		FCB086379	NA	174 µL	1.0 mmol	10
DMF	Fisher Scientific	1994431		NA		
DCM		1998076				

Table 34 - Chemicals and quantities used for *3*-maleimidopropionic acid coupling to *C*-terminal lysine of modified aurein-1.2.

Acid Cleavage

Scheme 12, Route 2 (Step 3)

Resin and side chain protecting group cleavage protocol applied was identical to the prior procedure followed. Please see 6.1.1 - acid cleavage for detail.

Chemical	Company	Lot #	Mass	Volume	Mol	Eq
TFA	Fluorochem	FCB009271	NA	3.8 mL	NA	
dH_2O	NA			100 µL		
DOD	Sigma Aldrich	SHBH9681				
TIS	Acros Organics	A0389936		100 µL		
Diethyl Ether	Fisher Scientific	1852837		1 mL		

Table 35 - Chemicals and quantities used for acid cleavage of modified aurein-1.2 comprised of *N*-terminal folate and *C*-terminal maleimide.

HPLC Isolation

Semi-preparation scale HPLC isolation protocol applied for obtaining *C*-terminal maleimide and *N*-terminal folate labelled aurein-1.2 was identical to the prior procedure followed for cyclic TAT. Please see 6.1.2 - HPLC Isolation for detail. Notable difference in this procedure was the gradient applied which was 45 – 70% acetonitrile in 30 minutes.

$^{M}/_{Z}$ = 1237.14 $[M+2H]^{2+}$ and 825.10 $[M+3H]^{3+}$

R_t = 18 minutes

Chemical	Company	Lot #	Mass	Volume	Mol	Eq
TFA	Fluorochem	FCB078391	NA	4 mL	NA	
CH_3CN	Fisher Scientific	2049762		2.0 L		
dH_2O	NA			2.0 L		

Table 36 - Chemicals used for HPLC isolation of modified aurein-1.2 comprised of *N*-terminal folate and *C*-terminal maleimide.

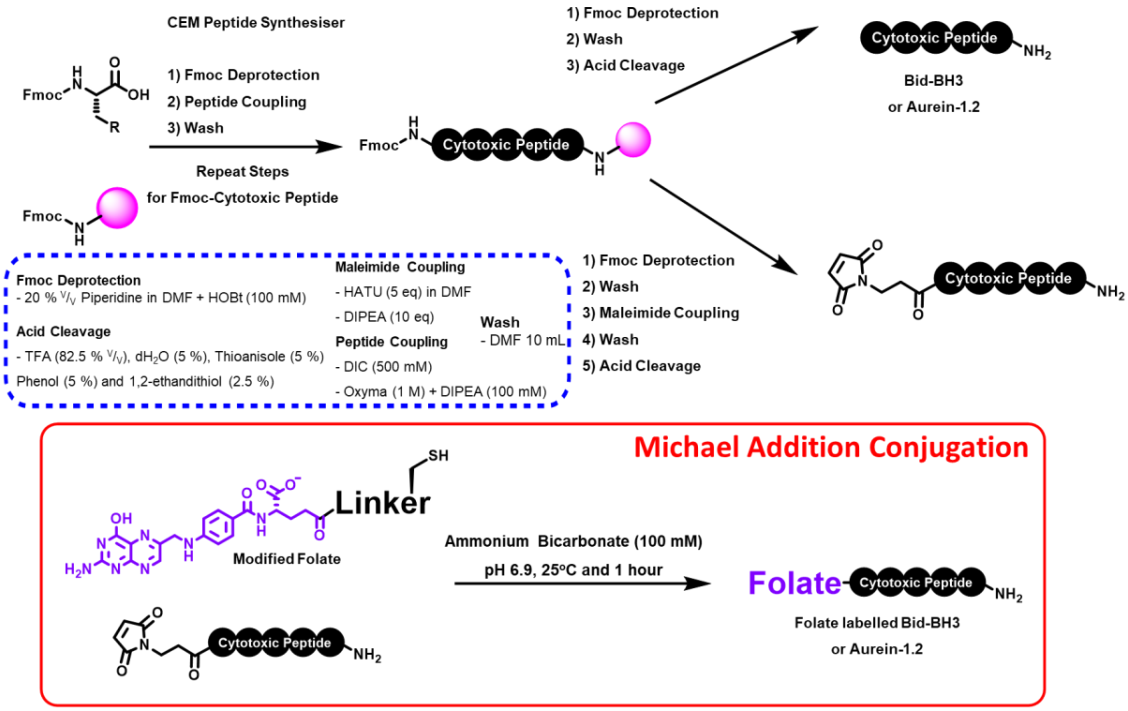

Scheme 19 - Construction of native cytotoxic peptides and folate labelled analogues.

6.1.6 Native Aurein-1.2

Automated Solid Phase Peptide Synthesis

Scheme 13, Top

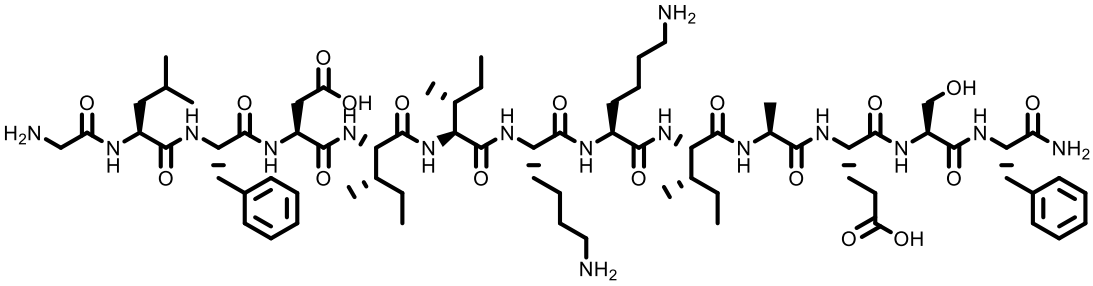

Chemical Formula: $C_{71}H_{114}N_{16}O_{18}$
Molecular Weight: 1479.79

Automated solid phase peptide synthesis protocol was identical to the prior procedure followed (see 6.1.3 Automated Solid Phase Peptide Synthesis). Notable differences applied to this procedure was the scale of synthesis, which was 100 µmole, the deprotection solution was switched to 20% piperidine in DMF $^{V}/_{V}$ and addition of DIPEA (100 mM) into oxyma solution.

Chemical	Company	Lot #	Mass	DMF Volume
DIC	Fluorochem	FCB099914	9.5 g	150 mL
Oxyma		FCB106481	21.3 g	
Fmoc-Ala-OH		FCC2009850	180 mg	2.8 mL
Fmoc-Lys(Mtt)-OH		FCB094528	240 mg	
Fmoc-Glu(^{t}Bu)-OH		FCB061859		
^{t}Boc-Gly-OH		FCC32924	100 mg	
Fmoc-Ile-OH		FCC3119988	1.17 g	16.5 mL
Fmoc-Leu-OH		FCC26151	400 mg	5.5 mL
Fmoc-L-Lys(^{t}Boc)-OH		FCB079060	520 mg	
Fmoc-Phe-OH	Sigma Aldrich	BCBV7517	430 mg	
Fmoc-Ser(^{t}Bu)-OH		BCBW0235	220 mg	2.8 mL
Fmoc-Asp(^{t}Bu)-OH		BCBX0738	240 mg	
Piperidine		STBH7898	116 g = 100 mL	500 mL
HOBt.H_2O	Cambridge Reagents	AG805160322	7.7 g	
DMF	Fisher Scientific	1994431	NA	

Table 37 - Chemicals and quantities used for automated SPPS of native aurein-1.2.

Acid Cleavage

Scheme 13, Top

Resin and side chain protecting group cleavage protocol applied was identical to the prior procedure followed. Please see 6.1.1 - acid cleavage for detail.

Chemical	Company	Lot #	Mass	Volume	Mol	Eq
TFA	Fluorochem	FCB009271	NA	3.8 mL	NA	
dH_2O	NA			100 µL		
TIS	Acros Organics	A0389936		100 µL		
Diethyl Ether	Fisher Scientific	1852837		1 mL		

Table 38 - Chemicals and quantities used for acid cleavage of native aurein-1.2.

HPLC Isolation

Preparation scale HPLC isolation protocol applied for obtaining native aurein-1.2 was identical to the prior procedure followed for *C*-terminal maleimide labelled aurein-1.2. Please see 6.1.4 - HPLC Isolation for detail. Notable difference in this procedure was the gradient which was 35 – 75% acetonitrile in 40 minutes.

$^{M}/_{Z}$ = 740.6 $[M+2H]^{2+}$ and 494.1 $[M+3H]^{3+}$

R_t = 26 – 29 minutes

Chemical	Company	Lot #	Mass	Volume	Mol	Eq
TFA	Fluorochem	FCB078391	NA	4 mL	NA	
CH_3CN	Fisher Scientific	2049762		2.0 L		
dH_2O	NA			2.0 L		

Table 39 - Chemicals used for HPLC isolation of native aurein-1.2.

6.1.7 *N*-terminal Folate Labeled Aurein1.2

Automated Solid Phase Peptide Synthesis

Scheme 13, Top

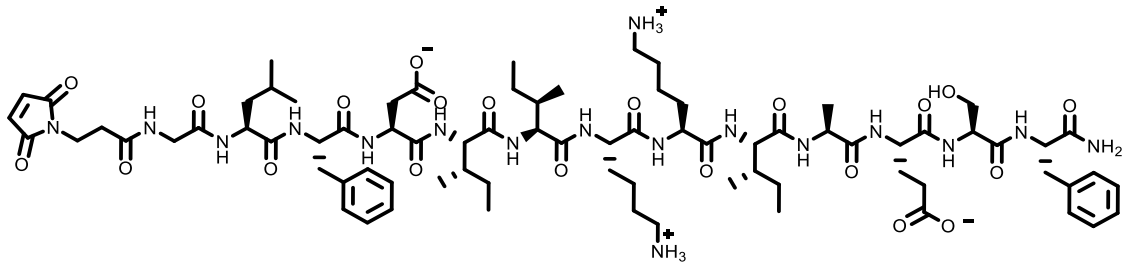

Chemical Formula: $C_{78}H_{119}N_{17}O_{21}$
Molecular Weight: 1630.91

Automated solid phase peptide synthesis protocol was identical to the prior procedure followed (see 6.1.3 - Automated Solid Phase Peptide Synthesis). Notable differences applied to this procedure was the scale of synthesis, which was 100 µmole, the deprotection solution was switched to 20% piperidine in DMF $^{V}/_{V}$, addition of DIPEA (100 mM) into oxyma solution and the introduction of an *N*-terminal maleimide into the peptide. Due to the reactivity of piperidine towards maleimides, a conscious effort was made to ensure that a final Fmoc deprotection sequence was switched off to maintain the structural integrity of the peptide on resin.

Chemical	Company	Lot #	Mass	DMF Volume
DIC	Fluorochem	FCB099914	9.5 g	150 mL
Oxyma		FCB106481	21.3 g	
DIPEA		FCB086379	1.94 g = 1.44 mL	
3-Maleimido Propionic Acid		FCC2010214	6 mg	2.8 mL
Fmoc-Ala-OH		FCC2009850	180 mg	
Fmoc-Lys(Mtt)-OH		FCB094528	350 mg	
Fmoc-Glu(^{t}Bu)-OH		FCB061859	240 mg	
Fmoc-Glu-O^{t}Bu		FCC200874		
Fmoc-Ile-OH		FCC3119988	1.17 g	16.5 mL
Fmoc-Leu-OH		FCC26151	400 mg	5.5 mL
Fmoc-L-Lys(^{t}Boc)-OH		FCB079060	520 mg	
Fmoc-Phe-OH	Sigma Aldrich	BCBV7517	430 mg	
Fmoc-Asp(^{t}Bu)-OH		BCBX0738	240 mg	2.8 mL
Fmoc-Ser(^{t}Bu)-OH		BCBW0235	220 mg	
Piperidine		STBH7898	116 g = 100 mL	500 mL
HOBt.H_2O	Cambridge Reagents	AG805160322	7.7 g	
DMF	Fisher Scientific	1994431	NA	

Table 40 - Chemicals and quantities used for automated SPPS of modified aurein-1.2 comprised of *N*-terminal maleimide.

Acid Cleavage

Scheme 13, Top

Resin and side chain protecting group cleavage protocol applied was identical to the prior procedure followed. Please see 6.1.1 - acid cleavage for detail.

Chemical	Company	Lot #	Mass	Volume	Mol	Eq
TFA	Fluorochem	FCB009271	NA	3.7 mL	NA	
dH_2O	NA			100 µL		
TIS	Acros Organics	A0389936		100 µL		
Diethyl Ether	Fisher Scientific	1852837		1 mL		

Table 41 - Chemicals and quantities used for acid cleavage of modified aurein-1.2 comprised of *N*-terminal maleimide.

Michael Addition Conjugation

Scheme 13, Bottom

An ammonium bicarbonate buffer solution was assembled in a falcon tube, and its volume was adjusted to 50 mL and pH altered under the guidance of a digital pH probe to 6.9 *via* dropwise additions of dilute acetic acid (2% $^{V}/_{V}$). This medium (10 mL) was used to solubilise a combination of modified folic acid with *C*-terminal cysteine (5 mg) and maleimide labelled aurein-1.2 (5 mg). For one hour this reaction would proceed by stirring with a magnetic stirrer bar at room temperature before attempting isolation by HPLC.

Chemical	Company	Lot #	Mass	Volume	Mol	Eq
dH_2O	NA			50 mL	NA	NA
Ammonium Bicarbonate	Acros Organics	A0383847	395 mg	NA	100 mM	
Acetic Acid	Fisher Scientific	1278359	NA			

Table 42 - Chemicals and quantities used for Michael addition conjugation of folate-PEG_9-DRDCG to *N*-terminal maleimide labelled aurein-1.2.

HPLC Isolation

Preparation scale HPLC isolation protocol applied for obtaining folate labelled aurein-1.2 was identical to the prior procedure followed for *C*-terminal maleimide labelled aurein-1.2. Please see 6.1.4 - HPLC Isolation for detail. Notable difference in this procedure was the gradient which was 20 – 80% acetonitrile in 60 minutes. In addition to isolating the desired folic acid aurein-1.2, the unreacted pre-cursor peptide was also isolated at 37 minutes.

$^{M}/_{Z}$ = 1382.64 $[M+2H]^{2+}$, 922.10 $[M+3H]^{+3}$ and 691.83 $[M+4H]^{4+}$

R_t = 28 minutes

Chemical	Company	Lot #	Mass	Volume	Mol	Eq
TFA	Fluorochem	FCB078391	NA	4 mL	NA	
CH_3CN	Fisher Scientific	2049762		2.0 L		
dH_2O	NA			2.0 L		

Table 43 - Chemicals used for HPLC isolation of *N*-terminal folate labelled aurein-1.2.

6.1.8 Native Bid-BH3

Automated Solid Phase Peptide Synthesis

Scheme 13, Top

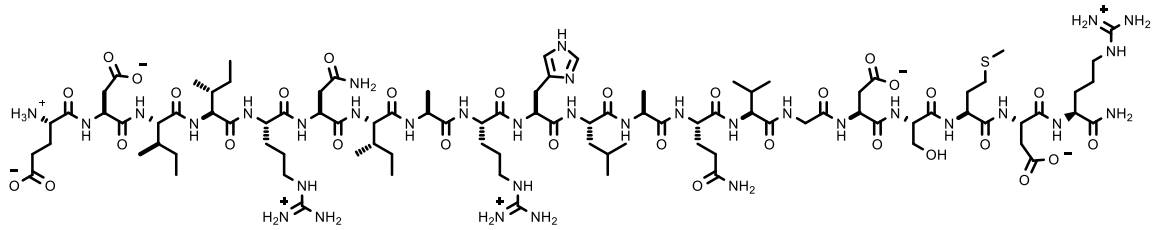

Automated solid phase peptide synthesis protocol was identical to the prior procedure followed (see 6.1.3 - Automated Solid Phase Peptide Synthesis). Notable differences applied to this procedure was the scale of synthesis, which was 100 µmole, the deprotection solution was switched to 20% piperidine and 1% formic acid in DMF $^{V}/_{V}$, addition of DIPEA (100 mM) into oxyma solution.

Chemical	Company	Lot #	Mass	DMF Volume
DIC	Fluorochem	FCB099914	9.5 g	150 mL
Oxyma		FCB106481	21.3 g	
DIPEA		FCB086379	1.94 g = 1.44 mL	
Fmoc-Ala-OH		FCC2009850	350 mg	5.5 mL
Fmoc-Arg(Pbf)-OH		FCC35262	2.15 g	16.5 mL
Fmoc-Asp(^{t}Bu)-OH		FCC30768	690 mg	8.3 mL
Fmoc-Asn(Trt)-OH		FCB081442	340 mg	2.8 mL
Fmoc-Gly-OH		FCB108354	170 mg	
Fmoc-Gln(Trt)-OH		FCC3127287	350 mg	
Fmoc-Ser(Trt)-OH		FCC530669	220 mg	
Fmoc-Glu(^{t}Bu)-OH	Cambridge Reagents	AG00335170905	240 mg	
Fmoc-His(Trt)-OH		AG802150801	690 mg	5.5 mL
Fmoc-Val-OH	Sigma Aldrich	BCCB0388	380 mg	
Fmoc-Leu-OH		BCBR5918V	390 mg	
Fmoc-Met-OH		BCBW0715	210 mg	2.8 mL
Fmoc-Ile-OH		BCBZ6720	1.17 g	16.5 mL
Piperidine		STBH7898	116 g = 100 mL	500 mL
Formic Acid	Acros Organics	A0400736	4.1 g = 5 mL	
DMF	Fisher Scientific	1994431	NA	

Table 44 - Chemicals and quantities used for automated SPPS of native Bid-BH3.

Acid Cleavage

Resin and side chain protecting group cleavage protocol applied was identical to the prior procedure followed. Please see 6.1.1 - acid cleavage for detail. Notable difference to highlight was the use of reagent K for resin cleavage (*e.g.* TFA 82.5% : dH_2O 5% : thioanisole 5%: phenol 5% : 1,2-ethandithiol 2.5% $^{V}/_{V}$).[203] This was employed due to the presence of a *C*-terminal methionine.

Chemical	Company	Lot #	Mass	Volume	Mol	Eq
Phenol	Merck	S7812296 926	200 mg	NA	NA	
TFA	Fluorochem	FCB009271	NA	3.3 mL		
Thioanisole		FCB04404		200 µL		
dH_2O	NA			200 µL		
1,2-ethandithiol	Sigma Aldrich	STBJ6018		100 µL		
Diethyl Ether	Fisher Scientific	1852837		40 mL		

Table 45 - Chemicals and quantities used for acid cleavage of native Bid-BH3 using reagent K

HPLC Isolation

Preparation scale HPLC isolation protocol applied for obtaining Native Bid-BH3 was identical to the prior procedure followed for *C*-terminal maleimide labelled aurein-1.2. Please see 6.1.4 - HPLC Isolation for detail. Notable difference in this procedure was the gradient which was 20 – 80% acetonitrile in 60 minutes.

$^{M}/_{Z}$ = 770.3 $[M+3H]^{+3}$, 578.1 $[M+4H]^{4+}$ and 462.6 $[M+5H]^{5+}$

R_t = 30 - 32 minutes

Chemical	Company	Lot #	Mass	Volume	Mol	Eq
TFA	Fluorochem	FCB078391	NA	4 mL	NA	
CH_3CN	Fisher Scientific	2049762		2.0 L		
dH_2O	NA					

Table 46 - Chemicals used for HPLC isolation of native Bid-BH3.

6.1.9 *N*-Terminal Folate Labelled Bid-BH3

Automated Solid Phase Peptide Synthesis

Scheme 13, Top

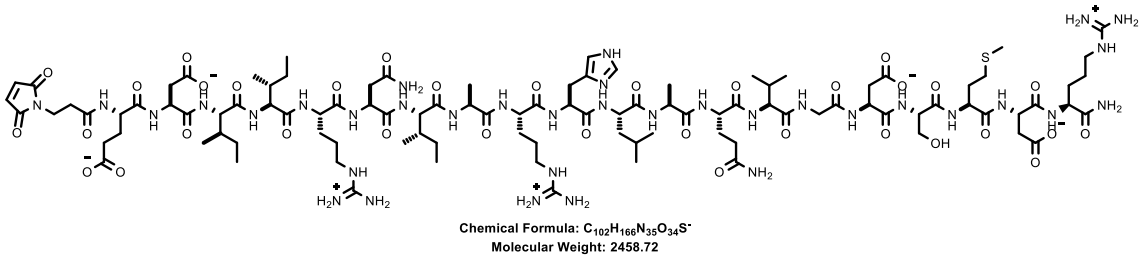

Automated solid phase peptide synthesis protocol was identical to the prior procedure followed (see 6.1.3 - Automated Solid Phase Peptide Synthesis). Notable differences applied to this procedure was the scale of synthesis, which was 100 µmole, the deprotection solution was switched to 20% piperidine and 1% formic acid in DMF $^{V}/_{V}$, addition of DIPEA (100 mM) into oxyma solution and the introduction of an *N*-terminal maleimide into the peptide. Due to the reactivity of piperidine towards maleimides, a conscious effort was made to ensure that a final Fmoc deprotection sequence was switched off to maintain the structural integrity of the peptide on resin.

6.1.10 Liquid Chromatography Mass Spectrometry (LC/MS)

Three LC/MS systems were used for the analysis of proteins and peptides in this work. The Bruker and Agilent LC/MS systems were connected to a C_{18} column for analysing peptides. The Waters synapt LC/MS was connected to a C_8 column for peptide analysis and a C_4 column for protein analysis. All samples were analysed *via* electrospray ionisation in positive mode.

Chemical	Company	Lot #	Mass	DMF Volume
DIC	Fluorochem	FCB099914	9.5 g	150 mL
Oxyma		FCB106481	21.3 g	
DIPEA		FCB086379	1.94 g = 1.44 mL	
Fmoc-Ala-OH		FCC2009850	350 mg	5.5 mL
Fmoc-Arg(Pbf)-OH		FCC35262	2.15 g	16.5 mL
Fmoc-Asp(^{t}Bu)-OH		FCC30768	690 mg	8.3 mL
Fmoc-Asn(Trt)-OH		FCB081442	340 mg	2.8 mL
3-Maleimido Propionic Acid		FCC2010214	6 mg	
Fmoc-Gly-OH		FCB108354	170 mg	
Fmoc-Gln(Trt)-OH		FCC3127287	350 mg	
Fmoc-Ser(Trt)-OH		FCC530669	220 mg	
Fmoc-Glu(^{t}Bu)-OH	Cambridge Reagents	AG00335170905	240 mg	
Fmoc-His(Trt)-OH		AG802150801	690 mg	5.5 mL
Fmoc-Val-OH	Sigma Aldrich	BCCB0388	380 mg	
Fmoc-Leu-OH		BCBR5918V	390 mg	
Fmoc-Met-OH		BCBW0715	210 mg	2.8 mL
Fmoc-Ile-OH		BCBZ6720	1.17 g	16.5 mL
Piperidine		STBH7898	116 g = 100 mL	500 mL
Formic Acid	Acros Organics	A0400736	4.1 g = 5 mL	
DMF	Fisher Scientific	1994431	NA	

Table 47 - Chemicals and quantities used for automated SPPS of modified Bid-BH3 with *N*-terminal maleimide.

Acid Cleavage

Resin and side chain protecting group cleavage protocol applied was identical to the prior procedure followed. Please see 6.1.1 - acid cleavage for detail. Notable difference to highlight was the use of reagent K for resin cleavage (*e.g.* TFA 82.5% : dH_2O 5% : thioanisole 5%: phenol 5% : 1,2-ethandithiol 2.5% $^{V}/_{V}$).[203] This was employed due to the presence of a *C*-terminal methionine.

Chemical	Company	Lot #	Mass	Volume	Mol	Eq
Phenol	Merck	S7812296 926	200 mg	NA	NA	
TFA	Fluorochem	FCB009271	NA	3.3 mL		
Thioanisole		FCB04404		200 µL		
dH_2O	NA			200 µL		
1,2-ethandithiol	Sigma Aldrich	STBJ6018		100 µL		
Diethyl Ether	Fisher Scientific	1852837		40 mL		

Table 48 - Chemicals and quantities used for acid cleavage of modified Bid-BH3 with *N*-terminal maleimide using reagent K.

HPLC Isolation

Preparation scale HPLC isolation protocol applied for obtaining Bid-BH3 with an *N*-terminal maleimide was identical to the prior procedure followed for *C*-terminal maleimide labelled aurein-1.2. Please see 6.1.4 - HPLC Isolation for detail. Notable difference in this procedure was the gradient which was 20 – 80% acetonitrile in 60 minutes.

$^{M}/_{Z}$ = 1230.62 $[M+2H]^{2+}$, 820.75 $[M+3H]^{3+}$ and 615.82 $[M+4H]^{4+}$

R_t = 24 minutes

Chemical	Company	Lot #	Mass	Volume	Mol	Eq
TFA	Fluorochem	FCB078391	NA	4 mL	NA	
CH_3CN	Fisher Scientific	2049762		2.0 L		
dH_2O	NA					

Table 49 - Chemicals used for HPLC isolation of modified Bid-BH3 with *N*-terminal maleimide.

Michael Addition Conjugation

Scheme 13, Bottom

Michael addition conjugation reaction protocol applied was identical to the prior procedure followed. Please see 6.1.7 - Michael Addition Conjugation for detail.

Chemical	Company	Lot #	Mass	Volume	Mol	Eq
dH_2O	NA			50 mL	NA	NA
Ammonium Bicarbonate	Acros Organics	A0383847	395 mg	NA	100 mM	
Acetic Acid	Fisher Scientific	1278359	NA			

Table 50 - Chemicals and quantities used for Michael addition conjugation of folate-PEG_9-DRDCG to Bid-BH3 with *N*-terminal maleimide.

HPLC Isolation

Preparation scale HPLC isolation protocol applied for obtaining folate labelled Bid-BH3 was identical to the prior procedure followed for *C*-terminal maleimide labelled aurein-1.2. Please see 6.1.4 - HPLC Isolation for detail. Notable difference in this procedure was the gradient which was 20 – 80% acetonitrile in 60 minutes.

$^{M}/_{Z}$ = 898.90 $[M+4H]^{4+}$, 719.33 $[M+5H]^{5+}$ and 599.45 $[M+6H]^{6+}$

R_t = 18 minutes

Chemical	Company	Lot #	Mass	Volume	Mol	Eq
TFA	Fluorochem	FCB078391	NA	4 mL	NA	
CH_3CN	Fisher Scientific	2049762		2.0 L		
dH_2O	NA					

Table 51 - Chemicals used for HPLC isolation of *N*-terminal folate labelled Bid-BH3.

6.2 Biological Chemistry

Conjugates based on sfGFP and the protease enzyme OaAEP1 were produced using bacterial gene expression systems. sfGFP was subjected to site selective labelling with folate and pteroate labelled peptides and OaAEP1 was employed in activity test assays. In this chapter the materials and methods used to generate these large polypeptides will be discussed.

6.2.1 Buffer Preparation

Chemical	Company	Lot #
NaCl	Fisher Scientific	1849132
KCl	Sigma Aldrich	20729
Tris base		SLBV5592
Na_2HPO_4	Acros Organics	A0376735
KH_2PO_4	Melford Biolaboratories Ltd	G25420-30006
Sodium dodecyl sulphate		L22010 B2008 (Batch # 13086)
Imidazole	Apollo Scientific	AS464818
Glycine		AS478393

Table 52 - Chemicals and quantities used for constructing buffered solutions.

Phosphate Buffer Saline (PBS) Stock Solution

To a 1 L Schott bottle, NaCl (80 g), KCl (2 g), Na_2HPO_4 (14.4 g) and KH_2PO_4 (2.4 g) was added with 800 mL of water (measured with a 1 L measuring cylinder). This solution was left to stir vigorously until all solid had dissolved. The solution was then measured in a 1 L measuring cylinder and the volume of solution was diluted up to 1 L. The pH of solution was measured using a pH probe (pH = 6.9).

Phosphate Buffer Saline 10x Dilution

A volume of 100 mL of PBS stock solution was diluted 10x (in 900 mL of water) to make up a total volume of 1 L. The pH of solution was measured using a pH probe (pH = 7.5).

Binding Buffer Solution

To a 1 L Schott bottle, tris base (50 mmol), NaCl (300 mmol) and imidazole (5 mmol) was added with 800 mL of water (measured with a 1 L measuring cylinder). This solution was left to stir vigorously until all solid had dissolved. The solution was then measured in a 1 L measuring cylinder and the volume of solution was diluted up to 1 L. The pH of solution was measured using a pH probe and adjusted using 11.6 M $HCl_{(aq)}$ (pH = 8.0).

Elution Buffer Solution

To a 1 L Schott bottle, tris base (50 mmol), NaCl (50 mmol) and imidazole (250 mmol) was added with 800 mL of water (measured with a 1 L measuring cylinder). This solution was left to stir vigorously until all solid had dissolved. The solution was then measured in a 1 L measuring cylinder and the volume of solution was diluted up to 1 L. The pH of solution was measured using a pH probe and adjusted using 11.6 M $HCl_{(aq)}$ (pH = 8.0).

Resolving Buffer

Tris base (36.3 g) was weighed in a 200 mL Schott bottle and 100 mL of deionised water was added with stirring *via* magnetic stirrer bar to aid solubilisation. Buffer pH was adjusted to 8.8 using 11.6 M $HCl_{(aq)}$ and the total volume was adjusted to 200 mL to bring concentration of tris to 1.5 M.

Stacking Buffer

Tris base (12.1 g) was weighed in a 200 mL Schott bottle and 100 mL of deionised water was added with stirring *via* magnetic stirrer bar to aid solubilisation. Buffer pH was adjusted to 6.8 using 11.6 M $HCl_{(aq)}$ and the total volume was adjusted to 200 mL to bring concentration of tris to 500 mM.

Running Buffer Stock Solution

Tris base (30.3 g), sodium dodecyl sulphate (10 g) and glycine (144 g) were weighed in a 1 L Schott bottle containing a magnetic stirrer bar. Deionised water (700 mL) was added, and the mixture was provided time for stirring to aid solubilisation of components. The volume of the buffer was made up to 1 L, and thus bringing the concentrations of tris base to 250 mM, sodium dodecyl sulphate to 35 mM and glycine to 1.9 M.

Running Buffer 10x Dilution

A volume of 100 mL running buffer stock solution was diluted in 900 mL of deionised water, and thus bringing the working buffer volume to 1 L.

6.2.2 Protein Production from Bacterial Gene Expression Systems

Lysogeny Broth (LB) Media Preparation and Sterilisation

A dry stock of Lysogeny broth (LB) was essembled using typtone, NaCl and yeast extract in a 2 : 2 : 1 ratio. From the dry stock, 2.5 g of LB was dissolved into 100 mL of dH_2O in a 100 mL glass bottle, and 25 g was placed into a glass flask filled with 1 L of dH_2O. The flask and glass bottle were subjected to sterilisation by using an Astell autoclave (120^oC for 4 hours, 1320 mBar, 15 minutes cooling time at 80^oC).

Chemical	Company	Lot #
Tryptone	Melford Biolaboratories	T60060 T1332 (33902)
NaCl	Fisher Scientific	1849132
Yeast Extract	Acros Organics	A0332869

Table 53 - Components assembled to produce LB media.

Small Scale Overnight E. coli Growth

From the sterilised 100 mL bottle of LB media, 10 mL was transferred under blue Bunsen burner flame on ethanol (70% $^V/_V$) washed surface into a sterile polypropylene steriline tube. To this sample, kanamycin sulfate (1.5 mg) was added to favour growth of genetically modified strain *E. coli* of interest.

BL21(DE3) *E. coli* strain comprised of *sfgfp* gene used for expression and production of sfGFP was introduced into the steriline tube shortly after, and over inoculation would proceed in an incubator with spinning (37^oC, 175 rpm for 16 hours). *E. coli* strain *Shuffle T7 express* containing *oaaep1* gene used for expression and production of OaAEP1 was subjected to the same conditions.

Chemical	Company	Lot #
Kanamycin Sulphate	Apollo Scientific	AS113963

Table 54 - Antibiotic used for overnight inoculation.

E. coli Growth Scale-up and Gene Expression

Following overnight inoculation *E. coli* strain, 1 mL of bactrerial cell suspension was transferred into a sterilised flask containing 1 L LB media and 50 mg kanamycin sulfate. This was performed on an ethanol (70% $^{V}/_{V}$) cleaned surface and under a blue Bunsen burner flame. Before the flask was placed into an incubator, a 1 mL aliquot of suspension was measured *via* UV-spectrometer at 600 nm to obtain OD_{600} values (time 0). After OD_{600} measurement the flask was placed into an Innova 44 Incubator Shaker (37°C, 200 rpm for 4 hours) to scale up *E. coli* growth. OD_{600} measurements would be taken to follow *E. Coli* and its optimal exponential growth (OD_{600} ~ 0.7). At 4 hours, optimal OD_{600} was achieved and 120 mg IPTG was added to the flask for gene expression. An additional 4 hours were granted for the cells to shake within the incubator before the cell suspension was transferred into centrifuge tubes subjected to centrifugation (6000 rpm, 4°C for 10 minutes). Pellets of fluorescent bacterial cells were collected and placed into 50 mL falcon tubes for storage in a -20°C freezer for later use.

Chemical	Company	Lot #
Kanamycin Sulphate	Apollo Scientific	AS113963
IPTG		AS473036

Table 55 - Antibiotic used for large scale E. coli growth and compound used for induction.

Cell Lysis

sfGFP

A sample of low concentration imidazole binding buffer (see 6.2.1 - Binding Buffer) was placed into a 50 mL falcon tube mixed with TCEP (114 mg). The pH of solution was measured using a digital pH probe and adjusted to pH 8.0 using 10 M NaOH (cautious dropwise addition *via* glass pasteur pipette). Adjusted buffer was then used to homogenise a cell pellet by vortex mixer (Scientific Industries SI™ Vortex-Genie™ 2) before resting the vessel in a water/ice bath and subjecting the suspension to 15 minutes of sonication (5 seconds on and 10 seconds off). Following sonication, the suspension was subjected to centrifugation (18000 rpm (110,000 x g), 4°C for 30 minutes) and after spinning, the lysate was separated from the pellet by decantation.

OaAEP1

Protocol applied was the same as the one used for cells containing sfGFP (see 6.2.2 - sfGFP). The only difference was the introduction of extra additives applied to the initial low imidazole binding buffer. Materials such as lysozyme (0.1 mg mL^{-1}) and PMSF (35 µg mL^{-1}) were employed along with TCEP, and following this, buffer pH was adjusted as previously documented.

Affinity Chromatography

A column filled with nickel nitrilotriacetic acid (Ni^{2+}-NTA) resin was washed with dH_2O (3 x 10 mL) to remove excess $NiCl_2$ with a gentle stream of nitrogen, and binding buffer (3 x 10 mL) was used to wash the resin. The lysate obtained from centrifugation was added into the column *via* 10 mL syringe fitted with a filter (0.22 µm) to allow proteins in the lysate comprised of His_6 tag to bind to the resin. Once all lysate was loaded onto the column, high concentration imidazole elution buffer (see 6.2.1 - Elution Buffer) was introduced to dissociate proteins bound to the resin and a stream of nitrogen to remove polypeptides from the column. The column was washed with the following materials in set order; dH_2O (2 x 10 mL), 0.5 M NaOH (10 mL), dH_2O (2 x 10 mL), 0.1 M EDTA pH 8.0 (2 x 10 mL), dH_2O (10 mL) and $NiCl_2$ (10 mL) before storage at 4ºC.

Chemical	Company	Lot #
PMSF	Fluorochem	FCB039886
TCEP		FCB062411
EDTA		FCB112739
$NiCl_2$	Fisher Scientific	1874363
NaOH		2041002
Lysozyme (14.4 KDa)	Sigma Aldrich	BCCD6905

Table 56 - Chemicals and quantities used for cell cracking and restoring affinity column.

Size Exclusion Chromatography

sfGFP Constructs

A Biorad FPLC pump was connected to a BioRad Next Generation Chromatography system connected to a HiLoad 26/600 superdex 75 pg (Cytiva)) size exclusion column (cross-linked agarose and dextran, 8.6 µm bead size) and fitted with a 6 mL loop. Phosphate buffer saline (see 6.2.1 - Phosphate Buffer Saline 10x Dilution) was prepared and degassed in a 2 L Schott bottle for 2 hours before use. After removing air bubbles, the buffer was connected to the FPLC pump, and the column was left to equilibrate overnight (flow rate = 0.5 mL min^{-1} and pressure = 0.1 MPa). The sequence applied for running overnight equilibration was an isocratic gradient that stopped column flow at 340 mL total volume.

Eluant obtained from affinity chromatography was concentrated using a 10 KDa spin column and centrifugation (6000 rpm at 4^{o}C) to volume corresponding to the 6 mL loop. Once the sample was injected into the loop an isocratic gradient was applied with a detection wavelength of 280 nm, flow rate of 2.5 mL min^{-1} and resulting pressure of 0.22 MPa. Fractions were collected autonomously *via* fraction collector and analysed by water synapt LC/MS.

OaAEP1

Protocol for obtaining OaAEP1 was the same as the one used for sfGFP construct isolations (see 6.2.2 - sfGFP Constructs), however, there were minor differences such as the buffer employed (150 mM NaCl, 50 mM sodium phosphate, 1 mM EDTA and 500 nM TCEP degassed at pH 6.5) and the immediate introduction of 20% $^{V}/_{V}$ glycerol into FPLC fractions to stabilise the target enzyme (1:1 dilution). Protein concentration was measured using a $^{1}/_{10}$ dilution (1 mL) *via* UV spectrometer and concentration measured was 7.4 µM (ε = 53290 mol^{-1} cm^{-1} L).[196]

SDS-PAGE

Resolving Gel (12%)

A mixture comprised of 30% acrylamide/bis-acrylamide (4 mL), deionised water (3.4 mL), resolving buffer (2.5 mL – see 6.2.1 - Resolving Buffer) and SDS 10% $^{W}/_{V}$ (100 µL) was assembled in a 20 mL steriline tube. Immediately before pouring, ammonium persulphate 10% $^{W}/_{V}$ (100 µL) and TEMED (20 µL) was added, and the concoction was gently mixed to initiate polymerisation.

Stacking Gel (5%)

A mixture comprised of 30% acrylamide/bis-acrylamide (850 µL), deionised water (2.85 mL), stacking buffer (1.25 mL – see 6.2.1 - Stacking Buffer) and SDS 10% $^{W}/_{V}$ (50 µL) was assembled in a 20 mL steriline tube. Immediately before pouring, ammonium persulphate 10% $^{W}/_{V}$ (50 µL) and TEMED (10 µL) was added, and the concoction was gently mixed to initiate polymerisation.

Electrophoresis

Bio-rad mini-PROTEAN tetra cell system and Bio-rad powerpack 3000 was used for SDS-PAGE experiments. Tris buffer gels were assembled using glass plates held together *via* casting clamp and stands. Resolving gel was assembled and poured between plates and provided time to polymerise. Stacking gel was subsequently added on top and provided time to polymerise. The gel was clamped into a running module along with a mini-cell buffer dam and placed into a gel box. Running buffer (see 6.2.1 - Running Buffer 10x Dilution) was used to fill the gel box. A lid comprised of electrodes was placed onto top of the gel box and connected to a powerpack. Conditions for SDS-PAGE were set to 200 V for 45 minutes.

Chemical	Company	Lot #
Quick Blue Protein Stain	Lubio Science	QC221601/2022-012
Unstained Protein Ladder Marker	Thermo Scientific	01051234
Ammonium Persulphate		1861583
TruPAGE™ LDS Sample Buffer	Sigma Aldrich	GR3378990-1
30% solution acrylamide/bis-acrylamide		SLCD3835
TEMED	Acros Organics	40159736

Table 57 - Chemicals used for SDS-PAGE.

6.2.3 Acetamide Capped sfGFP

BL21(DE3) *E. coli* gene expression system was used to obtain super folder sfGFP which was isolated from bacterial cells (see 6.2.2 - Cell Lysis and Affinity Chromatography). An excess of iodoacetamide was added to the eluate collected from the affinity column and given 1 hour for conjugation to the solvent exposed cysteine of sfGFP. The target conjugate was isolated by size exclusion column chromatography (see 6.2.2 - Size Exclusion Chromatography) and protein fractions were concentrated *via* spin column and centrifugation before concentration was determined by UV-spectroscopy (ε = 83,300 mol cm^{-1} L^{-1}).

Calculated Observed $^{M}I_{Z}$ = 26962.50

Chemical	Company	Lot #
Iodoacetamide	Fluka	397226/1 43599

Table 58 - Compound used for capping solvent exposed cysteine of sfGFP.

6.2.4 Aurein-1.2 Labelled sfGFP

The conjugation method employed to tether aurein-1.2 to sfGFP was like the off-resin technique used for thiol-acylation with iodoacetamide (see 6.2.3 Acetamide capped sfGFP). However, in this case, aurein-1.2 modified with *C*-terminal maleimide had to be solubilised in acetonitrile (2 mL) before introduction into the nickel column eluate containing sfGFP. Michael addition reaction was provided with 60 minutes before size exclusion column chromatography (see 6.2.2 - Size Exclusion Chromatography). Fractions comprised of conjugate were concentrated *via* spin column and centrifugation before concentration was determined by UV-spectroscopy (ε = 83,300 mol cm^{-1} L^{-1}).[204]

Calculated Observed $^{M}I_{Z}$ = 28,666 [M]

6.2.5 Pterin Labelled sfGFPs

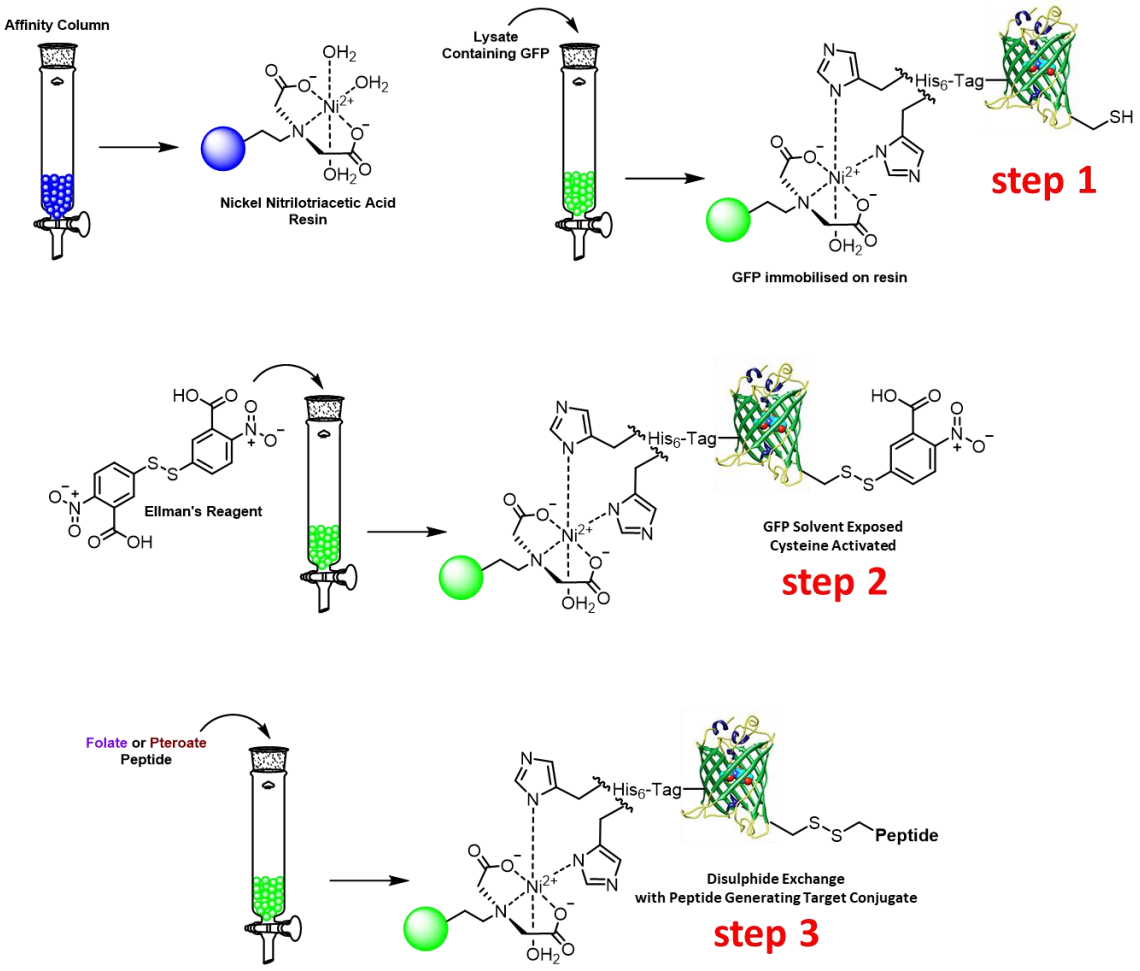

Scheme 20 - Site selective chemical modification of sfGFP via immobilisation on nickel resin.

Folate Labelled sfGFP

BL21(DE3) *E. coli* gene expression system was used to obtain super folder sfGFP which was isolated from bacterial cells (see 6.2.2 - Cell Lysis and Affinity Chromatography). In contrast to cysteine thiol acylation *via* iodoacetamide which occurred off resin (6.2.3 Acetamide Capped sfGFP), conjugation between pterin labelled peptide and sfGFP occurred on resin (**Scheme 2**). Whilst the protein was bound to Ni^{2+}NTA resin through interaction with its His_6 tag, the solvent exposed thiol was activated by introducing Ellman's reagent into the affinity column. After full saturation of all thiols, the column was washed with binding buffer to remove excess Ellman's reagent. Once cleared, 5 mg of pterin labelled peptide was solubilised in binding buffer and introduced into the affinity column for protein conjugation. This was given 1 hour before elution buffer (see 6.2.1 - Elution Buffer) was put into the column to dissociate conjugates from the nickel resin. The eluent was processed *via* size exclusion chromatography (see 6.2.2 - Size Exclusion Chromatography) and protein fractions were concentrated *via* spin column and centrifugation before concentration was determined by UV-spectroscopy (ε = 83,300 mol cm^{-1} L^{-1}).[204]

Calculated Observed $^{M}/_{Z}$ = 28036 [M] and 56072 [2M]

Pteroate Labelled sfGFP

Conjugation procedure used for the construction of folate labelled sfGFP was identical to the one applied in producing pteroate labelled sfGFP (see 6.2.5 - Folate Labelled sfGFP).

Calculated Observed $^{M}/_{Z}$ = 27905.0 [M], 13952.5 [$^{M}/_{2}$] and 55180.0 [2M]

6.2.6 OaAEP1 Mediated Test Reactions

Test peptide (GLPVSTKPVATRNGL) was used as the model system for enzyme mediated cyclisation reactions. Aliquots of peptide were prepared and comprised of 4 mg mL^{-1} and the planned ratio for this examination was 500 µM : 50 nM (peptide : OaAEP1). Test reactions were housed within eppendorfs and volumes were 50 µL. The buffer used for FPLC isolation of OaAEP1 was used in this experiment (see 6.2.2 - OaAEP1). Test reaction was given 60 minutes to proceed before diluting the system with buffer and analysing the sample *via* Waters synapt LC/MS.

6.3 Mammalian Cell Culture Work

Folate labelled conjugates based on sfGFP and naturally occurring cytotoxic peptides were tested on cancerous and non-cancerous mammalian cells. In this chapter the materials and methods used to investigate the behaviour of folate labelled polypeptides will be discussed.

6.3.1 Cell Maintenance

Freeze Thaw and Cell Growth

A 1 mL frozen stock of mammalian cells was taken from a -80°C freezer and placed into a 37°C water bath for 2 minutes of partial thawing. Once air bubbles had evolved, the cell stock was introduced to warm culture media in a 15 mL falcon tube and centrifugated (1200 rpm, 5 minutes at 25°C). The pellet formed was decanted to remove leftover materials such as DMSO that was present during prior cryogenic freezing process. Fresh culture media was used to re-suspend and homogenise the pellet, and this suspension was transferred into a sterile culture flask. The cells would be left to grow inside of a 37°C incubator (5% CO_2 / 95% humidified air) and media would be changed once every two days with a PBS wash in-between to remove dead cells. Mammalian cells were given time to grow to confluency (*e.g.* approximately 80% of vessel surface is covered with cells).

Cell Passage

Cell confluency was determined *via* microscopy and the media covering the cells was removed. PBS was used to wash off dead cells and a solution of 0.05% trypsin was added to the culture flask containing cells. The cells were placed into an 37°C incubator for 5 minutes to facilitate trypsin digestion of proteins anchoring cells to the flask. After this time, 5 mL of culture media (+ 10% $^{V}/_{V}$ FBS) was added to the flask to inhibit trypsin and the cells are removed from their flask and placed into a 15 mL falcon tube for centrifugation (1200 rpm, 5 minutes at 25°C). A cell pellet had formed, and media was decanted from the cell pellet to reduce trypsin concentration, and the pellet was resuspended in 5 mL of fresh media (+ 10% $^{V}/_{V}$ FBS). From this suspension 500 µL is taken and placed into a new flask pre-filled with appropriate culture media for further growth.

Cryogenic Freezing of Cells

Mammalian cells were grown to confluency, and this was determined *via* microscopy. Media covering the cells was removed and PBS was used to wash away dead cells. The cells were split from their flask by using 0.05% trypsin and submerged into media for resuspension and transfer into a flacon tube for centrifugation (1200 rpm, 5 mins at 25^{o}C). The cell pellet formed was decanted and re-suspended into a cryogenic freezing mixture comprised of 10% DMSO and 90% FBS $^{V}/_{V}$. From this suspension 1 mL was added into a 1.5 mL cryovial and placed into a Thermo Scientific Mr. Frosty freezing container filled with isopropanol. This was placed into a -80^{o}C freezer for cell preservation.

Trypan Blue Cell Viability Assay and Counting Cells

Mammalian cells were grown to confluency and split using 0.05% trypsin. Culture media was used to re-suspend and homogenise the cells. From this mixture 10 µL of cell suspension was mixed with 10 µL of trypan blue solution in a sterile Eppendorf. This concoction was pipetted in duplicate (2 x 10 µL) into either end of a plate reader, and this was placed into an Eve automated cell counter (NanoEnTek) to determine an approximate number of cells[205] and viability percentage.[206]

Chemical	Company	Lot #
DMEM (1X) + Glutamax Supplement	Gibco	2205979
RPMI Medium 1640 (1X)		2309569
Fetal Bovine Serum (FBS)		2275142
Trypsin (0.05%)		NA
Trypan Blue	NanoEntek	2C17761A
DMSO (Cell Culture Standard)	Fisher Scientific	175462
Isopropanol		1913436
Phosphate Buffer Saline (PBS)	Corining	322215009

Table 59 - Materials used for mammalian cell maintenance.

6.3.2 Polypeptide Concentration Determination

Native small polypeptide concentrations were analysed using a Shimadzu UV2600 UV-Vis spectrophotometer at 205 nm. A sample of pH 7.4 PBS (900 µL) was used to blank the spectrophotometer and the dilution employed was 1 in 10. Molar extinction coefficients used for concentration calculation was derived from a protein/peptide calculator (Protein Calculator (nih.gov)).[207]

All sfGFP constructs were analysed using the same buffer and UV-vis spectrophotometer. The wavelength set was 488 nm with a corresponding molar extinction coefficient (ε = 83,300 mol^{-1} cm^{-1} L)[204] for sfGFP used for calculating concentration. On the other hand, for small peptide sequences comprised of a folate motif, 100 mM NaOH was used for concentration measurement and a wavelength of 368 nm was used for obtaining an absorbance value.[208] Concentrations were determined using a known molar extinction coefficient (ε = 9,120 mol^{-1} cm^{-1} L).[208]

Polypeptide	**Extinction Coefficient (ε) – mol^{-1} cm^{-1} L**	**Wavelength (λ) - nm**
Acetamide Capped sfGFP	83,300	488
Folate labelled sfGFP		
Pteroate labelled sfGFP		
Aurein-1.2	50,560	205
Bid-BH3	64,700	
Folate labelled Aurein-1.2	9,120	368
Folate labelled Bid-BH3		

Table 60 - Polypeptide molar extinction coefficients and corresponding wavelengths.

6.3.3 Fluorescence Activated Cell Sorting (FACS)

Mammalian cells grown to confluency were split using 0.05% trypsin and re-suspended and homogenised in culture media. The cells were examined for viability and cell count *via* trypan blue before tests by using the protocol outlined previously (see 6.3.1 - Trypan Blue Cell Viability Assay and Counting Cells). Once a live cell population was established the cell suspension (2.0×10^5 cells mL^{-1}) was plated into 24 well plates in triplicate and provided with 24 hours to settle inside a 37°C incubator (5% CO_2 / 95% humidified air). Following overnight attachment, the cells were washed with PBS to remove dead cells, and subsequently, introduced to dilutions comprised of fluorescent protein in culture media (500 µL applied – varying concentrations). The cells were given 60 minutes to incubate with fluorescent protein before being detached from the 24 well plates *via* 0.05% trypsin. Fresh culture media was used to re-suspend the cells and transfer them through a filter into sterile test tubes. Each test tube was examined using a biorad S3e cell sorter. The cells sorter was calibrated using ZE-series quality control beads and 488 nm was the detection wavelength for green fluorescence. Each sample was given sufficient time for the cell sorter to collect a minimum of 10,000 cells. Shutdown of the cell sorter was performed at the conclusion of the experiments and a high-pressure wash using 70% $^{V}/_{V}$ ethanol in deionised water.

Chemical	Company	Lot #
ZE-Series QC Beads, 3-3.4 µm, 1×10^6 beads mL^{-1}	Bio-Rad	Catalogue # = 12004403 BR080712A
Ethanol	Fisher Scientific	2211390

Table 61 - Materials used for FACS calibration and cleaning.

6.3.4 Cell Titre Blue Cell Viability Assays

Mammalian cells grown to confluency were split using 0.05% trypsin and re-suspended and homogenised in culture media. The cells were examined for viability and cell count *via* trypan blue before tests by using the protocol outlined previously (see 6.3.1 - Trypan Blue Cell Viability Assay and Counting Cells). Once population count was established the cell suspension (2.0 x 10^5 cells mL^{-1}) was plated into 96 well plates and provided with 24 hours to settle inside a 37°C incubator (5% CO_2 / 95% humidified air). Following overnight attachment, the cells were washed with PBS to remove dead cells, and subsequently, introduced to dilutions comprised of varying concentration of polypeptide in culture media (100 µL). The cells were provided with 20 hours to incubate before cell titre blue (20 µL) was added to each well and incubated for an additional 4 hours before being analysed by a plate reader. The plate reader employed was a perkin elmer victor X5 multimode plate reader for resorufin fluorescence at 590 nm.

Chemical	Company	Lot #
DMEM (1X) + Glutamax Supplement	Gibco	2205979
RPMI Medium 1640 (1X)		2309569
Fetal Bovine Serum (FBS)		2275142
0.05% Trypsin		NA
PBS	Corining	322215009
Cell Titre Blue Cell Viability Assay	Promega	0000340854

Table 62 - Materials used for cell viability experiments.

IC_{50} Curves

The cell titre blue cell viability data was fitted according to the following equation in GraphPad Prism version 9 for Windows, San Diego, California USA, www.graphpad.com: log (inhibitor) vs response – variable slope four parameters, Y=bottom + (Top-Bottom)/(1+10^((LogIC_{50}-X)*Hillslope)).

Statistical Analysis

Calculation of statistical significance (FACS and cell titre blue cell viability data) was performed using, data analysis, t-test: paired two samples for means on Microsoft excel with α-value set to 0.05.

References

1 W. M. Strong, *J. Cancer Res.*, 1921, **6**, 251–256.

2 P. J. Landrigan, *Ann. Res. Oncol.*, 2022, **2**, 89–93.

3 A. Ferrari, D. Stark, F. A. Peccatori, L. Fern, V. Laurence, N. Gaspar, I. Bozovic-Spasojevic, O. Smith, J. De Munter, K. Derwich, L. Hjorth, W. T. A. van der Graaf, L. Soanes, S. Jezdic, A. Blondeel, S. Bielack, J. Y. Douillard, G. Mountzios and E. Saloustros, *ESMO Open*, 2021, **6**, 100096.

4 C. Haub and J. Gribble, *Popul. Bull.*, 2011, **66**, 1.

5 UK Population Estimates 1851 - 2014, https://www.ons.gov.uk/peoplepopulationandcommunity/populationandmigration/populationestimates/adhocs/004356ukpopulationestimates1851to2014, (accessed 1 April 2020).

6 Cancer Mortality Statistics, https://www.cancerresearchuk.org/health-professional/cancer-statistics/mortality, (accessed 1 April 2020).

7 Understanding Cancer, https://www.cancer.gov/about-cancer/understanding/what-is-cancer#genes-causing-cancer, (accessed 28 July 2022).

8 G. I. Evan and K. H. Vousden, *Nature*, 2001, **411**, 342–348.

9 A. Sharma, L. H. Boise and M. Shanmugam, *Cancers (Basel).*, 2019, **11**, 1144.

10 H. Elnakat and M. Ratnam, *Adv. Drug Deliv. Rev.*, 2004, **56**, 1067–1084.

11 H. Sung, J. Ferlay, R. L. Siegel, M. Laversanne, I. Soerjomataram, A. Jemal and F. Bray, *CA. Cancer J. Clin.*, 2021, **71**, 209–249.

12 B. Lin, F. Gao, Y. Yang, D. Wu, Y. Zhang, G. Feng, T. Dai and X. Du, *Front. Oncol.*, , DOI:10.3389/fonc.2021.644400.

13 D. De Ruysscher, G. Niedermann, N. G. Burnet, S. Siva, A. W. M. Lee and F. Hegi-Johnson, *Nat. Rev. Dis. Prim.*, , DOI:10.1038/s41572-019-0064-5.

14 P. Nygren, *Acta Oncol. (Madr).*, 2001, **40**, 166–174.

15 J. Hirsch, *J. Am. Med. Assoc.*, 2006, **296**, 1518–1520.

16 H. Joensuu, *Lancet Oncol.*, 2008, **9**, 304.

17 J. Drews, *Science (80-.).*, 2008, **1960**, 1960–1965.

18 P. T. R. Rajagopalan, Z. Zhang, L. McCourt, M. Dwyer, S. J. Benkovic and G. G. Hammes, *Proc. Natl. Acad. Sci.*, 2002, **99**, 13481–13486.

19 J. Selhub, *J. Nutr. Health Aging*, 2002, **6**, 39–42.

20 Goodman L. S., *J. Am. Med. Assoc.*, 1946, **132**, 126–132.

21 L. Holmboe, A. M. Andersen, L. Mørkrid, L. Slørdal and K. S. Hall, *Br. J. Clin. Pharmacol.*, 2012, **73**, 106–114.

22 M. Hospital, *Br. J. Dermatol.*, 1990, **36**, 127–133.

23 R. J. Hilsden, S. J. Urbanski and M. G. Swain, *ARTHRITIS Rheum.*, 1995, **38**, 1014–1018.

24 M. F. Dawwas and G. P. Aithal, *Aliment. Pharmacol. Ther.*, 2014, **40**, 938–948.

25 E. D. Simmons and K. A. Somberg, *Am. Cancer Soc.*, 1991, **67**, 2062–2065.

26 I. R. Vlahov and C. P. Leamon, *Bioconjug. Chem.*, 2012, **23**, 1357–1369.

27 M. Luyckx, R. Votino, J. L. Squifflet and J. F. Baurain, *Int. J. Womens. Health*, 2014, **6**, 351–358.

28 P. Pribble and M. J. Edelman, *Expert Opin. Investig. Drugs*, 2012, **21**, 755–761.

29 A. H. Maurer, P. Elsinga, S. Fanti, B. Nguyen, W. J. G. Oyen and W. A. Weber, *J. Nucl. Med.*, 2014, **55**, 701–704.

30 L. L. Albert and A. L. Lehninger, *Lehninger principles of biochemistry / David L. Nelson, Michael M. Cox*, 2005.

31 G. M. Cooper and R. E. Hausman, *The Cell: A Molecular Approach 2nd Edition*, 2007.

32 M. T. Dorak, *Am. J. Epidemiol.*, 2002, **5**, 69.

33 M. Nagl, L. Kacani, B. Müllauer, E. M. Lemberger, H. Stoiber, G. M. Sprinzl, H. Schennach and M. P. Dierich, *Clin. Diagn. Lab. Immunol.*, , DOI:10.1128/CDLI.9.6.1165-1168.2002.

34 C. Rosales and E. Uribe-Querol, *Biomed Res. Int.*, 2017.

35 H. T. McMahon and E. Boucrot, *Nat. Rev. Mol. Cell Biol.*, 2011, **12**, 517–533.

36 D. Ricotta, S. D. Conner, S. L. Schmid, K. Von Figura and S. Höning, *J. Cell Biol.*, 2002, **156**, 791–795.

37 S. D. Conner and S. L. Schmid, *J. Cell Biol.*, 2003, **162**, 773–779.

38 B. Chen, M. R. Dores, N. Grimsey, I. Canto, B. L. Barker and J. A. Trejo, *J. Biol. Chem.*, 2011, **286**, 40760–40770.

39 E. Ter Haar, S. C. Harrison and T. Kirchhausen, *Proc. Natl. Acad. Sci. U. S. A.*, 2000, **97**, 1096–1100.

40 L. Hinrichsen, A. Meyerholz, S. Groos and E. J. Ungewickell, *Proc. Natl. Acad. Sci.*, 2006, **103**, 8715–8720.

41 A. Musacchio, C. J. Smith, A. M. Roseman, S. C. Harrison, T. Kirchhausen and B. M. F. Pearse, *Mol. Cell*, 1999, **3**, 761–770.

42 S. M. Ferguson and P. De Camilli, *Nat. Rev. Mol. Cell Biol.*, 2012, **13**, 75–88.

43 A. M. Van Der Bliek, T. E. Redelmeier, H. Damke, E. J. Tisdale, E. M. Meyerowitz and S. L. Schmid, *J. Cell Biol.*, 1993, **122**, 553–563.

44 S. Mayor, R. G. Parton and J. G. Donaldson, *Cold Spring Harb. Perspect. Biol.*, 2014, **6**, 1–20.

45 J. Cherfils and P. Chardin, *Trends Biochem. Sci.*, 1999, **24**, 306–311.

46 K. L. Rossman, D. K. Worthylake, J. T. Snyder, D. P. Siderovski, S. L. Campbell and J. Sondek, *EMBO J.*, 2002, **21**, 1315–1326.

47 L. A. Quilliam, R. Khosravi-Far, S. Y. Huff and C. J. Der, *BioEssays*, 1995, **17**, 395–404.

48 R. Rohatgi, H. Y. H. Ho and M. W. Kirschner, *J. Cell Biol.*, 2000, **150**, 1299–1309.

49 H. N. Higgs and T. D. Pollard, *J. Cell Biol.*, 2000, **150**, 1311–1320.

50 W. Bu, A. M. Chou, K. B. Lim, T. Sudhaharan and S. Ahmed, *J. Biol. Chem.*, 2009, **284**, 11622–11636.

51 C. Endocytosis, A. P. A. Ferreira and E. Boucrot, *Trends Cell Biol.*, **28**, 188–200.

52 L. Johannes, R. G. Parton, P. Bassereau and S. Mayor, *Nat. Rev. Mol. Cell Biol.*, 2015, **16**, 311–321.

53 S. Sabharanjak and S. Mayor, *Adv. Drug Deliv. Rev.*, 2004, **56**, 1099–1109.

54 S. Sabharanjak, P. Sharma, R. G. Parton and S. Mayor, *Dev. Cell*, 2002, **2**, 411–423.

55 A. S. Wibowo, M. Singh, K. M. Reeder, J. J. Carter, A. R. Kovach, W. Meng, M. Ratnam, F. Zhang and C. E. Dann, *Proc. Natl. Acad. Sci. U. S. A.*, 2013, 110, 15180–15188.

56 R. G. Parton, *Encycl. Cell Biol.*, 2015, 2, 394–400.

57 R. Zhao, S. H. Min, Y. Wang, E. Campanella, P. S. Low and I. D. Goldman, *J. Biol. Chem.*, 2009, **284**, 4267–4274.

58 M. Fernández, F. Javaid and V. Chudasama, *Chem. Sci.*, 2018, **9**, 790–810.

59 S. Tyagi, *Int. J. Pharm. Sci. Res.*, 2016, **7**, 4278–4303.

60 M. Scaranti, E. Cojocaru, S. Banerjee and U. Banerji, *Nat. Rev. Clin. Oncol.*, 2020, **17**, 349–359.

61 N. Parker, M. J. Turk, E. Westrick, J. D. Lewis, P. S. Low and C. P. Leamon, *Anal. Biochem.*, 2005, **338**, 284–293.

62 R. M. Sandoval, M. D. Kennedy, P. S. Low and B. A. Molitoris, *Am. J. Physiol. - Cell Physiol.*, 2004, 287.

63 S. L. Samodelov, Z. Gai, G. A. Kullak-Ublick and M. Visentin, *Nutrients*, , DOI:10.3390/nu11102353.

64 F. Maguire, F. L. Henriquez, G. Leonard, J. B. Dacks, M. W. Brown and T. A. Richards, *Genome Biol. Evol.*, 2014, **6**, 2709–2720.

65 X. F. Le, F. Pruefer and R. C. Bast, *Cell Cycle*, 2005, **4**, 87–95.

66 G. Valabrega, F. Montemurro and M. Aglietta, *Ann. Oncol.*, 2007, **18**, 977–984.

67 A. Berchuck, A. Kamel, R. Whitaker, B. Kerns, G. Olt, R. Kinney, J. T. Soper, R. Dodge, D. L. Clarke-Pearson and P. Marks, *Cancer Res.*, 1990, **50**, 4087–4091.

68 J. Weber, U. Haberkorn and W. Mier, *Int. J. Mol. Sci.*, 2015, **16**, 4918–4946.

69 A. Cagaanan, B. Stelter, N. Vu, E. N. Rhode, T. Stewart, P. Hui, N. Buza, A. Al-Niaimi, C. Flynn, P. S. Weisman and S. M. McGregor, *Int. J. Gynecol.*

Pathol., 2022, **41**, 132–141.

70 I. D. Goldman, *Clin. Cancer Res.*, 2002, **8**, 4–6.

71 R. Krishna and L. D. Mayer, *Eur. J. Pharm. Sci.*, 2000, **11**, 265–283.

72 D. B. Longley and P. G. Johnston, *J. Pathol.*, 2005, **205**, 275–292.

73 J. Goebel, J. Chmielewski and C. A. Hrycyna, *Cancer Drug Resist.*, 2021, **4**, 784–804.

74 C. P. Leamon, J. A. Reddy, P. J. Klein, I. R. Vlahov, R. Dorton, A. Bloomfield, M. Nelson, E. Westrick, N. Parker, K. Bruna, M. Vetzel, M. Gehrke, J. S. Nicoson, R. A. Messmann, P. M. LoRusso and E. A. Sausville, *J. Pharmacol. Exp. Ther.*, 2011, **336**, 336–343.

75 J. C. Paulson and W. Mcclurei, *Ann. New York Acad. Sci.*, 1975, **253**, 517–527.

76 C. A. Hudis, *N. Engl. J. Med.*, 2007, **357**, 39–51.

77 J. A. Konner, K. M. Bell-McGuinn, P. Sabbatini, M. L. Hensley, W. P. Tew, N. Pandit-Taskar, N. Vander Els, M. D. Phillips, C. Schweizer, S. C. Weil, S. M. Larson and L. J. Old, *Clin. Cancer Res.*, 2010, **16**, 5288–5295.

78 E. Raymond, E. Pisano, C. Gatsonis, R. Boineau, M. Domanski, C. Troutman, J. Anderson, G. Johnson, S. E. Mcnulty, N. Clapp-channing, L. D. Davidson-ray, E. S. Fraulo, D. P. Fishbein and R. M. Luceri, *N. Engl. J. Med.*, 2011, **365**, 1273–1283.

79 P. Hillmen, A. B. Skotnicki, T. Robak, B. Jaksic, A. Dmoszynska, J. Wu, C. Sirard and J. Mayer, *J. Clin. Oncol.*, 2007, **25**, 5616–5623.

80 H. Kantarjian, A. Stein, N. Gökbuget, A. K. Fielding, A. C. Schuh, J. M. Ribera, A. Wei, H. Dombret, R. Foà, R. Bassan, Ö. Arslan, M. A. Sanz, J. Bergeron, F. Demirkan, E. Lech-Maranda, A. Rambaldi, X. Thomas, H. A. Horst, M. Brüggemann, W. Klapper, B. L. Wood, A. Fleishman, D. Nagorsen, C. Holland, Z. Zimmerman and M. S. Topp, *N. Engl. J. Med.*, 2017, **376**, 836–847.

81 K. Imai and A. Takaoka, *Nat. Rev. Cancer*, 2006, **6**, 714–727.

82 G. Piotrowski, R. Gawor, A. Stasiak, Z. Gawor, P. Potemski and M. Banach, *Arch. Med. Sci.*, 2012, **8**, 227–235.

83 P. Österlund, L. M. Soveri, H. Isoniemi, T. Poussa, T. Alanko and P. Bono, *Br. J. Cancer*, 2011, **104**, 599–604.

84 Y. Hanaoka, H. Soejima, O. Yasuda, H. Nakayama, M. Nagata, K. Matsuo, M. Shinohara, Y. Izumi and H. Ogawa, *Hypertens. Res.*, 2013, **36**, 829–833.

85 X. F. Hang, W. S. Xu, J. X. Wang, L. Wang, H. G. Xin, R. Q. Zhang and W. Ni, *Eur. J. Clin. Pharmacol.*, 2011, **67**, 613–623.

86 A. K. Alahmari, Z. S. Almalki, A. K. Alahmari and J. J. Guo, *Am. Heal. Drug Benefits*, 2016, **9**, 221–231.

87 P. Chames, M. V. Regenmortel, E. Weiss and D. Baty, *Brtish J. Pharmacol.*, 2009, **157**, 220–233.

88 S. Olsnes and A. Pihl, *FEBS Lett.*, 1972, **20**, 327–329.

89 S. Olsnes and A. Pihl, *Biochemistry*, 1973, **12**, 3121–3126.

90 S. Olsnes, R. Heiberg and A. Pihl, *Mol. Biol. Rep.*, 1973, **1**, 15–20.

91 C. P. Leamon and P. S. Low, *J. Biol. Chem.*, 1992, **267**, 24966–24971.

92 C. P. Leamon, I. Pastan and P. S. Low, *J. Biol. Chem.*, 1993, **268**, 24847–24854.

93 D. B. Thompson, R. Villaseñor, B. M. Dorr, M. Zerial and D. R. Liu, *Chem. Biol.*, 2012, **19**, 831–843.

94 M. Inagaki, Y. Sakakura, H. Itoh, K. Ukai and Y. Miyoshi, *Rhinology*.

95 G. M. Grass and J. R. Robinson, *J. Pharm. Sci.*, , DOI:10.1002/jps.2600770104.

96 M. Li, Y. Tao, Y. Shu, J. R. LaRochelle, A. Steinauer, D. Thompson, A. Schepartz, Z. Y. Chen and D. R. Liu, *J. Am. Chem. Soc.*, 2015, **137**, 14084–14093.

97 B. Tam, D. Sherf, S. Cohen, S. A. Eisdorfer, M. Perez, A. Soffer, D. Vilenchik, S. R. Akabayov, G. Wagner and B. Akabayov, *Chem. Sci.*, 2019, **10**, 8764–8767.

98 X. Ge, A. Oliveira, K. Hjort, T. Bergfors, H. G. de Terán, D. I. Andersson, S. Sanyal and J. Åqvist, *Sci. Rep.*, 2019, **9**, 1–10.

99 R. Ferreira, J. S. Schneekloth, K. I. Panov, K. M. Hannan and R. D. Hannan,

Cells, 2020, **9**, 266.

100 L. Benedetti, J. S. Marvin, H. Falahati, A. Guillén-Samander, L. L. Looger and P. De Camilli, *Elife*, 2020, **9**, 1–49.

101 D. Guimarães, A. Cavaco-Paulo and E. Nogueira, *Int. J. Pharm.*, , DOI:10.1016/j.ijpharm.2021.120571.

102 J. O. Eloy, M. Claro de Souza, R. Petrilli, J. P. A. Barcellos, R. J. Lee and J. M. Marchetti, *Colloids Surfaces B Biointerfaces*, 2014, **123**, 345–363.

103 M. Alavi, N. Karimi and M. Safaei, *Adv. Pharm. Bull.*, 2017, **7**, 3–9.

104 H. Daraee, A. Etemadi, M. Kouhi, S. Alimirzalu and A. Akbarzadeh, *Artif. Cells, Nanomedicine Biotechnol.*, 2016, **44**, 381–391.

105 S. Shah, V. Dhawan, R. Holm, M. S. Nagarsenker and Y. Perrie, *Adv. Drug Deliv. Rev.*, 2020, **154**–**155**, 102–122.

106 J. Shi, Y. Ma, J. Zhu, Y. Chen, Y. Sun, Y. Yao, Z. Yang and J. Xie, *Molecules*, , DOI:10.3390/molecules23113044.

107 A. Adamo, A. Arione, A. Sharei and K. F. Jensen, *Anal. Chem.*, 2013, **85**, 1637–1641.

108 D. Kalafatovic and E. Giralt, *Cell-penetrating peptides: Design strategies beyond primary structure and amphipathicity*, 2017, vol. 22.

109 V. Mukundan, C. Maksoudian, M. C. Vogel, I. Chehade, M. S. Katsiotis, S. M. Alhassan and M. Magzoub, *Arch. Biochem. Biophys.*, , DOI:10.1016/j.abb.2016.11.001.

110 K. Löfgren, A. Wahlström, P. Lundberg, Ö. Langel, A. Gräslund and K. Bedecs, *FASEB J.*, , DOI:10.1096/fj.07-099549.

111 P. E. G. Thorén, D. Persson, M. Karlsson and B. Nordén, *FEBS Lett.*, , DOI:10.1016/S0014-5793(00)02072-X.

112 C. Rüter, C. Buss, J. Scharnert, G. Heusipp and M. A. Schmidt, *J. Cell Sci.*, , DOI:10.1242/jcs.063016.

113 C. O. Pabo and A. D. Frankel, *Cell Press*, 1988, **55**, 1189–1193.

114 M. Gomarasca, T. F. C. Martins, L. Greune, P. R. Hardwidge, M. A. Schmidt and C. Rüter, *Antimicrob. Agents Chemother.*, 2017, **61**, 1–20.

115 J. Li, F. Liu, Q. Shao, Y. Min, M. Costa, E. K. L. Yeow and B. Xing, *Adv. Healthc. Mater.*, 2014, **3**, 1230–1239.

116 B. R. Meade and S. F. Dowdy, *Adv. Drug Deliv. Rev.*, 2007, **59**, 134–140.

117 M. Oba, Y. Demizu, H. Yamashita, M. Kurihara and M. Tanaka, *Bioorganic Med. Chem.*, , DOI:10.1016/j.bmc.2015.05.025.

118 T. Kato, H. Yamashita, T. Misawa, K. Nishida, M. Kurihara, M. Tanaka, Y. Demizu and M. Oba, *Bioorganic Med. Chem.*, , DOI:10.1016/j.bmc.2016.04.031.

119 S. G. Patel, E. J. Sayers, L. He, R. Narayan, T. L. Williams, E. M. Mills, R. K. Allemann, L. Y. P. Luk, A. T. Jones and Y. H. Tsai, *Sci. Rep.*, , DOI:10.1038/s41598-019-42456-8.

120 S. Reissmann, *J. Pept. Sci.*, 2014, **20**, 760–784.

121 H. C. Christianson and M. Belting, *Matrix Biol.*, 2014, **35**, 51–55.

122 D. A. Simon Davis and C. R. Parish, *Front. Immunol.*, 2013, **4**, 1–7.

123 A. Walrant, C. Bechara, I. D. Alves and S. Sagan, *Nanomedicine*, 2012, **7**, 134–143.

124 P. Säälik, K. Padari, A. Niinep, A. Lorents, M. Hansen, E. Jokitalo, Ü. Langel and M. Pooga, *Bioconjug. Chem.*, 2009, **20**, 877–887.

125 U. Soomets, M. Lindgren, X. Gallet, M. Hällbrink, A. Elmquist, L. Balaspiri, M. Zorko, M. Pooga, R. Brasseur and Ü. Langel, *Biochim. Biophys. Acta - Biomembr.*, 2000, **1467**, 165–176.

126 K. Montrose, Y. Yang, X. Sun, S. Wiles and G. W. Krissansen, *Sci. Rep.*, 2013, **3**, 1–7.

127 J. B. Rothbard, T. C. Jessop, R. S. Lewis, B. A. Murray and P. A. Wender, *J. Am. Chem. Soc.*, 2004, **126**, 9506–9507.

128 M. Di Pisa, G. Chassaing and J. M. Swiecicki, *Biochemistry*, 2015, **54**, 194–207.

129 S. R. Dennison, F. Harris and D. A. Phoenix, *Biophys. Chem.*, 2007, **127**, 78–83.

130 Y. Li, Y. Liu, Y. Zhou, W. Liu, Y. Fan, N. Jiang, M. Xue, Y. Meng and L. Zeng,

Dev. Comp. Immunol., 2021, **116**, 103935.

131 T. Rozek, K. L. Wegener, J. H. Bowie, I. N. Olver, J. A. Carver, J. C. Wallace and M. J. Tyler, *Eur. J. Biochem.*, 2000, **267**, 5330–5341.

132 S. Elmore, *Toxicol. Pathol.*, 2007, **35**, 495–516.

133 R. Singh, A. Letai and K. Sarosiek, *Nat. Rev. Mol. Cell Biol.*, 2019, **20**, 175–193.

134 P. Thiagarajan, C. J. Parker and J. T. Prchal, *Front. Physiol.*, 2021, **12**, 8–10.

135 J. J. Luke, C. I. van de Wetering and C. M. Knudson, *Cell Death Differ.*, 2003, **10**, 740–748.

136 C. Candé, N. Vahsen, C. Garrido and G. Kroemer, *Cell Death Differ.*, 2004, **11**, 591–595.

137 I. F. Sevrioukova, *Antioxid. Redox Signal.*, 2011, **14**, 2545–2579.

138 M. Tanaka, T. Suda, T. Takahashi and S. Nagata, *EMBO J.*, 1995, **14**, 1129–1135.

139 M. E. Peter and P. H. Krammer, *Cell Death Differ.*, 2003, **10**, 26–35.

140 M. Donepudi, A. Mac Sweeney, C. Briand and M. G. Grütter, *Mol. Cell*, 2003, **11**, 543–549.

141 L. D. Walensky, *Nat. Chem. Biol.*, 2019, **15**, 657–665.

142 C. Kantari and H. Walczak, *Biochim. Biophys. Acta - Mol. Cell Res.*, 2011, **1813**, 558–563.

143 D. I. Fernandez, J. D. Gehman and F. Separovic, *Biochim. Biophys. Acta - Biomembr.*, 2009, **1788**, 1630–1638.

144 M. A. Apponyi, T. L. Pukala, C. S. Brinkworth, V. M. Maselli, J. H. Bowie, M. J. Tyler, G. W. Booker, J. C. Wallace, J. A. Carver, F. Separovic, J. Doyle and L. E. Llewellyn, *Peptides*, 2004, **25**, 1035–1054.

145 D. I. Fernandez, A. P. Le Brun, T. C. Whitwell, M. A. Sani, M. James and F. Separovic, *Phys. Chem. Chem. Phys.*, 2012, **14**, 15739–15751.

146 I. R. Vlahov, H. K. R. Santhapuram, P. J. Kleindl, S. J. Howard, K. M. Stanford and C. P. Leamon, *Bioorganic Med. Chem. Lett.*, 2006, **16**, 5093–5096.

147 G. L. Ellman, *Arch. Biochem. Biophys.*, 1959, **82**, 70–77.

148 G. L. Ellman, *Arch. Biochem. Biophys.*, 1958, **74**, 443–450.

149 V. Ghetie, M. A. Ghetie, J. W. Uhr and E. S. Vitetta, *J. Immunol. Methods*, 1988, **112**, 267–277.

150 G. T. Hermanson, *Bioconjugation Techniques*, Academic Press, Rockford, Illinois, USA, 2nd edn., 2008.

151 A. Michael, *J. Pract. Chem.*, 1887, **35**, 349–356.

152 K. Renault, J. W. Fredy, P. Y. Renard and C. Sabot, *Bioconjug. Chem.*, 2018, **29**, 2497–2513.

153 P. Ochtrop and C. P. R. Hackenberger, *Curr. Opin. Chem. Biol.*, 2020, **58**, 28–36.

154 G. Marverti, C. Marraccini, A. Martello, D. D'Arca, S. Pacifico, R. Guerrini, F. Spyrakis, G. Gozzi, A. Lauriola, M. Santucci, G. Cannazza, L. Tagliazucchi, A. S. Cazzato, L. Losi, S. Ferrari, G. Ponterini and M. P. Costi, *J. Med. Chem.*, 2021, **64**, 3204–3221.

155 D. Wang, Z. Fan, X. Zhang, H. Li, Y. Sun, M. Cao, G. Wei and J. Wang, *Langmuir*, 2021, **37**, 339–347.

156 C. P. Leamon, R. B. DePrince and R. W. Hendren, *J. Drug Target.*, 1999, **7**, 157–169.

157 Y. Dai, X. Cai, X. Bi, C. Liu, N. Yue, Y. Zhu, J. Zhou, M. Fu, W. Huang and H. Qian, *Eur. J. Med. Chem.*, 2019, **171**, 104–115.

158 C. P. Leamon, I. R. Vlahov, J. A. Reddy, M. Vetzel, H. K. R. Santhapuram, F. You, A. Bloom, R. Dorton, M. Nelson, P. Kleindl, J. F. Vaughn and E. Westrick, *Bioconjug. Chem.*, 2014, **25**, 560–568.

159 D. Cardella, W. Deng, L. Y. P. Luk and Y.-H. Tsai, *Biomolecules*, , DOI:10.3390/biom12050725.

160 Z. Gong, M. T. Walls, A. N. Karley and A. J. Karlsson, *Mol. Biotechnol.*, , DOI:10.1007/s12033-016-9983-5.

161 M. Stawikowski and G. B. Fields, *Curr. Protoc. Protein Sci.*, 2002, **26**, 1–17.

162 A. Isidro-Llobet, M. N. Kenworthy, S. Mukherjee, M. E. Kopach, K. Wegner,

F. Gallou, A. G. Smith and F. Roschangar, *J. Org. Chem.*, 2019, **84**, 4615–4628.

163 M. Verlander, *Int. J. Pept. Res. Ther.*, 2007, **13**, 75–82.

164 G. W. Anderson, *New York Accademy Sci.*, 1960, **88**, 676–688.

165 P. D. W. and W. C. CHAN, *Fmoc SPPS - A pratical approach*, Oxford University Press, Oxford, 2000.

166 R. B. Merrifield, *J. Am. Chem. Soc.*, 1963, **85**, 2149–2154.

167 R. B. Merrifield, *Biochemistry*, 1964, **3**, 1385–1390.

168 R. B. Merrifield, *Endeavour*, , DOI:10.1016/0160-9327(65)90090-6.

169 A. Isidro-llobet, F. Albericio and M. Alvarez, *Chem. Rev.*, 2009, **109**, 2455–2504.

170 P. D. W. and W. C. CHAN, *Fmoc SPPS - A pratical approach*, Oxford University Press, Oxford, 2000.

171 S. B. H. Kent, *Annu. Rev. Biomchemistry*, 1988, **57**, 957–985.

172 M. Beyermann and M. Bienert, *Tetrahedron Lett.*, 1992, **33**, 3745–3748.

173 C. Y. Ke, C. J. Mathias and M. A. Green, *J. Am. Chem. Soc.*, 2005, **127**, 7421–7426.

174 P. C. Elwood, M. A. Kane, R. M. Portillo and J. F. Kolhouse, *J. Biol. Chem.*, 1986, **261**, 15416–15423.

175 K. Pal, A. Heinsch, A. Berkessel and A. L. Koner, *Chem. - A Eur. J.*, 2017, **23**, 15008–15011.

176 S. Gorle, M. Ariatti and M. Singh, *Eur. J. Pharm. Sci.*, 2014, **59**, 83–93.

177 B. A. Kamen and A. Capdevila, *Proc. Natl. Acad. Sci. U. S. A.*, 1986, **83**, 5983–5987.

178 J. A. Ledermann, S. Canevari and T. Thigpen, *Ann. Oncol.*, 2015, **26**, 2034–2043.

179 M. Divito, W. Miller, J. Uzarski and J. Wertheim, *Biomaterials*, 2017, **129**, 163–175.

180 T. Harayama and H. Riezman, *Nat. Rev. Mol. Cell Biol.*, 2018, **19**, 281–296.

181 J. Lombard, P. López-García and D. Moreira, *Nat. Rev. Microbiol.*, 2012, **10**, 507–515.

182 M. F. Mescher, *Trends Biochem. Sci.*, 1981, **6**, 97–99.

183 R. Zhang, X. Qin, F. Kong, P. Chen and G. Pan, *Drug Deliv.*, 2019, 26, 328–342.

184 G. L. Nicolson, *Biochim. Biophys. Acta - Biomembr.*, 2014, **1838**, 1451–1466.

185 B. B. Boycott and A. Curtis, *General Biology*, 2020.

186 M. M. Lacy, R. Ma, N. G. Ravindra and J. Berro, *FEBS Lett.*, 2018, **592**, 3586–3605.

187 S. Katayama, I. Nakase, Y. Yano, T. Murayama, Y. Nakata, K. Matsuzaki and S. Futaki, *Biochim. Biophys. Acta - Biomembr.*, 2013, **1828**, 2134–2142.

188 A. Fittipaldi, A. Ferrari, M. Zoppé, C. Arcangeli, V. Pellegrini, F. Beltram and M. Giacca, *J. Biol. Chem.*, 2003, **278**, 34141–34149.

189 A. Ferrari, V. Pellegrini, C. Arcangeli, A. Fittipaldi, M. Giacca and F. Beltram, *Mol. Ther.*, 2003, **8**, 284–294.

190 J. S. Wadia, R. V. Stan and S. F. Dowdy, *Nat. Med.*, 2004, **10**, 310–315.

191 N. Nischan, H. D. Herce, F. Natale, N. Bohlke, N. Budisa, M. C. Cardoso and C. P. R. Hackenberger, *Angew. Chemie - Int. Ed.*, 2015, **54**, 1950–1953.

192 K. Matsuda, H. Maruyama, F. Guo, J. Kleeff, J. Itakura, Y. Matsumoto, A. D. Lander and M. Korc, *Cancer Res.*, 2001, **61**, 5562–5569.

193 H. Park, Y. Kim, Y. Lim, I. Han and E.-S. Oh, *J. Biol. Chem.*, 2002, **277**, 29730–29736.

194 Z. Junmin and R. Marchant, *J. Pept. Sci.*, 2007, **14**, 690–696.

195 K. S. Harris, S. Poon, P. Quimbar and M. A. Anderson, *Methods Mol. Biol.*, 2019, **2012**, 211–235.

196 T. M. S. Tang, D. Cardella, A. J. Lander, X. Li, J. S. Escudero, Y. H. Tsai and L. Y. P. Luk, *Chem. Sci.*, 2020, **11**, 5881–5888.

197 B. R. McNaughton, J. J. Cronican, D. B. Thompson and D. R. Liu, *Proc. Natl. Acad. Sci. U. S. A.*, 2009, **106**, 6111–6116.

198 H. T. C. Ho, C. Lam, M. Chan, R. Cheung, L. Law, L. Lit, K. Ng, M. Suen, *Clin. Biochem. Rev.*, 2003, **24**, 3–12.

199 L. Armbrecht, G. Gabernet, F. Kurth, J. A. Hiss, G. Schneider and P. S. Dittrich, *Lab Chip*, 2017, **17**, 2933–2940.

200 J. Li, Y. Li, L. Liu, Y. Li, Q. He and H. Li, *Org. Biomol. Chem.*, 2014, **12**, 5435–5441.

201 D. Hong, A. J. Fritz, K. H. Finstad, M. P. Fitzgerald, A. Weinheimer, A. L. Viens, J. Ramsey, J. L. Stein, J. B. Lian and G. S. Stein, *Mol. Cancer Res.*, 2018, **16**, 1952–1964.

202 S. Finkin, H. Hartweger, T. Y. Oliveira, E. E. Kara and M. C. Nussenzweig, *Immunity*, 2019, **51**, 324-336.e5.

203 D. S. King, C. G. Fields and G. B. Fields, *Int. J. Pept. Protein Res.*, 1990, **36**, 255–266.

204 J. D. Pédelacq, S. Cabantous, T. Tran, T. C. Terwilliger and G. S. Waldo, *Nat. Biotechnol.*, 2006, **24**, 79–88.

205 S. Tolnai, *Tissue Cult. Assoc. Man.*, 1975, **1**, 37–38.

206 V. Stone, H. Johnston and R. P. F. Schins, *Crit. Rev. Toxicol.*, 2009, **39**, 613–626.

207 N. J. Anthis and G. M. Clore, *Protein Sci.*, 2013, **22**, 851–858.

208 *The Merck Index, 11th ed., Entry# 4140.*, 1986.

Appendix

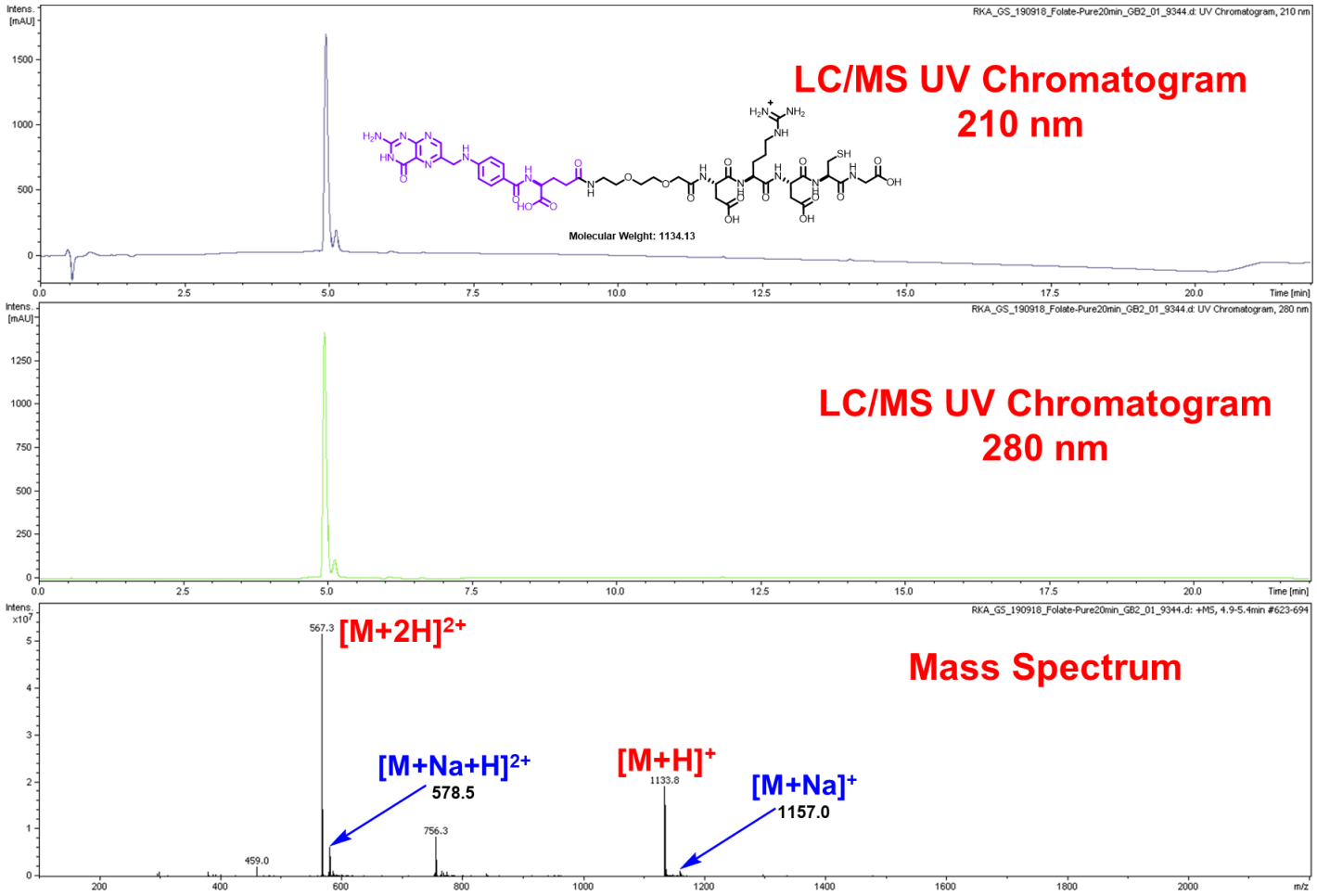

Bruker LC/MS Chromatogram and Mass Spectrum Derived from HPLC Fraction of Isolated Modified Folic Acid Labelled Peptide.

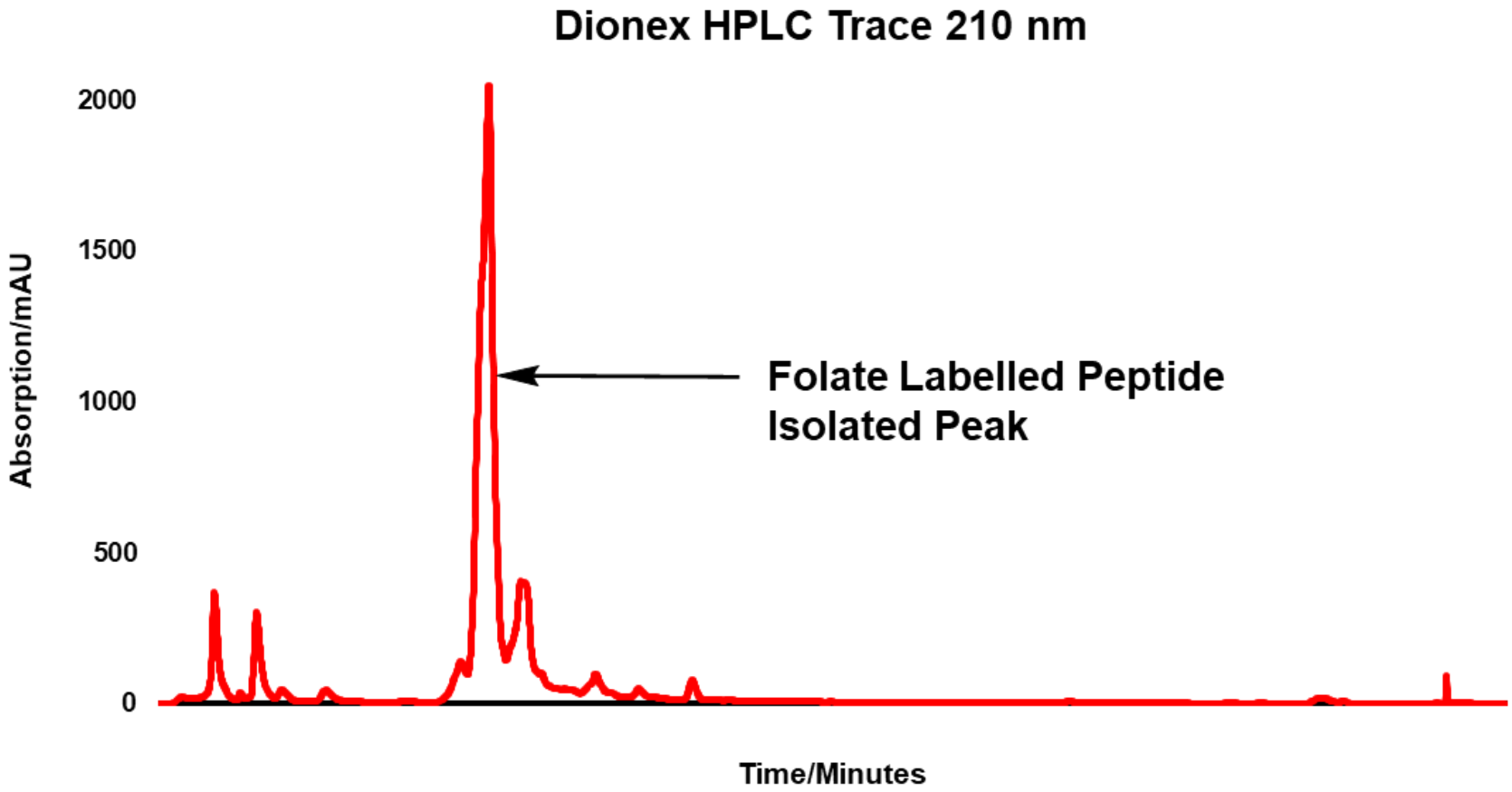

Dionex Preparation Scale HPLC UV Chromatogram (210 nm) from Isolation Attempt of Modified Folic Acid Peptide.

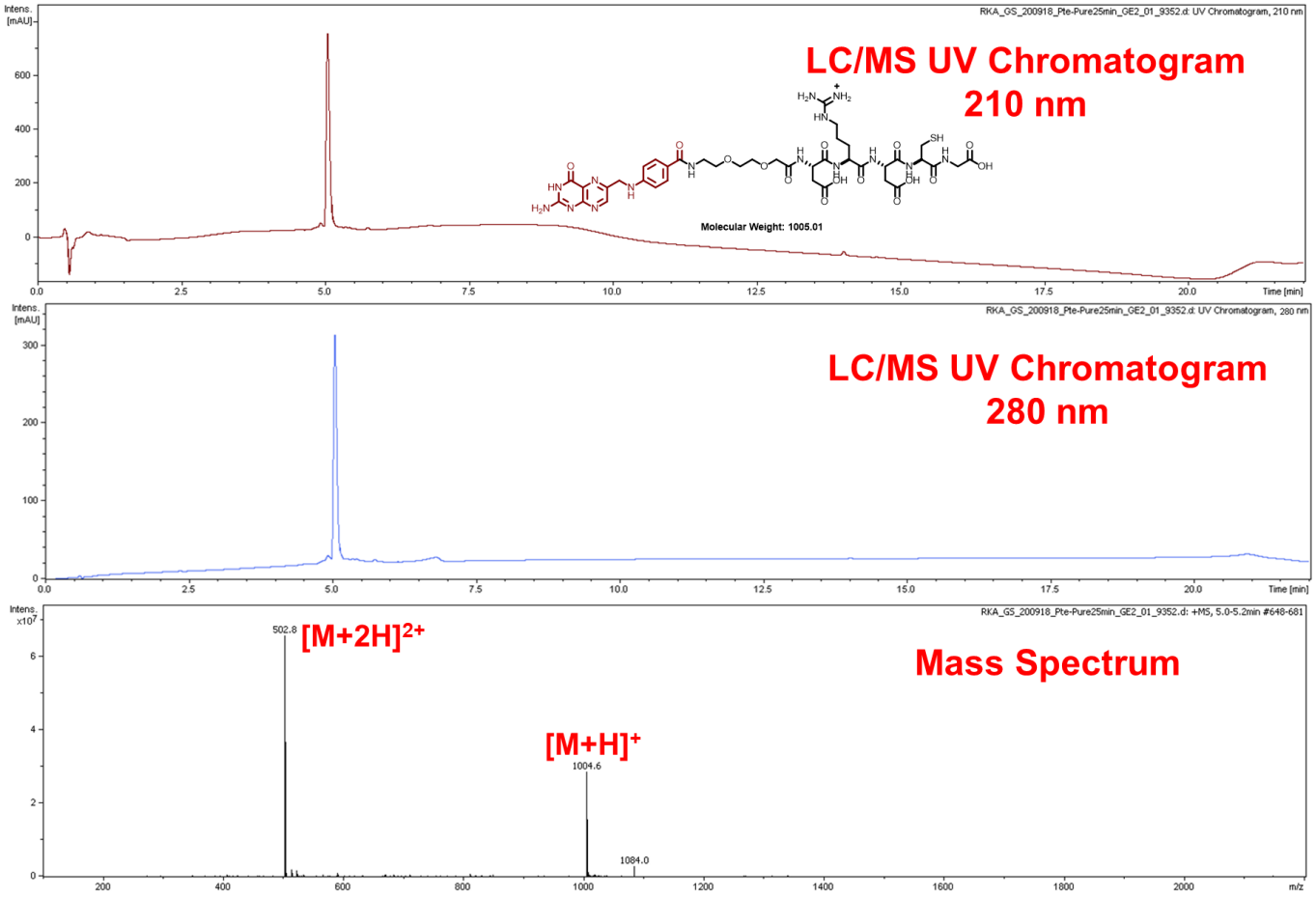

Bruker LC/MS Chromatogram and Mass Spectrum Derived from HPLC Fraction of Isolated Modified Pteroic Acid Labelled Peptide.

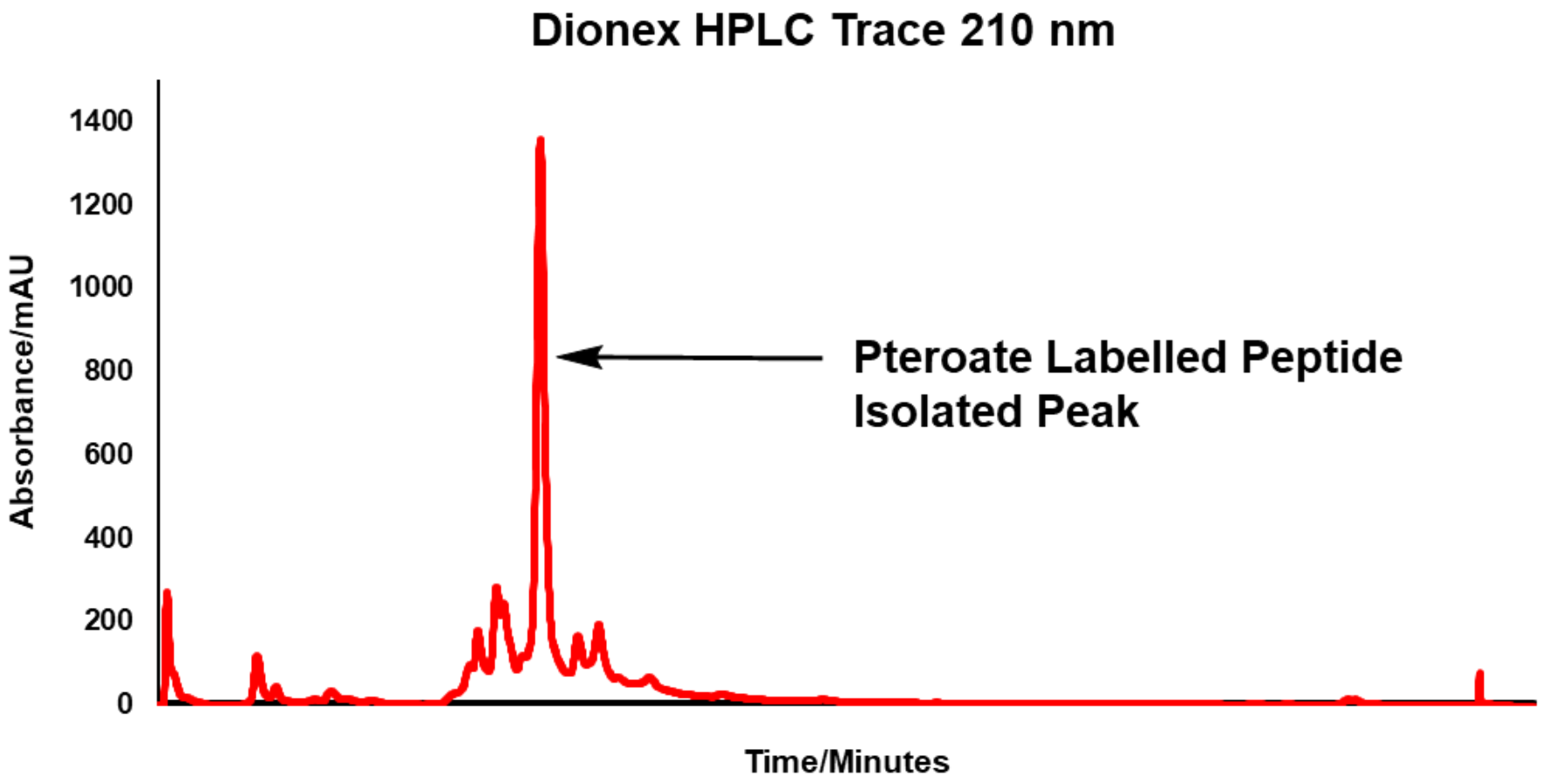

Dionex Preparation Scale HPLC UV Chromatogram (210 nm) from Isolation Attempt of Modified Pteroic Acid Peptide.

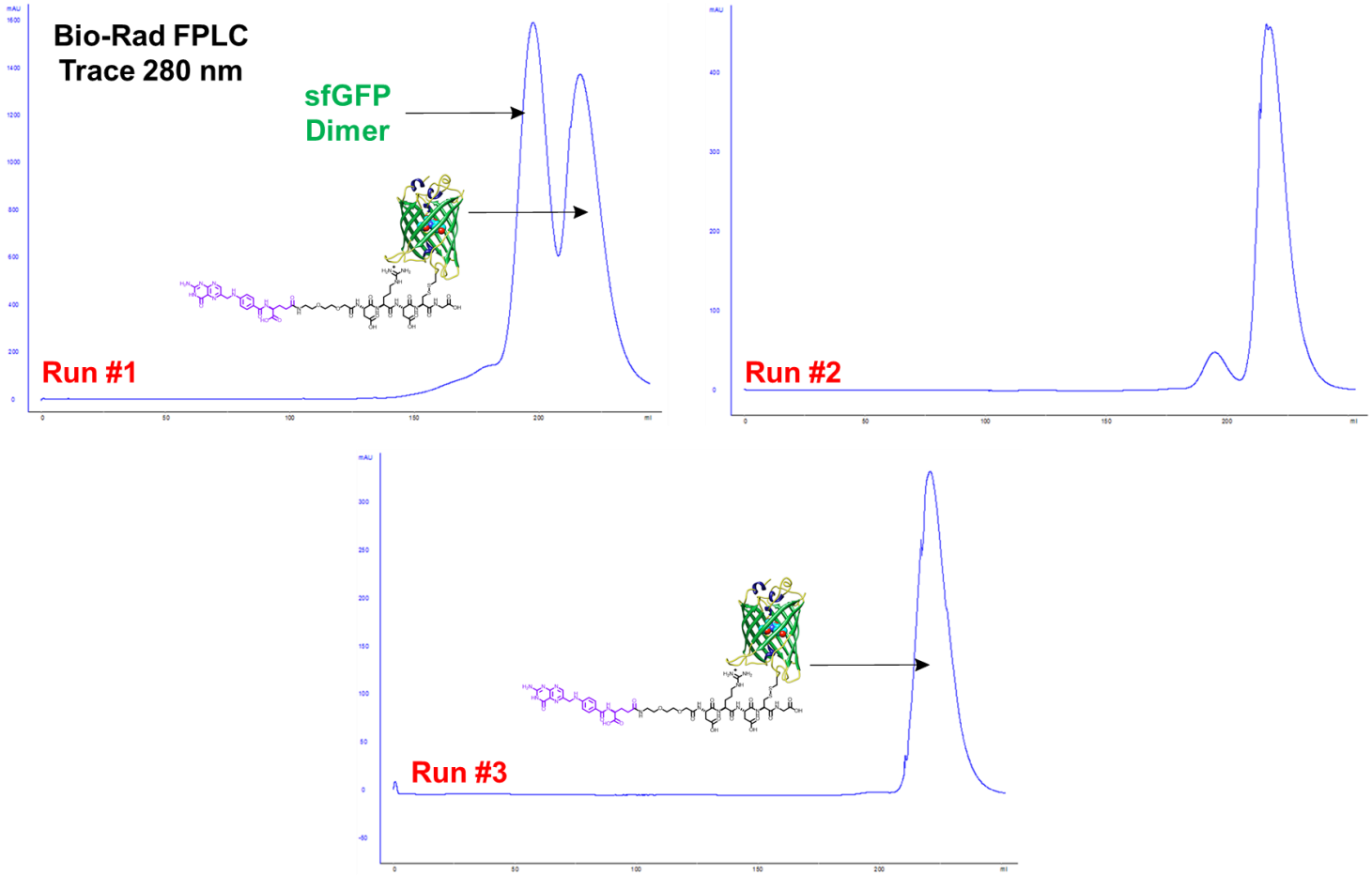

Bio-Rad FPLC Traces at 280 nm Derived from Isolation Attempt of Folate Labelled sfGFP.

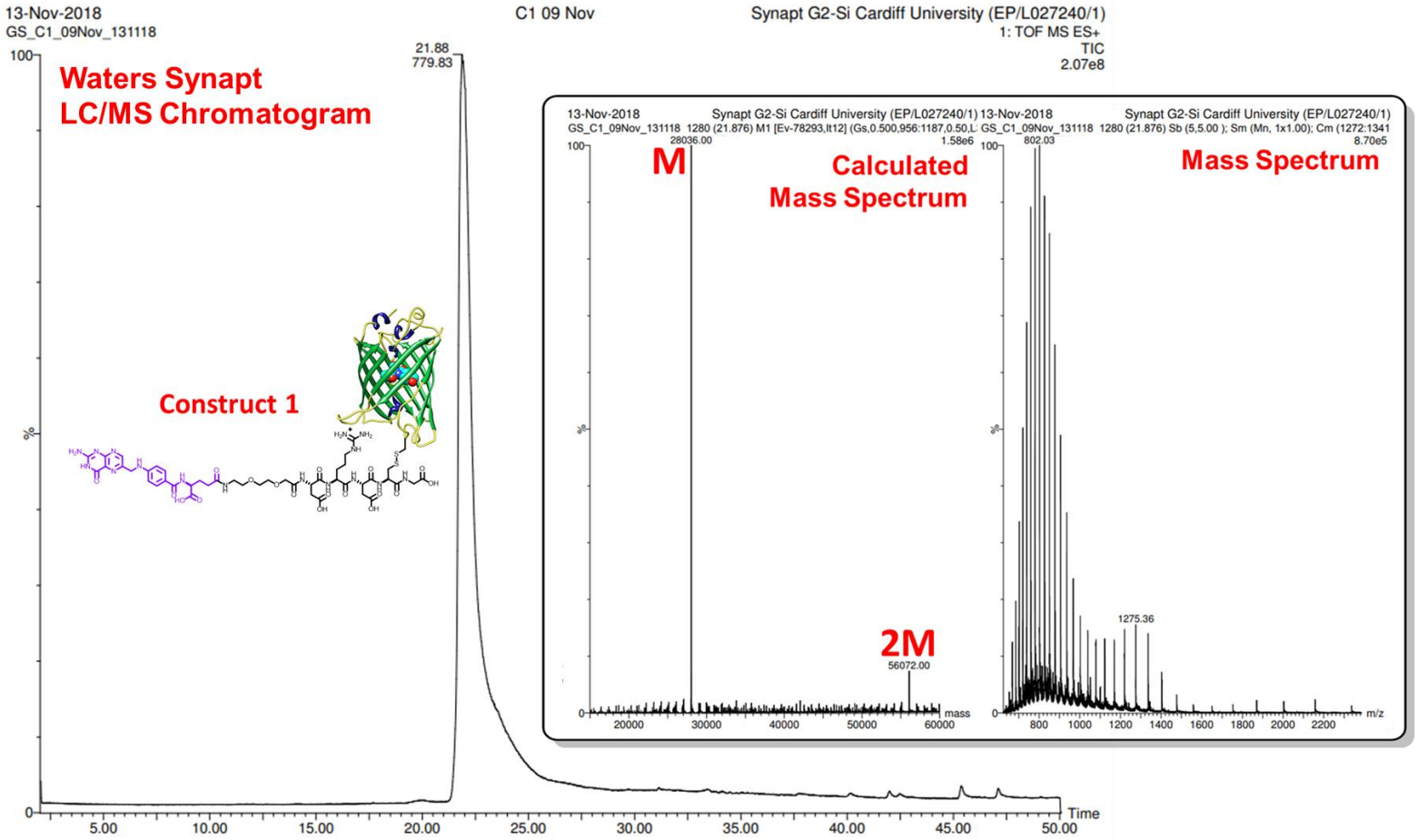

Waters Synapt LC/MS Chromatogram, Convoluted and Deconvoluted Mass Spectrum of FPLC Fraction of Isolated Folate Labelled sfGFP.

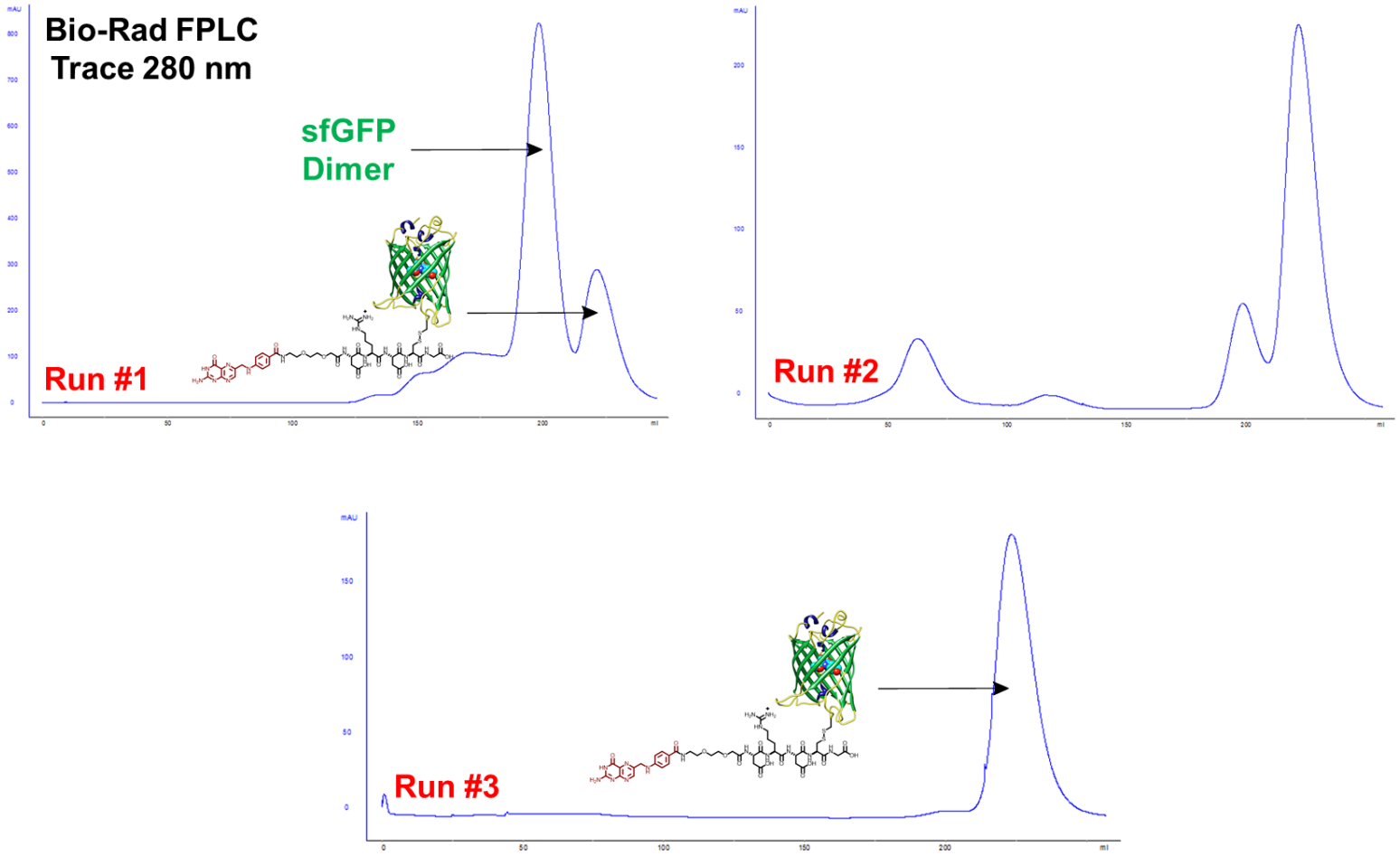

Bio-Rad FPLC Traces at 280 nm Derived from Isolation Attempt of Pteroate Labelled sfGFP.

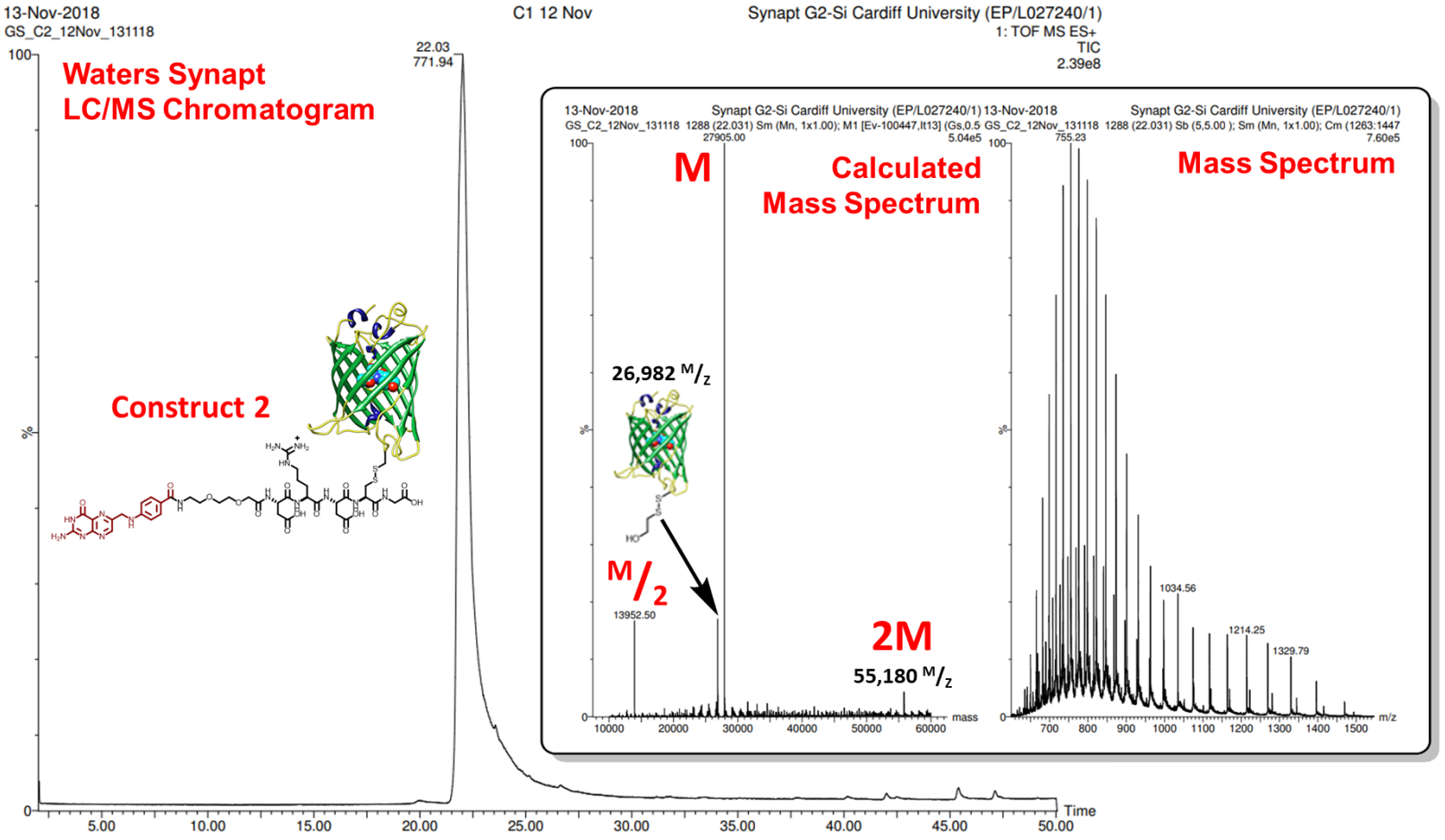

Waters Synapt LC/MS Chromatogram, Convoluted and Deconvoluted Mass Spectrum of FPLC Fraction of Isolated Pteroate Labelled sfGFP.

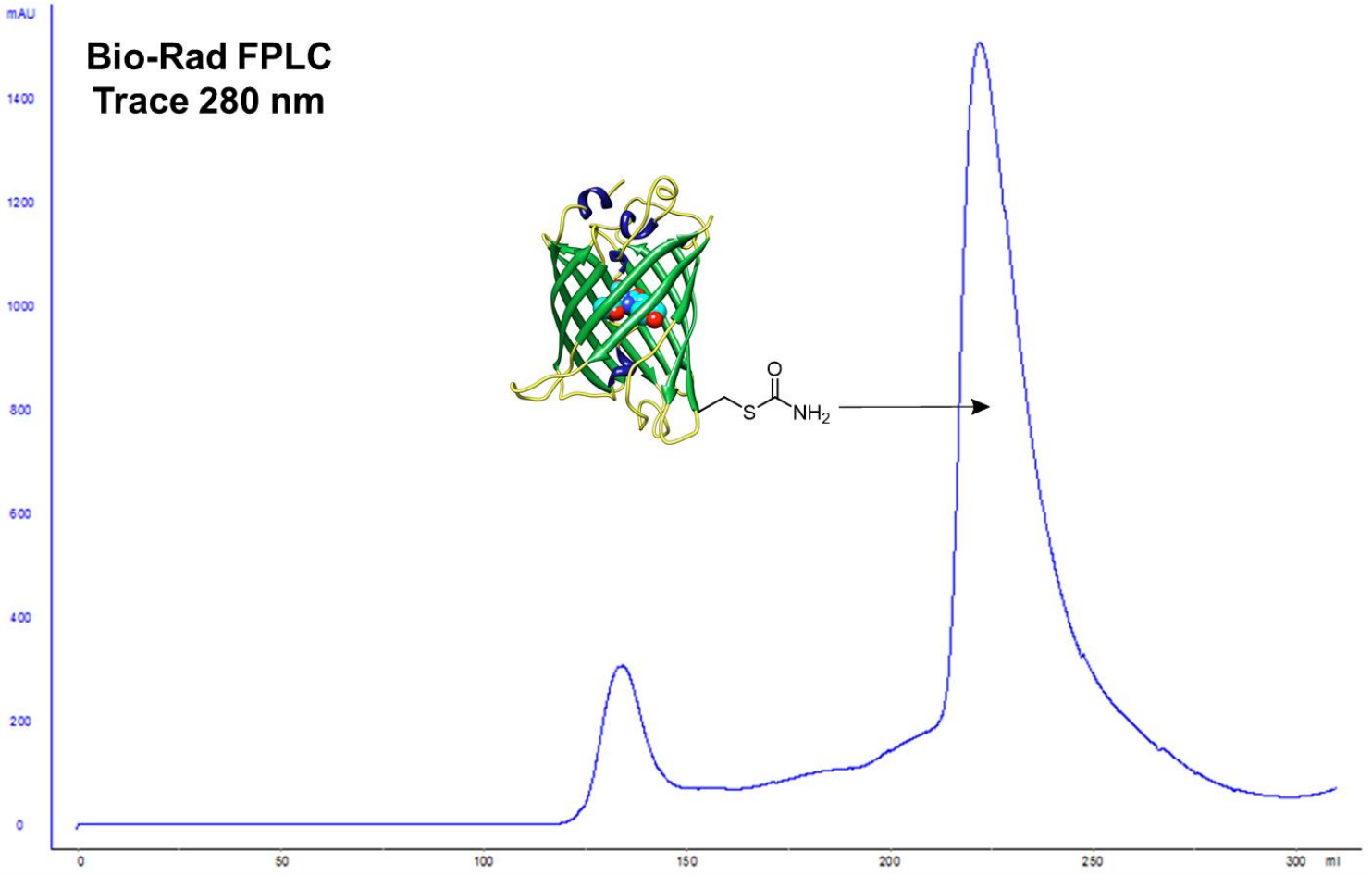

Bio-Rad FPLC Trace at 280 nm Derived from Isolation Attempt of Acetamide sfGFP.

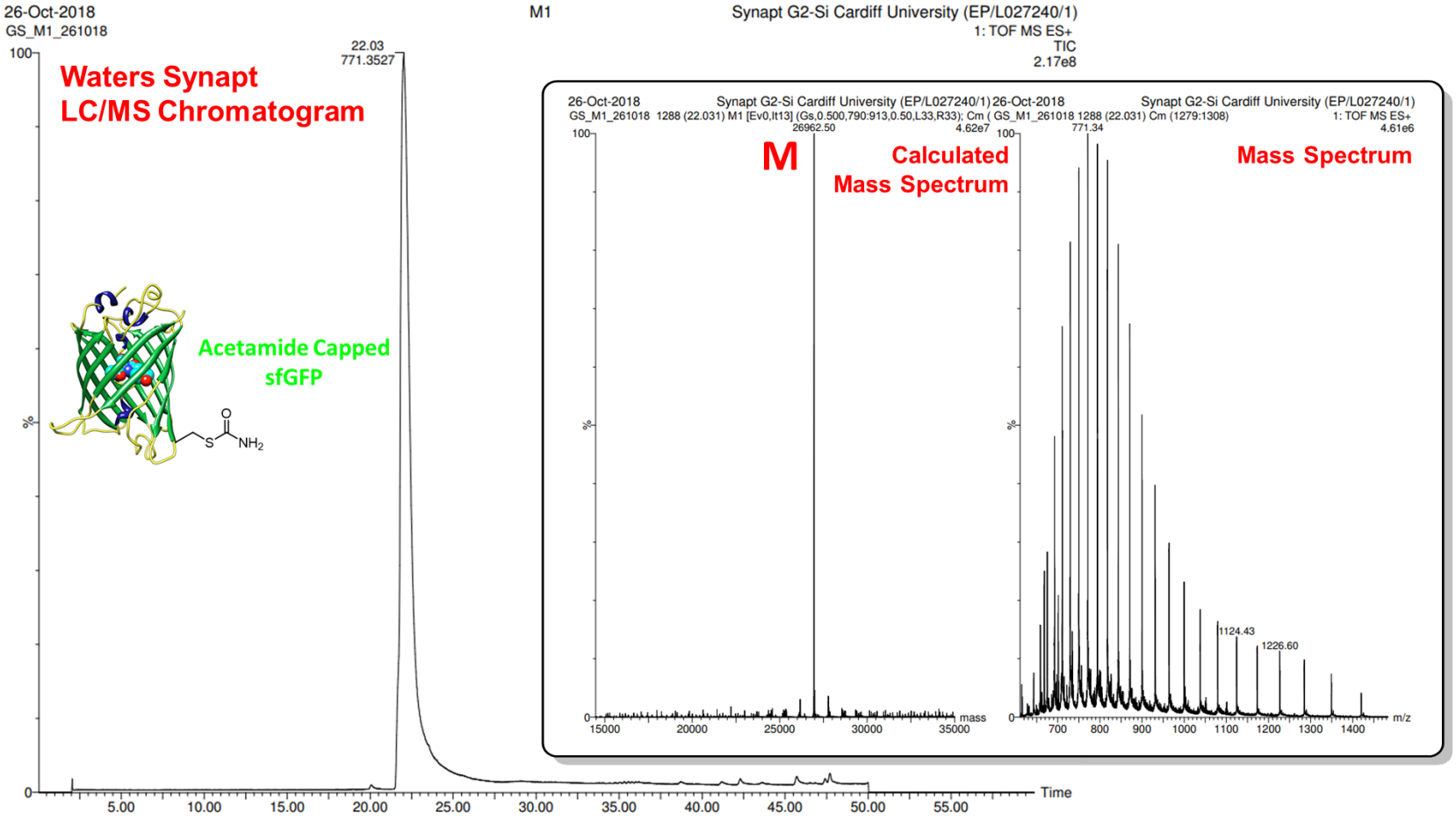

Waters Synapt LC/MS Chromatogram, Convoluted and Deconvoluted Mass Spectrum of FPLC Fraction of Isolated Acetamide Capped sfGFP.

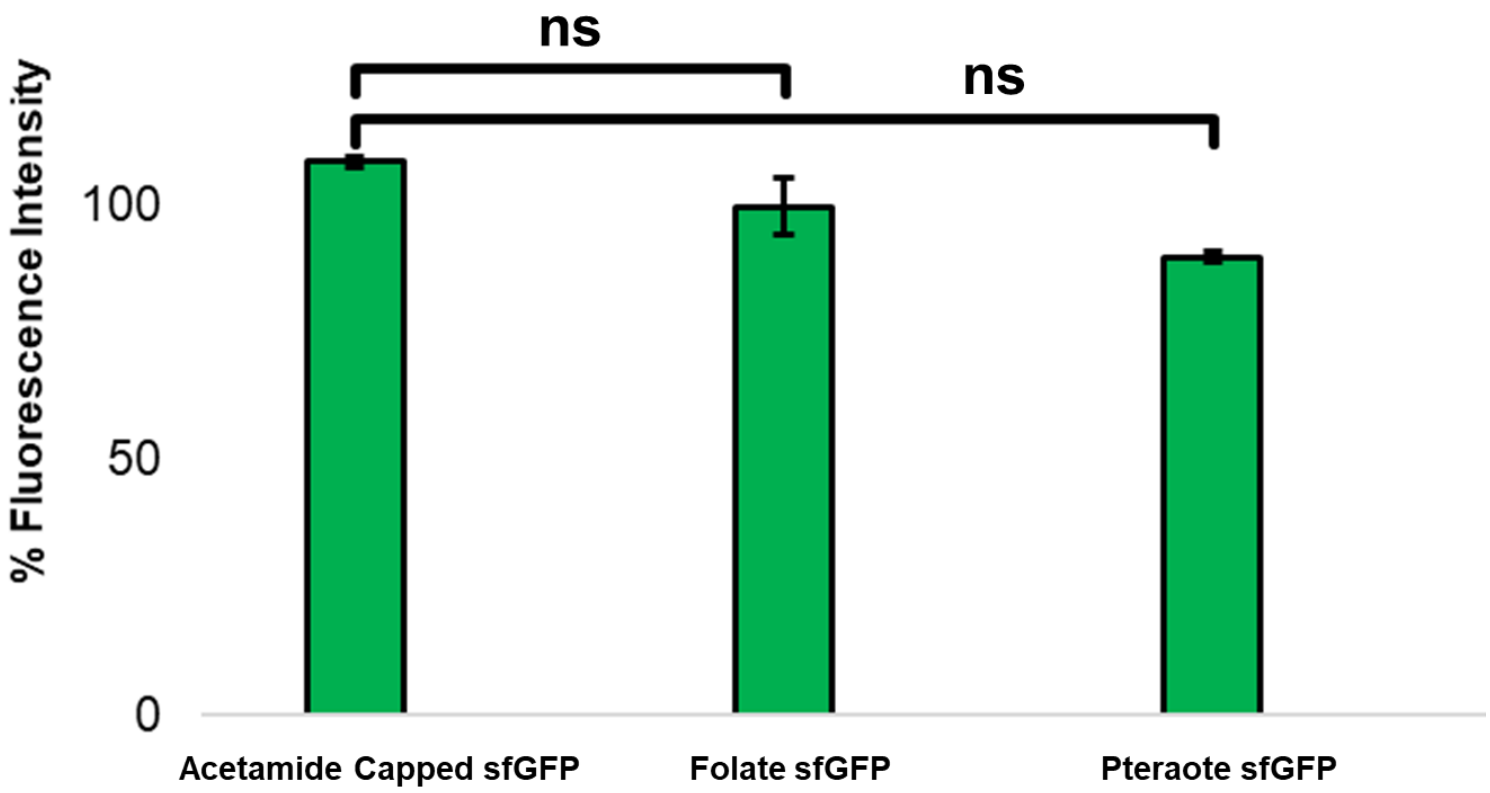

Bar chart derived from cell titre blue cell viability assay performed on KB cells exposed to all modified sfGFP constructs (10 μM) after 24-hour incubation.

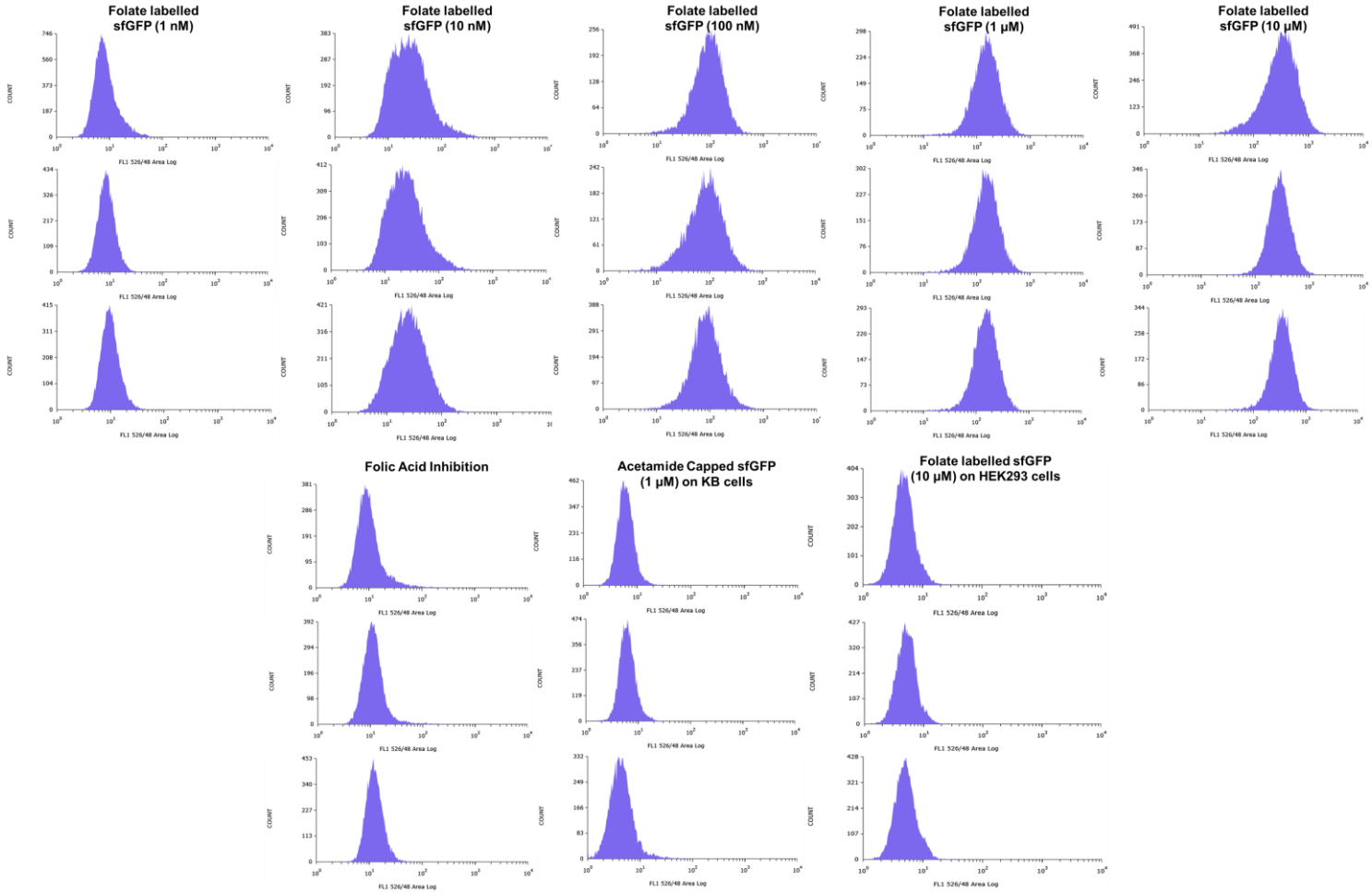

1D histograms derived from FACS experiments demonstrating the importance of folic acid labelling for sfGFP to selectively interact with FR-α positive cells.

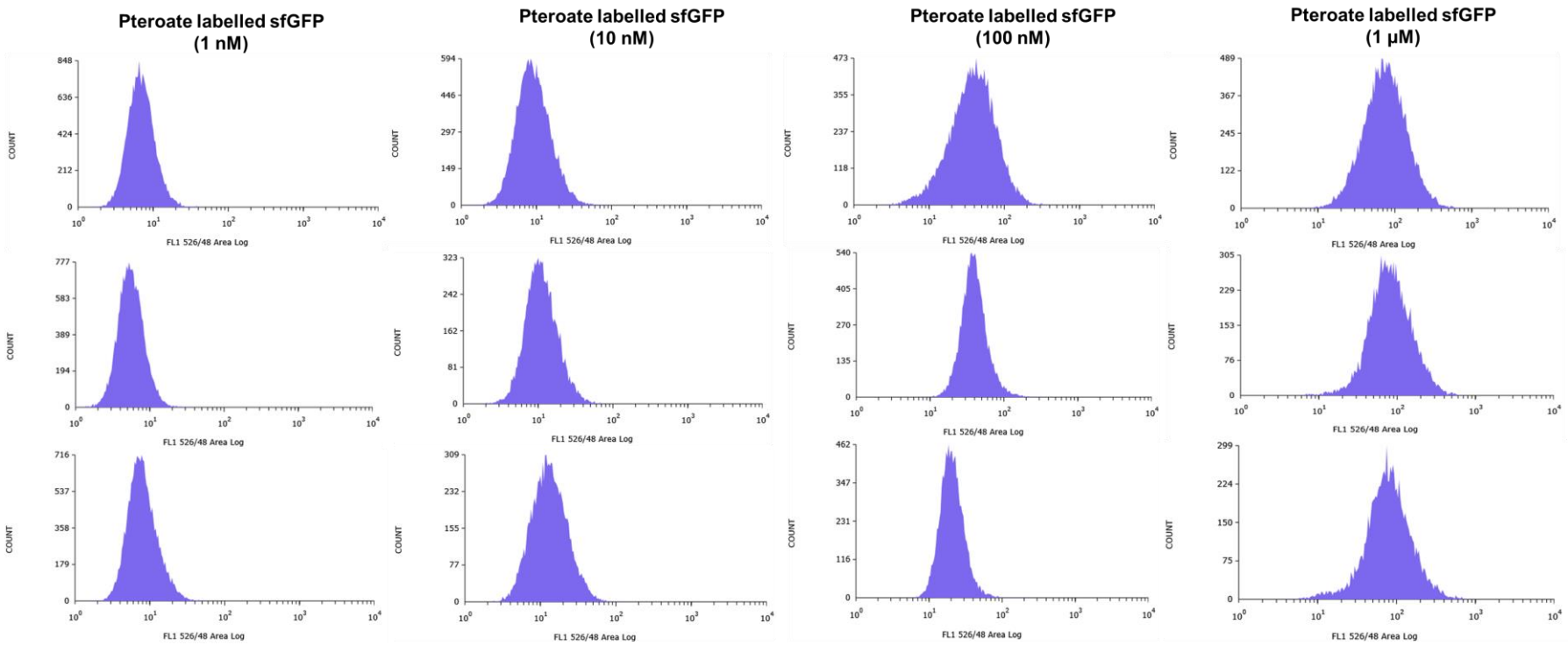

1D histograms derived from FACS experiments demonstrating pteroic acid labelled sfGFP interacting with FR-α positive cells.

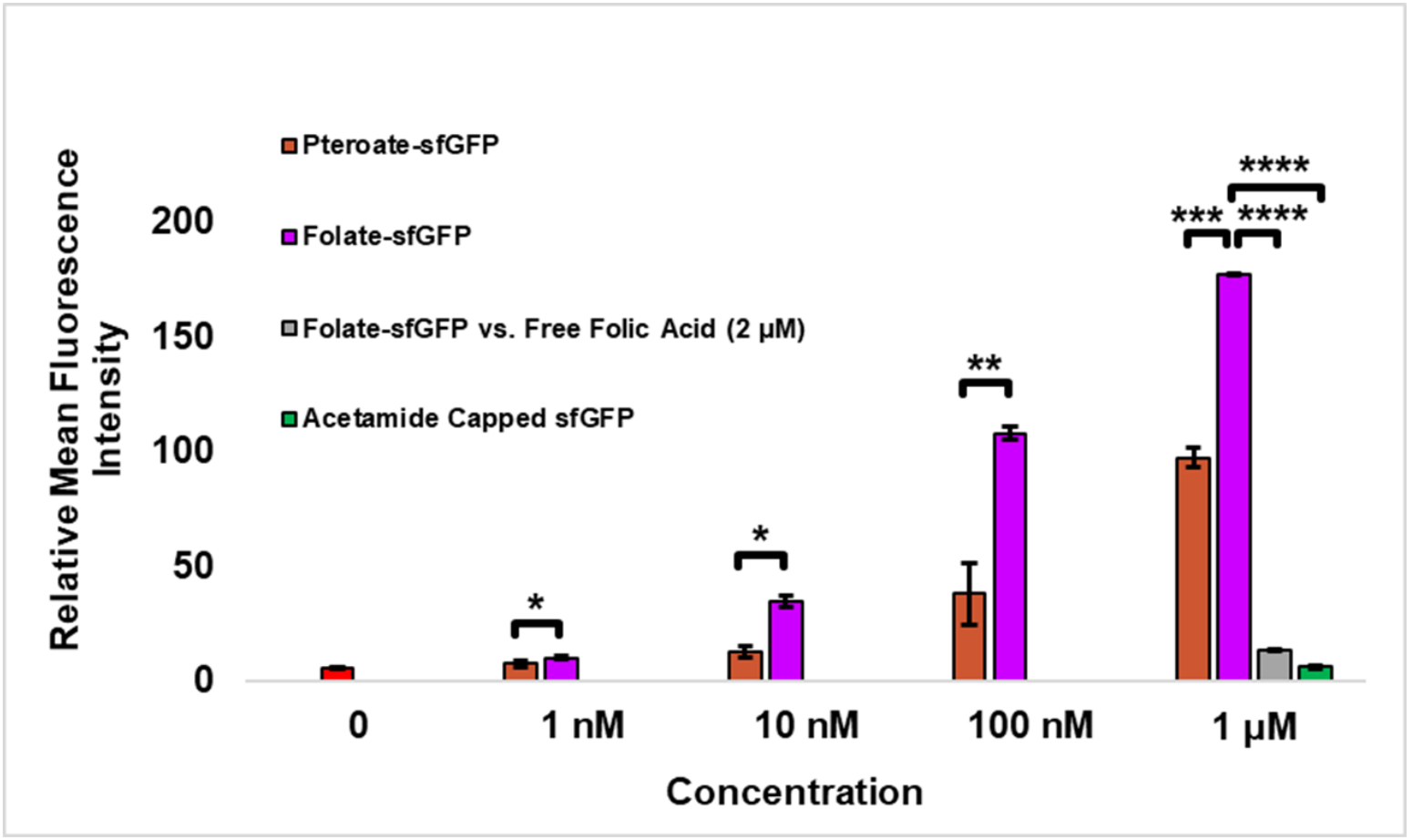

Bar Chart Derived from FACS Experiments Performed on KB Cells Exposed to Folate Labelled sfGFP (i.e. 1 – 10^3 nM) and Acetamide Capped sfGFP (i.e. 10^3 nM) After 1 Hour Incubation.

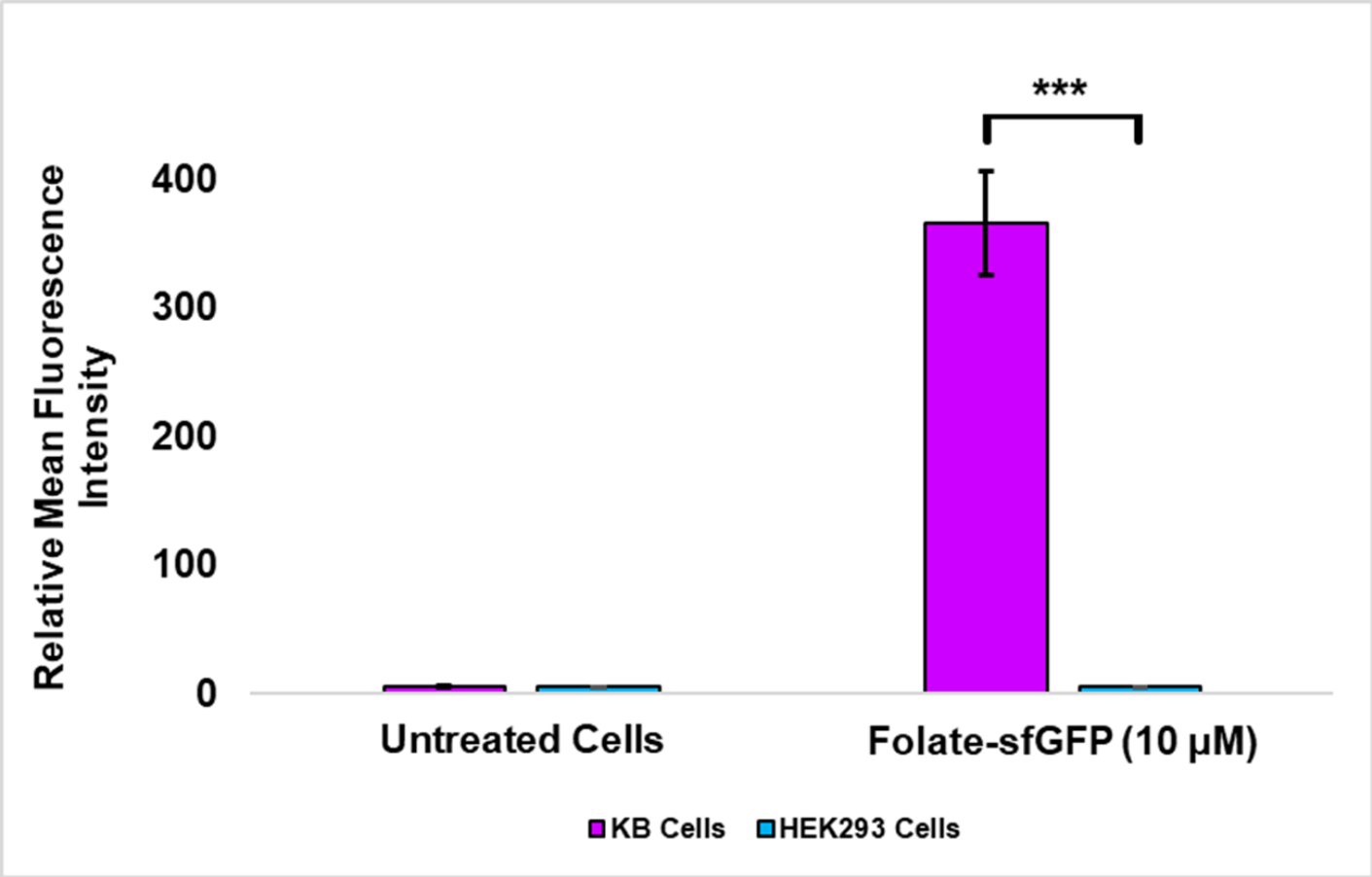

Bar chart derived from FACS experiments performed on KB cells and HEK293 cells exposed to folate labelled sfGFP (i.e. 10 µM) after 1 hour incubation and compared to untreated Cells.

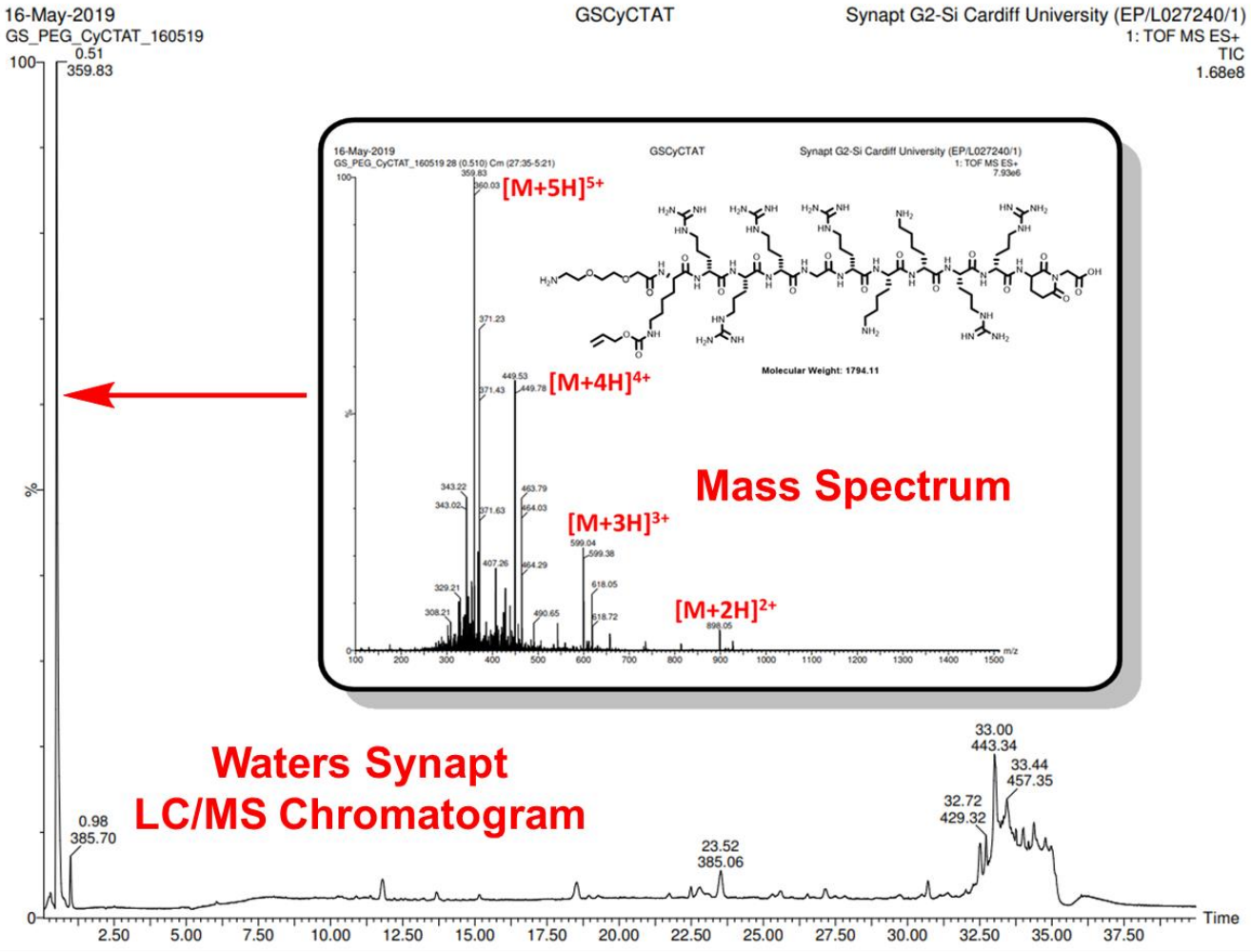

Waters synapt LC/MS chromatogram and mass spectrum derived from glutarimide formation.

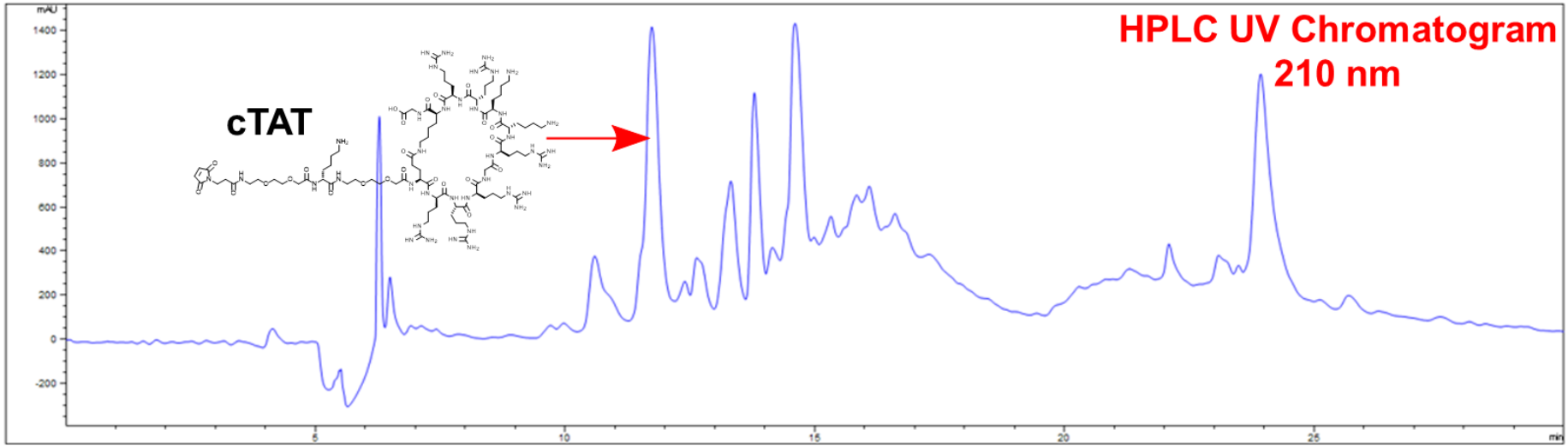

Agilent infinity semi-preparation scale HPLC UV chromatogram (210 nm) derived from isolation attempt of cyclic TAT sequence.

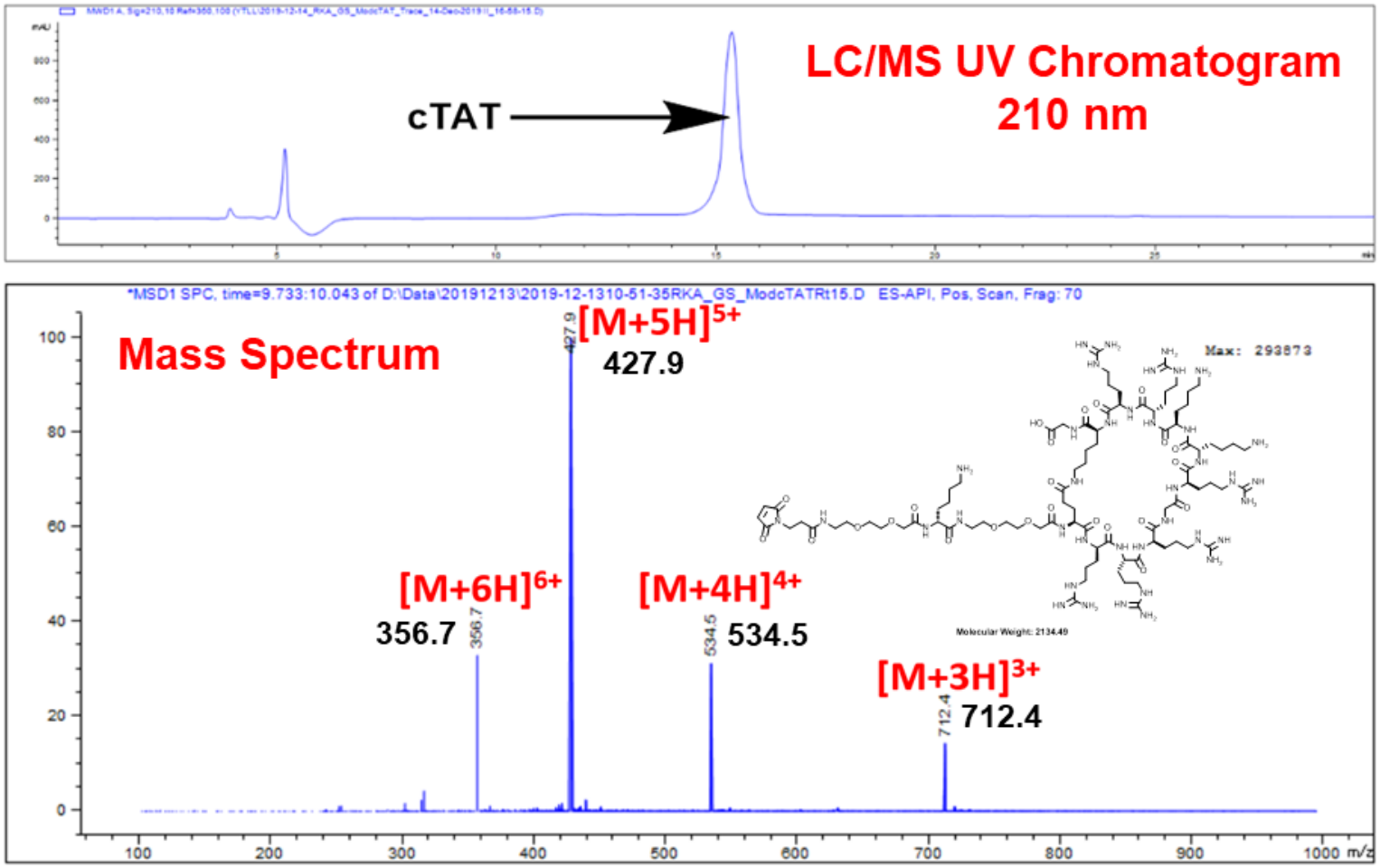

Agilent LC/MS chromatogram and mass spectrum derived from HPLC fraction of isolated cyclic TAT.

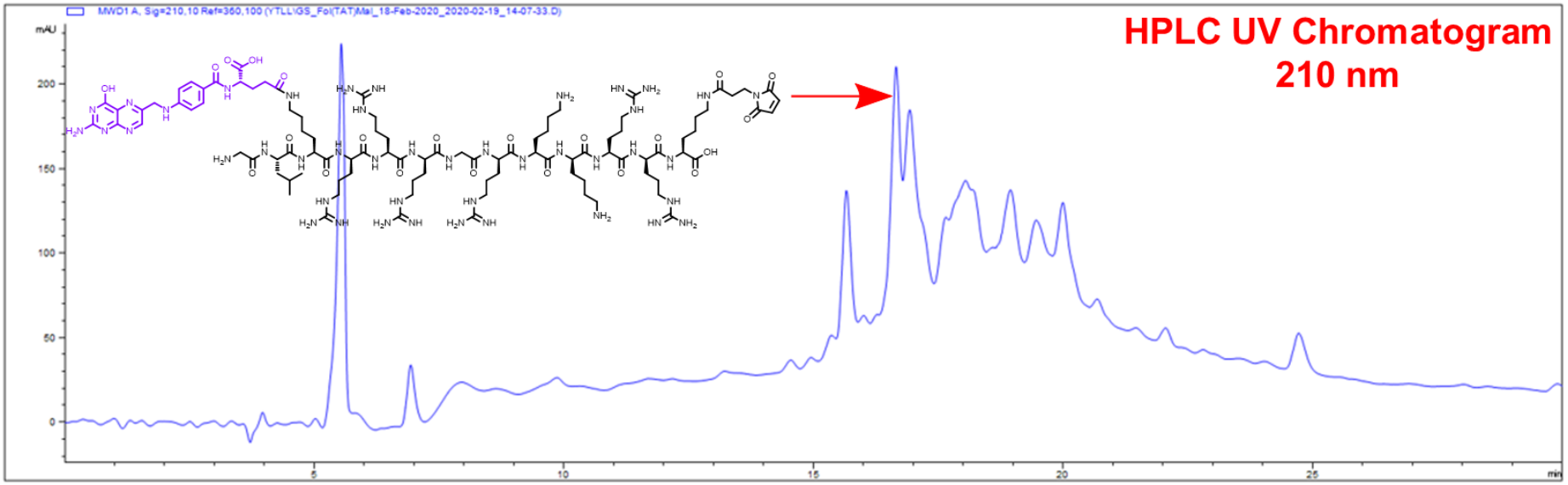

Agilent infinity semi-preparation scale HPLC UV chromatogram (210 nm) derived from isolation attempt of folate labelled TAT with N-terminal GL dipeptide motif and C-terminal maleimide.

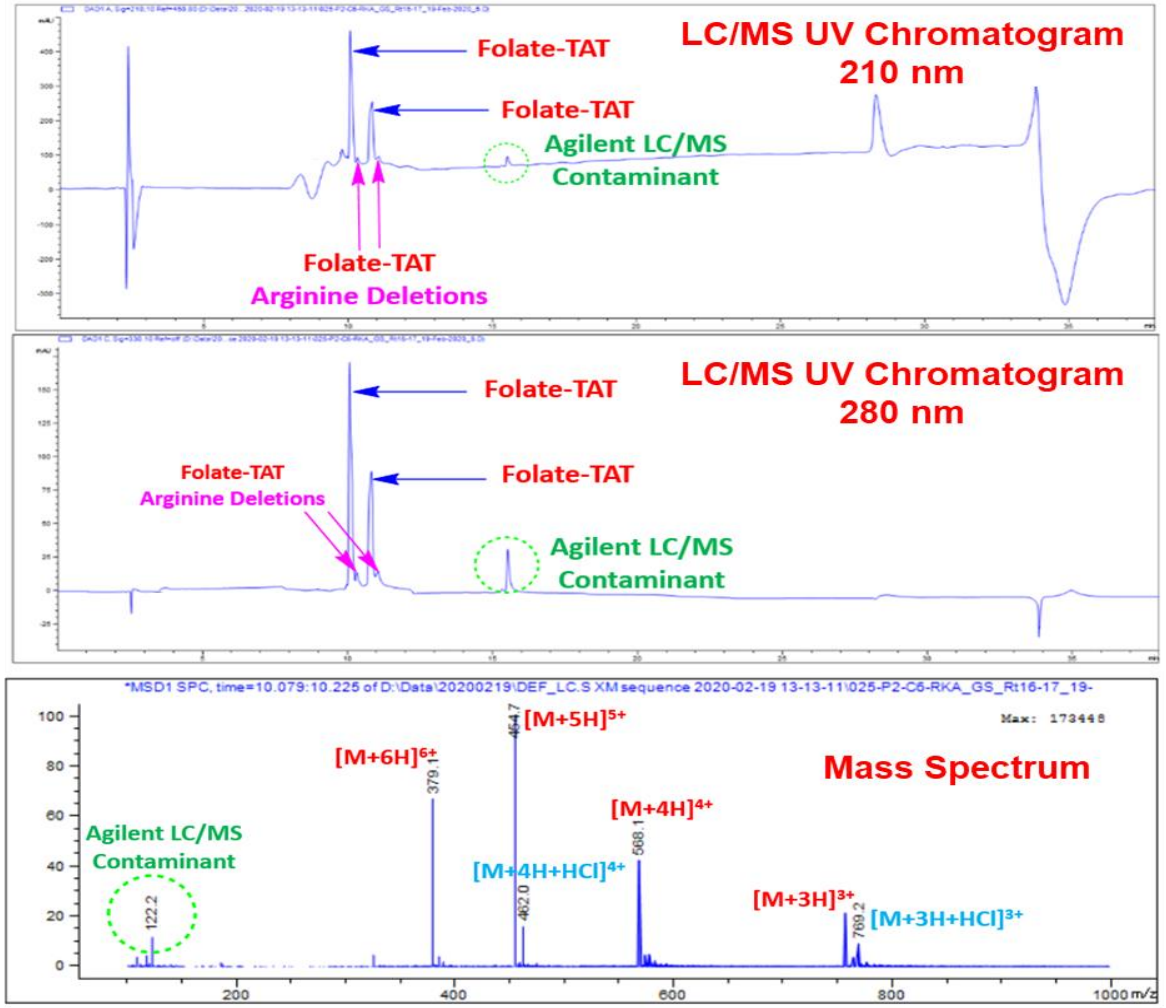

Agilent LC/MS chromatogram and mass spectrum of isolated folate labelled TAT with GL motif.

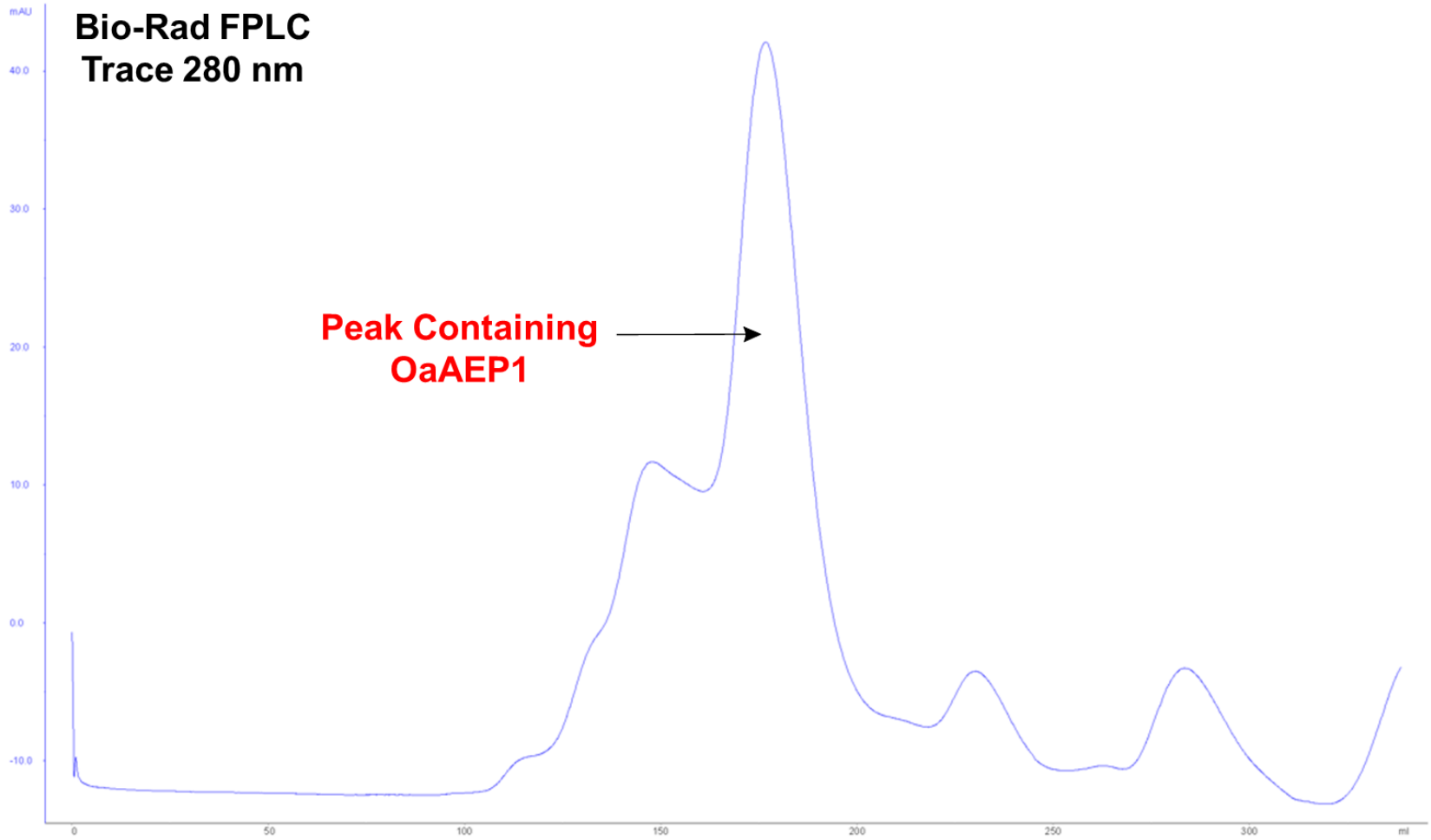

Bio-rad FPLC trace at 280 nm derived from isolation attempt of OaAEP1.

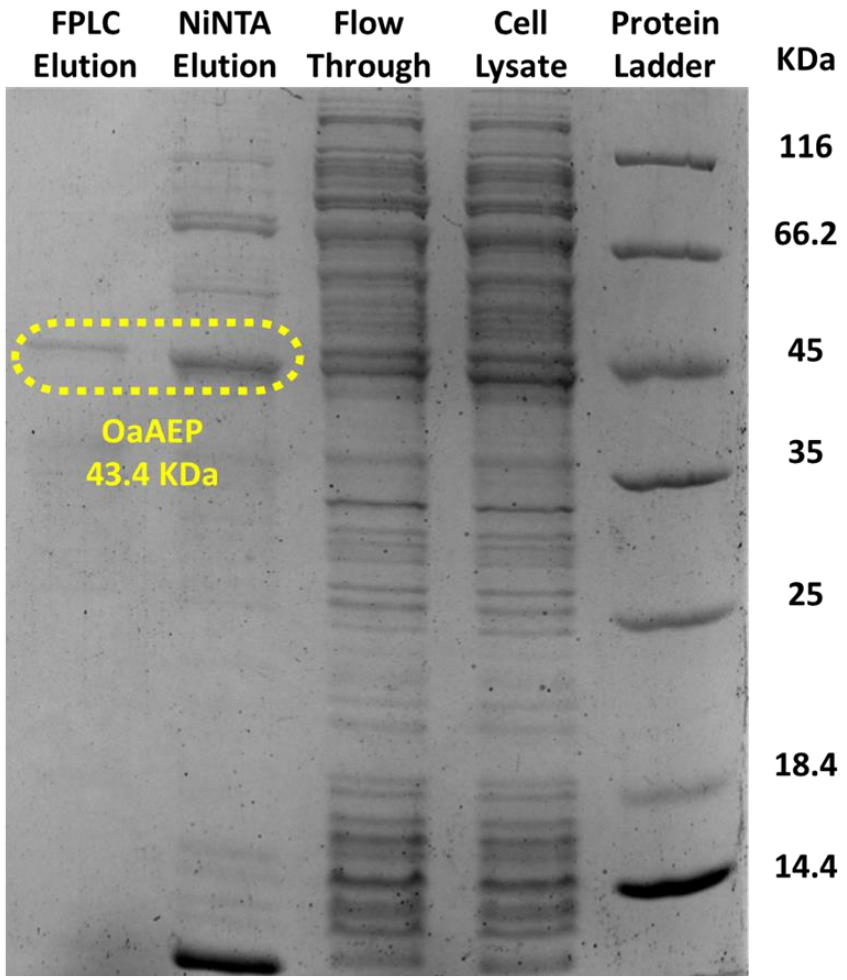

SDS-PAGE of FPLC fraction comprised of isolated OaAEP1 compared alongside affinity column isolate, flow through and cell lysate with a protein ladder for reference.

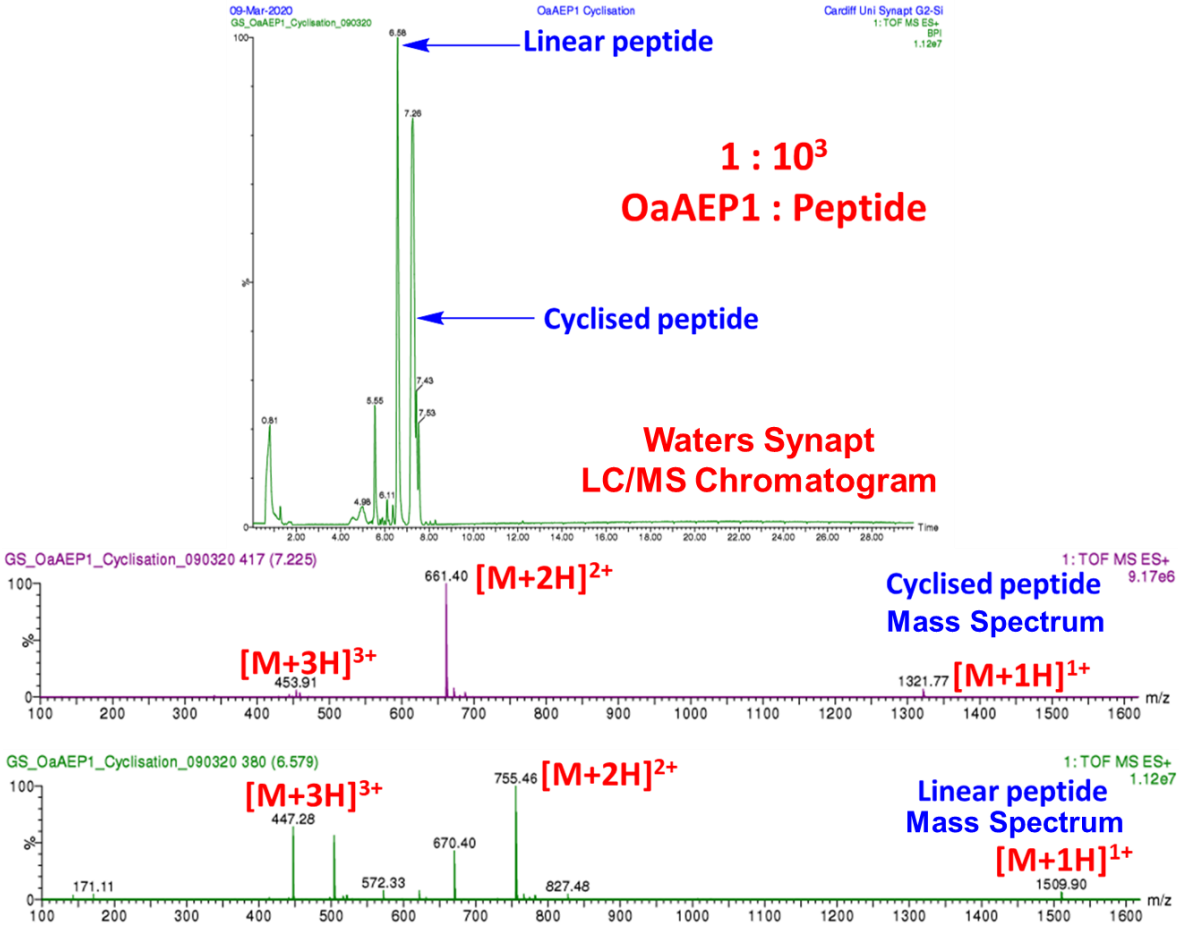

Waters synapt LC/MS chromatogram and mass spectrum derived from OaAEP1 cyclisation attempt with test peptide sequence (GLPVSTKPVATRNGL).

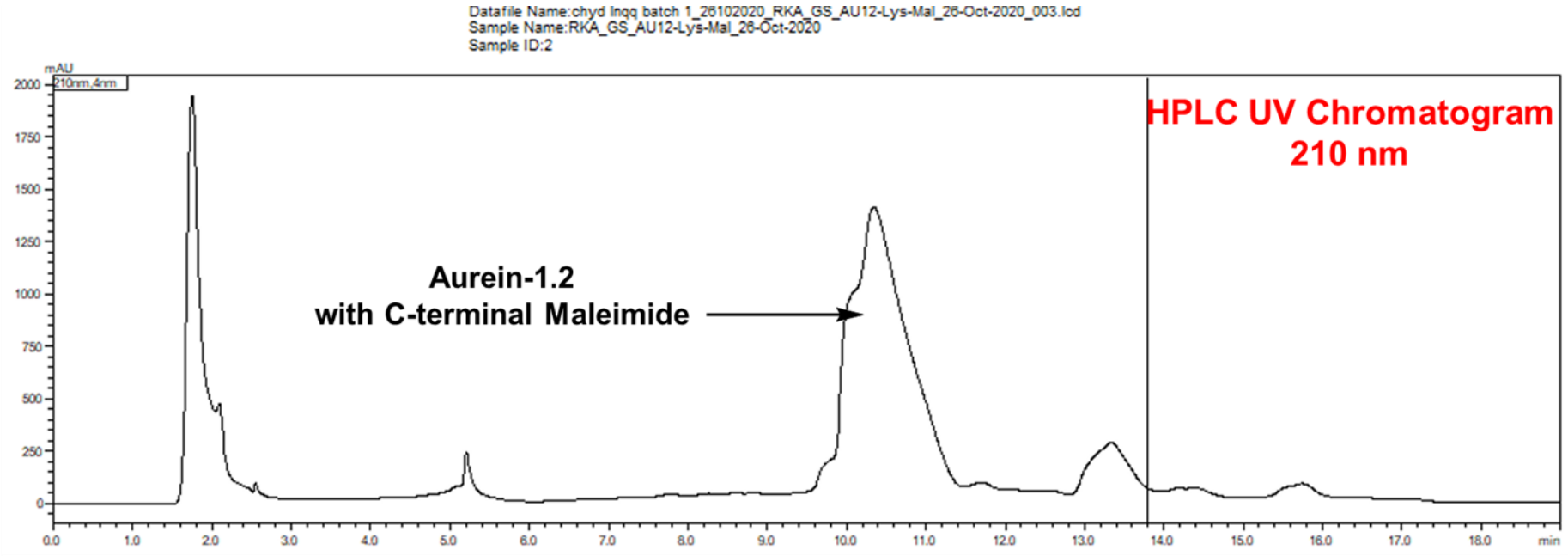

Shimadzu preparation scale HPLC UV chromatogram (210 nm) of isolated aurein-1.2 with C-terminal maleimide.

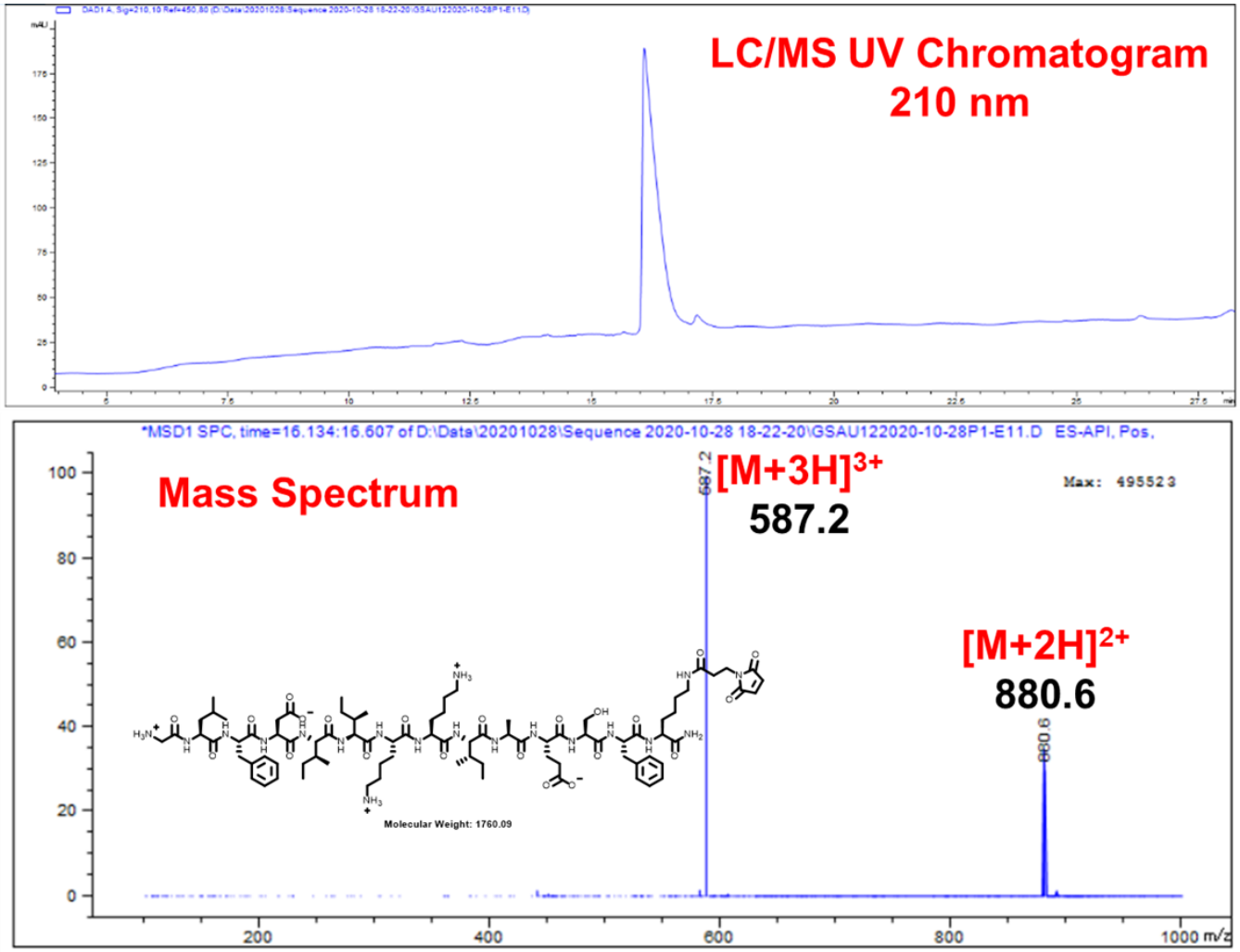

Shimadzu preparation scale HPLC UV chromatogram (210 nm) of isolated aurein-1.2 with C-terminal maleimide.

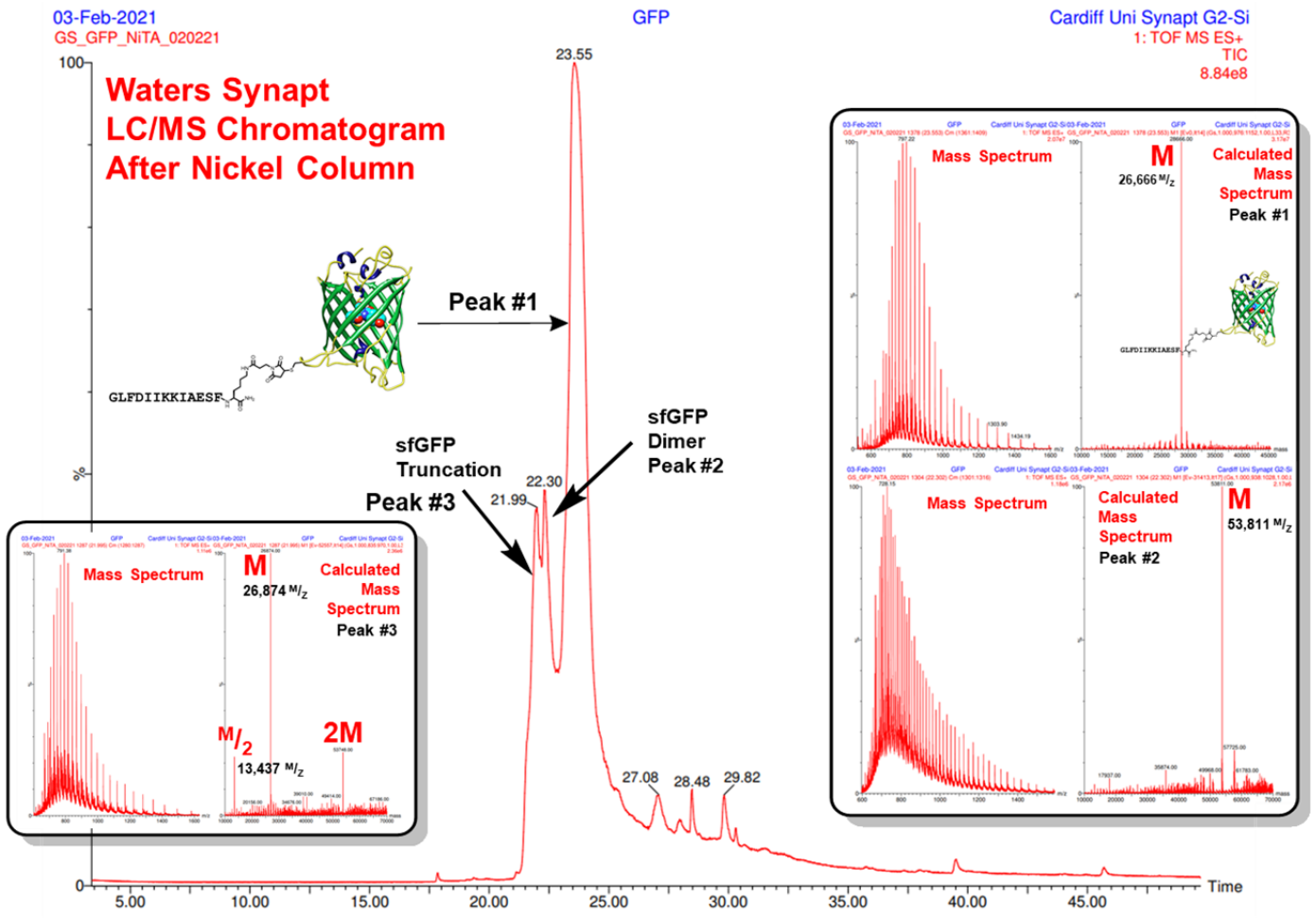

Waters synapt LC/MS chromatogram, convoluted and deconvoluted mass spectrum of affinity column isolated aurein-1.2 labelled sfGFP.

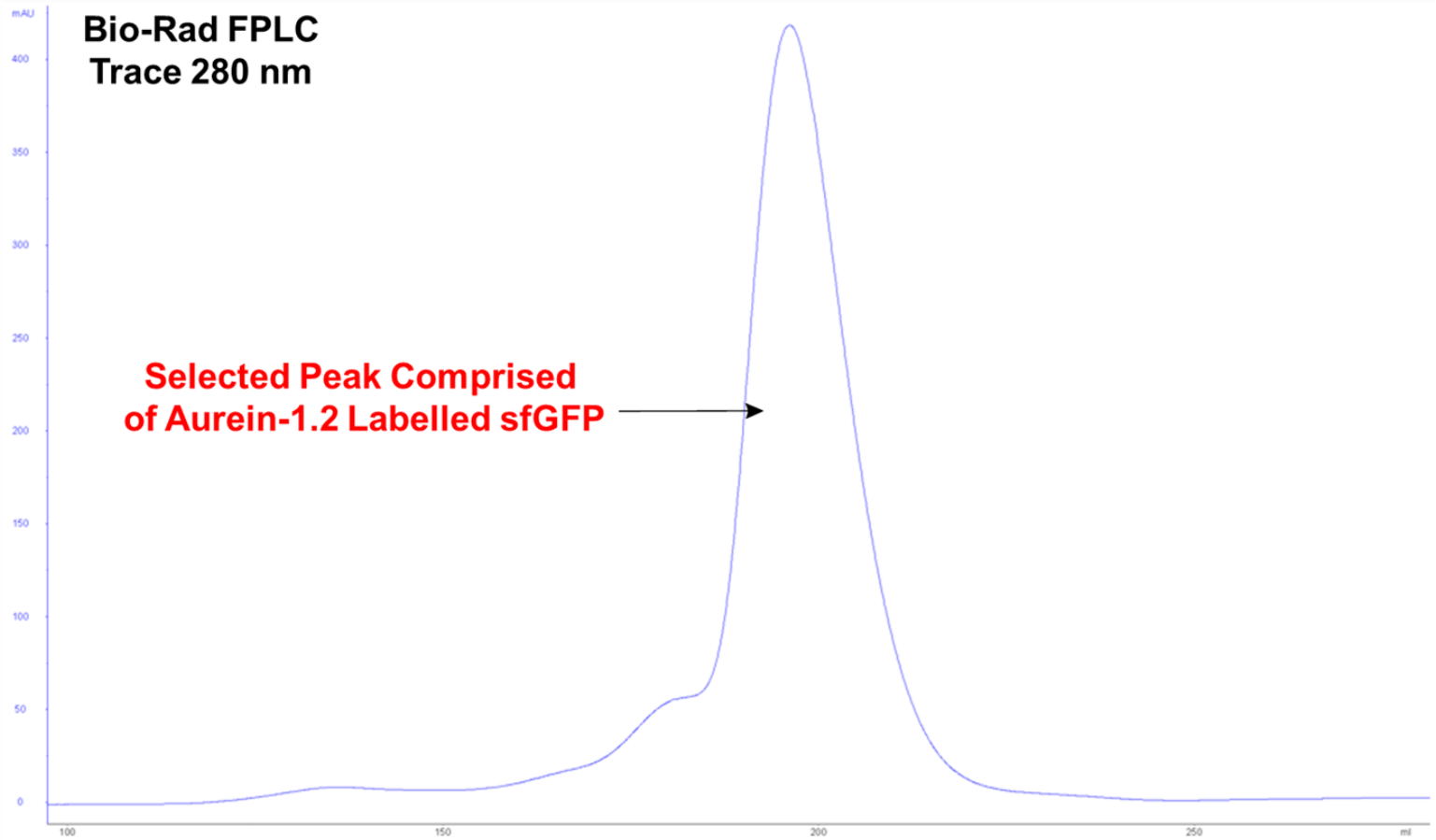

Bio-rad FPLC trace at 280 nm derived from isolation attempt of aurein-1.2 labelled sfGFP.

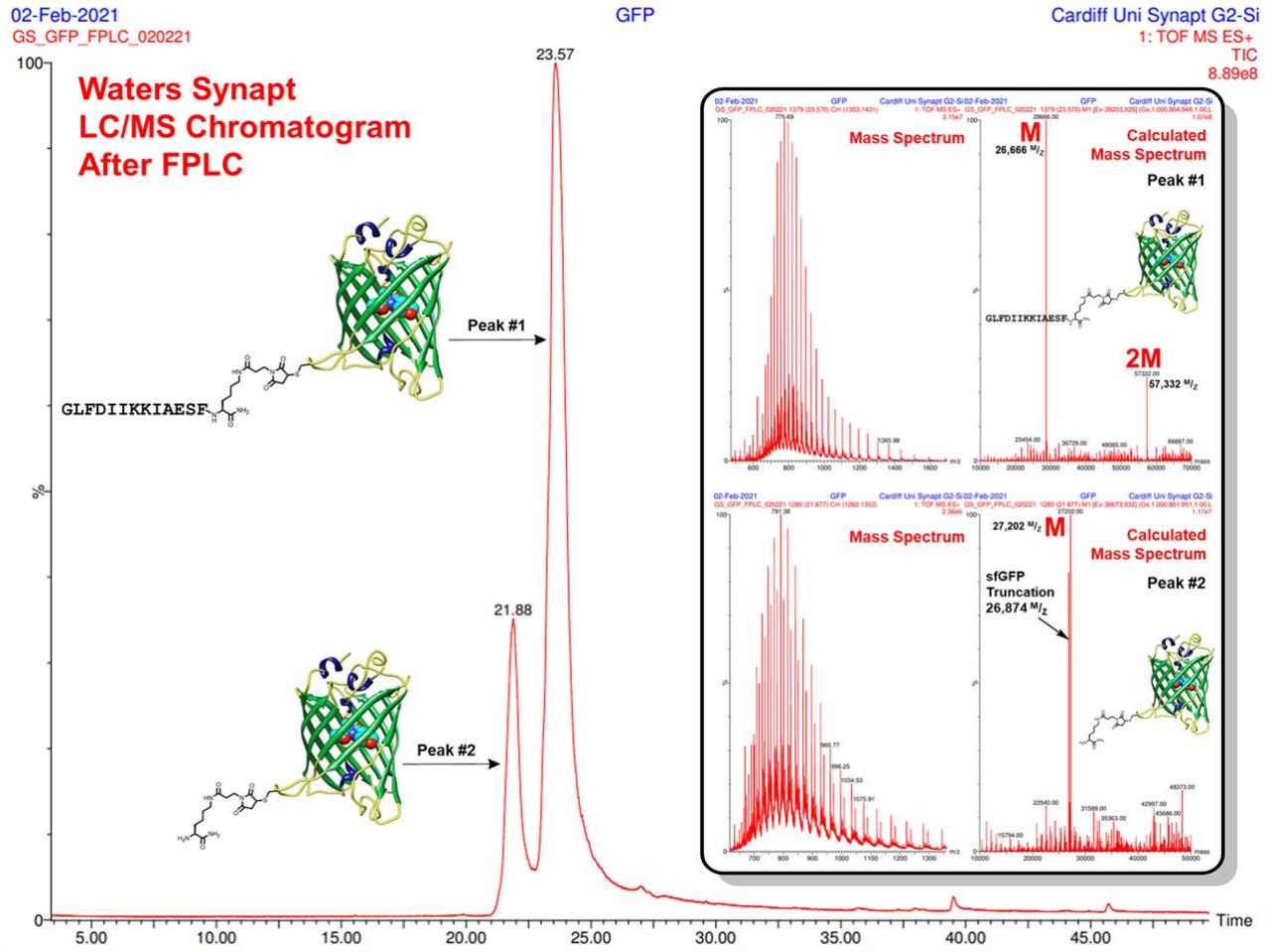

Waters synapt LC/MS chromatogram, convoluted and deconvoluted mass spectrum of FPLC fraction of isolated aurein-1.2 labelled sfGFP.

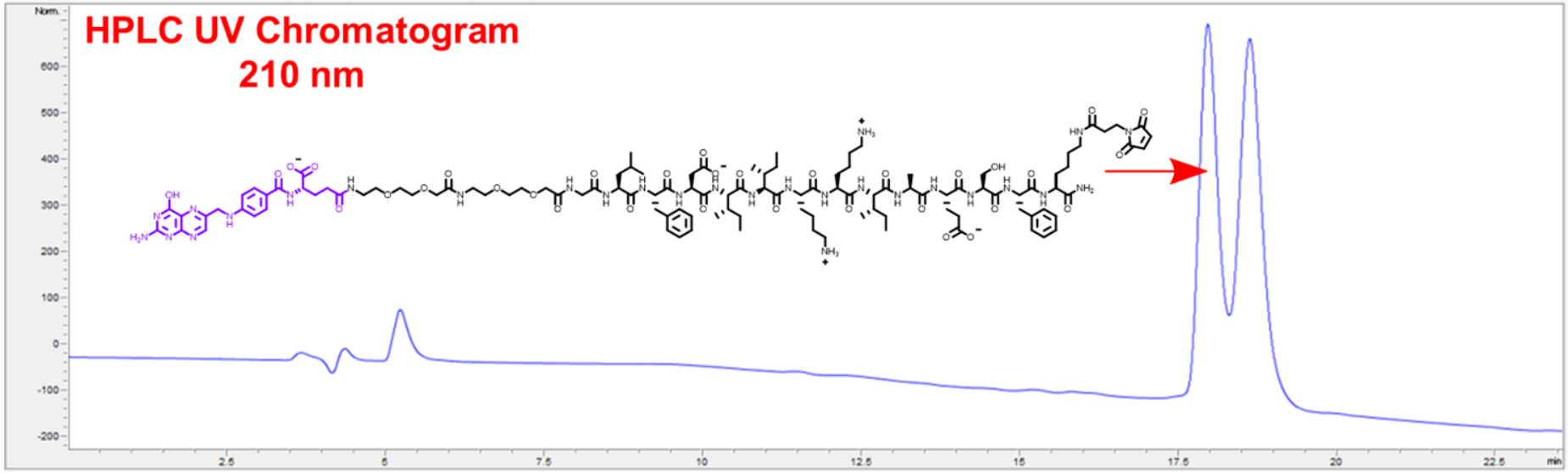

Agilent infinity semi-preparation scale HPLC UV chromatogram (210 nm) derived from isolation of folate labelled aurein-1.2 with C-terminal maleimide.

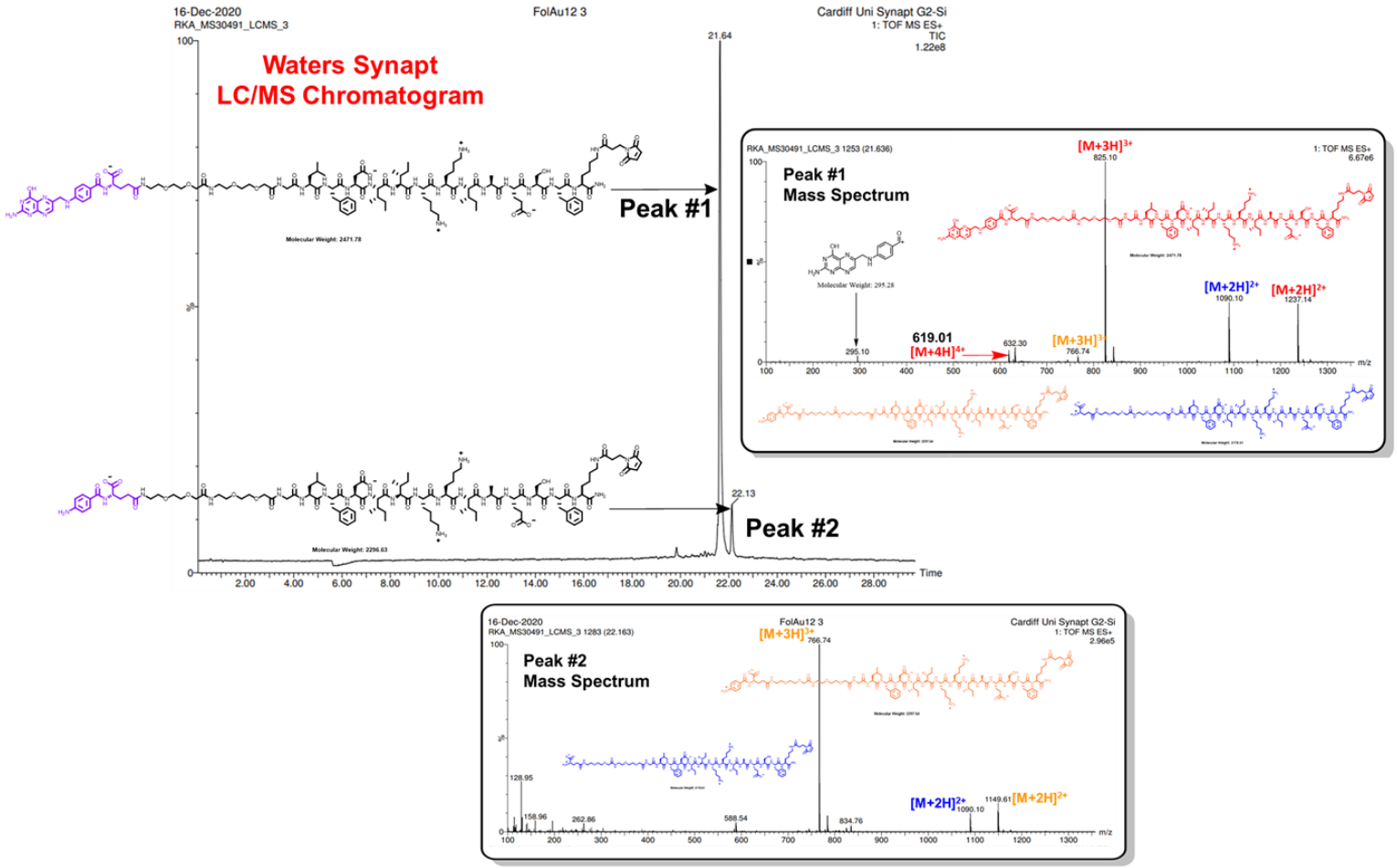

Waters synapt LC/MS chromatogram and mass spectrum derived from HPLC fraction of isolated folate labelled aurein-1.2 with C-terminal maleimide.

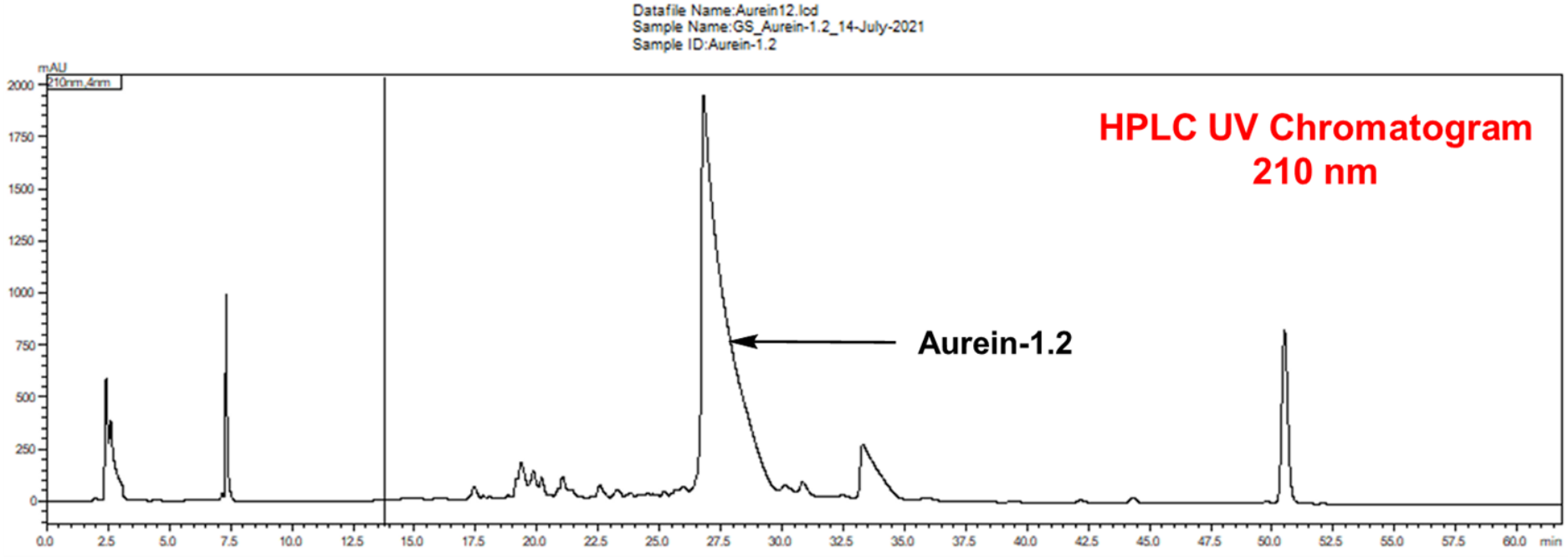

Shimadzu preparation scale HPLC UV chromatogram (210 nm) of isolated aurein-1.2.

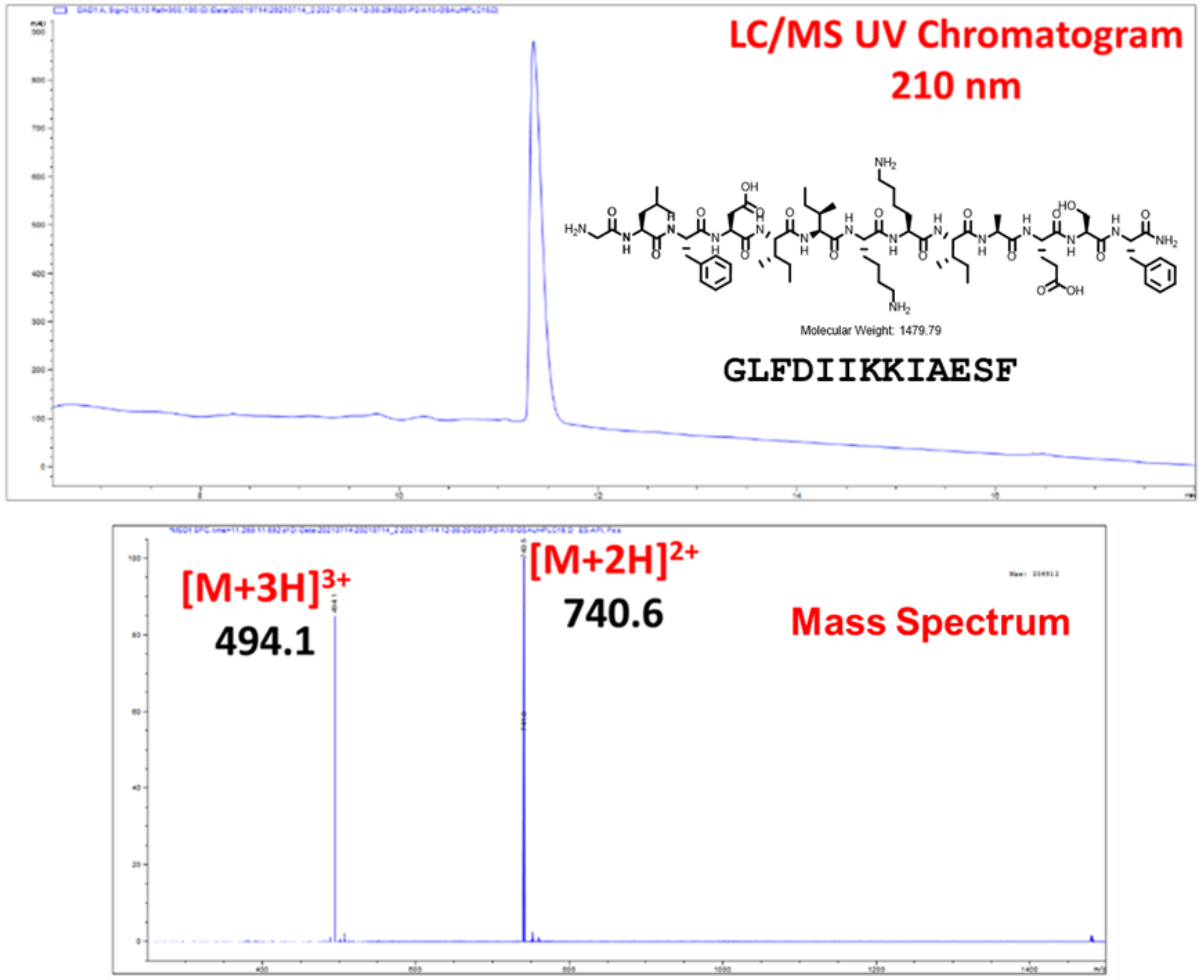

Agilent LC/MS chromatogram and mass spectrum of HPLC fraction of isolated aurein-

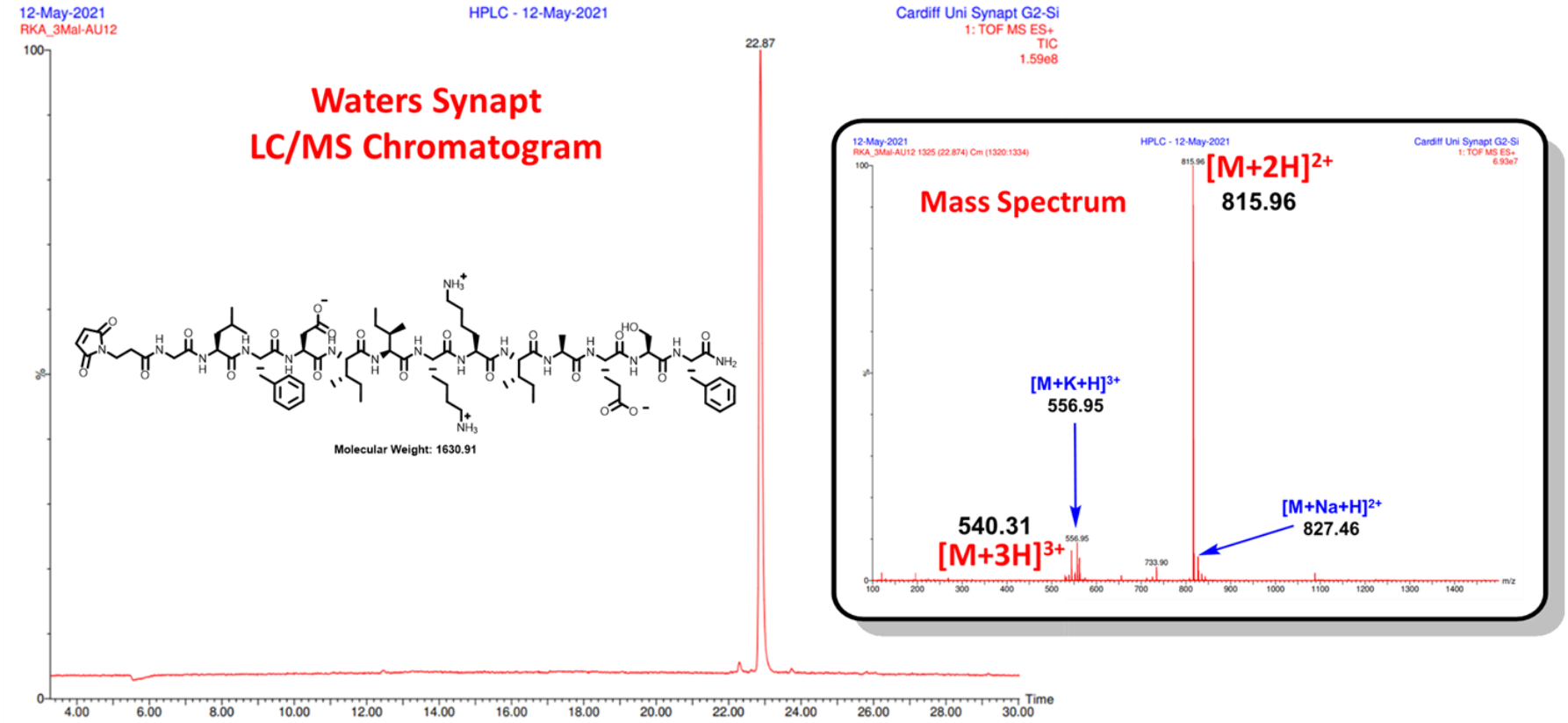

Waters synapt LC/MS chromatogram and mass spectrum of HPLC fraction of isolated aurein-1.2 with N-terminal maleimide.

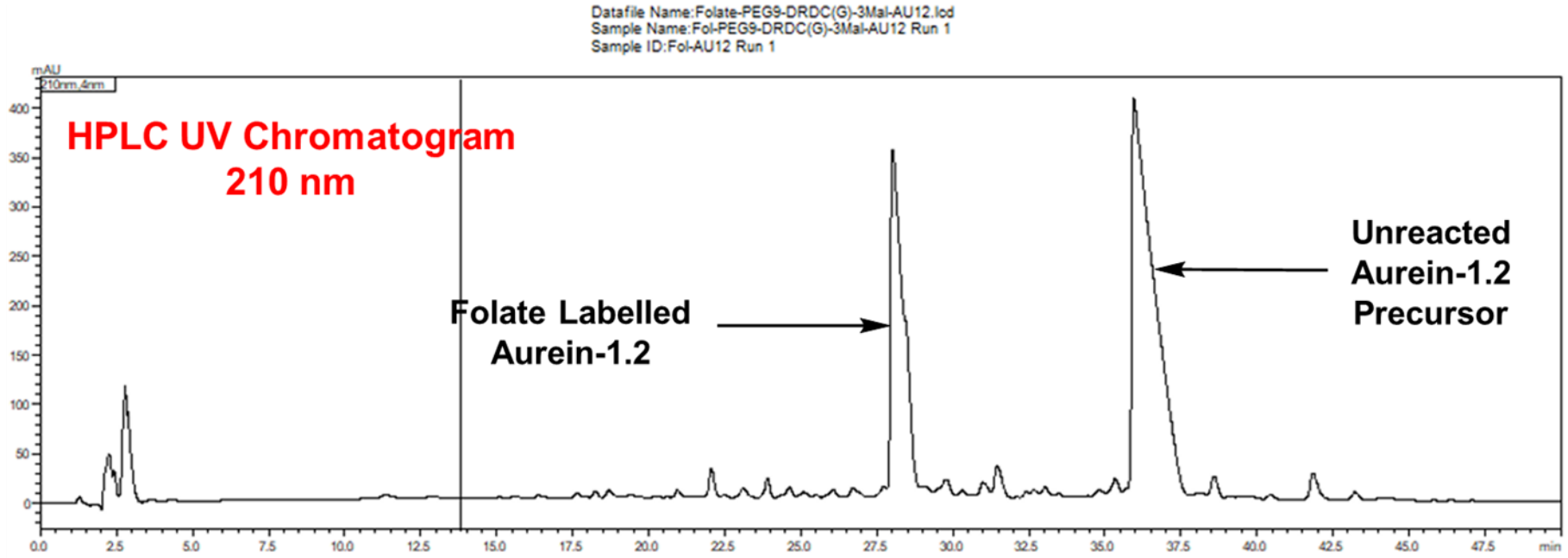

Shimadzu preparation scale HPLC UV chromatogram (210 nm) of isolated folate labelled aurein-1.2.

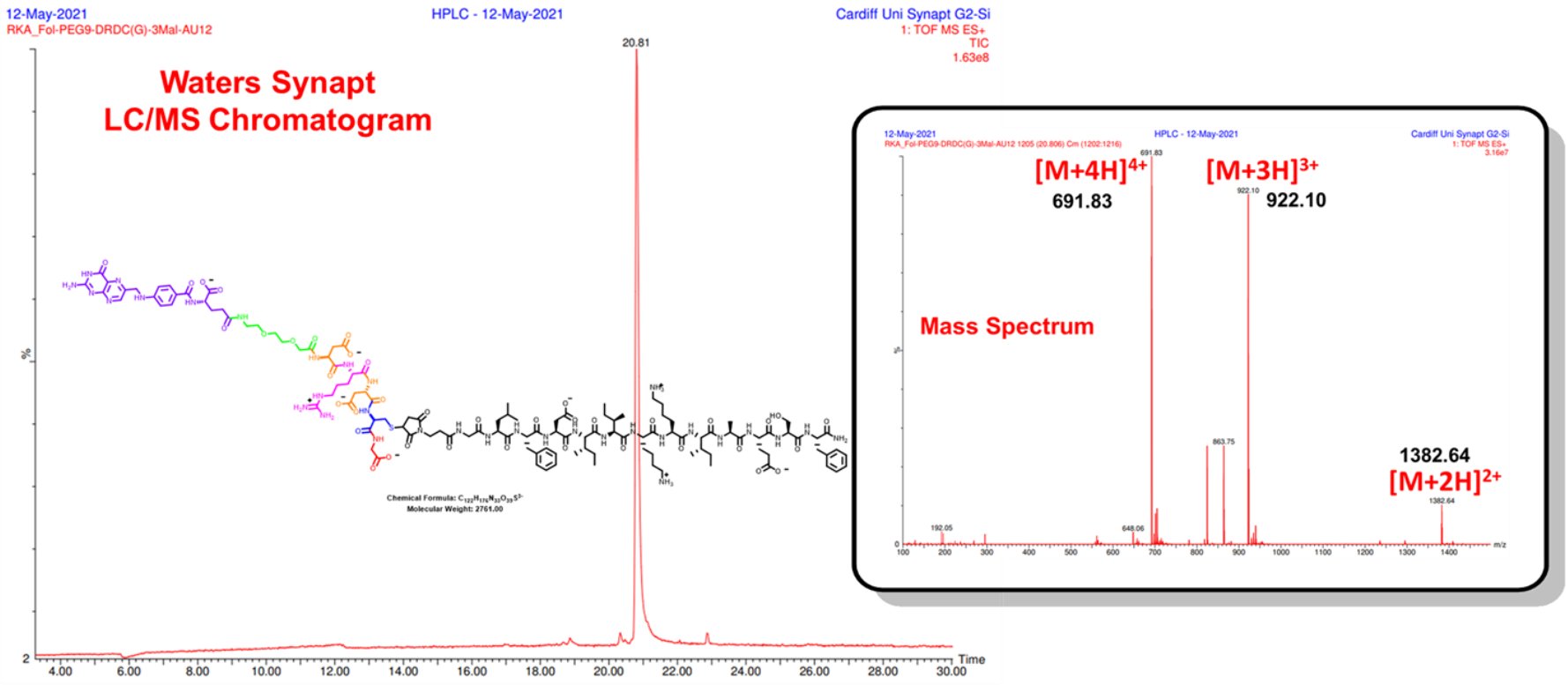

Waters synapt LC/MS chromatogram and mass spectrum of HPLC isolated folate labelled aurein-1.2.

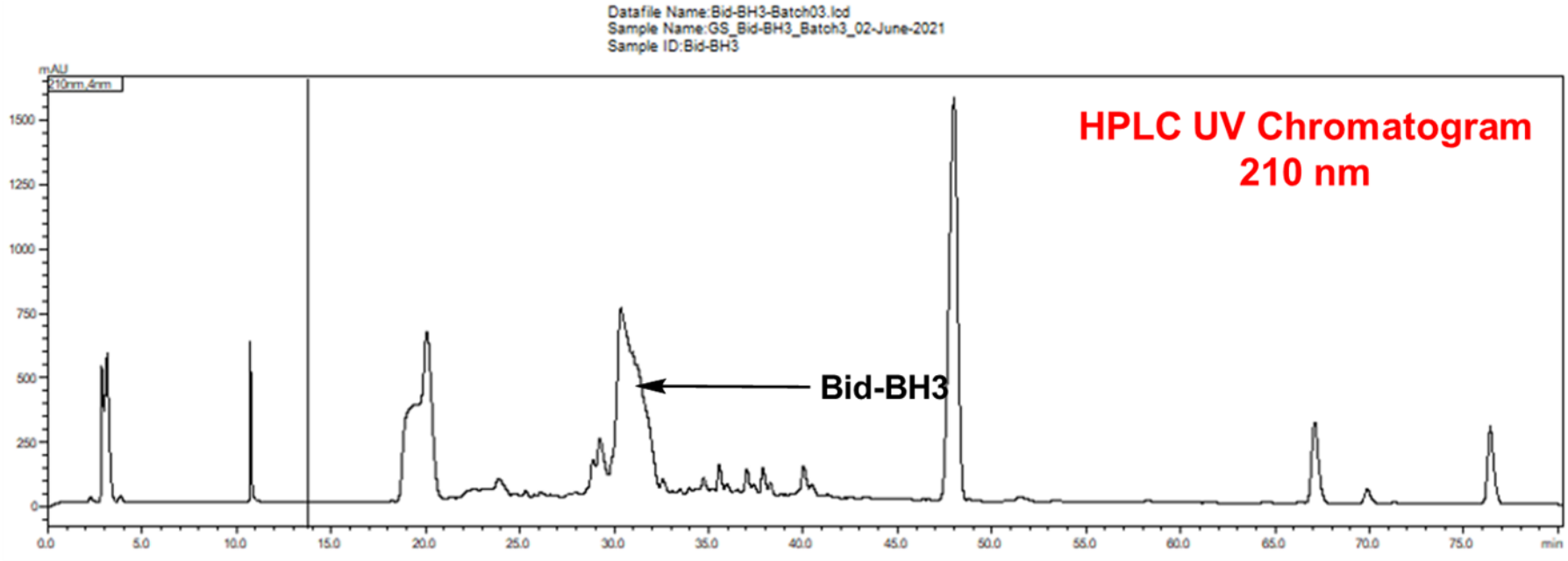

Shimadzu preparation scale HPLC UV chromatogram (210 nm) of isolated Bid-BH3.

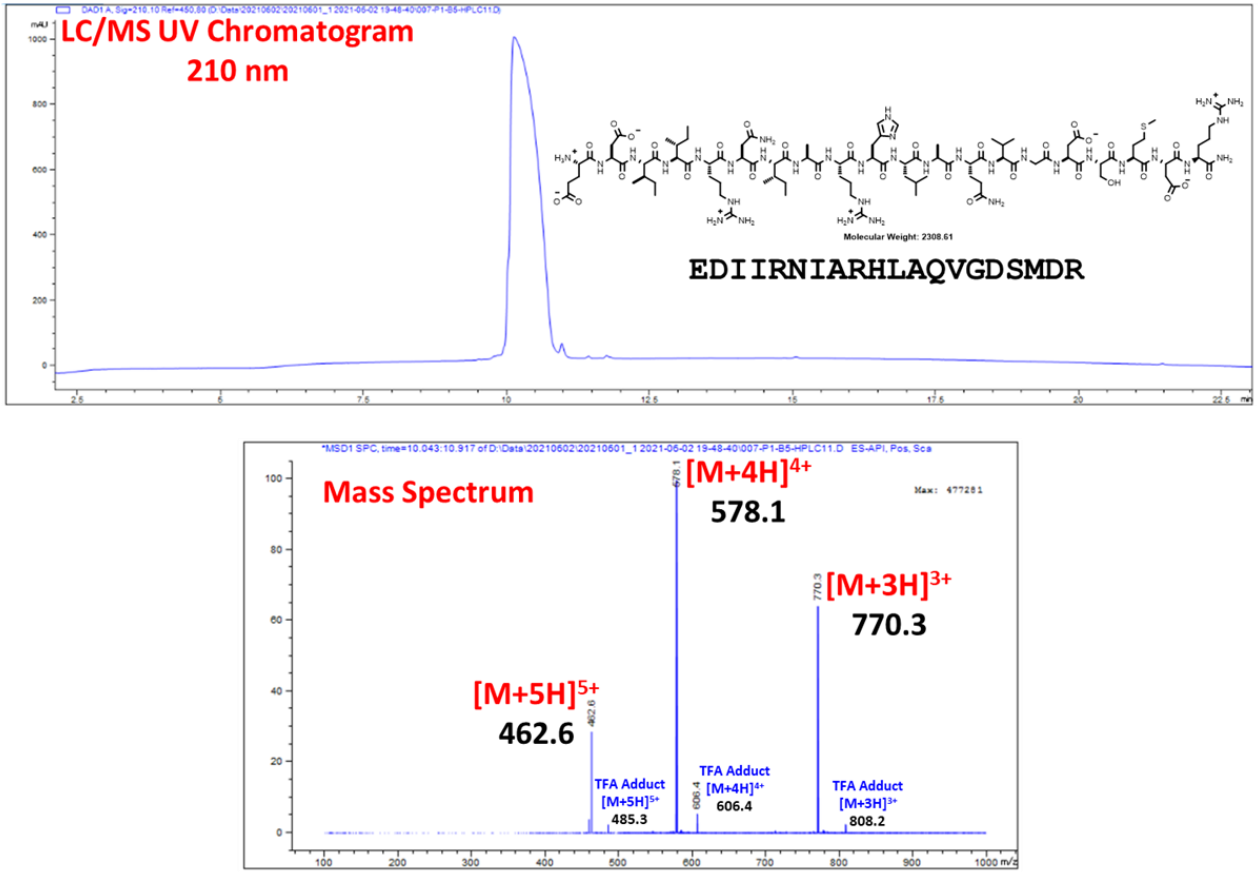

Agilent LC/MS chromatogram and mass spectrum of HPLC isolated Bid-BH3.

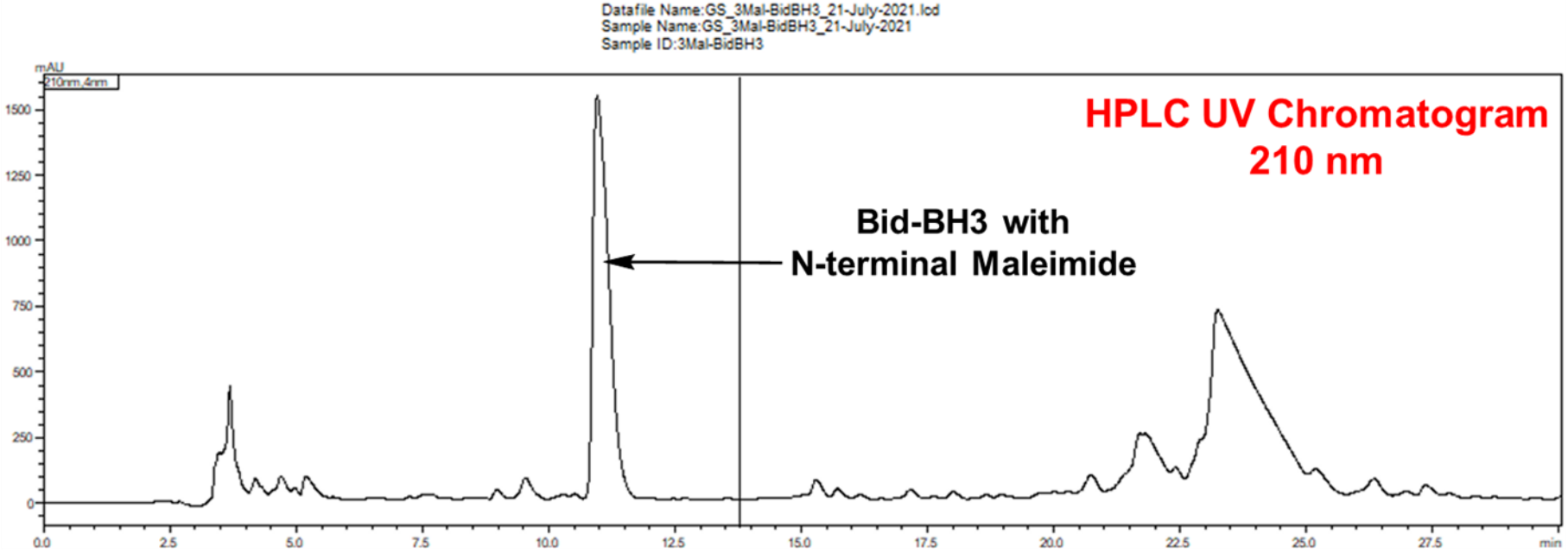

Shimadzu preparation scale HPLC UV chromatogram (210 nm) of isolated Bid-BH3 with N-terminal maleimide.

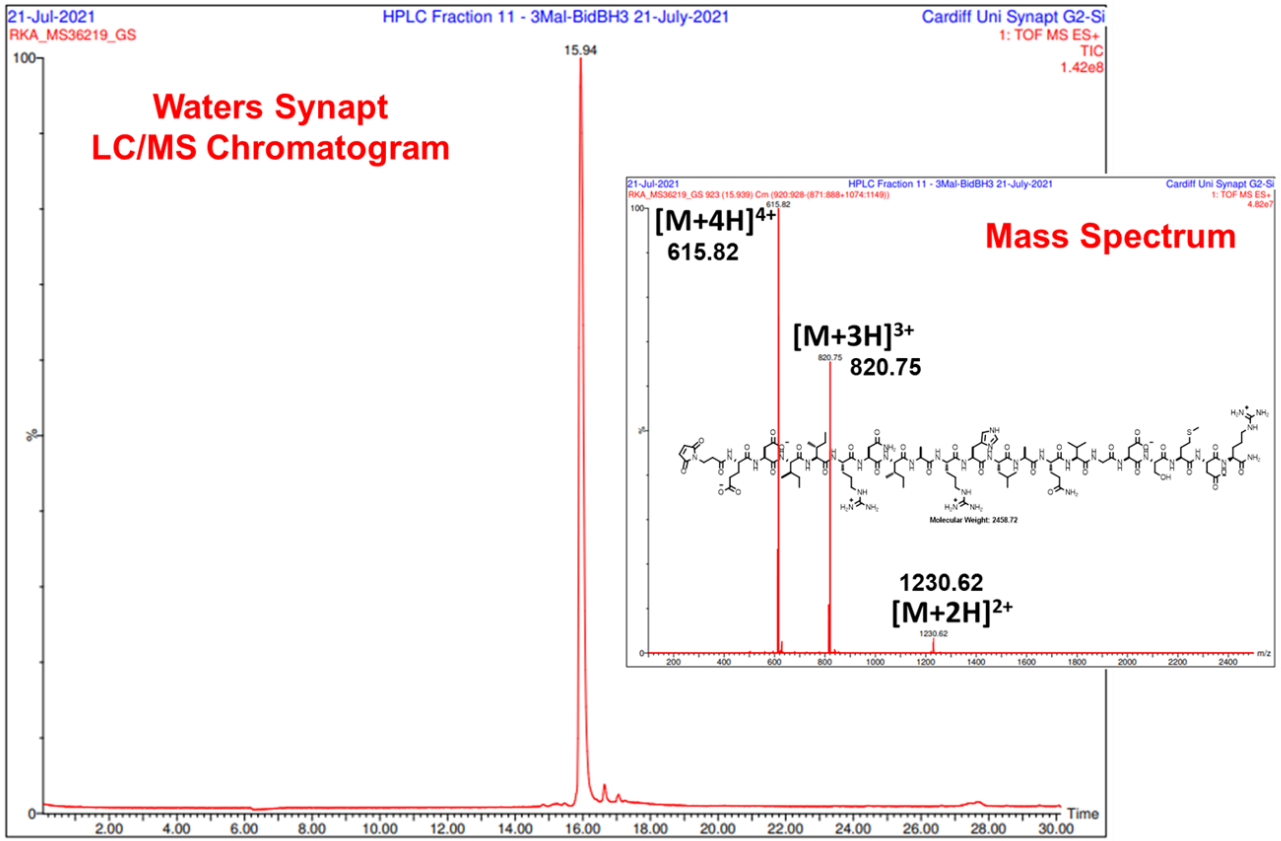

Waters synapt LC/MS chromatogram and mass spectrum of HPLC isolated Bid-BH3 with N-terminal maleimide.

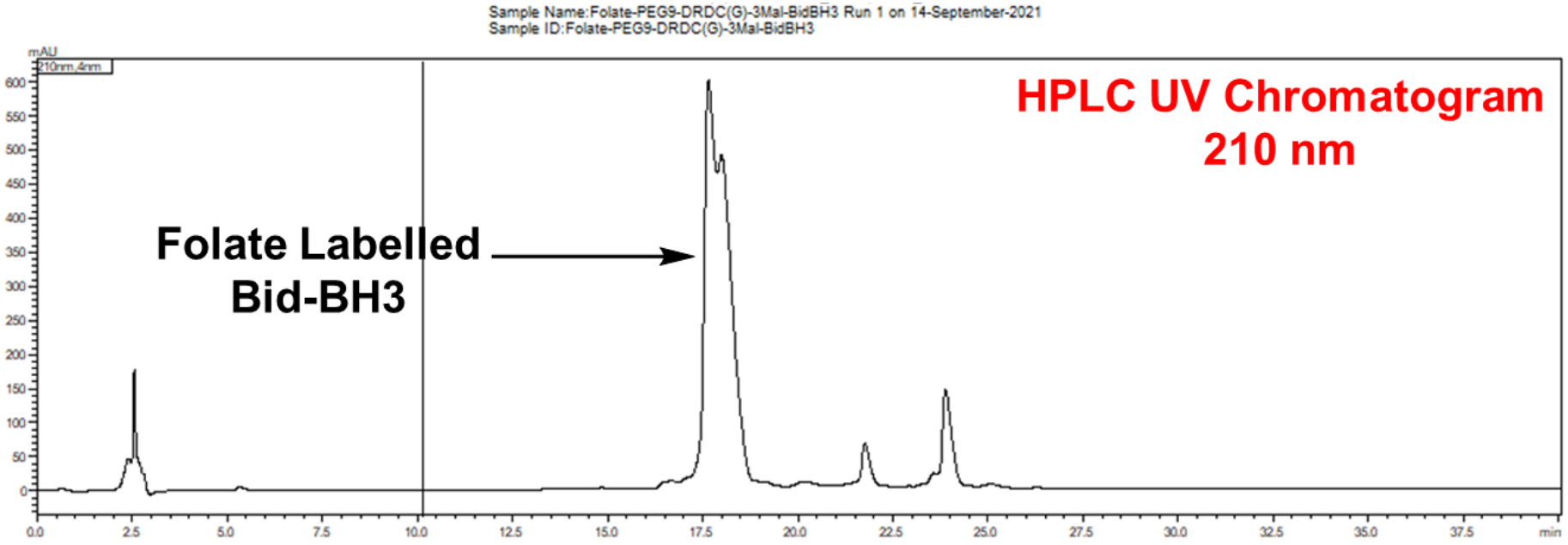

Shimadzu preparation scale HPLC UV chromatogram (210 nm) of isolated folate labelled Bid-BH3.

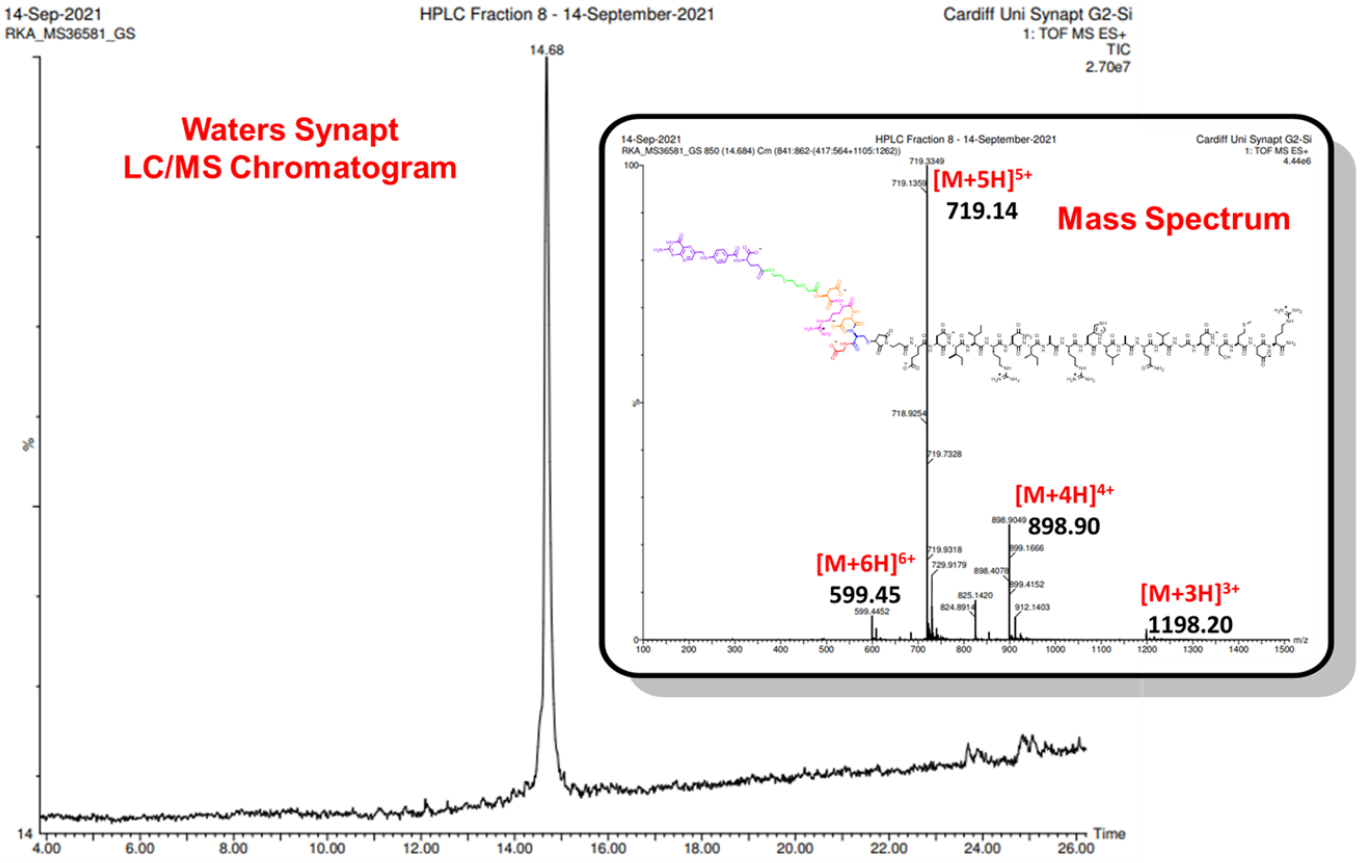

Waters synapt LC/MS chromatogram and mass spectrum of HPLC isolated folate labelled Bid-BH3.

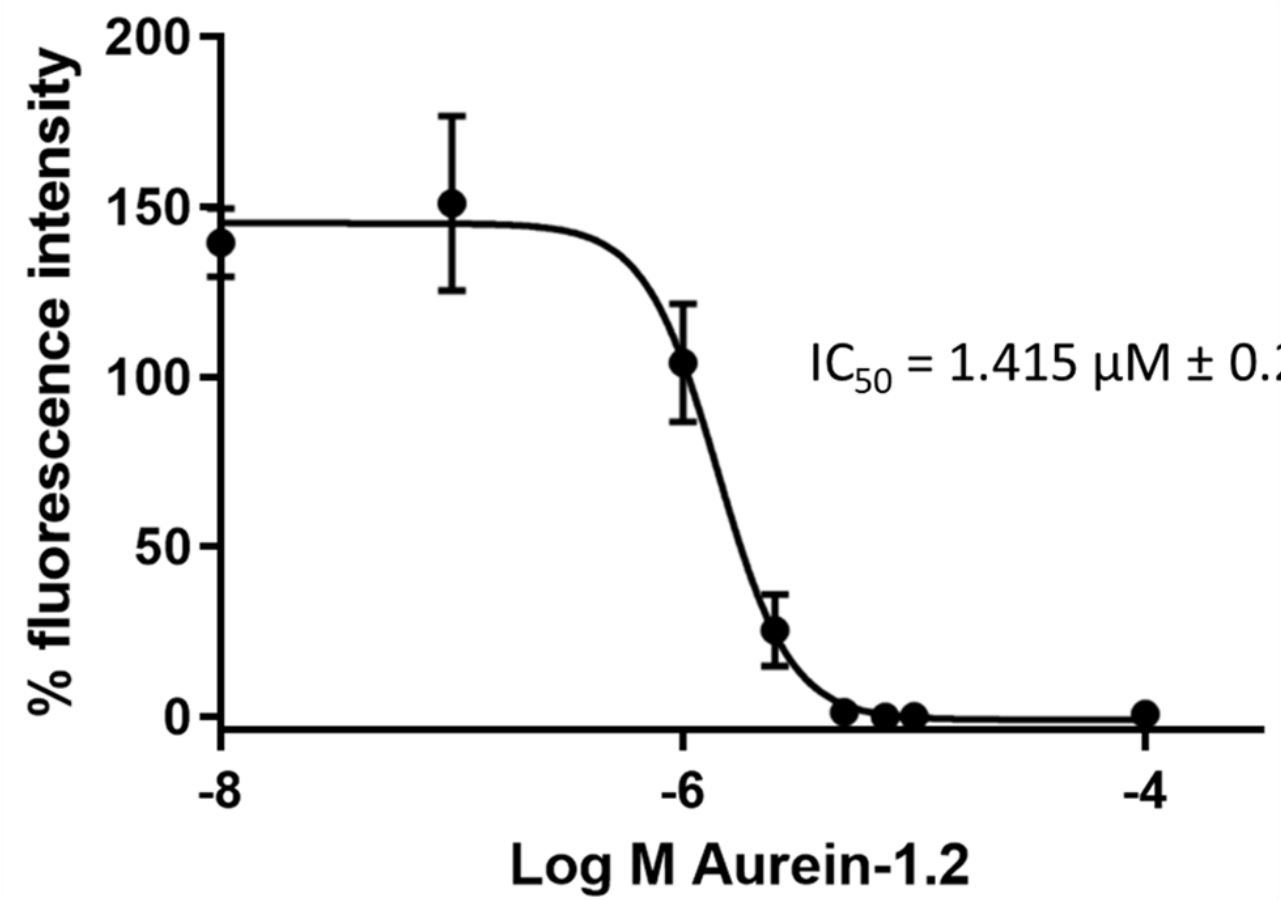

IC_{50} curve derived from cell titre blue cell viability assay applied to a single colony of KB cells exposed to varying concentrations of aurein-1.2 during 24-hour period.

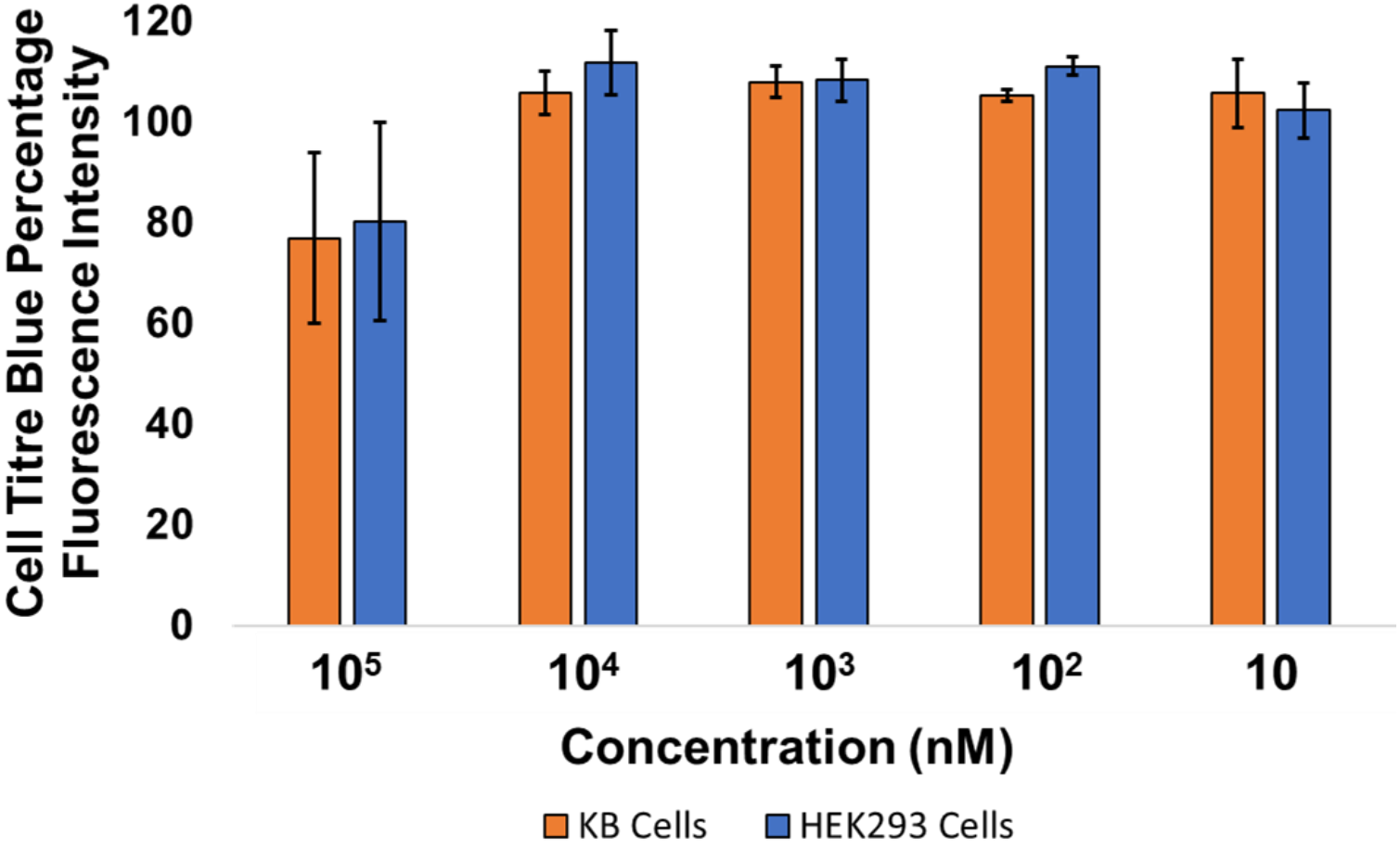

Bar chart showing cell titre blue cell viability assay applied to a single colony of KB cells and HEK293 cells tested side by side on varying concentrations of folate labelled aurein-1.2 During 24-hour period.

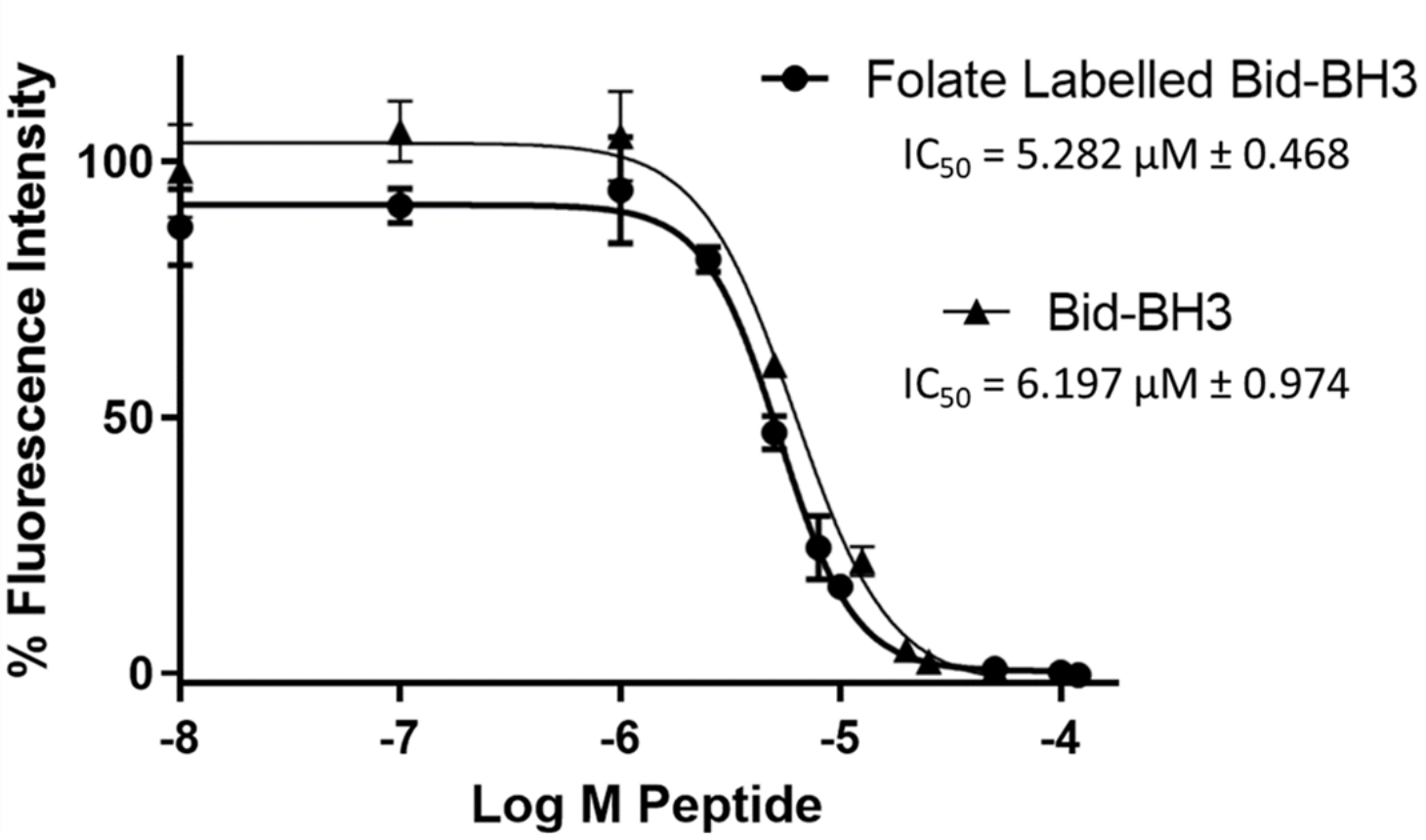

IC_{50} curve derived from cell titre blue cell viability assay applied to a single colony of KB cells exposed to varying concentrations of Bid-BH3 peptides (folate labelled vs. native) during 24-hour period.

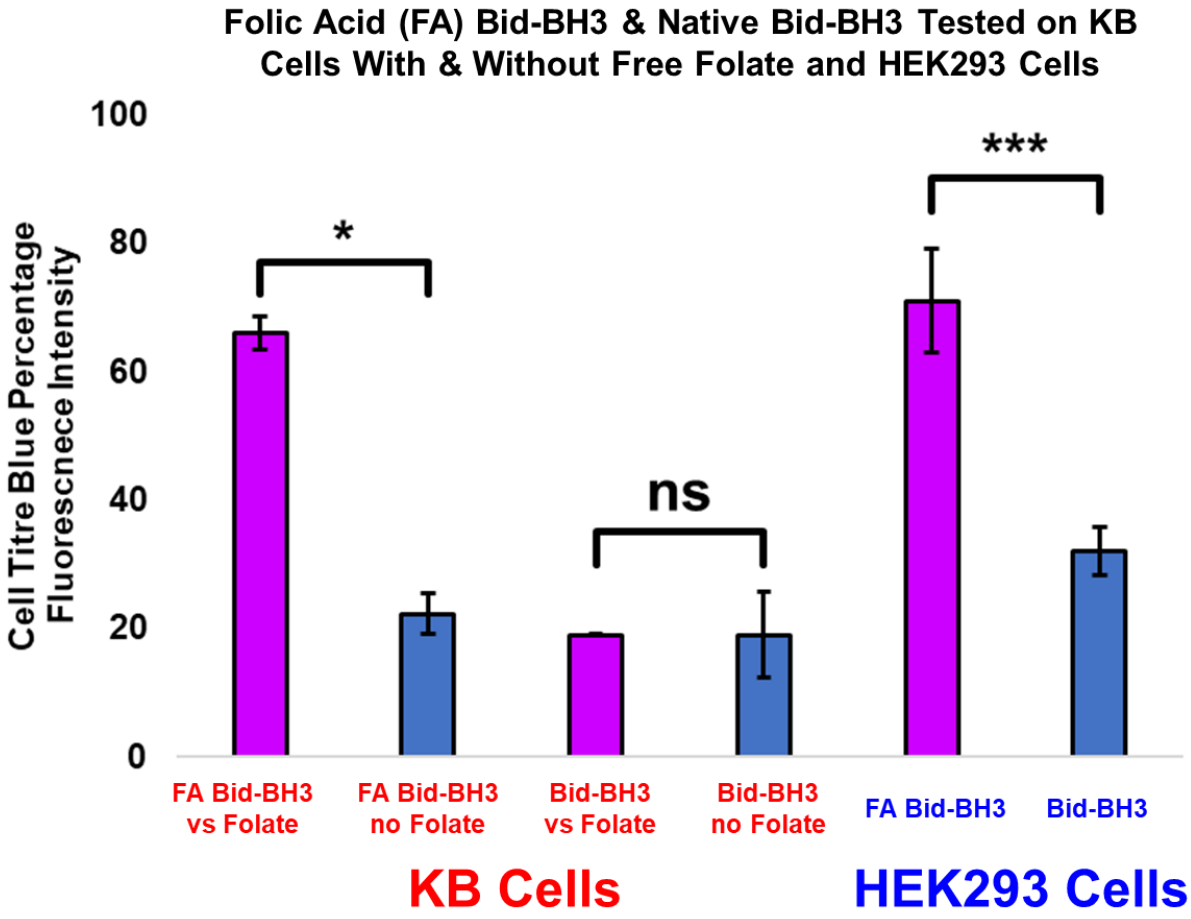

Bar chart derived from cell titre blue cell viability assay applied to KB Cells (left) and HEK293 cells (right) exposed to 5 μM Bid-BH3 peptides (folate labelled vs. native) during 24-hour period.

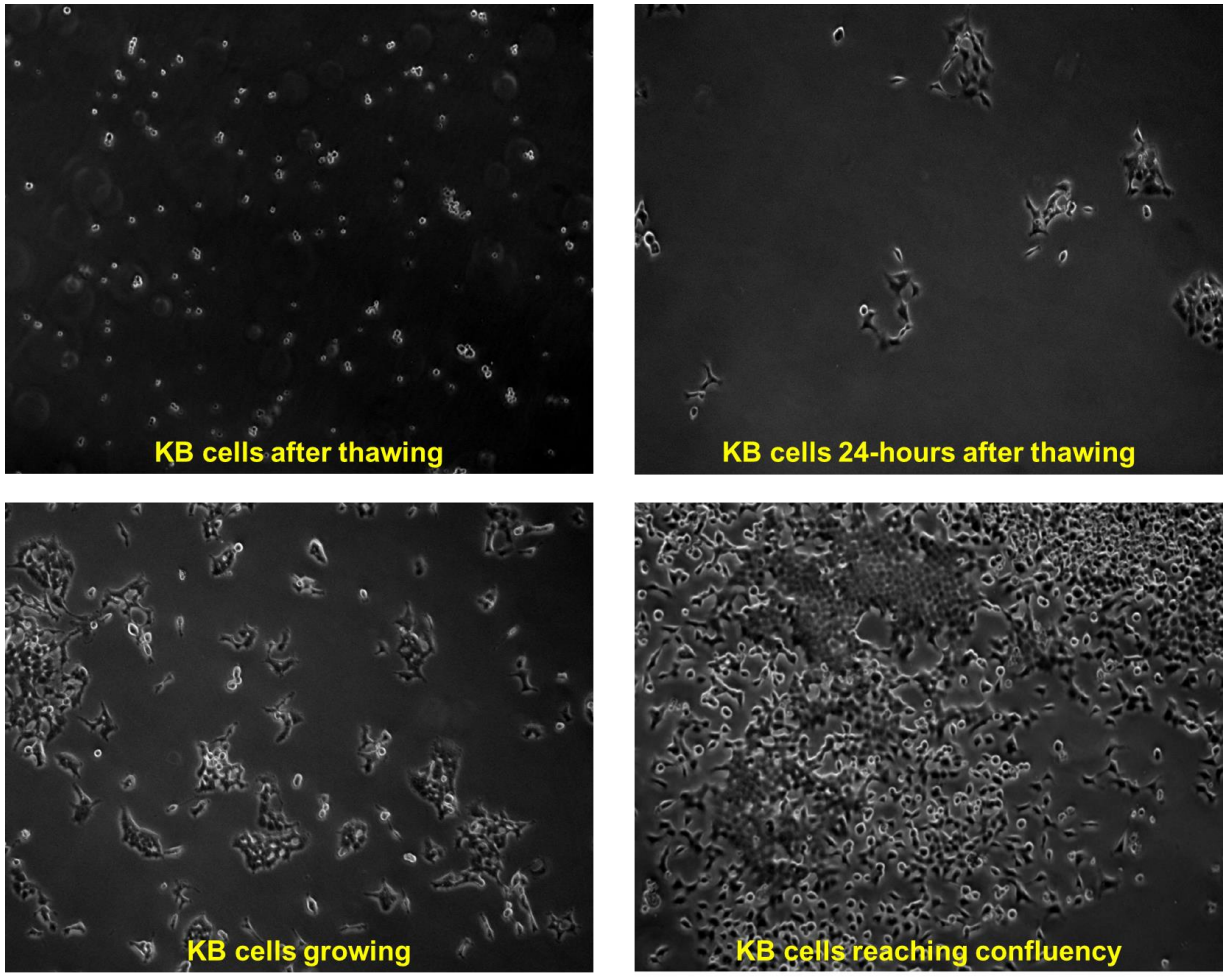

Light microscopy images of KB cells from freeze thawing to reaching confluency.

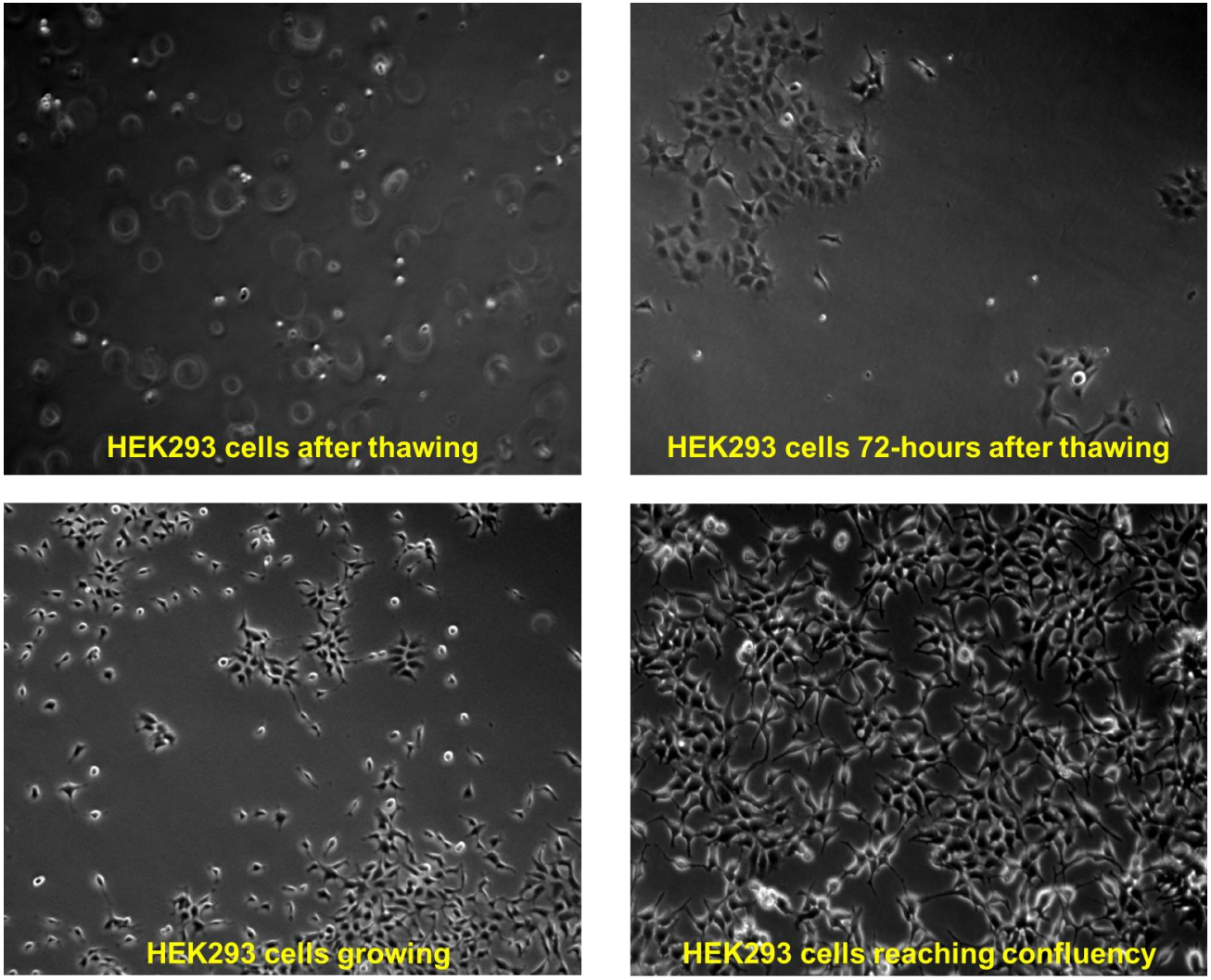

Light microscopy images of HEK293 cells from freeze thawing to reaching confluency.